

ISSN 0236-2945

LIGHT & ENGINEERING

Volume 25, Number 2, 2017

LLC “Editorial of Journal “Light Technik”, Moscow

LIGHT & ENGINEERING

(Svetotekhnika)

General Editor: **Julian B. Aizenberg**, Dr. of Sc., Prof., Academician of AESc.RF

Editor-in-Chief: **Vladimir P. Budak**, Dr. of Sc., Prof. Moscow Power University

Deputy Chief Editor: **Raisa I. Stolyarevskaya**, Dr. of Sc., LLC "Editorial of Journal "Light Technik"

Editorial Board Chairman: **George V. Boos**, Ph.D., Moscow Power University

Editorial Board:

Sergey G. Ashurkov, Ph.D., LLC "Editorial of Journal "Light Technik"

Vladimir P. Budak, Dr. of Sc., Prof. Moscow Power University

Vladislav E. Bugrov, Dr., Prof., ITMO University rector, S. – Petersburg

Natalya V. Bystryantseva, Ph.D., ITMO University, S.-Petersburg

Alexei A. Korobko, Ph.D., BL Group, Moscow

Leonid G. Novakovskiy, Ph.D., Closed Corporation "Faros-Aleph"

Alexander T. Ovcharov, Dr. of Sc., Prof., Tomsk State Arch. – Building University, Tomsk

Leonid B. Prikupets, Ph.D., VNISI named by S.I. Vavilov, Moscow

Vladimir M. Pyatigorsky, Ph.D., VNISI named by S.I. Vavilov, Moscow

Anna G. Shakhparunyants, Ph.D., General Director of VNISI named by S.I. Vavilov, Moscow

Nikolay I. Shchepetkov, Dr. of Arch., prof. of SA MARchi, Moscow

Alexei K. Solovyov, Dr. of Sc., Prof., State Building University, Moscow

Konstantin A. Tomsky, Dr. of Sc., Prof., St.-Petersburg State University of Film and Television

Leonid P. Varfolomeev, Ph.D., Moscow

Pavel P. Zak, Dr. of Biol. Sc., Prof., Emanuel Institute of Biochemical Physics of Russian Academy of Science (IBCP RAS)

International Editorial Advisory Board:

Lou Bedocs, Thorn Lighting Limited, United Kingdom

Tony Bergen, Technical Director of Photometric Solutions International, Australia

Wout van Bommel, Philips Lighting, the Netherlands

Peter R. Boyce, Lighting Research Center, the USA

Lars Bylund, Bergen's School of Architecture, Norway

Stanislav Darula, Academy Institute of Construction and Architecture, Bratislava, Slovakia

Peter Dehoff, Zumtobel Lighting, Dornbirn, Austria

Marc Fontoynt, Ecole Nationale des Travaux Publics de l'Etat (ENTPE), France

Franz Hengstberger, National Metrology Institute of South Africa

Warren G. Julian, University of Sydney, Australia

Zeya Krasko, OSRAM Sylvania, USA

Evan Mills, Lawrence Berkeley Laboratory, the USA

Yoshi Ohno, NIST Fellow, (CIE President 2015-2019), USA

Lucia R. Ronchi, Higher School of Specialization for Optics, University of Florence, Italy

Eino Tetri, Dr. of Tech.Sc., Lighting Expert, Finland

Nicolay Vassilev, Sofia Technical University, Bulgaria

Jennifer Veitch, National Research Council of Canada



Moscow, 2017

Editorial Office:

VNISI, Rooms 327 and 334
106 Prospekt Mira, Moscow 129626,
Russia
Tel: +7.495.682.26.54
Tel./Fax: +7.495.682.58.46
E-mail: lights-nr@inbox.ru
<http://www.sveto-tehnika.ru>

Scientific Editors:
Sergey G. Ashurkov
Evgeny I. Rozovsky
Raisa I. Stolyarevskaya
Style Editor
Marsha Vinogradova
Art and CAD Editor
Andrei M. Bogdanov

Light & Engineering" is an international scientific Journal subscribed to by readers in many different countries. It is the English edition of the journal "Svetotekhnika" the oldest scientific publication in Russia, established in 1932.

Establishing the English edition "Light and Engineering" in 1993 allowed Russian illumination science to be presented the colleagues abroad. It attracted the attention of experts and a new generation of scientists from different countries to Russian domestic achievements in light and engineering science. It also introduced the results of international research and their industrial application on the Russian lighting market.

The scope of our publication is to present the most current results of fundamental research in the field of illumination science. This includes theoretical bases of light

source development, physiological optics, lighting technology, photometry, colorimetry, radiometry and metrology, visual perception, health and hazard, energy efficiency, semiconductor sources of light and many others related directions. The journal also aims to cover the application illumination science in technology of light sources, lighting devices, lighting installations, control systems, standards, lighting art and design, and so on.

"Light & Engineering" is well known by its brand and design in the field of light and illumination. Each annual volume has four issues, with about 80–140 pages per issue. Each paper is reviewed by recognized world experts.

To promote the work of the Journal, the editorial staff is in active communication with Thomson Scientific (Citation index) and other international publishing houses and agencies, such as Elsevier and EBSCO Publishing.

CONTENTS

VOLUME 25

NUMBER 2

2017

LIGHT & ENGINEERING

Leonid P. Varfolomeev Lighting Equipment for Manned Spacecraft.....	4
Sergei I. Lishik, Valery S. Posedko, Yuri V. Trofimov, and Vitaly I. Tsvirko Current State, Trends and Perspectives of the Development of Light Emitting Diode Technology.....	13
Alexander V. Sibrikov and Andrei I. Kirichyok Application of Light Emitting Diodes for Illumination of Moscow and Operational Challenges.....	25
Lale Erdem Atilgan and Mustafa BerkerYurtseven Thermal Design of an LED System: A Special Lantern for Turkish Historical Mosques.....	30
Banu Tabak Erginöz and Cenk Yavuz A Survey and Measurement Based Study on Dimmable Lighting to Evaluate Visual Performance and Lighting Energy Savings	42
Musa Demirbaş, Türker Fedai Çavuş, Ceyda Aksoy Tirmikçi, and Cenk Yavuz Investigation of Energy Saving Performance and Other Related Parameters of a Daylighting Scenario for an Industrial Building	51
Mustafa Zeytin and Nazım İMAL Lighting Quality Supported by Software and Application of Increasing the Efficiency.....	56
Nikolai L. Pavlov A Chromatic Conceptualisation of Natural Life	62
Mária Ferencíková and Stanislav Darula Availability of Daylighting in School Operating Time.....	71
Natalya A. Saprykina Sunlight as an Arranging Factor of Forming Dynamic Architecture.....	79
Alexei K. Solovyov Reflective Facades and their Influence on Illumination of Nearby Buildings.....	88
Mikhail V. Osikov, Oksana A. Gizinger, Olga I. Ogneva, Olga R. Bokova, and Victoria G. Chudinova A Comparative Analysis of the Influence Artificial Illumination on Behaviour of Laboratory Animals.....	94
Guy Durinck, Frédéric B. Leloup, Jan Audenaert, and Peter Hanselaer Modeling the Spectrum of a Luminaire Including a Dichroic Filter By Spectral Ray Tracing.....	103
Viktor S. Zheltov and Vladimir P. Budak Mathematical Simulation of Lighting Installations Using a Computer.....	113
Sergey V. Alkov, Mikhail L. Belov, and Viktor A. Gorodnichev An Approximation Formula for Angular Distribution of Irradiance From an Irregular Surface with Complex Indicatrix	121
Leihong Zhang, Bei Li, Haojun Zhang, Yi Kang, Wenjie Zhan, Wenjuan Yi, and Zhiwen Chen Study on the Comparison of Two Spectral Reflectance Reconstruction Methods Based on Agile Spectrum Imaging and Liquid Crystal Modulation	128
Kadirvel Sindhubala and Baba Vijayalakshmi Design and Implementation of Optical Receiver for Visible Light Communication to Reduce Ambient Light Noise	139
Content #3 2017	147

LIGHTING EQUIPMENT FOR MANNED SPACECRAFT

Leonid P. Varfolomeev

E-mail: galeo.varfol@yandex.ru

ABSTRACT

The article presents a retrospective of the achievements in Russian domestic scientific, design and manufacturing efforts, headed by the VNISI, on the creation of illumination and irradiation devices for manned spacecraft.

Keywords: space, manned spacecraft, luminaire, irradiator, VNISI

All materials connected with space exploration were considered secret for many years in the USSR, and the first open access publication concerning «space lighting engineering» was article [1]. In order to publish it, it was necessary to involve astronaut Yu.P. Artyukhin who completed a 15 day flight mission at the Salyut-3 station. In the article, the main problems of illuminating space craft intended for long flights were formulated in the most general terms.

The Salyut stations (beginning from Salyut-3) were the first space objects for which illumination equipment was completely developed and manufactured at the VNISI. Before, for illumination of manned space craft, incandescent lamps (IL) and SI-3 luminaires with fluorescent lamps (FL) of ЛБ4–2BY type were developed in the experimental design bureau (EDB) of the Flight-test Institute of M.M. Gromov. In the luminaire, two FLs were used of 4 W each with luminous flux of 90 lm, and the both lamps could simultaneously work no more than 3 h a day. It is clear that illuminance of operational surfaces was at the level of utility rooms (not higher than 30 lx).

The first scientific progress in the determination of optimal illumination conditions for

manned spacecraft was represented by the work of S.M. Zalkind, who worked at the Scientific Research Institute of Civil Air Fleet, and made it the subject of her dissertation defended in 1972. This dissertation became the basis of industrial standards of the Ministry of General Mechanical Engineering coordinated with the Ministry of Health of the USSR, and the standards were implemented for the first time at Salyut station. Compared to Building regulations and other regulating documents, these standards did not meet the requirements for normal working and functioning conditions, especially in the context of arduous long space flights. Illuminance on operational surfaces and in resting places should reach 100 lx, and illuminance of auxiliary rooms should be 30 lx. The light source type was regulated as FLs of white light. Irregularity of luminance distribution in the field of vision and other illumination parameters were not regulated in any way.

Such low requirements for illumination conditions were primarily a result of a very high price of electric energy on manned spacecraft and due to payload limitation for placement into orbit. According to American sources for 1970, the cost of lifting 1 kg of payload into orbit was \$2200, cost of 1 kW power from solar batteries was \$25000 [2]. During the design stage of the Salyut-5 station, all system of inner illumination were assigned 250 W of average daily power and 14 kg of total mass. It should be said that the first part of these requirements was met, and the second was not (the total mass of the inner illumination system was equal to about 24 kg).

An important feature of manned spacecraft illumination is that their only source of electric

energy is solar powered rechargeable batteries. The total area of solar batteries at the International Space Station (ISS) is about 2000 m², and their power is 110 kW. In the Russian segment, the voltage is 28 V, in the American – 124 V, and in the Japanese – 28, 50 and 124 V is traditionally used. The presence of direct voltage only complicates the use of FLs as in order to avoid cataphoresis, they can only operate with an alternating current. Therefore, a critical element of FL luminaires is the converter of direct voltage into alternating. ILs can successfully work both with direct, and with alternating current but they require a stable voltage. The challenge is that onboard voltage can vary widely (from plus 7 to minus 4 V while rating value is 27 V). IL parameters, primarily lifetime and luminous flux, strongly depend on voltage, and therefore an indispensable unit of all IL luminaires is a voltage stabilizer.

The first manned spacecraft with acceptable illumination conditions was Soyuz –19 created for the ASTP Soviet-American space programme (the Apollo-Soyuz Test Project). СД1–5М and СД1–6 luminaires for operational and local illumination were specifically developed for this craft in a short time frame. For illuminating TV reporting in space, the СТ2–9 luminaire was developed. The first two luminaires were equipped with U-type amalgam FLs of 8 W, and the third had a halogen incandescent lamp (HIL) of 27 W. By their structure, the FL luminaires were identical but СД1–6 was the world's first «space» luminaire with controlled luminous flux (axial luminous intensity was varied from 1 to 40 cd). By request of the All-Russian Research Institute of Television responsible for telecasting from the orbit, in these luminaires, FLs of improved colour rendition (“ЛДЦ”) were used providing a better colour rendition quality in comparison with the “ЛБ” (white light lamp) FLs.

Illuminance of working spaces on the Soyuz –19 was about 200 lx and could be dimmed by the astronauts to 2–5 lx depending on the nature of the work undertaken. Illuminance for black-and-white TV reports reached 300 lx, at colour – of about 100 lx and provided TV reports and camera recording of acceptable quality. When they arrived at the Zvyozdny Gorodok training facility, the American astronauts were shocked by the quality of the Soyuz illumination, as Apollo illumination at that time was much worse, and

the American astronauts had not even considered the possibility adjustable FL luminaires.

СД1–5М and СД1–6 luminaires (Fig. 1) consisted of two units: a power supply unit, which was stably installed onboard and a detachable light unit. The light unit was manufactured from polycarbonate as the most shock-resistant plastic. Electrical junction of the units was a PC 10Б connector, and clamping of the light unit on the power supply unit used thrown-over locks.

This luminaire structure was also used in subsequent developments. It provided a high degree of reliability and operational convenience on numerous flights and during long-term missions at the Salyut and Mir stations and at the ISS.

Due to obviously insufficient illumination levels according to the standards in place at that time, the VNISI together with specialists from the Institute of Medical and Biological Problems (IMBP), the State Optical Institute (SOI), the Design Bureau of General Machinery Industry of V.P. Barmin, with the Institute of Aircraft and Space Medicine (IASM) and with the Scientific Research Institute of Industrial Aesthetics, in 1977–80 a large-scale study was undertaken («Study of creating ways of rational illumination installation for closed ecological objects»), the results of which were partly published [3–9].

For long-term experiments, two unique illumination installations were developed and manufactured.

In an isolation vacuum chamber of the IASM, four luminaires with six FLs of 18 W power each were mounted. Power supply of the lamps was implemented using a high frequency current (20kHz), with a possibility of independent adjustment of luminous flux from two places: from within and outside of the chamber. Luminaires ЛБ (white lamp) FLs were used for two of them and improved colour rendition FLs were used for the other two. The experiment participants working in the chambers could set a desirable illuminance level for working spaces within an interval of 0–350 lx, as well as a desirable spectrum of the lamps. There were no limitations by power consumption. The experimental team performed a continuous three-day project of work very close to the real activity of astronauts in space flights. To imitate zero gravity conditions, the operators were in the orthostatic position (lying on the back with body axis tilt of 6° and head down). Physio-



Fig. 1. CD1–5M (CD1–6) luminaire:
a – assembled; *b* – light unit from the back; *c* – power supply unit

logical parameters of all participants were measured: blood pressure and heart rate. Visual working capacity and state of visual analyzer were determined by correction tasks, achromatic adisparometry, contrast sensitivity and critical flicker fusion frequency. Without a certain periodicity, several times a day, adjustors outside the chamber set illuminance levels different from those selected by the participants inside the chamber so that they would set a desired level again.

In another experimental installation, a desired illuminance for recreational spaces was determined (level, irregularity of luminance distribution, room saturation with light, radiation chromaticity, colour finish of rooms). For this purpose, in full-scale models of the real rooms, installations of cornice illumination with standard FLs of different types were mounted, as well as of coloured FLs (red, green and blue) developed especially of 36 W each. As well as in the luminaires for the isolation vacuum chamber, FLs were supplied with a high frequency current and could be adjusted.

The participants voluntarily installed illuminance levels and radiation spectrum for different colours of walls, providing the most comfortable conditions for rest.

The results of these experiments, which formed the basis of O.I. Okara's (1980) and T.S. Leonova's theses (1982)), found that:

- The illuminance level, which provides comfortable conditions for work during a long stay in closed spaces, is about 200 lx for “ЛДЦ” FLs and about 270 lx for “ЛБ” FLs.

- In terms of visual working capacity and fatigue “ЛДЦ” FLs were no worse than ЛБ FLs (apparently, due to an absence of luminous flux pulses at a high-frequency power supply of the lamps).

- To create comfortable working conditions, the illumination system should allow the user to adjust illuminance levels, and for rest conditions – to adjust the spectrum.

- To decrease the unpleasant impacts of long term operations in a small closed spaces in the recreational areas, it is desirable to create light-and-colour dynamics.

To meet these requirements, in the All-Russian Research and Design Institute of Light Sources (RDILS) responding to a task set by the VNI-SI, developed a series of 8 W FLs, steady against high mechanical loads and climate conditions: ЛБ, ЛЕ and ЛДЦ FLs of red, green and blue FLs, as well as of erythemal and bactericidal mercury LP lamps. The VNISI created luminaires based on these lamps, which have functioned successfully in space for more than thirty years and continue to equip illumination facilities of the Russian ISS modules.

The listed special FLs created at the beginning of the 1980s still remain the leading world specimens; the luminous efficacy of red and green FLs is 75 lm/W, of ЛБ FLs is 55 lm/W; their guaranteed lifetime (with 0.95 probability of no-failure operation) is 5000 h.

ЛБ8–4 and ЛДЦ-8 FLs remain the basic light sources for the Russian ISS modules, and CD1–7, СПР-1 and CP-2 luminaires (Figs. 2–4) are developed to be used within them.

The CD1–7 luminaire was the main illumination device at the Mir station [10]. Seventeen such stationary luminaires were installed there with two ЛБ8–4 or ЛДЦ8 FLs each. The lamps were operated using one voltage converter and could be switched on separately. Output voltage frequency was 20 kHz, which completely excluded lamp luminous flux pulsations and acoustic noises from the luminaire. The luminaire's structure was similar to the above listed CD1–5M and CD1–6



Fig. 2. CD1-8 (CD1-7) luminaire

luminaires: the power supply unit was rigidly fixed onboard, and the detachable light unit of polycarbonate was clamped by thrown-over locks. No smooth adjustment of luminous flux was provided for. Later on, the CD1-8 luminaire was developed, the structure of which completely coincided with CD1-7 but its luminous flux was adjustable within (100–1)%. However, for the reasons listed below, development of this luminaire was stopped at the prototype stage, and they did not participate in real space flights.

The CIP-1 luminaire (Fig. 3) was developed for illumination during TV reports and filming, as well as still photographs at the Mir station. It was made as a monoblock with six 8 W FLs, and to protect them, the luminaire outlet was covered with a plate of especially strong material PMMA – CO 140 of 4 mm thickness. For convenient carrying and operation, there were two handles on end face sides of the case. There were four such luminaires at the station. They could be easily fastened in any place on the station using arms attached to the back of the case with captive screws but also using Velcro stickers. The CIP-1 luminaires were widely used by astronauts for not only TV reports and filming but also whenever an increased illuminance was required.

One more «space» luminaire, the CP-2 (Fig. 4), is similar to the CIP-1 luminaire by the electric circuit and parameters but it has a stationary fastening. CP-2 luminaires successfully work in Russian ISS modules today as well.

Finally, an additional version of the universal luminaire was developed suitable both for illumination of reports and filming, and for working light: CP-3 (Fig. 5). The luminaire contains three detachable light units unified with the main luminaire of working illumination CD1-7, which is fastened to the general power supply unit using thrown-over locks. Each unit can be turned on separately, which makes the illumination installation quite flexible. As well as portable CIP-1 re-



Fig. 3. CIP-1 luminaire (portable for reports)

porting luminaire, the CP-3 luminaire is designed for different methods of its fastening and carrying.

Unfortunately, the collapse of the USSR and destruction of the uniform space-rocket industry which followed, did not allow for a complete implementation of a comfortable light environment in manned spacecraft. Nevertheless, since July 1997, GOST [11] standard came into operation regulating some illumination parameters obtained from the 1977–80 study. It was created without participation of the VNISI (the illumination section was developed by the IMBP by the results of the above mentioned study) and therefore from the lighting point of view it is not quite correct. In Table 1, the illumination requirements normalised by the standard are presented.

They are as follows:

- In inhabited compartments, the following illumination types should be provided for: general (working); standby; emergency; to provide TV reports, video filming and still photographs; portable for repair work; portable with autonomous power supply;

- In technologically reasonable cases, combining different types of illumination. When switching off standby illumination, emergency illumi-



Fig. 4. CP-2 luminaire

Table 1. Requirements to illuminance for operational surfaces of manned spacecraft inhabited compartments [11, Table 13]

Illumination place	Optimum illuminance, lx, not less	Notes
1.Desktop	150	White light lamps are used Illumination uniformity, not less than: 1:3 – for control panels and work places 1:5 – for separate inscriptions and designations on panels 1:10 – for panels in central and peripheral part of the vision field
2.Control panel (dash board)	200	
3. Astronaut rest places	100	
4. Installation places of radio and special equipment	40	
5. Auxiliary compartments	50	In the ACS, washing cabin, and shower areas, a reduction to 30 lx is permitted
6. Astronaut sleep stations	10	Constant emergency illuminatin using blue filters
7. Indication facilities with need of detail distinction of the size: to 1 mm to 10 mm	200 75–100	For indication facilities of especially important parameters, luminance increase relative to basic elements by 40 % takes place (including control panels and systems for physical trainings)

nation should automatically switch on. Local illumination, switching on working illumination at astronaut bunks and a possibility of full illumination switching off including standby should be provided for;

– In the inhabited compartment, formation of flares on the reflecting surfaces of devices, windows, control panels, astronaut dazzle, shading of the working equipment when carrying out working operations by the astronauts and exposure of direct solar rays on the astronaut eyes should be excluded;

– Illuminance in case of emergency illumination should be not less than 20 % of the values specified in Table 1 but not less than 20 lx;

– To provide optimum conditions of information perception from devices, illumination control of indication facilities should be provided for. Illumination facilities of inhabited compartments should provide a smooth illuminance adjustment from 300 to 50 lx.

When carrying out the Buran space programme, (an analogue of the American Space Shuttle programme), the CF2–12 luminaire with HILs was developed to illuminate the untight loading and unloading site (Fig. 6). This choice of light source was motivated by the impossibility

of discharge lamp operation, including FLs in a preset temperature interval, and light emitting diodes then did not exist in practice. As the on-board voltage had a wide dispersion, the luminaire was turned on via a voltage stabilizer (in Fig. 6 at the left). As it is known, the Soviet orbital Buran ship made the only pilotless space flight, and its model is now shown at the Exhibition of Economic Achievements (EEA).

According to the Customer requirements, TV report illumination from the descent of manned spacecraft, in which astronauts are present during placing the ship into orbit and during descent, should be implemented using ILs only. In accor-



Fig. 5. CP-3 luminaire



Fig. 6. CF2-12 luminaire

dance with the ASTP programme, CF2-9 luminaire with KFM27-27 HILs was developed for this purpose. Later on it was modified, and as the CF2-14 luminaire (Fig. 7) was used on many Soviet and Russian Soyuz crafts. Due to a specially computed aluminium reflector with electrochemical polishing of the surface, the luminaire forms a uniform illuminance of about 300 lx within a circle of 1 m diameter from 1 m distance, which fully provides for high quality of TV reports. Four such luminaires work with one general power supply unit stabilising onboard voltage.

Besides illumination devices, the VNISI together with the IMBP developed and delivered onto the Salyut-7 UV BUF irradiator intended to compensate UV insufficiency, and to be exact, to prevent disturbances of the calcic exchange¹ [12]. The irradiator contained six erythemal ЛД8 FLs developed by the RDILS. Selection of a material to close the outlet appeared to be a big problem, because neither polycarbonate, nor polymethyl methacrylate (PMMA), nor other shock-resistant plastics pass through UV radiation of a necessary interval. As a result of studying material spectral transmission characteristics, polytrifluorochlorethylene (ftoroplast-3) was selected as a film of 0.4 mm thickness. Protection of the lamps and film closing was provided by a metal lattice (Fig. 8).

¹ Astronauts faced the “solar deprivation” problem, when flight duration continued for several months. It is known that vitamin D₃ regulating calcic exchange of an organism is not practically assimilated from food and is formed when skin radiating by UV radiation of about 365 nm wave length. A shortage of this vitamin leads to washing away of calcium from the bones and associated negative consequences (thinning and brittleness of bones, osteoporosis, etc.).



Fig. 7. CF2-14 luminaire

The IMBP has developed methodological instructions for astronauts concerning the BUF irradiator. To meet the instructions, the irradiator had a built-in timer with a preset radiation time: from 5 to 45 min. The irradiator was installed over the race track training device. The same irradiator operated at the Mir station as well.

Further, the illumination of the ISS American segment modules was implemented according to document [13]. The correspondent requirements for this illumination are presented in Table 2, from which it is seen that they are significantly higher than in accordance with GOST [11], and mainly meet the recommendations obtained from the research work of 1977-80.

For illumination of the American ISS modules, FLs are also used but it is already known that NASA intends to change to light emitting diodes (Fig. 9) [14]. One of the reasons for this is the disturbance of circadian rhythms and astronauts' chronic lack of sleep. It is known that during flights, the astronauts are short of approximately two hours of sleep daily. As light emitting diodes can practically radiate light of any chromaticity and can be easily adjusted, it is possi-



Fig. 8. BUF irradiator

Table 2. Requirements to illumination of ISS American segment module interiors

ISS area or activity type	Illuminance, lx not less
Servicing	100
Passages	50
Hatches	100
Hand-rails	100
Ladders	100
Working place	320
Maintenance	270
Control devices	200
Assembly	320
Recordings	540
Filling of tables	540
Repair	320
Panels	50
Reading	540
Night-time illumination	20

ble to simulate circadian change of light environment not only by illuminance, but also by radiation chromaticity, which facilitates maintenance of normal daily rhythms of the astronauts². It was planned to replace FLs with light emitting diodes in 2016.

One more important objects of lighting engineering manned spacecraft are «space greenhouses». Plant growing experiments in zero gravity conditions began at the Salyut station (1971), onboard which there was a small greenhouse – «Oasis». To illuminate the plants, CD1–4 luminaire with two FLs of 4 W each was used on the station. According to astronaut Yu.P. Artyukhin working on the station, the Oasis was the lightest place on the station, and astronauts spent considerable time near it. Incidentally, the CD1–4 luminaire was the first device develo-

² The problem of disturbance of circadian rhythms and of the possibility to control them using light was studied in the USSR already in the 1970s (VNISI, IMBP, IKM), however technical facilities of that time did not allow to implement the results.



Fig. 9. Luminaire with light emitting diodes for replacement of FL luminaires in the American ISS modules [14]

ped by the VNISI, which went to space. Later on, the Malachite greenhouses and others appeared, which showed a possibility of growing taller plants in manned spacecraft through a full cycle (from seed to seed).

Since 1996, a completely automatic greenhouse Svet (Light) developed at the IMBP, has worked on the Mir station. Its luminaire has two FLs of 8 W each and was developed in Bulgaria. In the greenhouse, wheat, leaf vegetables and garden radish were grown up. The astronauts gathered the harvest at a certain development stage, fixed it in special solutions, and then biologists on Earth studied the anatomy and morphology of the selected material.

On the ISS, experiments with growing taller plants are carried out both in the Russian and in the American segments. In the Russian segment the Lada greenhouse was operated, in which leaf salad, dwarf tomatoes, dwarf peas, barley, garden radish and wheat were grown (Fig. 10).

To illuminate, more precisely – to radiate, plants, FLs were used. The Lada greenhouse



Fig. 10. Lada space greenhouse

failed in 2010. In December 2016 the Lada-2 automatic greenhouse, which used light emitting diodes (white, red and blue in a combination optimum for growth of plants) should have replaced it. However, on the 1st of December, the Progress supply ship, which was to deliver the greenhouse to the ISS, did not enter orbit and was lost.

In the American segment of the ISS since April 2014 the Veggie (Vegetable) dismountable greenhouse is in operation. By planting area (30×36 cm) it is now the largest greenhouse, and a unit of red, blue and green light emitting diodes is used inside it. In this greenhouse, salad and other vegetable crops are grown, as well as for the first time zinnia flowers are grown under space flight conditions.

There is no information available on illumination of the Japanese, Canadian and European ISS segments.

For warning light systems, Russian manned spacecraft only use ILs. On unmanned craft search beacons with pulse xenon lamps are applied. The VNISI has developed and manufactured several types of external and signal lights for manned spacecraft [15, 16].

Searchlights for illumination of docking units should be mentioned separately. Searchlights are installed on all manned spacecraft models of the Soyuz type. They are used when manually coupling manned spacecraft with the space station. For this purpose the CMИ3–3 searchlight with KГM27–100 HIL type was developed. Its luminous efficacy of 33 lm/W was a record for HILs. However, because of a wide dispersion of on-board voltage and of a considerable wire voltage difference (up to 5 V) the lamps often operated at a voltage lower than the rated, which resulted in a noticeable deterioration of the searchlight lighting parameters.

To eliminate this disadvantage, in the late 1980th a new illumination unit CMИ-4 was developed (Fig. 11). In the unit searchlights, new KГM12–100 halogen incandescent lamps (HIL) developed in the RDILS were used. A pulse voltage stabilizer was assembled according to an original circuit. It was located near the lamps and had an efficiency of more than 92 %. Therefore, at any oscillations of the onboard voltage, the lamps were supplied with exactly 12 V. Dimensions of the lamp filament were 2×3 mm only, which allowed obtaining a radiation angle 4° and



Fig. 11. Set of CMИ-4 searchlights

axial luminous intensity more than 10000 cd with rather small dimensions of the reflectors. The CMИ-4 unit contained three searchlights: two with radiation angle 4° to illuminate the docking unit directly and one with radiation angle of 20° for general illumination and overlook of the station. When coupling, one of the «four-degree» searchlights operates, and another serves as a reserve and automatically switches if the first one fails. This provides a very high reliability of the searchlights. However, it should be noted that throughout their long history there were no failures of the main searchlight. Attempts to use MHL instead of HILs were not successful because of a very wide interval of surrounding temperatures (from – 150 to + 100 °C).

* * *

Obviously, light emitting diodes open up completely new opportunities for both inner illumination of manned spacecraft and in the light warning system and illumination of the docking units. Using LEDs can easily provide for a light- and colour-dynamic environment and meet all recommended illumination parameters with a lower energy consumption and with more suitable payloads and dimensions.

Meanwhile, «for reasons beyond our control», the space lighting engineering work in the VNISI was stopped a few years ago. According to unofficial figures, the work today is carried out in Zelenograd.

REFERENCES

1. Artyukhin Yu.P., Varfolomeyev L.P., Leonova T.S., Motylkov V.A., Okara O.I., Chernyshyov V.P., Shtal-

tovny N.A. Problems of inner illumination of manned space crafts // Svetotekhnika, 1980, #7, pp. 6–8.

2. Information sheets «Rocket and space facilities». GONTI-1, 1973–76.

3. Varfolomeyev L.P., Leonova T.S., Okara O.I., Chernyshyov V.P. Choice of optimum illumination modes for operator rooms of a limited volume // Svetotekhnika, 1981, #6, pp. 6–8.

4. Varfolomeyev L.P., Leonova T.S. On the choice of fluorescent lamps for operator rooms // Svetotekhnika, 1983, #5, pp. 9–11.

5. Varfolomeyev L.P., Leonova T.S. Illumination of small isolated rooms intended for active rest // Electrotechnical industry. Lighting Products series, 1981, Issue 3 (69), pp. 1–2.

6. Leonova T.S. Illumination of operator rooms in closed ecological volumes // Electrotechnical industry. Lighting Products series, 1981, Issue 4 (70), p.2

7. Leonova T.S. On assessment of light environment comfort in closed ecological volumes // The Electrotechnical industry. Lighting Products series, 1981, Issue 5 (71), p. 2.

8. Bolyinov V.A., Varfolomeyev L.P., Leonova T.S. A colour dynamics illumination installation // Electrotechnical industry. Lighting Products series, 1982, Issue 2 (74), p. 2.

9. Okara O.I. On dynamics of light environment of operator rooms // Svetotekhnika, 1978, #11, pp. 12–14.

10. Varfolomeyev L.P., Gusev V.G., Magiyev G.V. Illumination of the Mir manned space system // Svetotekhnika, 1995, #4–5, pp. 33–34.

11. GOST P 50804–95 «The astronaut life environment in manned space crafts. General medical and technological requirements».

12. Varfolomeyev L.P. A compensation of ultra-violet insufficiency of astronauts at the Mir station // Svetotekhnika, 1997, #5, pp. 29–30.

13. Specification of the systems for the International Space Station. Type 1. Contract # NAS15–1000 CDRL # M G 02.

14. NASA: light emitting diodes will help inhabitants of the ISS to fight against insomnia // Svetotekhnika, 2013, #1, pp. 17.

15. Baryshnikov V.G., Vodovatov B.M., Zhiltsov V.P., Konkov V.E., Magiyev G.V. Development of light-signal facilities for visual search from air // Svetotekhnika, 1977, #2, pp. 1–4.

16. Leonidov A.V. Determination of optimum energy parameters of light beacons as elements of the visual warning system // Electrotechnical industry. Lighting Products series, 1982, Issue 5 (77), pp. 1–2.



Leonid Varfolomeev,

Ph.D. Graduated from the Moscow Power Institute in 1959 as a Lighting engineer and light sources specialist. For many years he has been the head of a scientific laboratory of the VNISI by S.I. Vavilov. At present, he is an editorial board member of the Light and Engineering Journal

CURRENT STATE, TRENDS AND PROSPECTIVES OF THE DEVELOPMENT OF LIGHT EMITTING DIODE TECHNOLOGY

Sergei I. Lishik, Valery S. Posedko, Yuri V. Trofimov, and Vitaliy I. Tsvirko

*Centre of light emitting diode and optoelectronic technologies of the National Academy of Sciences
of Belarus State enterprise, Minsk*

*Test laboratory of the Centre of light emitting diode and optoelectronic technologies of the National
Academy of Sciences of Belarus State enterprise, Minsk*

*E-mails: sergey.lishik@gmail.com; nioledcenter@gmail.com; trofimo119@gmail.com;
vitalii.tsvirko@gmail.com*

ABSTRACT

The current state of research and development of LED hardware components, LED lamps of direct replacement, street and industrial luminaires with light emitting diodes, irradiating devices with light emitting diodes for hothouse crop production, etc. are considered. Some examples of prospective directions for LED engineering development, such as medical equipment, UV disinfection and mobile facilities are mentioned. Conclusions and forecasts are made on the further development of lighting and irradiating equipment with light emitting diodes.

Keywords: LED hardware components, energy efficiency, luminaires with light emitting diodes, LED lamps of direct replacement, lighting characteristics, hothouse crop production, prospective directions

Many articles, reviews and monographs are accumulating around the world on the subject of light emitting diodes. This has significantly complicated the objective of this article: to provide readers with new and useful information. As a result, the authors formed the article based primarily on their own research. In doing so, we have collected many materials, because our research into LEDs began in 1977 [1, 2].

Our analysis of the modern level of development of light emitting diode (LED) equipment is based on results of tests performed in the accredited Test laboratory of the Centre of light emitting diode and optoelectronic technologies of the National Academy of Sciences of Belarus (TL), which was established in 2010 and accredited in 2012 (accreditation certificate ISO 17025 # BY/11202.1.0.1714 of 8/13/2012). The TL is outfitted with modern test equipment and measuring instruments, experienced and trained personnel. Its purpose is the measurement of lighting and thermal characteristics of LEDs and of products with LEDs: luminaires, lamps, modules, displays, devices for back illumination, light-signal equipment, traffic lights and indicators.

The scope of work performed by the TL grows constantly. In 2015, about 300 luminaires and 100 lamps were tested, and for January and November of 2016, 280 luminaires and 80 lamps were tested. Many of these tests was carried out by request of the *Lumen&ExpertUnion* journal. The results of these tests are open access on the journal website under the TESTED heading [3]. They were used during the competition for the Euroasian lighting prize in 2015.

In 2016, the TL also performed measurements of thermal characteristics of LEDs and of lamps by request of the *Lumen&ExpertUnion* journal us-

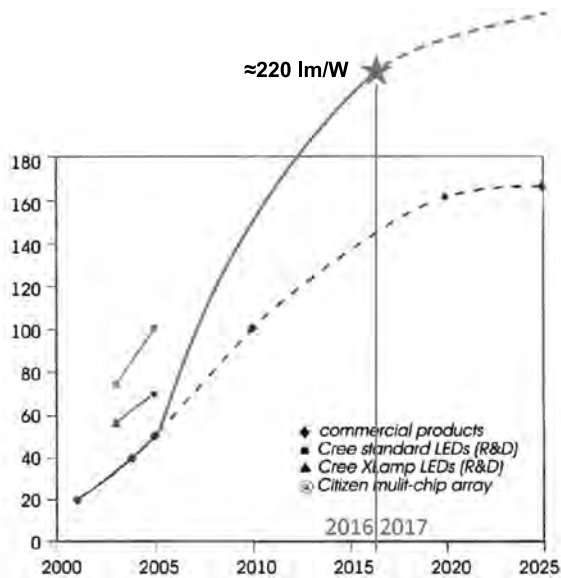


Fig. 1. Luminous efficacy of light emitting diodes η_v : forecast and reality

ing Flir A325 TV camera. The test results are presented on the same website.

In some cases customers ask to estimate and to analyse engineering and technological levels of development and production of LED products: therefore we have accumulated information both on separate structural units and on technological operations, as well as on products as a whole.

Let us consider some factors of hardware component development. It is known that LED light efficacy (η_v) mainly determines the η_v of the LED luminaire as a whole.

Fig. 1 shows a forecast of LED η_v growth dynamics by data [4] and a correspondent real picture [5, 6].

It should be also noted that the presented η_v data in articles and advertising materials until 2012 correspond to lowered operation currents (1/3 of the rated) and to a working temperature 25°C. At present, for complete consumer satisfaction, η_v of LEDs as a rule corresponds to normal operation currents and to a temperature of 85°C.

Looking at the dependencies in the presented graph, it is clear that the actual level of η_v for white LEDs is higher than that predicted for 2016 by 70 lm/W (47 %). Let us try to establish the reason for such an abrupt growth in η_v .

At the beginning of the 2000s the world market portion of hyper-luminous white LEDs was worth \$1.2 billion for total volume, manufacturing such LED products as billboards, signboards and LCD panels with back illumination, which

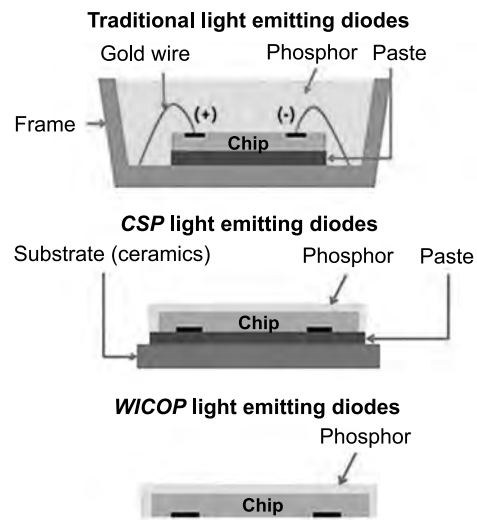


Fig. 2. Development of LED crystal manufacturing and encapsulation technology

amounted to 56 % of the total number of LEDs, and the demand for them grew constantly (their portion of the general illumination segment was only 4 %) [7, 8]. This situation became a catalyst for the fast development of white LEDs, which were the main hardware components for creating the devices for back illumination. Challenges around household appliance energy efficiency, image quality of LCD television panels and of computer monitors, were mainly addressed by improving the quality of LEDs. These processes are still ongoing.

At the same time, requirements to LED design and to technological effectiveness of their use when assembling LCD panels, have risen.

Fig. 2 shows the stages of *SMD-LEDs* development: traditional LEDs, *CSP*- and *WICOP*-/*WICOP2-LEDs* [9].

WICOP- and *WICOP2-LEDs* have the following advantages: minimisation of dimensions of the correspondent lighting devices (decrease of their material consumption and miniaturisation); improved heat removal (reduction of degradation speed, increased reliability). Their disadvantages are high requirements of the assembly equipment (vacuum manipulators, positioning accuracy), as well as the selection of printed circuit board materials and their flatness, giving them reflecting properties and selection of materials with the closest values of thermal expansion coefficients.

The need for such LED's to be airtight (moisture- and gas- impermeable) is not addressed very well. For this reason, they can be referred to LEDs

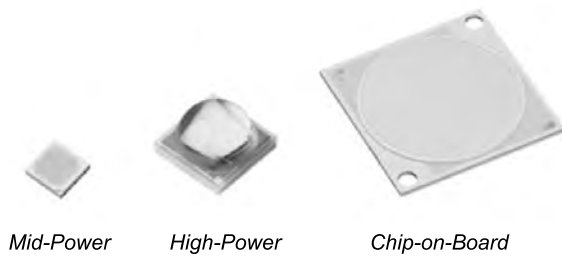


Fig. 3. Most widespread types of light emitting diodes

for «domestic use» (for example, inside LCD TV cases), though there have been attempts to use them in street luminaires.

Further, let us assess the economic and practical feasibility of LED type selection when creating street luminaires. Let us consider the most widespread LED types used for this task and presented in Fig. 3, as well as data concerning quantity of kilolumen of luminous flux, which can be bought for \$1 (klm/\$) at the following LED parameters: correlated colour temperature $T_{cc} = 5000$ K, general colour rendering index $R_a \geq 80$ and $\eta_v \geq 135$ lm/W at operation temperature equal to $+85$ °C.

According to our information, when using *Mid-Power* LEDs (with case 3030, of about 1 W power and of about \$0.06 cost¹) when purchasing batches up to 500,000 pieces). Hence one can buy 2.25 klm luminous flux for \$1. And when using *High-Power* LEDs (with 3535 housing, about 2.1W power and about \$0.45 cost) when purchasing them up to 100,000 pieces, or LED matrices of *Chip-on-Board (COB)* (of about 90 W power and about \$19 cost) when purchasing them up

¹ The prices are given approximately for LED leading brands available in the market of the Customs union, as of the IIIrd quarter 2016.

to 200 pieces, one can buy 0.6 klm luminous flux for \$1.

It is known that an LED module's thermal properties determine the degradation of light characteristics and the reliability of a LED luminaire as a whole. In this case, total thermal resistance levels of the LED array providing luminous flux of 12 klm (typical for most street luminaires with LEDs), for *Mid-Power* and *High-Power* LEDs and for LED matrices of *Chip-on-Board (COB)*, are equal to 0.087, 0.095 and 0.14 K/W respectively.

Analyzing these results, one can assume that low-power *Mid-Power* LEDs during the next several years will dominate by their price factor and reliability on the LED consumption market of hardware components for creation of LED street luminaires.

Further, we will consider the state of development and introduction of street and industrial luminaires, looking at measurement results of their specimens in the Test laboratory of the Centre of light emitting diode and optoelectronic technologies of the National Academy of Sciences of Belarus. During 2015, for the research tests, 21 LED street luminaires and 55 industrial LED luminaires were presented, and in 2016, 40 and 46 pieces respectively were selected. All of the studied specimens were the latest developments of known companies presented at the Customs union market.

In Fig. 4, total η_v and luminous flux values of the LED equipment specimens studied and their weighted average value are presented.

Best η_v results among LED street luminaires are close to 145 lm/W and average η_v values for 2015 and 2016 did not change, however average η_v values of industrial LED luminaires significantly increased: from 90 to 114 lm/W.

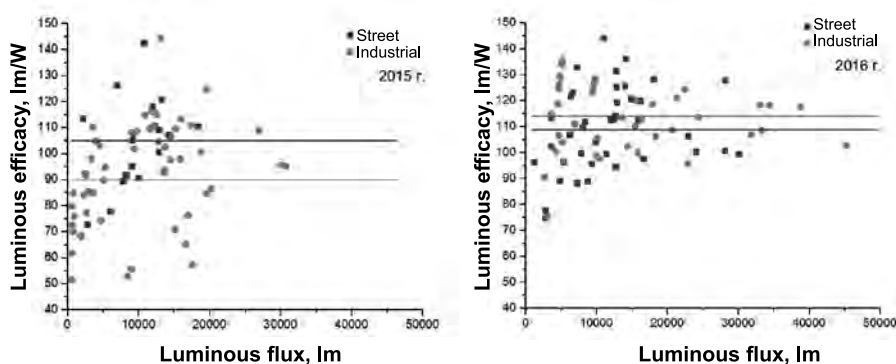


Fig. 4. Luminous efficacy and luminous flux values of the studied specimens of LED devices



Fig. 5. In national park Tsianfoshan, Tsinan, China

This situation can be explained as follows. In 2015, a minimum five-year warranty period was fixed for tendered procurement of LED equipment. In addition, the number of luminaires sharply increased, which did not correspond to the warranty period requirements (no less than three years), mainly because of failure of the control units («drivers») and because of insufficient air tightness of the light-optic parts. The problem is so acute that many companies are now close to bankruptcy.

It should be stated that at present the main problems of LED and LED module degradation are caused not only by electric and thermal phenomena but also by chemical and electrochemical processes connected with the interaction of LED equipment components with corrosive gases (HCl , CO_2 , SO_2 , etc.), moisture, salt vapours and solutions.

At the same time, a niche opens for industrial luminaires operated in rooms, which significantly reduces requirements for air tightness of these devices due to the absence of adverse environmental factors.

Based on the analysis of the obtained data, we assume that target indices for the development of LED street luminaires, for example of 100 W power, will reach the following values by 2020: average value of luminous efficacy will be 180 lm/W, mass will be no more than 5 kg, operational warranty period will be 8 years.

Besides, the luminaires should have the following features: smart functions (remote and automatic control), thermal regulation, self-cleaning surface of the case.

Moving on to LED lamps of direct replacement (LDR), in Tsianfoshan national park

in China, LED lamps are being sold, which lie in bulk unpacked and without labels. And they are transported and stored in bags (Fig. 5). According to the cardboard price tags, these are lamps of 3 to 12W power, and price of a 12-watt bulb is about \$0.30.

What does this mean and what are the risks? Under certain conditions, such products can appear in our shops decently packed and bearing any label. This is the underbelly of the market. Fortunately, in China, there also exist LED products of much better quality.

When consider the state of LED lamp development in more detail, it can be stated that there are two approaches used for the creation of these products:

1. A traditional composition method, when a bulb is close to the norm by its appearance and the main components are assembled in layers, which significantly facilitates automation of the assembly processes (Fig. 6) [10, 11];

2. Production as an analogue of a normal IL by replacement of tungsten wires with multielement linear radiators (filaments) [12].

To analyse the situation, we will use the rating information on ten of the best normal LED lamps [13, 14] and of controlled smart lamps presented on a consumer website [15]. Website information [13–15] is topical from both engineering and economic viewpoints. So website [13] contains

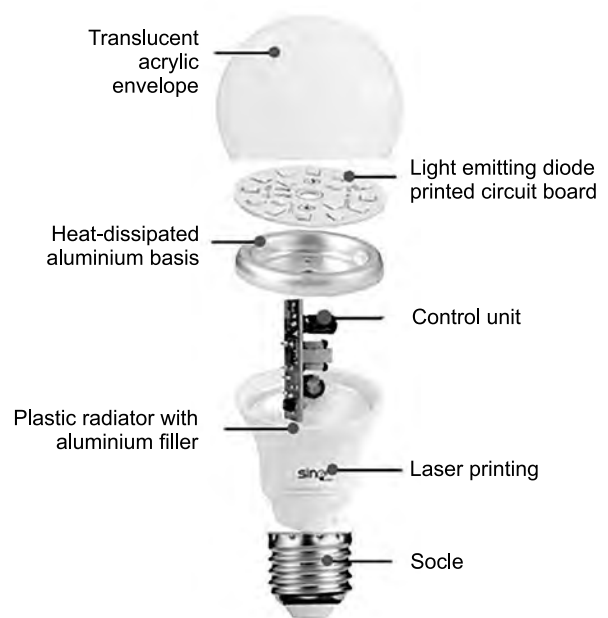


Fig. 6. Main components of direct replacement LED lamp





			
Incandescent lamp	Compact fluorescent lamp	Direct replacement lamp	Filament lamp
60 W	14 W	12,5 W	12,5 W
800 lm	800 lm	800 lm	800 lm
1 200 h	10 000 h	25 000 h	?

Fig. 7. Lamp light sources

more than 2000 detailed protocols of LED lamp research, and at website [15], price indices of the LED lamps sold via the *Amazon* retail network are given, which allows assessing the price-to-quality ratio of the presented light sources. Despite the high cost (\$159.9), products of *Philips Hue Connected Bulb* have some advantages in this category. They are supplied as sets of three controlled LED lamps, which additionally include a control panel.

We will consider approach 2 i.e. so-called «filament lamps» in more detail. We will reduce known lamp light sources to one luminous flux va-

lue of 800 lm (lamps with such luminous flux are mostcommonly used in everyday life). As can be seen from Fig. 7, the presented lamps significantly differ by power consumption and lifetime. LED lamps of different types are identical by energy efficiency but vary by lifetime. Wherein:

- A prototype of a filament lamp was first developed in 2008 by the Japanese company *Ushio Lighting*. In 2011, a lamp produced by *Panasonic* won the Good Design Gold Award [16]. These lamps were introduced into mass distribution from 2012–2013, and their market portion has gradual-

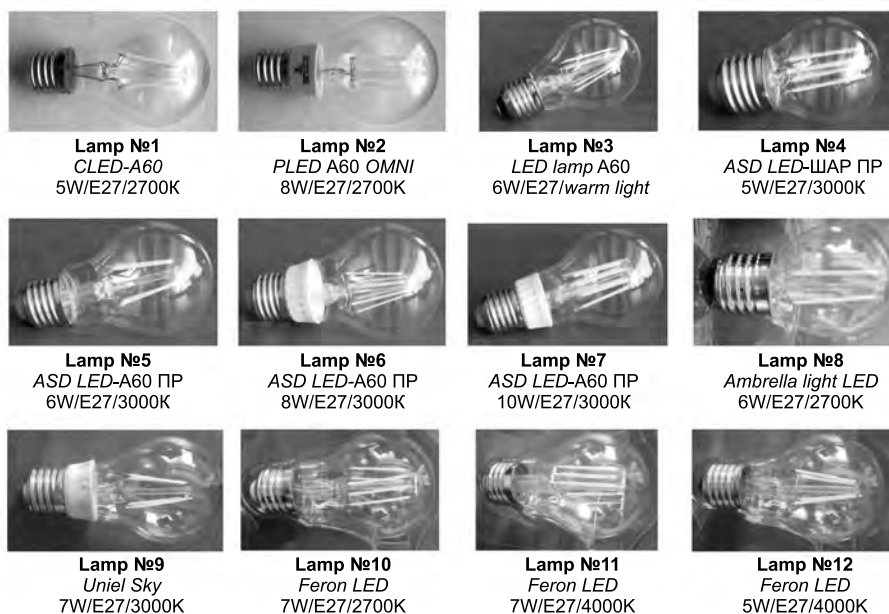


Fig. 8. The studied lamps specimens

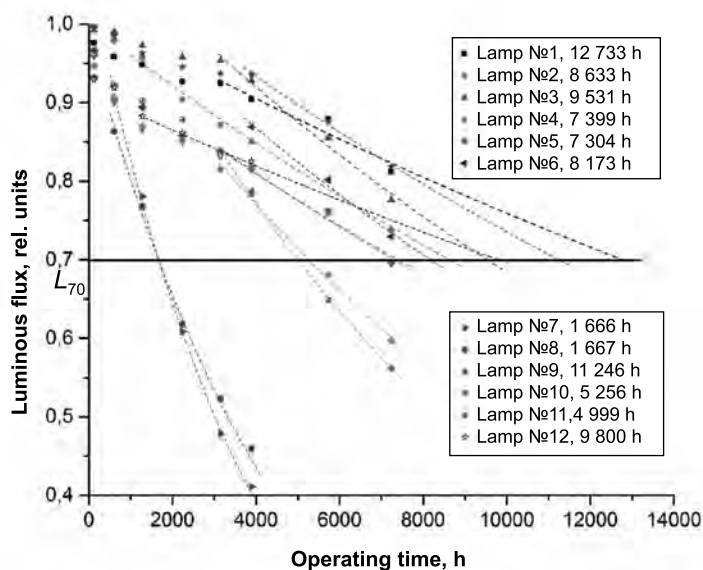


Fig. 9. Time dependence of luminous flux and lifetime of the tested lamp specimens

ly grown since then. Test results of filament lamps in comparison with the reference lamps are presented in the Table.

- The measured specimens of filament lamps were obtained through the retail network of the Customs Union, and their appearance is given in Fig. 8.

- The lighting characteristics of the filament lamps declared by producers, in most cases considerably differ from those obtained during measurement. In particular, the measured value of power consumption appeared on average to be 15 % lower than the declared value, and the measured value of luminous flux is 18 % lower than the declared value. These results unambiguously show that consumer rights are being infringed, and demand response measures from the state authorities.

Fig. 9 and the Table show the lamp test results concerning dynamics of luminous flux decrease. The lamp specimen lifetime was assessed using

the IES TM-21–11 technique «*Projecting Long Term Lumen Maintenance of LED Light Sources*» by decrease of luminous flux level to 70 % from the initial value. For the calculations, the data of the last 3000–4000 h of the service hours were used as they give the most reliable assessment of the lifetime according to this technique. The general service hours of most specimens amounted to 7239 h. For four lamp specimens, decrease of luminous flux exceeded 30 % during operating time of less than 6000 h. Lamps #7 and 8 were removed from tests after 4000 h as they degraded by luminous flux more than by 50 %. Lamp #12 failed after 5352 h work: therefore, the assessment of its lifetime was overestimated in our opinion, because for the calculations, operating time of an earlier period was used. Lifetime values of the tested lamp specimens are also given in Fig. 9, and so lifetime of the filament lamps changes from 1680 to 12700 h, and over the tested specimen sample, the average value amounts to about 7200 h.



Fig. 10. The Green Creative BR30 Cloud LED lamp

Table. Comparison of the declared and measured values of the studied lamp specimen main characteristics

#	Product type	Power			Luminous flux		
		Declared value, W	Measured value, W	Deviation, %	Declared value, lm	Measured value, lm	Deviation, %
1	<i>CLED-A60 5W/E27/2700K</i>	5	5.2	4	800	819	2
2	<i>PLED A60 OMNI 8W/E27/2700K</i>	8	7.3	-9	720	741	3
3	<i>LED Filament Lamp A60 6W/E27/warm light</i>	6	5.9	-1	-	642	-
4	<i>ASD LED-IIIAP IIP 5Bm/E27/3000K</i>	5	4.0	-20	450	350	-22
5	<i>ASD LED-A60 IIP 6Bm/E27/3000K</i>	6	4.5	-25	540	457	-15
6	<i>ASD LED-A60 IIP 8Bm/E27/3000K</i>	8	5.8	-27	720	582	-19
7	<i>ASD LED-A60 IIP 10Bm/E27/3000K</i>	10	7.4	-26	900	850	-6
8	<i>Ambrella light LED6W/E27/2700K</i>	6	2.6	-56	510	227	-56
9	<i>Uniel Sky 7W/E27/3000K</i>	7	5.0	-28	-	642	-
10	<i>Feron LED7W/E27/2700K</i>	7	5.9	-16	740	618	-16
11	<i>Feron LED7W/E27/4000K</i>	7	6.1	-13	760	695	-9
12	<i>Feron LED5W/E27/4000K</i>	5	3.8	-25	550	394	-28

The next characteristic studied is T_{cc} time change. The test results showed a significant change in this parameter for some specimens of filament lamps: to 100 K and more. Summarising the results, it should be noted that the use of LED filaments and placing them into a glass envelope without solving the problems of heat removal and vibration resistance gives rise to serious doubts as to the future of this direction. The same doubts arise when considering production technology of these lamps. The use of glass envelopes, installation of filaments in operation positions, pumping-out, subsequent filling with a special gas mixture and soldering of the envelope are poor objects to automation and demand considerable time unlike LED lamps of «traditional» structure.

The above listed problems can be solved by means of carrying out some scientific and technical research with additional time.

To conclude this section, it is worth making a few comments about some of the sample LED lamps. In 2016 the Chinese company *Wellmax*, which is growing intensively, presented LED lamps with a power consumption of 65 W and with a luminous flux of 4500 lm manufactured in a case

of heat-conducting plastic with local aluminium deposition [17]. It is supposed that this lamp is a substitute of 125-watt HPSLs. The lamp has a passive cooling system with channels of special configuration for effective heat removal due to air convection.

The second sample LED lamp, which differs by the novelty of its solution, is the *Green Creative BR30 Cloud LED* lamp [18], inside which the LED radiator card placed in the light emitting unit is separated from the case part, where the control device and socle are located. This significantly improves the thermal properties of the product as a whole (Fig. 10).

Further we will compare some new prospects and directions for the development of LED equipment. One such direction is the radiation of plants in greenhouses: «the sweet cherry on top of the financial pie» of the irradiation facilities market. The presented schematic image of the plant growing process (Fig. 11) allows drawing some conclusions and identifying problems. A plant is a complex multiple-factor system, and light is only one of many factors influencing the plant growth processes. Different plants at different stages of their

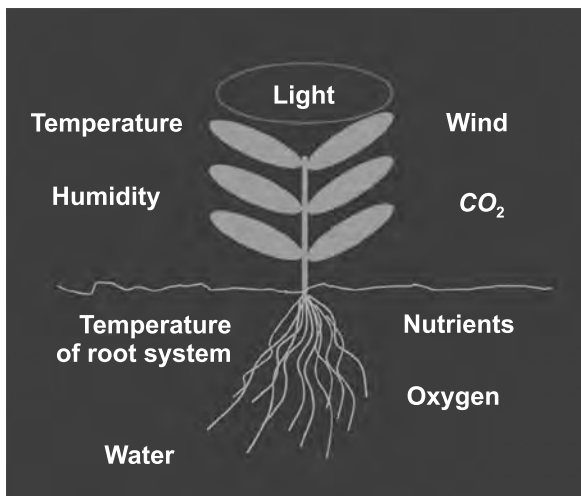


Fig. 11. A schematic image of plant growing process

growth cycle require different radiation intensities and intervals, as well as different growing procedures. The existing crop variety dependence adds ambiguity to the interpretation of the results. Experiments on the choice of LED illumination technological parameters are rather long and expensive. Confirmation of the results under different geographical conditions in greenhouses of different design is required. All components and units of LED irradiators should be resistant to high air humidity and temperature, as well as to all types of chemical treatment typical for greenhouse operation.

Lately, along with traditional hothouse systems, an interest in LED radiation (illumination) appears in industrial greenhouses [19], where multi-level storage racks (14–18 levels) are used.

These green cultures (salad, basil, parsley, etc.) are grown using hydroponic systems. This type of venture has launched into large-scale production, and information appears [20] that using these methods *Spread* company in Japan grows and supplies retailers (restaurants, pizzerias, etc.) with up to 30000 heads of salad a day.

There is also another direction, which appeared and develops vehemently beginning from creation of the installations sometimes called «food computers» or «kitchen gardens» for household use to provide a family with fresh produce.

For all the mentioned technologies (Fig.12), high levels of luminous efficacy and reliability are necessary, as well as a special radiation range.

A marketing method is rather widespread, when the developer and the producer release LED irradiators with a set of different radiation intervals and different luminous fluxes, thereby transferring responsibility for the results of the LED crop-growing irradiator use to the consumer. The Finnish company *Valoya* proposes an entire irradiator range of different power with different intervals (Fig. 13) [21] accompanying them with a general recommendation: «for strengthening generative development», «for strengthening vegetative growth», «for research purposes», etc. A similar approach is taken by *Illumitex*, a leading US company [22], except LED irradiators with a wide interval set, in addition proposes irradiators with a monochromatic radiation of 450, 525, 624, 660 and 730 nm wavelengths (i.e. they offer many



Fig. 12. Directions of light emitting diode hothouse radiation use:

a) Minsk vegetable factory (2015): hothouse radiation (Test laboratory of the Centre of light emitting diode and optoelectronic technologies of the National Academy of Sciences of Belarus); b) many-storey systems; c) a device for house use (Test laboratory of the Centre of light emitting diode and optoelectronic technologies of the National Academy of Sciences of Belarus)

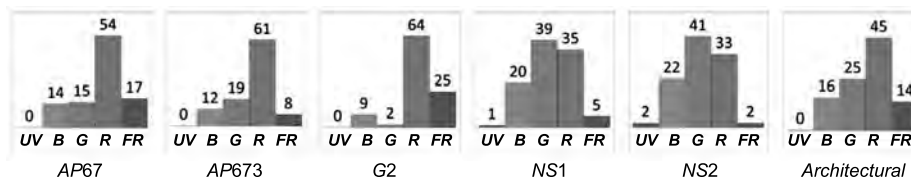


Fig. 13. Radiation spectra of LED irradiators (Valoya company)

«tools» but customers should know, how to use them).

Other prospective applications of LED technologies can be mentioned briefly. Lately, LED equipment has enjoyed a serious development boost due to the increase of LED light quality requirements, which allows expanding the LED luminaire sphere to such fields as the illumination of museums, film and photo studios, cosmetology consulting rooms, etc. After studying the consumer requirements, the Test laboratory of the Centre of light emitting diode and optoelectronic technologies of the National Academy of Sciences of Belarus has created an experimental luminaire specimen for photographic studios (Fig. 14), which confirms this. By lighting characteristics, this luminaire is an analogue of an FL standard luminaire but with an ability to adjust T_{cc} and luminous flux and with a low dimensional glare. Its main technical parameters are as follows: $Ra \geq 90$; T_{cc} is adjustable value within 2700–6500 K range with the pace 50 K; luminous flux is 4500 lm adjusted within 0–100 % interval; power consumption ≤ 60 W.

Similar requirements need to be met when creating LED equipment of medical purposes. After LED light quality needs were met (correct human tissue colour transmission), surgical and dental LED luminaires have been developed and applied widely. LED light sources for special medical tasks are used more widely (Fig. 15) [23]. According to our assessments, this direction will be intensively developed in the near future.

The questions rose when considering LED light quality and applying LED luminaires in medicine, have something in common with the issue of photobiological safety. Photobiological safety is sometimes considered an unsubstantiated problem, because there are obvious ways to solve it: to shift peak wave length λ_{max} of blue LED crystals applied in phosphor white LEDs from 455 nm to 405 nm or, for example to install light filters weakening the blue range. However, the latter reduces η_v of the white LEDs.

One more way to provide photobiological safety is the correct design of luminaires with LEDs, which takes into consideration requirements of the regulatory basis by dimensional luminance and glare. In this case, the presence of a strict metrological support for the production and control of access of these products to the market is very important.

The introduction of LED facilities into the UV disinfection field (Fig. 16) has begun. Two prototypes of UV disinfection devices are known. They consist of a reactor for radiation of flowing water and of a LED module with 150 mW radiation flux in spectral range of 250–300 nm ($\lambda_{max} = 275$ nm). The device effectively neutralises bacteria in the water including *E. coli*, *R. Terrigena* and *P. aeruginosa*, as well as MS2 phage and fr phage viruses with water consumption of 0.5–2.0 l/min. Use of UV diodes makes the device compact. Other information is not known.

A prototype of the device for UV disinfection and water purification is also known,



Fig. 14. A luminaire for photographic studios (Test laboratory of the Centre of light emitting diode and optoelectronic technologies of the National Academy of Sciences of Belarus)



Fig. 15. LED light sources for search and visualisation of veins

in which UV disinfection and a photocatalysis effect by means of titanium dioxide TiO_2 are used. A consortium headed by the Cork Technology Institute (Ireland) is actively developing this direction [24]. The process in essence consists of water flowing through a helicoid channel filled with tiny balls with TiO_2 coating. Under the influence of UV radiation, in the subsurface layer of this coating, polluting organic compounds are split into elementary hydrocarbons and minerals. It is expected that these prototypes will appear in real practice within the next 3–5 years.

As discussed above, display technologies at the beginning of the 21st century were the driving motive of the development of white LEDs in order to create LCD panels with effective back illumination. At present, another ambitious task has appeared: to create a mobile gadget (smartphone) with the function of video projection. The first specimens have been created and are already available (Fig. 17) [25].

The *Moto Z* mobile phone and *Moto Insta-Share* projector, have resolution 480 (854×480), contrast 1:400, luminous flux 50 lm, screen size up to 70 inches (178 cm) and duration of autonomous work to 1 h. According to some information, *Samsung S8* will be supplied with a built-in projector. Similar developments are carried out by *Huawei* Company as well. For a further development in this direction, LEDs with $\eta_v \geq 250$ lm/W and with $R_a \geq 90$ are needed. Besides, problems of cooling such LEDs, increase of rechargeable battery capacity and decrease of light losses in the image formation channel need to be addressed. These problems are likely to be solved in the short term (5–8 years), and each user will have a cinema in his/her pocket.

Lighting companies increasingly interact with *IT* companies and together address smart illumination to gain income of additional opportunities given by illumination. They want to make light an integral part of the “the Internet of things”, in which inanimate objects could interact with each other automatically and perform co-ordinated actions based on the transmitted data increasing efficiency of energy use and facilitating everyday life.

It is suggested that street illumination will also transition to smart illumination, and many companies invest considerable funds to upgrade street illumination by means of empowering it with additional functions [26, 27]. Addition of sensors, cameras and even loudspeakers make the illumination system more expensive but its expanded possibilities help various services to operate replacing multiple highly specialised sensor systems. Such combinations allow not only controlling illumination switch on and off but also at the same

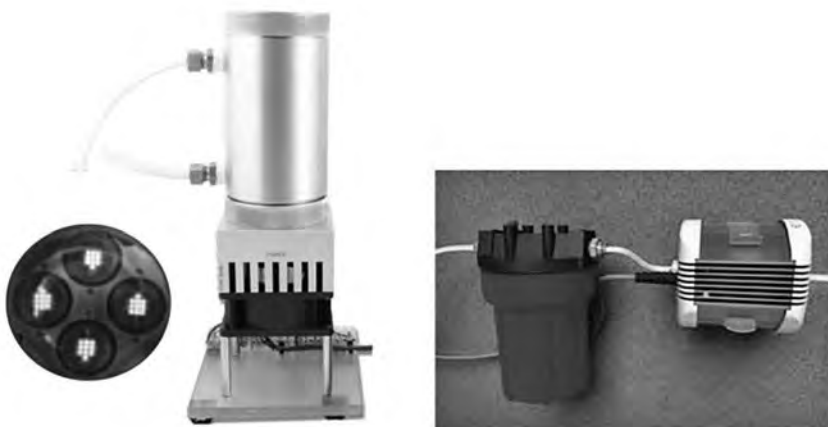


Fig. 16. Main units and appearance of devices with UV diodes for UV disinfection



Fig. 17. Mobile phone of the Moto Z series and projector of the Moto Insta-Share Projector series

time monitoring air quality, road traffic and parking load, notifying municipal services of snowfall and providing sound messages on emergency situations. The novelty of these functions is relative but they are seldom used in practice in their totality. Fig. 18 shows a schematic image of an LED street luminaire with a universal set of functions [28].

Lately a new «inner» function of luminaires appeared. This is so-called Li-Fi function, which has some advantages and disadvantages. Some examples of its possible use are given in [29]. The provided information allows drawing some conclusions.

LED illumination equipment will develop in many directions, and it is difficult right now to foresee the end results of improving its main characteristics. The possibilities of implementing highly reliable LED luminaires of low and middle power have already been demonstra-

ted in practice. Due to further increases in LED energy efficacy, which will lead to decreased heat loss and improved environmental resistance, highly reliable lighting devices of large and superlarge power with a high quality of light and adaptive functions will be implemented. These directions should be supported by the development of metrological assurances, test equipment and a sound regulatory basis for LED lighting equipment. With all this in mind, let us lighting engineers work towards a better LED future!

REFERENCES

1. Lishik S. I., Pautino A.A., Posedko V.S., Trofimov Yu. V., Tsvirko V.I., Problems of application of light emitting diodes in illumination and light-signal devices and methods of their solution // Svetotekhnika, 2008, #4, pp. 22–26.
2. Trofimov Yu.V. How to take place under the LED sun. Postulates of development of LED facilities // Modern lighting engineering, 2010, #1(02), pp.14–17.
3. URL: <http://www.lumen2b.ru/catalog-luminaries> (addressing date: 12/6/2016).
4. Whitaker T. LEDs in the mainstream: technical hurdles and standardization issues // LEDs Magazine Lighting, 2005, October, pp. 11–13.
5. Steele R.V. LCD display backlighting and illumination markets drive HB-LED demand // LEDs Magazine Review, 2006, April, pp. 5–6.
6. URL: <http://www.electronics-eetimes.com/news/5630-packaged-led-delivers-210–220lmw> (addressing date: 12/7/2016).



Fig. 18. Schematic image of a street LED luminaire

7. *Trofimov Yu. V.* Semiconductor light emitting diodes – new application spheres and trends of market development // *Electronic components*, 2003, #3, pp. 31–35.

8. *Trofimov Yu. V.* Semiconductor light emitting diodes – new application spheres and trends of market development. Part II // *Electronic components*, 2004, #11, pp. 1–6.

9. URL: http://www.seoulsemicon.com/WICOP/WICOP_en.asp (addressing date: 10/28/2016).

10. *Lishik S. I., Pautino A.A., Posedko V.S., Trofimov Yu. V., Tsvirko V.I.*, On LED lamps of direct replacement // *Svetotekhnika*, 2010, #1, pp. 48–54.

11. *Lishik S. I., Pautino A.A., Posedko V.S., Trofimov Yu. V., Tsvirko V.I.*, Structural and technology solutions of LED lamps of direct replacement // *Svetotekhnika*, 2010, #2, pp. 7–12.

12. *Trofimov Yu. V., Kaleda I.A., Taugenov A.S., Lishik S.I.* Evolution of LED lamps of direct replacement // *Science and innovations*, 2015, #10 (152), pp. 13–17.

13. URL: <http://www.olino.org/advice/us/retrofit/step> (addressing date: 12/5/2016).

14. URL: <http://www.pcmag.com/article2/0,2817,2483488,00.asp> (addressing date: 12/5/2016).

15. URL: <http://www.toptenreviews.com/home/smart-home/best-led-light-bulbs> (addressing date: 12/5/2016).

16. Panasonic LED Bulb Wins Gold Award at Good Design Award 2011 // URL: <http://news.panasonic.com/global/topics/2011/7682.html> (addressing date: 12/5/2016).

17. URL: <http://wellmaxgroup.com> (addressing date: 12/6/2016).

18. URL: <http://gc-lighting.com/products/cloud-br30-8w/> (addressing date: 12/7/2016).

19. *Wright M.* LED lighting advances in horticultural applications, boosts productivity // *Leds Magazine*. – 2014. – July. – P. 10–11.

20. URL: http://www.theguardian.com/environment/2016/feb/01/japanese-firm-to-open-words-first-robot-run-farm?CMP=share_btn_link (addressing date: 12/6/2016).

21. URL: <http://www.valoya.com> (addressing date: 12/6/2016).

22. URL: <http://www.illumitex.com> (addressing date: 12/6/2016).

23. URL: <http://www.accuvein.com> (addressing date: 12/6/2016).

24. URL: http://www.aqua-pulse.org/images/pdf/Aqua-pulse_Brochure.pdf (addressing date: 12/6/2016).

25. URL: <https://www.motorola.com/us/products/moto-mods/moto-insta-share-projector> (addressing date: 12/6/2016).

26. URL: <http://www.pennsmartlighting.com> (addressing date: 12/6/2016).

27. URL: <http://www.lightwell.eu> (addressing date: 12/6/2016).

28. URL: <http://www.lightinginsight.com/light-motion-lightwells-intelligent-lamppost> (addressing date: 12/6/2016).

29. URL: <http://luxreview.com/article/2016/06/lifi-innovators-on-track-to-complete-paris-metro-installation> (addressing date: 12/6/2016).



Sergei I. Lishik,
Ph.D. Graduated from the Physical department of the Belarus State University in 1999. Academic secretary of the “LEDs and Optoelectronic Technology Centre” of the National Academy of Sciences of Belarus



Valery S. Posedko,
Ph.D. Graduated from the Radio physics and electronics department of the Belarus State University in 1981. The research department manager of the “LEDs and Optoelectronic Technology Centre” of the National Academy of Sciences of Belarus



Yuri V. Trofimov,
Ph.D. Graduated from the Chemical Department of the Belarus State University in 1972. The Director of the “LEDs and Optoelectronic Technology Centre” of the National Academy of Sciences of Belarus



Vitaly I. Tsvirko,
an engineer. Graduated from the Radiophysics and electronics department of the Belarus State University in 2000. The chief of the Test laboratory of the CDB of the National Academy of Sciences of Belarus

APPLICATION OF LIGHT EMITTING DIODES FOR ILLUMINATION OF MOSCOW AND OPERATIONAL CHALLENGES

Alexander V. Sibrikov and Andrei I. Kirichyok

Svetoservis TM Open Company, Moscow
E-mail: info@svs-tm.ru

ABSTRACT

The problems inherent in a great number of lighting installations with light emitting diodes and ways of solving them are considered.

Keywords: luminaires with light emitting diodes, control system, architectural-art illumination, design and operation, start-up current limit switches

1. INTRODUCTION

Publications concerning the practical application of light emitting diodes (LED) as light sources for external illumination installations (utilitarian, architectural, landscape and decorative) appear regularly in specialist scientific and engineering journals, as well as publications intended for the lay reader. In the latter case, the questions of LED application tend to be of a commercial character, directed to promote products by specific manufacturers. Less attention, or none at all, is given to aspects of operational reliability of installations with light emitting diodes and their application problems. The experience of working with LED luminaires and their control systems is insufficiently described.

Back in 2013, the Svetotekhnika Journal published an article [1] in which the state and trends of Moscow's functional illumination and its development were considered. The necessity for interconnected application of external illumination all types and facilities, in order to create

harmonious light-and-colour city spaces was noted. It was specially designated in the Concept of a uniform light-and-colour environment for Moscow, which was confirmed by order № 1037-ПП of the 11th November, 2008 by the Moscow government. Even at that time, the authors noted "that there should be a certain line beyond which gains in energy efficiency should not be sought at the expense of illumination quality".

There is a need to explore in this journal the theme of LED lighting device selection and their operation in architectural and functional illumination. It is not proposed that rules of application of static and dynamic light emitting diode illumination installations should be sought, but instead that a platform for experience exchange can be developed, especially in terms of operational challenges and methods overcoming them.

2. Development of Moscow city illumination from 2011 till today

In 2011, two orders of the Moscow government № 98-ПП of 31.03.2011 were approved: "On the development of external illumination, architectural-art local illumination and festive light decoration of Moscow city for 2011" and № 451-ПП of 27.09.2011 "On confirmation of the State programme of Moscow city "Development of municipal-and-engineering infrastructure". These orders were the beginning of a new stage in the development of the city's light and colour medium.

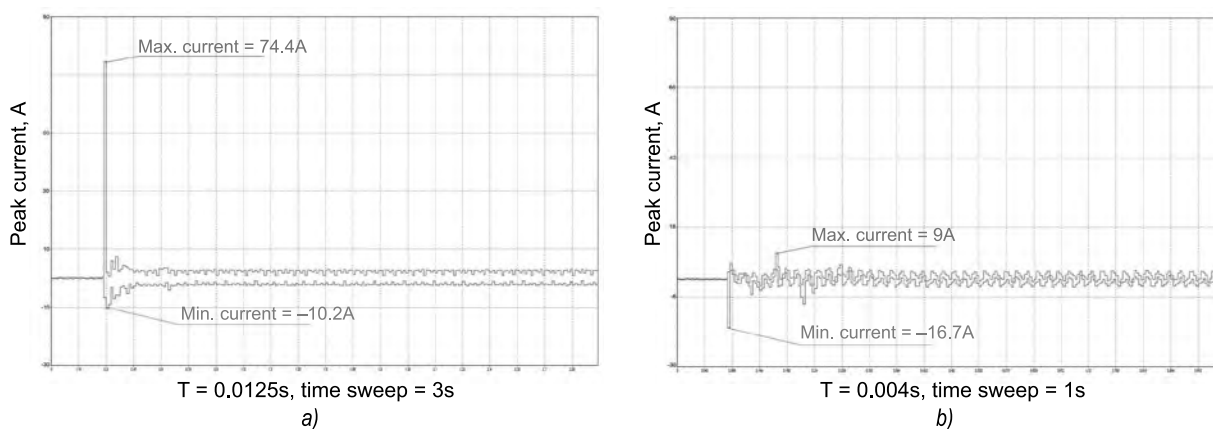


Fig. 1. A diagram of architectural illumination current installation of a building located in Sadovaya-Triumfalnaya street: a) without SCL, b) after SCL installation

Implementation of these programmes was carried out stage by stage with financial funds increasing. Object commissioning was carried out from the city centre to the periphery.

During 2011–2015, the following was achieved:

- Architectural illumination installations were mounted on more than 900 buildings and constructions;
- 74,000 lighting devices with LEDs were installed;
- More than 500,000 new functional illumination luminaires were installed or replaced (including 20,000 with LEDs);
- Decorative illumination installations were mounted in 80 streets, boulevards and squares.

2. EXPERIENCE

Within a relatively short period the number of operational lighting devices of domestic and foreign production in Moscow increased rapidly. And this trend will continue.

In order to understand, how to work with LED luminaires in such a situation and to determine a systematic approach to design, equipment selection, construction and subsequent operation, as well as saving budgetary funds, it is important to analyze the existing operational experience and to determine the practical questions at the start, which will require attention at later stages.

There are many companies in today's market, which provide design, installation, adjustment and operation services for lighting installations using illumination equipment with LEDs. In external, and especially in architectural illumi-

nation, most problems appeared at the early stages of LED luminaires use, are already solved. But questions of a management and technological nature remain, which need addressing. This is especially important due to the rapid growth in the number of LED light sources, and with the sudden expansion of their product range. Solving these issues will ensure progressing to a higher level of production and application of the lighting equipment.

3. DISADVANTAGES OF THE PROJECTS

Most projects do not take into account the processes in electric installations working with LED luminaires, especially with high concentrations of LEDs, as for example in architectural illumination. Automatic switches of many lighting switchboard objects installed both on input, and on group lines, disconnect the circuit at the start-up moment. As an example, one can mention lighting installations in the New Arbat street, Tverskaya street, Sadovoye Koltso (Garden ring), which were installed in the period from 2011 to 2015.

During operation, the objects often were completely or partly disconnected, which caused a great deal of discontent. Therefore, switching mode change was required at most objects of architectural illumination installations, for example of New Arbat street buildings. A similar situation occurred in Sadovoye Koltso and Tverskaya streets. According to the dispatch service, for the 2014–2015 period of time, 610 cases of protection device response took place. And according

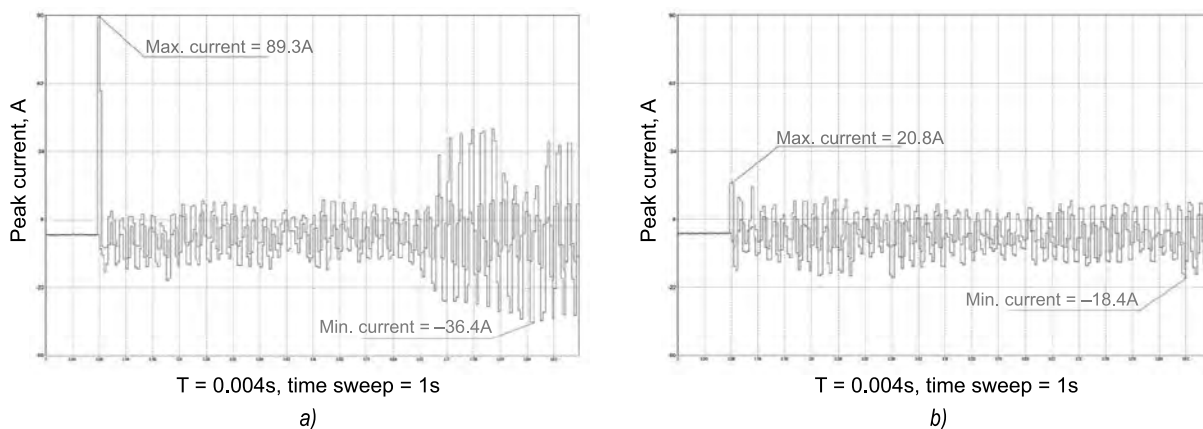


Fig. 2. A diagram of architectural illumination current installation of a building located in Tverskaya street: a) without SCL, b) after SCL installation

to the design specifications, preset values of automatic switches were selected with due regard for start-up currents according to the Electrical installation code 6.1.33 requirements.

With the aid of the operating company's laboratory, measurements of start-up currents of some installations in operation were made. The measurement results are given in Figs. 1 and 2. The measurements were performed for each phase separately. Figs. 1 and 2 show "A" phase lighting installation current diagrams. The installations are located in Sadovaya-Triumfalnaya and Tverskaya streets. As it can be seen from Fig. 1a, at 5A average value of working current, the start-up current is equal to **74.4 A**. In other words, the start-up current exceeds the rated by a factor of **15**.

A similar situation is displayed in Fig. 2.a, where start-up current exceeds the rated by a factor of **6**.

According to GOST P 50345–2010, automatic switches are divided into the following types (classes) by instant disconnection current:

- B type: more than 3·In to 5·In inclusive,
- C type: more than 5·In to 10·In inclusive,
- D type: more than 10·In to 20·In inclusive.

Type C is used most often. If in the second example, there is nothing that can be done, in the first example, a choice is available: to replace the circuit breakers with D class devices, or to install protection devices of a greater specific power. In both cases, it is needed to conduct inspection and current measurement, and acquisition of new protection devices is required. And this means an increase in operating costs.

The cost increase can be estimated by with simple calculations. Each architectural illumination installation usually includes from 4 to 8 three-phase outgoing lines, and general number of the lighting installations with LEDs is about 900 pieces.

Each one of them needs to be measured, and a decision should be made concerning protection device specific power or current class change. This means that from 10,800 to 21,600 measurements need to be made, and a similar number of decisions should be made about the selection and replacement of the protection devices.

One of the simplest methods to deal with start-up currents without considerable financial costs is, for example, the installation of start-up current limit switches (SCL). Start-up current diagrams after SCL installation are presented in Figs. 1b, and 2b. An appearance of OPT3–16 limiter is given in Fig. 3.

Production of the OPT3–16 limit switches is arranged at MOSZ TM Open Company (Moscow experimental telemechanics factory). These limit switches can be manufactured both in three- and in single-phase versions. The rated current can be equal to 16 A, or to 32 A for one phase.

Unfortunately, this and many other aspects are rarely taken into consideration when developing design specifications because of a low level of qualification amongst designers. Such design defects are being corrected while in service. This work is carried out by emergency teams in the process of eliminating disconnections of lighting installations.



Fig. 3. Appearance of the OPT3-16 limit switch

To eliminate these defects, typical solutions should be developed and regular seminars arranged to teach specialists from the design companies, customer representatives and experts.

4. PROBLEMS AND ERRORS IN SELECTING LUMINAIRES

1. Product range of the LED luminaires is extensive and varied. Luminaires of domestic and of imported production are available. Each manufacturer presents equipment characteristics in their own way. The main characteristics, such as power, power line voltage, luminous intensity curves etc., are provided by all manufacturers. But characteristics like power factor, consumed current (especially at the moment of switching) are rarely specified by anybody, and these characteristics are not taken into consideration in the design process. All design errors and defects are being corrected while already in service. But manufacturers and light equipment dealers have little interest in this issue.

2. Modern luminaires are not dismountable and frequently cannot be repaired under operating conditions. Therefore, in case of their total failure and after warranty period termination, it becomes necessary to buy new luminaires. Due to the extensive product range of the installed luminaires, lighting installation can be made simpler by having a reserve of many different luminaires and of their accessories.

It is easy to compute that if according to the effective regulations and specifications, one should have a 10 % reserve of the all operated equipment,

then with the availability of 74000 luminaires on 900 buildings and constructions, the reserve must have **7400** lighting devices of different types.

3. Modern luminaires, especially working in dynamic illumination are complex devices requiring a highly qualified approach and individual programming. There is a need to train a considerable number of specialists to do this. And as the product line is constantly upgraded, this process will be constant and inevitable. Unfortunately, the operating companies cannot affect the process of luminaire selection during designs. But they can provide an objective analysis based on operational experience. This type of analysis should be performed for each lighting device type, and the developers should be made aware of the results.

5. ERRORS DUE TO CONTROL SYSTEM OPERATION

1. Design companies often do not fully meet the specifications requirements regarding climate version of control system components. During the last five years, there have been many such systems in the market. Operation of the commissioned architectural illumination installations shows that when selecting a control system, designers and frequently builders, use cheap, single-use solutions. For example, equipment, which uses hardware components of control units or modules, not intended to be operated under -40°C or above $+70^{\circ}\text{C}$ conditions. It leads to the device as a whole being unable to operate within the set temperature interval. Specifically for products of foreign manufacturers, especially those from China, even the recognised brands do not provide working capacity warranty within the declared interval. Equipment is bought, which besides appears to be «grey», uses non-standard elements.

2. There are cases when equipment manufacturers try to adapt modules developed previously and not intended for illumination system work, to illumination tasks. One example is devices intended for automated information and measuring systems of commercial energy metering systems, where work algorithms are used, which are absolutely not suited for illumination.

3. One more problem is control equipment, which operates using utilitarian protocols of data exchange between actuators and con-

trol points. To avoid single supplier dependence, a comprehensive system of Moscow architectural-art illumination control was developed in 2013 and is successfully operated now by a contract organisation. The system is constructed using data transmission open protocols, a confirmed signal list and typical solutions approved by expert evaluations. Building companies often ignore the requirement of joining with this system specified in the technical requirement, which leads to loss of controllability and information by the operating company and by the customer, and further to cost increase. Sooner or later such control equipment needs to be replaced, even if its life time has not expired, and this causes additional expenditure.

6. PROPOSALS

Based on the problems described and errors in luminaire and control system selection, and in order to avoid problems and additional expenditure during future project, the authors propose the following:

- The operating companies together with the customers should analyse the control system work over the last five years.

- Equipment manufacturers and construction companies should be advised to test lighting equipment together with the control system in an accredited reputable laboratory, for example in VNISI Open Company.

- Based on test reports, the customer should form a restricted list of permitted illumination control systems and pass it on to the design companies together with other specifications.

7. CONCLUSION

The success of implementing utilitarian and architectural illumination projects requires not only sufficient allocated funds but also the close interaction of the design, assembly and operating companies during the implementation process, as well as of the manufacturers and suppliers of the lighting equipment and control systems.

REFERENCES

1. Bukatov A.S., Kirichok A.I. Functional Energy-Effective Illumination of External Spaces of the Capital: The State And Development Trends // Svetotekhnika, 2012, # 6, pp. 38–41.



Alexander V. Sibrikov

is the director of Svetoservis TM Open Company. He was graduated from the Leningrad Higher Military Engineering School of Communications of Lensovyet with a specialization in Automated control systems in 1989



Andrei I. Kirichyok

is the development deputy director of Svetoservis TM Open Company, graduated from the Leningrad Higher Military Engineering School of Communications of Lensovyet with a specialization in Automated control systems in 1989

THERMAL DESIGN OF AN LED SYSTEM: A SPECIAL LANTERN FOR TURKISH HISTORICAL MOSQUES

Lale Erdem Atilgan¹ and Mustafa BerkerYurtseven²

¹ *Istanbul Technical University, Electrical Engineering Department, Istanbul, Turkey*

² *Istanbul Technical University, Energy Institute, Istanbul, Turkey*

E-mail: erdeml@itu.edu.tr; byurtseven@itu.edu.tr

ABSTRACT

In this study, LEDs are used to design a modern lantern for the interior lighting of Turkish historical mosques, aiming at achieving substantial energy savings and preserving the historical texture of the mosque at the same time. One of the most important methodologies in designing a lighting system with LEDs is the thermal design aspect. For the application of the system, the thermal design process of the modern mosque lantern is elaborated in detail; photometric measurements of selected LEDs are made, thermal simulations are carried out, the design approach is ameliorated according to the results of the simulations, a prototype is produced and verification measurements are performed. The resulting system provides a satisfactory thermal performance which translates into a long lifetime and sustainability. Thus, the study forms an important example of how an ancient system can be turned into an LED lighting system to be used in the lighting of a historical place of worship.

Keywords: light emitting diodes (LEDs); thermal design; lighting

1. INTRODUCTION

Mosques are religious buildings Muslims use for worship. The Turkish Republic has inherited an enormous cultural heritage from the Turkish-Islamic civilizations that were established on the same lands and one of the touch-

stones of this heritage is the historical mosque. According to the IES Lighting Handbook, electric lighting approximately corresponds to 28 % of the electricity used in places of worship [1]. The statistics published by the Turkish Directorate of Religious Affairs showed that there were 86.101 mosques in Turkey in 2014, the number rising 1.1 % every year, pointing to a number of 88.000 mosques at the end of 2016 [2]. According to another survey by the Directorate made in 2004, the average monthly electricity bill for a mosque is 43 Turkish Liras, corresponding to roughly 390 kWh of energy consumption per month [3, 4]. For 88.000 mosques, this number adds up to a monthly average consumption of 34.3 GWh, which is higher than the monthly energy production of Hirfanlı, an important Hydroelectric Power Plant founded on Kızılırmak River, Turkey [5].

Energy consumption is not the only problem with the current lighting systems in Turkish historical mosques. Incandescent lamps (ILs), which constitute the majority of the lighting solution in historical mosques, create major maintenance problems due to their short lifetimes. As a candidate for European Union membership, Turkey is directly affected by the phase-out of ILs in the EU and this means that ILs will not be available in the market in the following years. An investigation of historical mosques show that most failed lamps have either been left inside the lanterns or the lamps have been turned off to maintain energy savings. Some mosques

have exchanged the failed ILs with compact fluorescent lamps (CFLs), however as most CFLs are aesthetically not compatible with the lanterns, due to the fact that the glass lanterns are too small for the CFLs to fit inside, this utilization destroys the aesthetic view of the lighting system. In addition to this, as the purchasers of these lamps lack the necessary technical knowledge, the chosen lamps end up not meeting the warm colour temperature values of the ILs. These problems result in lower and non-uniform illuminance levels and in the same time aesthetical failures. While some highly touristic mosques have adopted LED (light emitting diode) retrofits instead of ILs, the number of these mosques are unsatisfactory, mostly due to the high initial purchase price of LEDs. In addition, similar to the problem with CFLs, as the lower priced LED retrofit lamps in the Turkish market are usually with high colour temperature values, the light colour of the preferred low priced / low quality lamps do not comply with the ambience of the mosques.

In this study, LEDs are used to design a modern mosque lantern to overcome the problems of the interior lighting of Turkish historical mosques. However, with high power LEDs, the majority of the input power is turned into heat, which should continuously be removed from the LED. The operating temperature of an LED is the most important indicator of LED reliability and durability. Continuous operation of LEDs at high temperatures accelerates the deterioration of luminous flux and shortens the lifetime [6]. In addition to these, the luminous efficacy of LED chips is reduced with the additions of thermal, optical and driver losses. Considering these inputs, the thermal design of LED lighting systems is ex-

tremely important. For the application of the proposed modern mosque lantern, the thermal design process of the system is elaborated in detail, forming an example of how an ancient system can be turned into an energy efficient LED lighting system through careful design, sensitive measurements and thorough simulations.

2. INTERIOR LIGHTING OF TURKISH HISTORICAL MOSQUES

The lighting system inside a mosque enables religious acts, creates the visual comfort for worshippers and emphasizes the architectural property. For artificial lighting, light sources fixed on chandeliers or circular concentric iron elements suspended from the ceiling are utilized [7]. The general approach is to use 60 or 40 W, 2700 K incandescent lamps placed inside glass lanterns. In the ancient times, these lanterns were filled with olive oil and lit using a wick, sending their light directly to the dome of the mosques. Today, however, due to electric cabling and the form of the lanterns, most of the light is sent to the mosque floor, rather than the dome as the lamp socket blocks an important amount of light going to the dome. This poses an important problem; the dome, which is designed to serve as a diffuser and reflector, does not receive enough light. Fig.1 (a) and (b) show the lanterns used in the interior lighting of the world renowned Architect Sinan's Semsî Ahmed Pasha Mosque and the previous lighting system, of the famous Hagia Sophia serving as a church, a mosque and a museum throughout its history, which was replaced by classic LED retrofits in the recent years.



Fig. 1. Lanterns used in the interior lighting of (a) Semsî Ahmed Pasha Mosque, (b) Hagia Sophia Museum

Table 1. Properties of the chosen LEDs

Properties	
Luminous Flux	93.9 lm
Maximum Drive Current	1000 mA
Thermal Resistance	6° C/W
Maximum Junction Temperature	150°
Viewing Angle	120°
Colour Temperature	2600–3700 K
Colour Rendering Index	80

3. PHOTOMETRIC APPROACH AND THE CHOICE OF LEDS

The photometric approach in designing the new LED lantern is to incorporate all positive characteristics of the current lantern and the historical system. The historical system sends most of the light to the dome of the mosque while the current system sends most of the light to the mosque floor. The novel design aims at sending light to all directions.

As the designed system will be used in historical places of worship and may also penetrate into all historical buildings using lanterns as light sources, colour temperature, colour rendering index and the spectral distribution of the LEDs are very important. Turkish historical mosques are embellished with antique carpets, ornamental works, painted tiles and many other delicate items, the colours of which should be meticulously showcased and protected. The interior lighting of a mosque is identified with warm colours. Thus the chosen LEDs should have high colour rendering values and should refrain from including infra-red and ultraviolet components. Table 1 gives details of the LEDs chosen for the study [8].

The catalogue values of the chosen LEDs are given for a 350 mA of constant drive current, at a junction temperature of 25 °C. However, in practice, it is not possible to keep the junction temperature at 25 °C. For luminous flux values at actual operating temperatures, it is necessary to consult the lifetime values obtained according to IES LM 80–08 (Illuminating Engineering Society Approved Method for Measuring Lumen Maintenance of LED Light Sources) as well as IES TM-21–11 (Lumen Depreciation Lifetime Estimation Method for LED Light Sources) [9, 10]. The values obtained by these two methods can be seen in Table 2 for a drive current of 350 mA, for the selected temperatures of 85 and 105 °C for these specific LEDs [11].

Here T_C is case temperature, T_A is ambient temperature and I is drive current.

Comparing the predicted lifetime values for temperatures of 85 °C and 105 °C, it is clearly seen that in a design with these specific LEDs, it would be highly preferable to keep the case temperature below or equal to 85 °C to provide a valuable useful lifetime with 80 % lumen maintenance of over 60,500 hours. A rise of 20 °C in case temperature results in losing approximately half the predicted

Table 2. IES LM80–2008 test results for the chosen LEDs

T_C , °C	T_A , °C	I , mA	Average lumen maintenance at 6000 hours, %	Reported TM-21 Lifetimes, h
85	85	350	99.8	L90(10k)=32,800 L80(10k)>60,500 L70(10k)>60,500
105	105	350	95.7	L90(6k)=15,600 L80(6k)=34,100 L70(6k)>36,300

Table 3. Change of LED Properties with Temperature

T, °C	Luminous Flux, lm				Efficacy, lm/W			
	LED1	LED2	LED3	Average	LED1	LED2	LED3	Average
25	92.24	93.81	92.75	92.93	88.79	88.22	88.54	88.52
35	89.61	91.82	89.90	90.44	87.23	87.33	86.93	87.16
45	87.12	89.80	87.38	88.10	85.66	86.32	85.46	85.81
55	84.70	87.59	84.96	85.75	84.04	85.04	83.96	84.34
65	82.27	85.44	82.61	83.44	82.31	83.75	82.38	82.81
75	79.95	83.32	80.34	81.20	80.61	82.39	80.81	81.27
85	77.73	81.12	78.04	78.96	78.94	80.96	79.11	79.67
T, °C	Luminous Efficiency, %				Power, W			
	LED1	LED2	LED3	Average	LED1	LED2	LED3	Average
25	28.25	28.33	28.55	28.38	1.04	1.06	1.05	1.05
35	27.85	28.22	28.18	28.09	1.03	1.05	1.03	1.04
45	27.44	28.00	27.84	27.76	1.02	1.04	1.02	1.03
55	27.05	27.67	27.52	27.41	1.01	1.03	1.01	1.02
65	26.62	27.39	27.04	27.02	1.00	1.02	1.00	1.01
75	26.19	27.04	26.64	26.62	0.99	1.01	0.99	1.00
85	25.71	26.66	26.08	26.15	0.98	1.00	0.99	0.99
T, °C	Correlated Colour Temperature, K				Colour Rendering Index			
	LED1	LED2	LED3	Average	LED1	LED2	LED3	Average
25	3003	3039	3036	3026	81.96	83.03	83.35	82.78
35	2999	3033	3031	3021	82.04	83.17	83.40	82.87
45	2995	3031	3029	3018	82.22	83.30	83.53	83.02
55	2993	3029	3025	3016	82.33	83.37	83.66	83.12
65	2991	3026	3025	3014	82.49	83.49	83.77	83.25
75	2992	3027	3027	3015	82.67	83.66	84.00	83.44
85	2992	3031	3031	3018	82.83	83.83	84.15	83.60

lifetime for this specific LED. Therefore, in the thermal design of the mosque lantern the initial target for the maximum case temperature has been chosen as 85 °C.

4. MEASUREMENTS

The influence of temperature on the chosen LEDs' luminous flux, efficacy, luminous efficiency, voltage, power, correlated colour temperature, colour rendering index and spectral distribution have been measured using a temperature

controlled Ulbricht sphere of 1 m diameter at the Energy Efficiency and Lighting Technique Laboratory of Istanbul Technical University's Energy Institute. 3 samples of LEDs, separately mounted on round metal core printed circuit boards (MCPCB) have been positioned on a thermoelectric plate. While the LED was driven at a constant current of 350 mA, the temperature at the lower face of the MCPCB has been raised from 25 °C to 85 °C at intervals of 10 degrees and the characteristic values have been measured using a spectroradiometer in the 2 π configuration of the Ul-

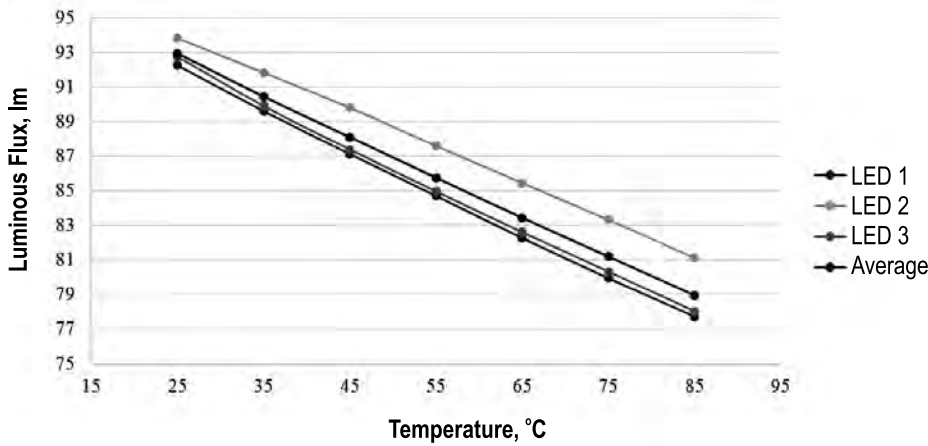


Fig. 2. Luminous Flux vs. Temperature

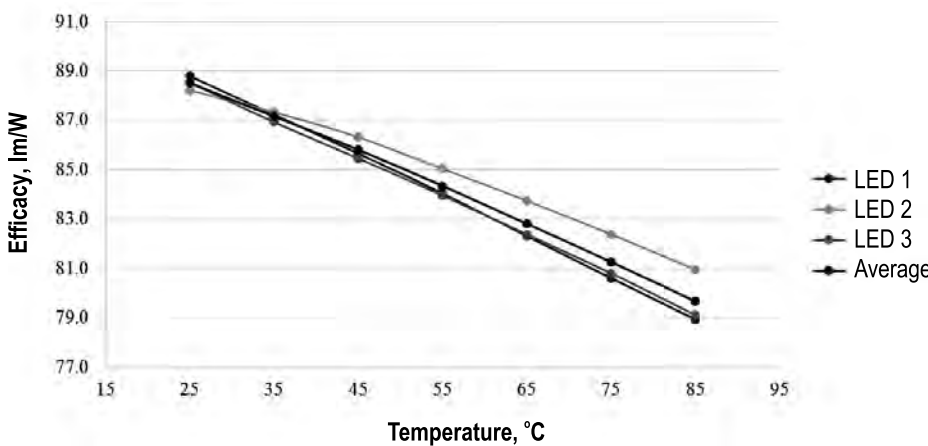


Fig. 3. Efficacy vs. Temperature

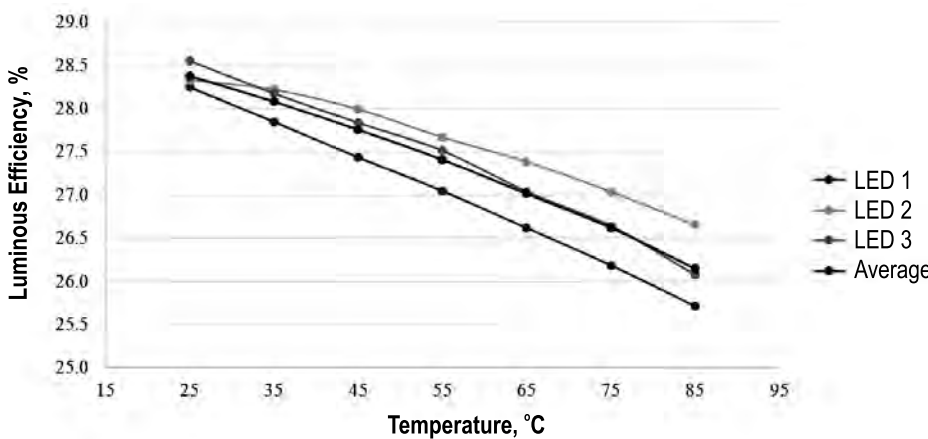


Fig. 4. Luminous Efficiency vs. Temperature

bright sphere. The obtained values can be seen in Table 3.

The measurement results show that with the increase of temperature, luminous flux, efficacy, luminous efficiency and power values of the LEDs decrease, as expected. From 25 °C to 85 °C, there’s an average of 15 % luminous flux drop. The colour temperature of the LEDs stays more or less constant and the colour rendering index increases with temperature, a satisfactory out-

come for the lighting of a historical place of worship. The measurement results have been plotted in Figs. 2–7.

As the changes in luminous flux and efficacy are fundamental to this study, to efficiently see the effect of temperature on these two important properties, the following formulas were obtained through line fitting, describing the relationship between luminous flux and temperature (1) and

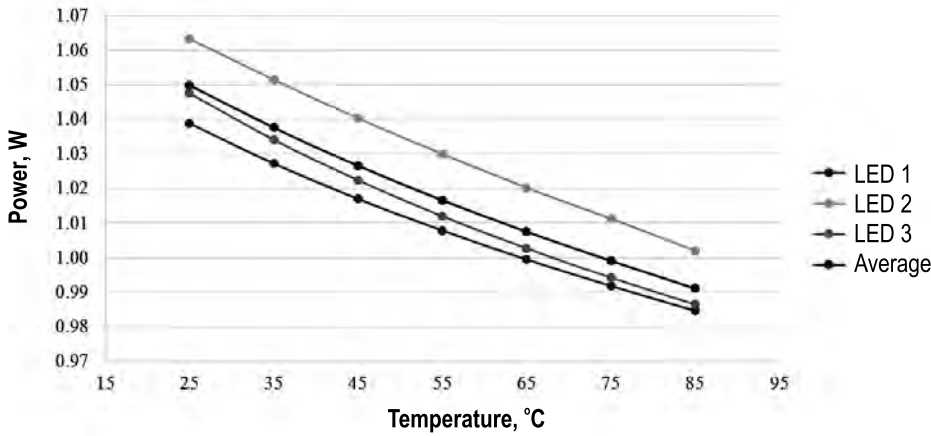


Fig. 5. Power vs. Temperature

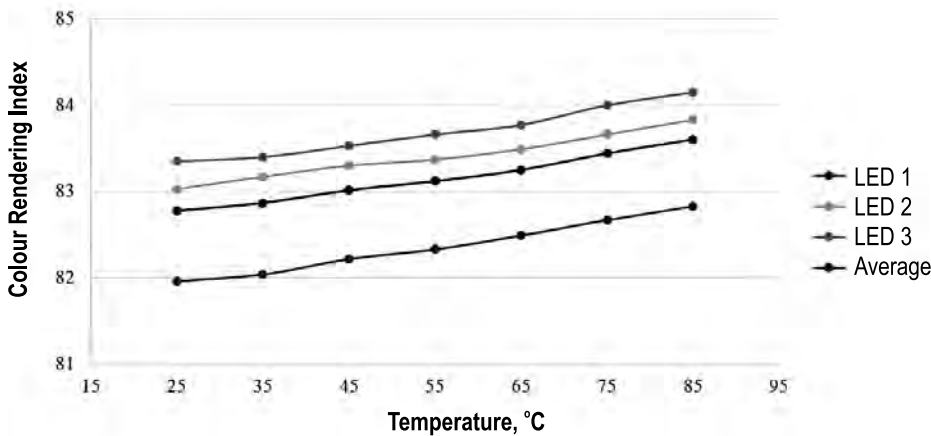


Fig. 6. Colour Rendering Index vs. Temperature

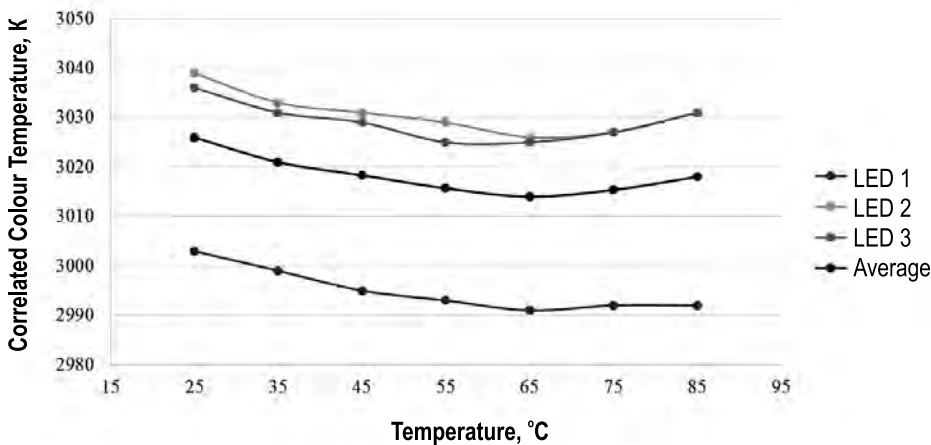


Fig. 7. Correlated Colour Temperature vs. Temperature

efficacy and temperature (2) for these specific LEDs in the measured configuration.

$$\phi_v = -0.2323 \cdot T + 98.61. \quad (1)$$

$$\eta_v = -0.1476 \cdot T + 92.34. \quad (2)$$

The obtained luminous efficiency values will be used to determine the thermal power of the LEDs for the thermal simulations and the equa-

tions obtained through line fitting will be used to determine the luminous flux and the efficacy values of the end product.

5. HEAT SINK DESIGN

The main approach in the design phase of the heat sink has been to create the most suitable form that is capable of providing the necessary cooling while in the same time can be fitted into the glass

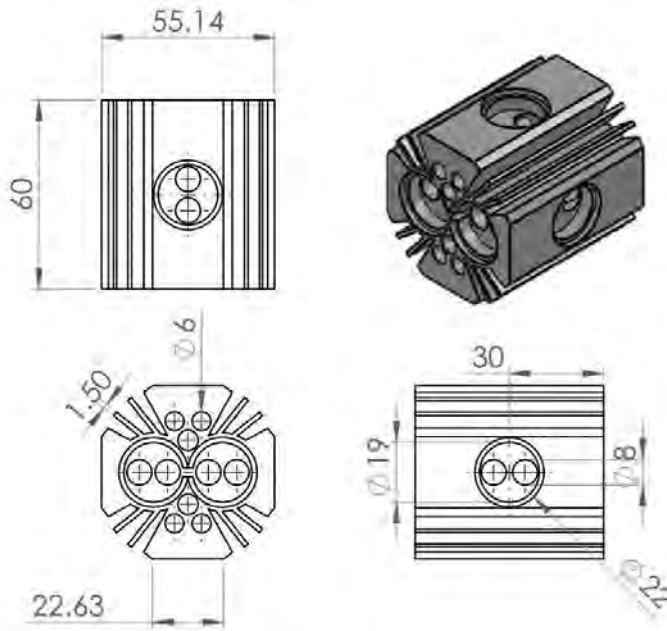


Fig. 8. Shape and dimensions of the designed heat sink

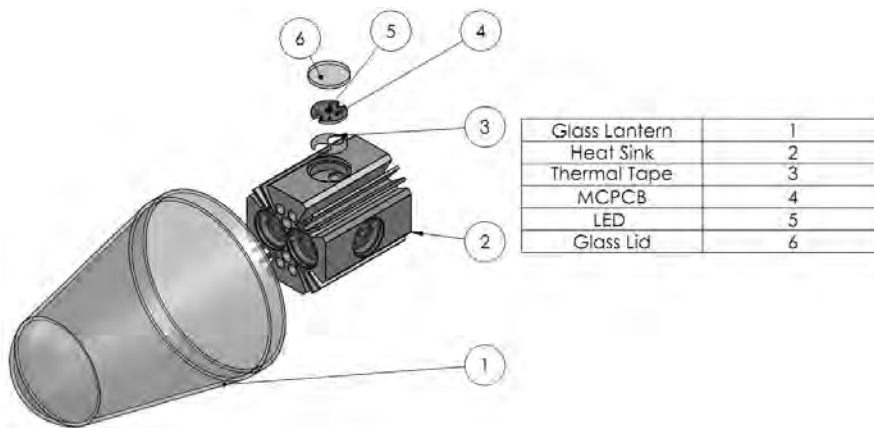


Fig. 9. Exploded view of the designed lighting system

mosque lantern; be light weight as to not cause any harm to the historical structure; and send its light to the whole space. Thus the design comprised of three major constraints: size, weight and photometric distribution. The size of the glass lantern posed several constraints on the dimensions and the form of the new system; the dimensions had to be small enough to fit into the lantern and comply with the shape of the lantern as well. As the second constraint, keeping the total weight of the lighting system equal to the current system was of utmost importance, due to the fact that exertion of extra weight on the lantern holder may in the long run ruin the holder and the dome, resulting in a collapse of the lighting system causing not only harm to the historical building but also to the users of the mosque. The photometric distribution created by the lantern proved to be the

third constraint. The positioning of the LEDs as well as the physical design of the system was based on this third constraint.

The investigations showed that using 1x4 LEDs on the side faces of the heat sink along with 2x1 LEDs on the top and the bottom faces of the heat sink has proved to provide sufficient luminous flux values as well as the targeted luminous intensity distribution. Originating from the number and configuration of LEDs and taking the constraints brought by the shape of the lantern as well as manufacturing constraints all into consideration, a special heat sink has been designed in Solid works. Fig. 8 demonstrates the shape and dimensions of the designed heat sink and Fig. 9 shows an exploded view of the lighting system with the heat sink; the adhesive thermal tape used for connecting the base of the MCPCB on which the LEDs

Table 4. Material properties used in the thermal simulation

Material	Thickness, mm	Thermal Conductivity, W/mK
LED	0.65	11.62
Solder	0.075	58
Copper	0.07	390
Dielectric	0.10	2.2
Aluminium	1.43	170
Adhesive Tape	0.13	0.17
Heat Sink (Aluminium)	58	218

are mounted to the heat sink, the MCPCB, the LED and finally the glass lids to protect the LED from dust, dirt and exterior impacts.

5.1. Thermal analysis

In order to evaluate the thermal performance of the designed system, the computational fluid dynamics software, Solid works Flow Simulation was used. For accurate results, the properties of each different part of the system, given in Table 4, have been introduced to the program. The material properties have been selected according to the catalogue values of the materials that will be used in the production of the proposed system.

For the construction of the simulation, the luminous efficiency values previously measured and given in Table 4 were utilized. The values show the amount of energy that turns into light; using these values and Equation (3), the amount of energy that turns into heat was calculated.

$$P_{th} = P_e \cdot (1 - \eta_l). \tag{3}$$

Here,

P_{th} : Thermal power

P_e : Electrical power

η_l : Luminous efficiency

According to the measurements and the initial target temperature value of 85 °C, the thermal power per LED has been designated as 0.74 W. The computational domain has been defined to provide enough space to enable air motion around the lantern. The laboratory conditions in which the measurements will be held for the validation of the

system provide an average ambient temperature of 21 °C, therefore the simulations were made for this ambient temperature value. In the simulation, a mesh was constructed using 1,499,402 cells including fluid, solid and partial cells. The simulation converged after 229 iterations. The temperature distribution obtained from the simulation can be seen in the cross section of the system given in Fig. 10. The figure shows that the LED modelled as a whole package reaches a maximum temperature value of 88.73 °C. The solder point temperature is 84.61 °C, and the temperature on the top of the heat sink is 79.18 °C.

The simulation results showed that the modelled system falls shortly above the target case temperature value of 85 °C. The maximum allowed junction temperature of the chosen LEDs

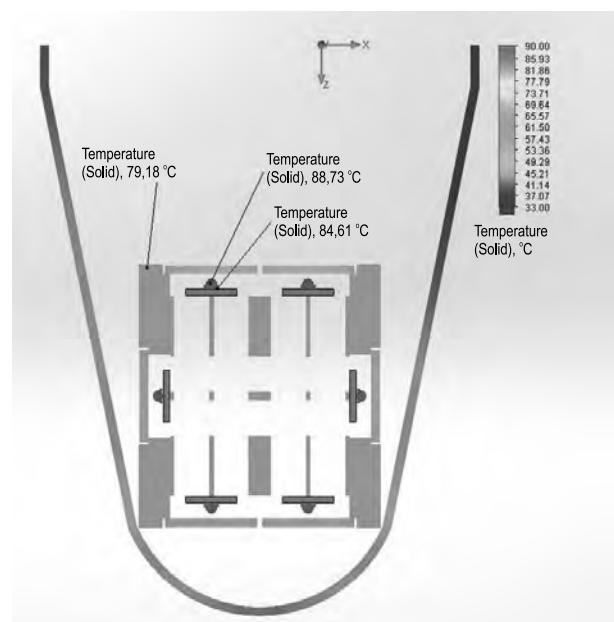


Fig. 10. Thermal simulation results for the designed lantern



Fig. 11. The new lantern design with a cut-off bottom

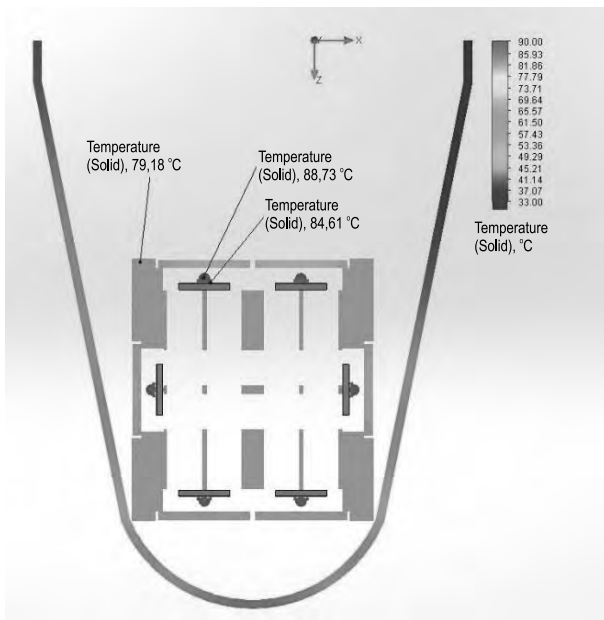


Fig. 12. Temperature distribution of the initial approach

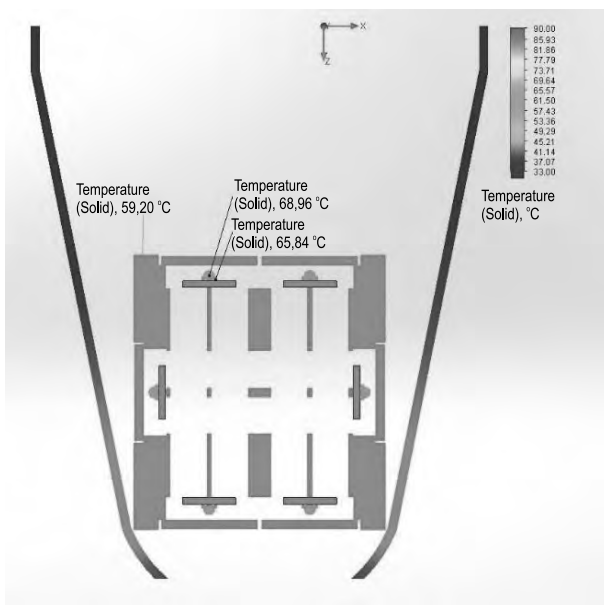


Fig. 13. Temperature distribution of the final approach

are 150 °C. The long term testing results given in Table 3 for 85 °C and 105 °C of case temperatures show that the lumen maintenance and lifetime predictions for 10,000 hours in between these two temperatures provide efficient results. However, using formulas (1) and (2) obtained from the integrating sphere measurements, showing the relationship between case temperature, luminous flux and efficacy, a case temperature of 85 °C translates into a 15 % luminous flux drop and a 10 % efficacy drop compared to 25 °C values.

In order to decrease the drops in luminous flux and efficacy, ways to remove more heat from the LEDs have been investigated. As a radical approach, the bottom part of the lantern was cut off, creating a circular opening right below the heat sink and providing much better air movement, as can be seen in Fig. 11.

In order to test the improvement achieved by cutting the bottom off, a new simulation was performed. The simulation resulted in 227 iterations, using a grid made up of 1,455,288 cells. The temperature distributions for both the original and the cut off lantern are given in Figs. 12 and 13. To compare the results objectively, the colour scale has been kept constant. The results show that the maximum package temperature has been lowered down from 88.73 °C to 68.96 °C through the new lantern, which enables a much more efficient cooling due to the ameliorated air motion. The flow of air through both systems can be seen in Figs. 14 and 15. Introducing the new case temperature value into equations (1) and (2) the luminous flux and efficacy values for one LED are calculated as 82.59 lm, and 82.16 lm/W respectively. In addition to the increase of luminous flux, the predicted lifetimes according to TM 21–11 measurements for 32,800 hours of L90 and more than 60,500 hours of L80 and L70 at 85 °C have definitely been guaranteed with a case temperature much lower than 85 °C.

5.2. Measurements and model verification

As the simulation results confirmed that the new system established the desired temperature values effectively, a prototype of the system was produced to see actual results and verify the model. The produced prototype lantern can be seen in Fig. 16.

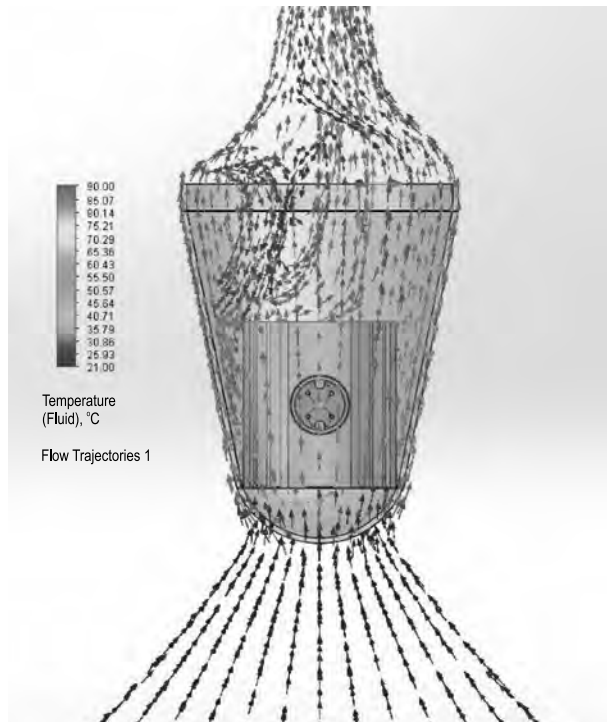


Fig. 14. Air flow in and around the lantern, initial approach

Temperature measurements on the solder point of the topmost LEDs were taken to compare the results to the simulation and to validate the prototype. The prototype posed a difficulty in terms of measurement; the LEDs were covered by glass lids to prevent dust and dirt entering the luminaire, however, the glass lids prevented the insertion of thermal probes to the system. Therefore, the measurements were made without the glass lids and to validate the simulation model effectively, the simulations were repeated for the system without the glass lids. For the measurements, the system was operated for 6 hours, and the temperature values at the solder point where the LED is mounted on the MCPCB were measured. In order to calculate the temperature value at the junction, the closest point that is available for mea-

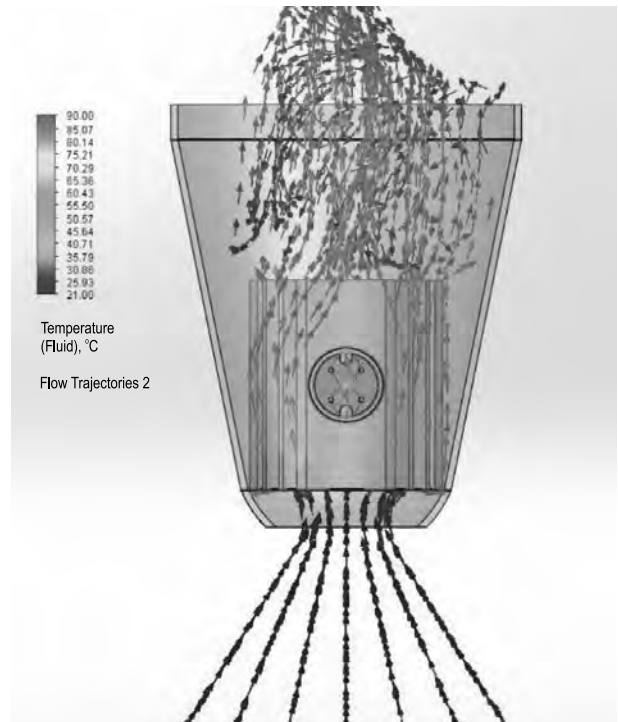


Fig. 15. Air flow in and around the lantern, final approach

surement, which is the solder point, can be used [12]. The temperature value at the junction point can be calculated using this measurement value, using formula (4).

$$T_j = T_{SP} + \theta_{TH} \cdot P_e \tag{4}$$

Here,

T_j : Junction temperature in °C

T_{SP} : Solder point temperature in °C

θ_{TH} : Thermal resistance of the LED in °C/W

P_e : LED electrical power in W

The measurements were taken at an ambient temperature of 21.7 °C, the temperature stabilizing at a value of 66.3 °C on the solder point. The simulation was repeated for the ambient tempera-

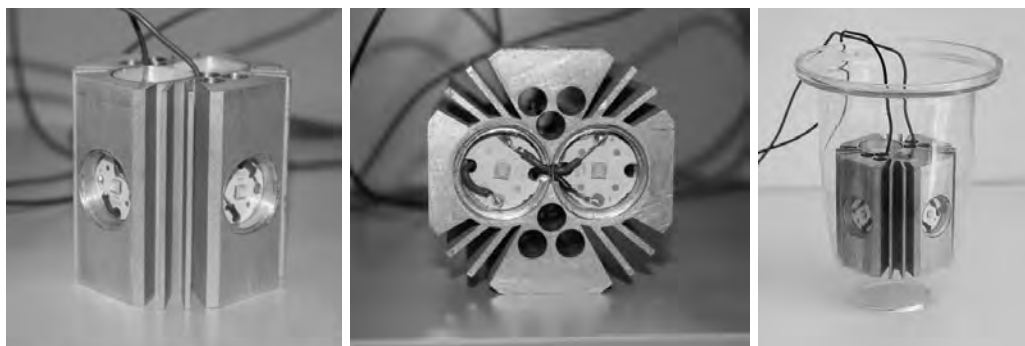


Fig. 16. The prototype of the novel LED Mosque Lantern

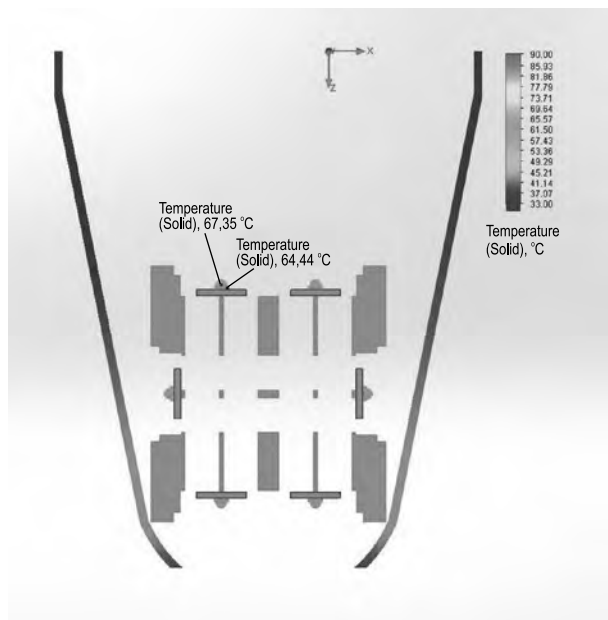


Fig. 17. Temperature distribution for the new lantern without the glass lids

ture of 21.7 °C and resulted in 225 iterations, using a grid made up of 1,422,605 cells. The obtained temperature distribution can be seen in Fig. 17. The results of the simulation show that the case temperature is equal to 67.35 °C and the solder point temperature is 64.44 °C. Thus the absolute difference between the measurement and the simulation is 1.86 °C, and the relative difference is 2.8 %, showing that the simulation model has been verified with an error range of less than 5 %.

As the simulation model has been verified with a small margin of error, it is possible to say that the package temperature for the proposed LED lantern is approximately equal to 69 °C, as obtained from the second set of simulations. Introducing this value into formulas (1) and (2), the luminous flux and efficacy of each LED is calculated as 82.6 lm and 82.1 lm/W, respectively. For the most preferred lighting systems in Turkish historical mosques, incandescent lamps of 40 or 60 W, the efficacy values are approximately 10–12 lm/W. Thus with the proposed system, the luminous efficacy of the light source used in the lantern has been ameliorated nearly to a value 8 times better compared to the incandescent lamp.

6. CONCLUSION

The main reasons behind this study were the lack of energy efficient and sustainable light sources in most Turkish historical mosques as well as

anaesthetic and non-uniform photometric conditions in terms of illuminances and colour properties. While some mosques are trying to adopt energy efficient alternatives such as CFLs or LED retrofits, these lamps are not as suitable as a custom designed lighting system due to the shape of the lanterns, the created luminous intensity distributions and the texture of the historical interiors.

In this study, an LED lighting system which can be adapted to the original lighting systems of Turkish historical mosques was meticulously designed. One of the most important methodologies in designing a lighting system with LEDs is no doubt the thermal design aspect. Without a proper thermal design, the end product could prove to be extremely unsatisfactory in terms of performance. In this study, for the thermal analysis, two different approaches have been evaluated in the finalization of the designed LED lighting system. The initial approach uses the designed heat sink directly with the available glass lantern. The final approach aims at a lower case temperature and proposes to cut a circular hole in the bottom part of the glass lantern to enable a more efficient natural ventilation, which will definitely aid in the cooling process. The thermal analysis of the system was started with the photometric measurements of the selected LEDs and carried out through simulations; a prototype originating from the results of the simulations were produced and verification measurements were performed. With the final system, cool air can easily enter the lantern through the opening on the bottom, flow through the fins of the heat sink and provide a much more efficient cooling. For the initial simulation, the case temperature stabilizes at 88.73 °C, while for the second simulation the case temperature is lowered down to 68.96 °C with the enhanced air flow due to the hole at the bottom of the glass lantern. Inserting the temperature values obtained from the simulation into equations (1) and (2) the luminous flux of one LED used in the lighting system is calculated as 82.6 lm and the efficacy of the LED is calculated as 82.1 lm/W. In addition to the luminous flux values, 32,800 hours of L90 as well as more than 60,500 hours of L80 and L70 lifetime values predicted by the TM 21–11 measurements can be guaranteed through achieving much lower case temperature values than 85 °C.

7. REFERENCES

1. The Lighting Handbook: Reference and Application. 10th Edition ed.: Illuminating Engineering Society, 2011.
2. Turkish Directorate of Religious Affairs, Statistical Tables 2014. Retrieved 12 May 2016 from <http://www.diyenet.gov.tr/tr/kategori/istatistikler/136>.
3. Radikal Newspaper, "Türkiye'de 79 bin 96 camiayda 42 milyonYTL'likelektriktüketiyor" (79096 mosques consume 42 million new Turkish Liras worth of electricity per month). 2008, Turkey. Retrieved 12 May 2016 from <http://www.radikal.com.tr/ekonomi/turkiyede-79-bin-96-cami-ayda-42-milyon-ytlik-elektrik-tuketiyor-886600/>.
4. Turkish Electricity Distribution Corporation, Electric Tariffs, 2004. Retrieved 12 May 2016 from http://www.tedas.gov.tr/#!/tedas_tarifeler.
5. Turkish General Directorate of State Hydraulic Works. Hirfanlı Dam. Retrieved 12 May 2016 from <http://www2.dsi.gov.tr/baraj/detay.cfm?BarajID=9>.
6. Yurtseven MB, Mete S, Onaygil S. The effects of temperature and driving current on the key parameters of commercially available, high-power, white LEDs. *Lighting Research and Technology* 2015; 0: 1–23.
7. Ünver R, Enarun D. *A Comparative Investigation of Lighting of Mosques and Churches in Istanbul*. 24–30 June 1999, Warsaw, Poland, CIE24th Session Proceedings, 288–292.
8. Cree XLamp XP-E High-Efficiency White LEDs. Retrieved 12 May 2016 from <http://www.cree.com/LED-Components-and-Modules/Products/XLamp/Discrete-Directional/XLamp-XPE-HEW>.
9. Illuminating Engineering Society (IES). *IES LM 80–08 Approved Method: Measuring Lumen Maintenance of LED Light Sources*. New York, USA, 2008.
10. Illuminating Engineering Society (IES). *TM-21–11 Projecting Long Term Lumen Maintenance of LED Light Sources*. New York, USA, 2011.
11. Cree LED Components IES LM-80–2008 Testing Results. Retrieved 12 May 2016 from http://www.cree.com/~/media/Files/Cree/LED%20Components%20and%20Modules/XLamp/XLamp%20Application%20Notes/LM80_Results.pdf.
12. Cree. Optimizing PCB Thermal Performance for Cree XLamp LEDs. Retrieved 12 May 2016 from http://www.cree.com/~/media/Files/Cree/LED%20Components%20and%20Modules/XLamp/XLamp%20Application%20Notes/XLamp_PCB_Thermal.pdf.



Lale Erdem Atılgan

received her B. Sc., M. Sc. and Ph.D. from Istanbul Technical University in 2004, 2007 and 2014 respectively. She worked as a research and teaching assistant at the Electrical Engineering Department of Istanbul Technical University through 2005–2011. She spent over a year at the Light Technology Institute of Karlsruhe Institute of Technology, Germany as a visiting researcher. She has been teaching lighting courses in the Electrical Engineering Department of Istanbul Technical University since the end of her Ph.D. Her research interests include interior lighting, LEDs, glare from LEDs and energy efficiency



Mustafa Berker Yurtseven

graduated from Istanbul University, Mechanical Engineering Department in 2003. He received his M. Sc. degree from Istanbul Technical University, Energy Institute in 2006. He is at the final phase of his Ph.D. work which focuses mainly on thermal management of LED light sources. His research interests include photometric and radiometric measurements of LEDs, thermal management and statistical analyses

A SURVEY AND MEASUREMENT BASED STUDY ON DIMMABLE LIGHTING TO EVALUATE VISUAL PERFORMANCE AND LIGHTING ENERGY SAVINGS¹

Banu Tabak Erginöz and Cenk Yavuz

Sakarya University, Turkey

E-mails: btabak@sakarya.edu.tr; cyavuz@sakarya.edu.tr

ABSTRACT

Energy saving has been one of the most important issues discussed in lighting systems lately. One of the most common applications to provide energy savings in lighting are scenarios involving the utilization of dimmable gears. Although applying dimming provides good results in energy savings, its negative effects on the power network should not be ignored. Among the main negative effects are values such as harmonic distortion and power factor. These measurable magnitudes have been the most strongly emphasized parameters in scientific studies that have been carried out lately. When it comes to energy efficiency, parameters such as the visual perception, visual comfort, and the associated working performances of users should also be considered. These parameters cannot be as easily measured as the current, voltage, and harmonic distortions parameters. In this study, the disturbing effects of dimmable systems, which have an important value with regards to energy savings and efficiency on the power network, were investigated, while the negative effects experienced by users were also emphasized.

Keywords: lighting energy savings, energy quality, current harmonics, light spectrum

INTRODUCTION

Given the ever growing energy demand both in our country and the world, great emphasis should be put on the issue of energy savings. Considering that lighting systems have a 20 % share in energy consumption, it can be clearly understood that making improvements in these systems is crucial for the country's economy.

In their study, M. Chiogna et al. analyzed performances in different scenarios in order to improve energy efficiencies in environments illuminated either with lighting control or with conventional methods and showed that energy saving up to 65 % can be achieved in an environment where lighting control is applied [1]. In a study carried out by CA. Majithia, AV. Desai, and AK. Panchal, the current and voltage waveforms, total harmonic distortions, displacement power factors, and the net power factors of some commonly used light sources such as fluorescent and LED lamps were measured. It was determined that among the lighting appliances that were analyzed harmonically, the incandescent and halogen lamps had the lowest total harmonic distortion value, while the compact fluorescent and LED lamps had the highest total harmonic distortion value [2].

In order to determine the power quality and luminous characteristics of different light sources suitable for office use at different light levels, HC. Albu et al. carried out a simulation study on January 21, 2010 at 17:00 o'clock, in a 60 m² room that had 4 equally distanced rooms on its northern

¹ On basis of report at the 1st International Conference on Green Technologies and Energy Efficiency". Sakarya, Turkey, 28 September – 01 October.

wall. The study revealed that the illumination effectiveness values and the total harmonic distortion values of the LED luminaires were higher than the other lighting appliances [3].

In the studies of C. Yavuz, E. Yanıkoğlu, and Ö. Güler, dated 2010 and 2012, which investigated energy savings and energy quality parameters of daylight responsive lighting control systems, important findings on dimmable electronically addressable ballasts were revealed. According to the results of this study, these systems provided considerable energy savings and efficiency, while especially with respect to current harmonics they also led to a disturbing effect that was much higher than the international standards and also significantly reduced the energy quality of the power network [4,5].

A. Logadottir et al. carried a study in two separate rooms of 18 m² area, where they investigated user preferences for different illuminance levels. They determined that the intermediate illuminance level was preferred more than the low and high illuminance level [6].

George et al. compared the economic advantages of LED lamps and CFL's and investigated the power quality problems caused by these in the power system network. They determined that LED lamps, which had lower thermal losses and higher power factor values, were much more economically advantageous compared to compact fluorescent lamps, the THD values of which may reach 100 %. The team suggested and designed a passive filter in order to eliminate the negative effects of both lamps on the power network and they concluded that the greatest advantage of this filter circuit was the reduction in costs and the 3rd harmonic, while the greatest disadvantage was that it did not reduce higher harmonics and its design was very difficult [7]. In order to analyze the characteristics of 12 LED and 2 CFL lamps from various brands that have different power levels, S. Uddin et al. performed a test using a power quality analyzer and analyzed all combinations of the lamps from different brands at different power levels. At the end of the experiment, the purpose of which was to identify the combination with the lowest THD value, it was revealed that the combined use of LED and CFL lamps resulted in lower harmonic generation compared to lighting systems with only LED or only CFL lamps [8].

S. Uddin et al. investigated the harmonics generation from dimmable LED appliances. They carried out tests with various LED lamps in a laboratory environment and observed the load current behaviour at different conditions. Then, they analyzed the generated harmonics in the frequency domain. They evaluated and compared experimentally the harmonic levels of dimmable and non-dimmable LED lamps and dimmable compact fluorescent lamps from different brands that had different wattages. The experimental results showed that during the dimming operation LED lamps generated very high harmonics, at a level that could affect the power quality of the AC mains [9].

Distortions that take place in the power network when applying methods of energy saving in lighting are important and have been lately emphasized by researchers, and research on this subject has intensified. The problems created by these distortion effects for users are similarly very important and are another subject that has to be investigated.

A. Sivaji stated in their study that light colour and colour temperature have significant effects on office workers and that office workers who work especially under warm white coloured artificial lighting devices have greater alertness and perception levels [10].

In a survey based study carried out by Wei et al. on the satisfaction level of office workers, it was observed that visual comfort in offices illuminated with high colour temperature artificial lighting devices was lower than offices illuminated with low colour temperatures even when the brightness level was high. As a result, luminaires with colour temperatures of 3500 K were preferred when selecting the light colour [11].

M. Islam et al. investigated, which of the two luminaire types -those with fluorescent or LED lamps- having the same illuminance level, made office workers feel more comfortable and increased their visual perception. It was revealed that luminaires with LED lamps, which have lower colour temperatures, were preferred by the workers [12].

In their studies, Charness and Dijkstra determined experimentally that young adults had increased perception levels at lower illuminance levels compared older adults [13]. As a result of a wide scale experimental field study, Chung

and Burnett determined that office users preferred working at high illuminance levels [14]. In a field study by Philips Company, investigating the productivity performance as well as worker psychology and biology, illuminance levels required by workers at different sectors were determined and it was observed that under working conditions with higher illuminance levels, the working performance increased considerably. In addition, the increase in the production of sleep hormones at low illuminance levels was also addressed [15].

In the study carried out by Karin Tetlow, it was revealed that the illuminance level needs varied according to age groups. It was found that the illuminance level needed between the ages of 60–70 was 250 % higher compared to that need at the ages of 20's [16].

In the experimental study carried out by B.M.T Shamsul et al. with students from University Putra Malaysia, Faculty of Medicine and Health Sciences, the effects of natural day light, cold white lighting, and warm white lighting on the working performance and visual comfort were investigated. The experimental results showed that the best visual comfort was experienced under daylight conditions where a high illuminance level could be achieved [17]. In a study by Sanaz Ahmadpoor Samani, it was claimed that adequate lighting increased the learning performance and thus there was a direct relationship between lighting and learning. It was also pointed out in the same study that there was a direct relationship between age and the need to work in an environment with a higher illuminance level [18].

In his study, Ateş Bayazıt Hayta addressed problems such as occupational accidents and worker health and examined the close relationship between working environment conditions and labour productivity. In the study it was stated that adequate lighting is a key factor for productivity increase as well as the health, safety, and effectiveness of workers, while in an insufficiently illuminated environment; visual impairments, accidents, and material losses take place and the productivity decreases. It was stressed that inadequate lighting especially decreased the efficiency of workers in jobs that required precision. The light level standard values required for an efficient working environment were presented and the importance of the light source colours was emphasized [19].

In a study carried out by Linhart and Scartezini in Switzerland, 2 different test rooms with lighting devices of the same luminous colour temperature were constructed. The room that was illuminated with a lighting device of a higher effectiveness demonstrated a higher illuminance level. However, this test room had a higher probability of producing discomfort glare. In the study, it was revealed that in the test room, that was illuminated with devices having higher energy efficiencies, the visual comfort was higher and the participants preferred working in this room despite the higher probability of experiencing a discomfort glare [20].

In the thesis study carried out by Siti Mardiah Binti Jamian, it was claimed that dim lighting reduced worker productivity and also resulted in negative consequences such as eye strain and headache. In the same study, it was experimentally shown that a normal lighting without dimming increased worker motivation and was more appropriate with respect to eye comfort and health [21].

A limited number of studies similar to those mentioned above revealed that visual performance decreased at low illuminance levels and the needed level of brightness increased; the working performance was associated with light colours; the colour temperature was important with respect to visual comfort and perception and was an important element of environment visibility.

When the issues of energy efficiency and savings in lighting are being investigated, all of the effects that take place during these should be addressed as a whole. Considering these, this study concentrates on the measurement of the perceptions of users who work in similar or the same working environments, under different light levels, different light colours, and different energy consumption levels, and the relationship of these with electrical distortions.

EXPERIMENTAL DESIGN

Sakarya University, Department of Electrical and Electronics Engineering allocated 3 testing and experimenting rooms for this study and experiment Figs. 1–3. The rooms were located on the M-6, 3rd floor of the 4-storey Engineering Department building. The exact coordinates of the rooms were 40° 74' north latitude and 30° 33' east longitude. The surface area of the rooms



Fig. 1. Test and experiment room 1 (fluorescent)



Fig. 2. Test and experiment room 2 (hybrid)

was 24 m² and each room had 1 window on their northwest wall. A thin film layer was applied to the windows in order to eliminate daylight glows. As a result, the inflow of 100 % direct daylight from the windows was prevented. The light transmittance of the windows was measured as 67 %. The dimensions of the window on the northwest direction were 1.5 m × 1.2 m and its total area was 1.8 m². According to section 21 of the IEA report, the effective window surface area was 1.2 m² and similarly the effective window height was 1.5 m. The Lighting Laboratory (TR4), which was used to check reliability of the results, was located on the 40° 74' North latitude and 30° 33' East longitude, on the ground floor of the M-4 Engineering Department. The room faced the west and northwest direction and although it had an actual ceiling height of 3.80 m, the apparent ceiling height was 2.85 m because of an installed suspended ceiling. The window dimensions in the room were 2.45 m × 1.75 m and the total window area was 4.29 m².

The old artificial lighting system (6 units of 4 × 18 fluorescent lamps, with double parabolic mirror louver) of test and experiment room 3 (TR3), which was the most important test and experiment room of the thesis study, was replaced with a LED system equipped with 1 × 41W middle class LED panels (6 units of 60 cm × 60 cm LED panels). The ballasts of the old system in test room 1 (TR1) were replaced with dimmable electronic DALI ballasts. Both rooms had systems with a dimming feature. Philips LED drivers with DALI feature (92 % efficiency, PF=0.95) were used in TR3 and OSRAM DALI RC BASIC lighting automation system was used in TR1. TR2 was designed as a hybrid room; the conventional ballasts of a lumi-

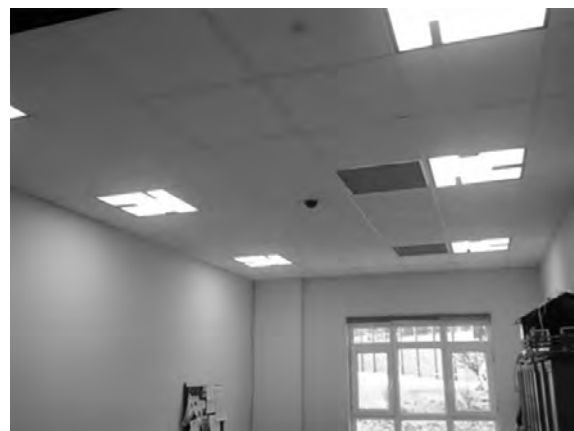


Fig. 3. Test and experiment room 3 (LED)

naire that had 3 fluorescent lamps were replaced with DALI ballasts, while 3 luminaires were replaced with LED luminaires that had DALI ballast and were used in TR3. The fluorescent luminaires that were used in TR2 and TR1 were 4 × 18 W luminaires. With a switch level of 100 %, the following illuminance levels were obtained in the rooms, respectively: 510 lx with the artificial lighting system in TR3, 275 lx with the system in TR1, and 400 lx with the hybrid system in TR2.

Electrical parameters such as the voltage, lamp currents, active/reactive powers, total harmonic distortion (THD, THD₁) were measured individually several times in periods of 1 second, 10 seconds, 15 seconds, 30 seconds, 1 minute, and 5 minutes with an electrical energy analyzer (Janitza UMG 503) that was connected at the input point of the systems.

While dimming in TR2 and TR3 was carried out manually using a system remote control, manual switch, and software provided by the luminaire provider Arlight Company; in TR1 and TR4, this was carried out via DALI RC BASIC.

Table 1. THD₁ ratios in TR1 and TR3 according to the dimming levels

Level	Dimming Levels, %	Lighting levels, %	TR3 LED THD ₁ , %	TR3 LED PF	TR1 FL THD ₁ , %	TR1 FL PF
DL1	0	100	21.7	0.94	24.6	0.98
DL2	25	75	24.92	0.89	30.99	0.91
DL3	50	50	29.02	0.84	36.35	0.83
DL4	75	25	33.21	0.79	42.73	0.77
DL5	95	5	37.60	0.75	49.05	0.68

The total energy consumption for an operation at a switch level of 100 % was measured as 250.2 W·h for TR3, 444 W·h for TR1, 346 W·h for TR2, and 1030 W·h for TR4, respectively. 5 different dimming levels were applied for each of the four lighting systems in two different buildings of Engineering Faculty.

THD values measured at different dimming levels are given in the Table 1. The harmonic distortion values obtained at different dimming levels for the hybrid room are given in the Table 2.

Considering the electronic circuits used in the dimming gears, the high values measured for harmonic distortion are a well expected result.

Another purpose of our study was determining how these disturbing effects affected the more difficult-to-measure parameters such as visual comfort and working performance. Before commenting on whether a specific lighting design is economic and energy efficient, first, user satisfaction and visual comfort should be investigated [22]. For this purpose, a study based on a survey evaluation was carried out with a group of 40 participants in the test rooms where we had carried out our measurements. In this study, after reviewing previous studies and evaluating different attitude scales, the Likert Scale was chosen as the survey attitude scale to determine user satisfaction and visual comfort at the lighting conditions applied in the constructed experiment rooms. The Likert Scale is a 5-point scale. In the Likert scale, answers include statements such as “strongly agree, agree, don’t know, disagree, and strongly disagree” or an attitude scale ranging between parameters equivalent to these. Every answer is assigned with a numerical value. The Likert scale is highly recognized worldwide and is a scale with high reliability.

The constructed survey consists of 2 parts. Part 1 are questions of “Personal Information”, which consists of demographic questions, and the Part 2 is measuring user reactions on “visual comfort and visual perception in the Experiment Room”. The survey was carried out with 40 volunteering participants and the survey results were analyzed using the SPSS16.0 statistical data analysis software package [23].

The survey was applied to the participants in the 3 different experiment rooms. The first room was an experiment room that had a total of 6 conventional type fluorescent luminaires with 4 × 18 W and a luminous correlated colour temperature (CCT) of 4000 K. In the second experiment room, there were 3 double parabolic fluorescent luminaires with 4 × 18 W and a CCT of 3000 K and 3 LED luminaires each of 41 W and a CCT of 3000 K. In the third room there were 6 LED luminaires, each of 41 W and a CCT of 3000 K.

The survey participants spent 20 minutes in Room 1 and approximately 30 minutes in the other rooms. The participants were asked to evaluate the visual conditions and the different lighting

Table 2. THD₁ ratios in TR2 according to the dimming levels

Level name	Dimming Levels, %	TR2 THD ₁ Levels, %
DL1	0	23.40
DL2	25	28.07
DL3	50	34.14
DL4	75	38.87
DL5	95	44.46

conditions in rooms 2 and 3 when the switching levels of lighting systems were at 100 % and 50 %.

Before performing the survey, the participants were allowed 15 minutes in order to adapt to the conditions of the room and they were asked to answer the survey questionnaire after this period. The participants were told that during these 15 minutes they could use the computers allocated for their use as they like, while they were only asked to select and read any 2 pages from the books that were placed before them.

At the end of the 15 minute period, the users were asked to look at previously specified points in the experiment rooms and then open specific documents on the desktop of the computers allocated for their use and read the text in that document. Then after carrying out these procedures, the participants were asked to adjust the switch level of the lighting systems to 50 % using the remote controls that they were handed and repeat the same procedures 2 minutes later.

The survey was comparative and contained determining questions regarding the personal satisfaction and visual comfort at the applied lighting conditions.

The survey questions that were asked to the participants were based on the following:

- The visual comfort experienced in the room;
- The distribution of light in the room;
- The light colour in the room;
- Evaluation of the effect of the lighting conditions in the room on the working performances of the participants;

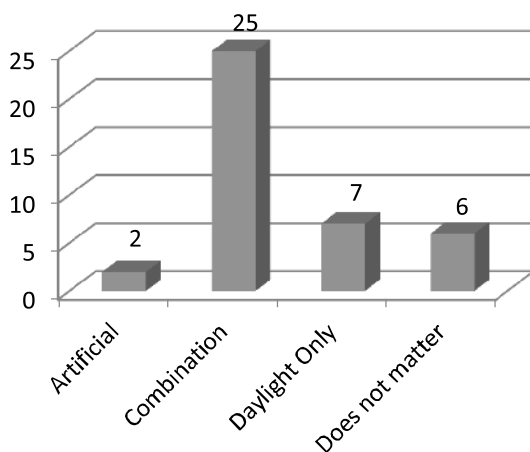


Fig.4. The lighting conditions that were preferred by the survey/experiment participants

- Evaluation of the ability of participants to discriminate the colours and patterns of the door cases;

- Participant evaluations regarding the ability to read the document in the computer;

- Evaluations by participants who experienced reading difficulties.

In addition, the light spectrum in the rooms was measured with the UPRTEK MK350S instrument and was compared with the survey results.

ASSESSMENT AND COMPARISON OF THE SURVEY RESULTS

When the answers obtained from the survey were assessed, it was revealed that the experiment room with the cold white light colour was the room that the users were least satisfied with and evaluated its visual comfort as the lowest. Experiment Room 2, which can be defined as a hybrid room, was ranked second in terms of satisfaction and visual comfort, while the highest visual comfort and user satisfaction was reported for Experiment Room 3. These results were obtained for a lighting switch level of 100 %. In the second case, when the switch level was reduced to 50 %, it was observed that the visual comfort level was higher in Experiment Room 3. Generally, the lighting type preferred by the participants was the system that combined artificial and daylight, Fig. 4.

The survey participants reported that generally when the lighting systems performed at their full capacity their visual comfort was high and their perception levels were higher. In the second case, when the illumination capacity was decreased by 50 %, the survey results obtained from both Experiment Room 2 and 3 indicated that some colours were difficult to distinguish and the perception level and visual comfort were reduced. However, the most important and distinctive outcome of this study was proving that both lower illuminance levels and dimming of fluorescent and LED luminaires with DALI ballasts resulted in energy loss in the light spectrums of the luminaires, Figs.5, 6. It is surprising that this subject has not been empathized previously in the literature. Actually, in the presence of energy losses in its light spectrum, the colour rendering index of a light source decreases with respect to some specific colours. In this study, the reduction of the illuminance level to 50 % in order to represent

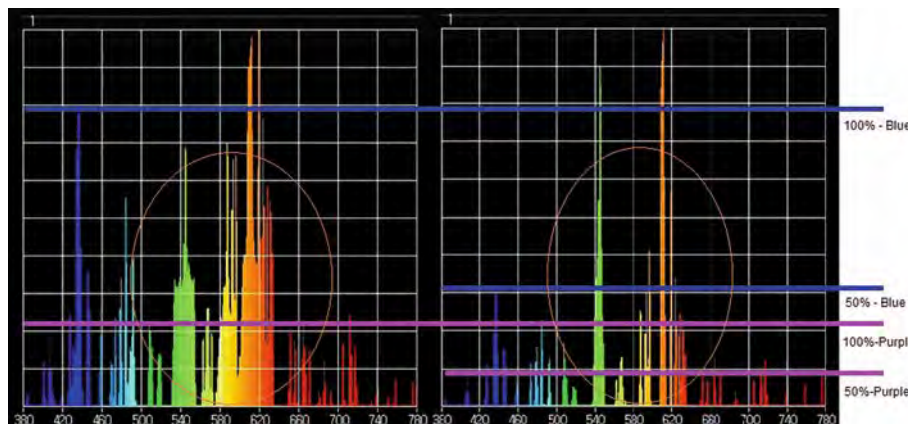


Fig. 5. Light spectrum energy losses in the fluorescent lamp after 50 % dimming

a lower power lamp was carried out using a control system with the DALI ballast.

The survey participants reported that they had difficulty in reading and discriminating the colours when dimming was applied and emphasized that they especially had difficulty in perceiving the purple, blue, and green colours. The participants observed that the best working conditions were those in Experiment Room 3 (LED).

The measurements revealed that the colour rendering index (CRI) of the room with the fluorescent gears decreased from 83.2 % to 81.9 % after dimming by 50 %. When the same measurements were carried out in the room with the LED luminaires, the initial CRI value was initially 80 % and it decreased to 78.9 % after dimming.

In the results obtained for the fluorescent luminaire in Experiment Room 2, i.e. the hybrid room, it can be seen that considerable energy losses occurred in the purple, blue, and green colour regions of the light spectrum. The results showed that dimming achieved using a DALI ballast system damaged visual comfort and visual perception and this was also supported by the survey results. It was observed that the participants who

had difficulties discriminating colours in Experiment Room 2 had problems in discriminating especially the purple and blue colours. In order to obtain the most reliable results, the measurements were carried out after the lighting system operated for at least 30 minutes, and the same results were obtained in the measurements that were repeated for several times.

The CRI was measured as 83.2 % for the fluorescent luminaire at a switch level of 100 %, while this value decreased to 81.9 % when the switch level was reduced to 50 %. While there were energy losses in the spectral region of specific colours, considerable loss was also determined in the visibility of all colours.

When Experiment Room 3 was analyzed, as can be clearly seen from the spectrum graphs, it was observed that again there were energy losses in the spectral region of the purple, blue, and green colours of the LED Luminaire light spectrum. The loss was minimal at the spectral region of the yellow, orange, and red colours. The fact that the survey participants who experienced difficulties in seeing and reading in Experiment Room 3 had problems in discriminating the blue,

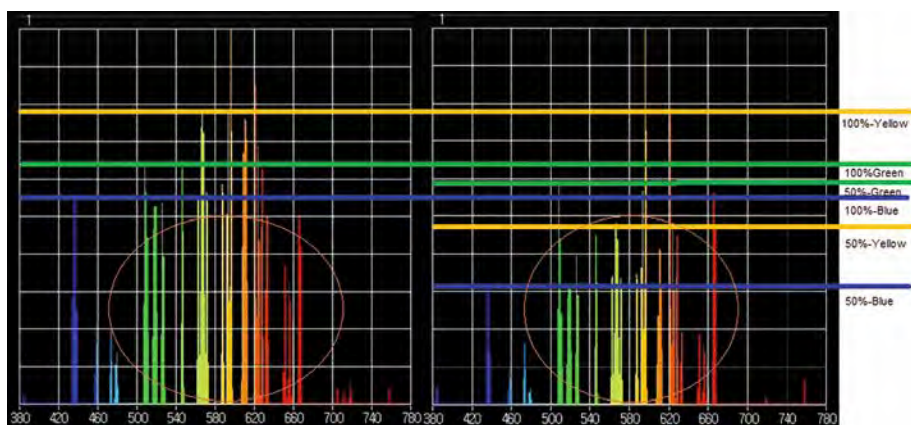


Fig. 6. Light spectrum energy losses in the LED lamp after 50 % dimming

green, and yellow colours was a proof that this spectral energy loss affected the visual perception. Another proof, which supported the observation that the energy loss in the spectrum made seeing difficult, was the fact that the colour rendering index (CRI), which was measured as 80 at an illuminance level of 100 %, was reduced to 78.9 at an illuminance level of 50 %.

CONCLUSIONS AND RECOMMENDATIONS

Although visual performance and associated parameters after dimming were investigated in scientific studies up until now, the light spectrum emitted by dimmed lighting devices were not investigated in detail. The comparison of electrical data obtained from the experiment rooms constructed within the scope of this study with the results of the survey that was conducted with 40 participants produced important results. In terms of savings, while the energy consumption, current and active power drawn to decrease, the harmonics is increasing and the power factor values are decreasing too. When the visual performances of the individuals present together in the office are analyzed, observations such as inability to discriminate colours and difficulty in reading suggest that electrical distortions that unavoidably arise as a result of dimming lead to visual problems.

On the other hand, one of the most important problems, which are ignored when transforming to LED systems, is the disturbing effect of LED lighting devices on the power quality of the power network. It is compulsory to apply filter systems in order to minimize the damage that will be created by LED luminaires, which have the highest harmonic distortion value (up to 159 %), when these are integrated to the power network system as a whole. Instead of applying filters for each LED luminaire, LED luminaires can be grouped and a filter system can be applied for each group.

When the overall findings, test and experiment results, user feedbacks, and electrical parameters that were obtained in this study were assessed, the following conclusions were reached:

- Although energy consumption can be reduced by using dimmed lighting systems, distortions arise in other electrical parameters;
- The maximum total harmonic distortion increases as a result of dimming;

- Harmonic distortions that arise as a result of dimming lead to energy loss in the light spectrum;
- The CRI decreases to a certain degree as a result of dimming;
- The visual performance declines as a result of dimming;
- The decline in the visual performance reduces the perception level;
- Dimming can result in performance and alertness reduction in older workers;
- In order to eliminate harmonic distortions, the active filtering method can be applied. However, this method is expensive in today's technological conditions;
- With increase in the number of electronic components used with the purpose of providing dimming, harmonic distortions and thus energy losses in the spectrum increase as well;
- Utilization of LED lamps, which are more energy efficient, have higher saving rate, and provide higher brightness level compared to conventional lamps- without dimming is an option that can prevent electrical distortions;
- While designing the lighting system of a volume, the use of unnecessary quantities of light as well as the application of unnecessary light controlling and, thus, the formation of electrical distortions can be prevented by paying attention to the visual perception level required for a certain job, instead of applying dimming.

ACKNOWLEDGEMENTS

This study was supported by the Sakarya University Scientific Research Projects Commission, Engineering Faculty and Electrical and Electronics Engineering Department.

REFERENCES

1. Chiogna, M., Mahdavi, A., Albatici, R., Frattari, A., "Energy Efficiency of Alternative Lighting Systems", *Lighting Res. Technology*, 2012, 44: 397–415.
2. Rosillo FG., Castejon F., Egido MA., "Emissions and Economic Costs of Cycling Compact Fluorescent Lamps With Integrated Ballasts", *Lighting Res. Technology*, 2012, 45:102–123.
3. Majithia CA., Desai AV., Panchal AK., "Harmonic Analysis Of Some Light Sources Used For Domestic Lighting", *Lighting Res. Technology*, 2011, 43: 371–380.

4. Yavuz C; Yanikoglu, E; Guler, O, "Determination Of Real Energy Saving Potential Of Daylight Responsive Systems: A Case Study From Turkey", LIGHT & ENGINEERING, Vol. 18, pp. 99–105, ISSN: 0236–2945, June 2010.
5. Yavuz C; Yanikoglu, E; Guler, O, "Evaluation Of Daylight Responsive Lighting Control Systems According To The Results Of A Long Term Experiment", LIGHT & ENGINEERING, Vol. 20, ISSN: 0236–2945, December 2012.
6. Logadottir A., Christoffersen J., Fotios SA., "Investigating The Use Of An Adjustment Task To Set The Preferred Illuminance In A Workplace Environment", Lighting Res. Technology, 2011, 43: 403–422.
7. George V., Bagaria A., Prakash S., Sankalp R.P. and Swati P., "Comparison of CFL and LED Lamp – Harmonic Disturbances, Economics (Cost and Power Quality) and Maximum Possible Loading in a Power System", Utility Exhibition on Power and Energy Systems: Issues & Prospects for Asia (ICUE), 2011.
8. Uddin S., Shareef H., Mohamed S., Hannan M.A., "Investigation of harmonic generation from dimmable LED lamps", Przegład Elektrotechniczny, Issn 0033–2097, 2013/4, 151–155.
9. Uddin S., Shareef H., Mohamed S., Hannan M.A., "Investigation of Harmonic Generation from Low Wattage LED Lamps", Journal of Applied Sciences Research, 2012, 8(8): 4215–4221.
10. Sivaji A., Shopian S., Mohd Z., Chuan N., Bahri S., "Lighting does Matter: Preliminary Assessment on Office Workers", Procedia-Social and Behavior Sciences, 2013, 97: 638–647.
11. Wei M., Houser K., Lang D., Ram N., Sliminski M., Bose M., "Field Study Of Office Worker Responses To Fluorescent Lighting of Different CCT and Lumen Output", Journal of Environmental Psychology, 2014, 39: 62–76.
12. Islam MS., Dangol R., Hyvarinen M., Bhusal P., Poulakka M., Halonen L., "User Acceptance Studies For LED Office Lighting: Lamp Spectrum, Spatial Brightness and Illuminance", Lighting Res. Technology, 2013, 47: 54–79.
13. Charness N., Dijkstra K., "Age, Luminance and Print Legibility in Homes, Offices and Public Places", Human Factors: The Journal of the Human Factors and Ergonomics Society, 1999, 41(2): 173–193.
14. Chung T.M., Burnett J., "Lighting Quality Surveys in Office Premises", Indoor and Built Environment, 2000, 9(6): 335–341.
15. Ir W J M van Bommel Ir G J van den Beld, "Industrial Lighting and Productivity", Philips Lighting, The Netherlands, 2003.
16. Tetlow K., "Task Lighting Solution: Their Economic And Ergonomic Benefits", Educational Advertising Section, Continuing Education, Human Scale, 173–180.
17. B.M.T Shamsul, C.C. Sia, Y.G Ng, K. Karmegan," Effects of Light's Colour Temperatures on Visual Comfort Level, Task Performances, and Alertness among Students", American Journal of Public Health Research, Vol. 1, No. 7, 159–165, 2013.
18. Sanaz Ahmadpoor Samani, "The Impact of Indoor Lighting on Students' Learning Performance in Learning Environments: A knowledge internalization perspective" International Journal of Business and Social Science Vol. 3 No. 24, 2012.
19. Hayta A.B., "The Effect of the working Environment Conditions to Management Fertility" Journal of Commerce and Tourism Education Faculty, 2007(1): 21–41.
20. Linhar F., Scartezini J., "Evening Office Lighting – Visual Comfort vs. Energy Efficiency Vs. Performance?", Building and Environment, 2011, 46(5): 981–989.
21. Siti M.B.J., "Employees Perceptions On Effect Of Lighting That Affect Employee Performance In The Workplace", Faculty of Cognitive Sciences and Human Development University Malaysia, 2015.
22. Erdem, L., Enarun, D., "Aydınlatmanın subjektif analizinde kullanılan anket yöntemleri, EMO 5. Ulusal Aydınlatma Sempozyumu", İzmir, Türkiye, 2009.
23. Eymen, E.U., SPSS, Veri Analiz Yöntemleri, www.istatistikmerkezi.com, 2007.



Banu Tabak Erginöz

received the Electrical and Electronics Engineering degree from Sakarya University (SAU), Turkey in 2000. Later, she obtained her M. Sc. and Ph.D. degrees in Electrical Engineering from SAU in 2005 and 2016 respectively.

Dr. Erginöz has been working as assistant researcher at SAU Electrical and Electronics Engineering Department since 2001. Her current research interests include interior lighting design, energy savings, energy efficiency and energy quality in electrical systems



Cenk Yavuz

received the Electrical and Electronics Engineering degree from Sakarya University (SAU), Turkey in 2002. Later, he obtained his M. Sc. and Ph.D. degrees in Electrical Engineering from SAU in 2004 and 2010

respectively. He is currently an Associate Professor at SAU Electrical and Electronics Engineering Department. His current research interests include daylighting applications, lighting energy savings, energy efficiency and energy quality in lighting. Dr. Yavuz is a member of Turkish National Illumination Committee

INVESTIGATION OF ENERGY SAVING PERFORMANCE AND OTHER RELATED PARAMETERS OF A DAYLIGHTING SCENARIO FOR AN INDUSTRIAL BUILDING*

Musa Demirbaş¹, Türker Fedai Çavuş², Ceyda Aksoy Tırmıkçı² and Cenk Yavuz²

¹*Arçelik R&D,*

²*Sakarya University*

E-mails: musa.demirbas@arcelik.com; tfcavus@sakarya.edu.tr, caksoy@sakarya.edu.tr, cyavuz@sakarya.edu.tr

ABSTRACT

Field measurement method is used in this paper to analyze the energy saving potential of an industrial building. A daylight responsive automated lighting control system application is implemented and the energy consumption of the building is observed for a year. Daylight trespass enabled by using two holes at the roof of the building which have spherical lenses. In conclusion energy savings of the building is related to the sunshine duration parameter.

Keywords: light automation, daylighting, energy efficiency, lighting energy savings

INTRODUCTION

Worldwide energy consumption has been growing rapidly. However, the ways that the energy is produced are not sustainable in most of the countries. It is not easy to switch these ways to alternative clean technologies in a very short time. Thus improving energy savings are essential to reduce the environmental effects of energy production [1].

The buildings have a large share in energy consumption, 30 % of global total final energy con-

sumption [2]. A considerable portion of this share, more than 25 %, is used for lighting [3]. Studies have shown that daylight responsive lighting control systems can significantly reduce this share [4–6]. Different methods have been used for estimating the energy saving potential of these systems: field measurement, software simulation and manually calculation [7].

Literature shows that lighting energy savings vary between 20 % and 68 % with field measurement [8–11], 25 % and 87 % with software simulation [12–14], 30 % and 95 % with manually calculation [15–17]. Software simulation and manually calculation are easy, economic, and effective methods. However, field measurement method, is more accurate since a real measurement is performed including all the design parameters.

In this paper lighting energy savings of an industrial building in Turkey are obtained by field measurement method in a 1-year period.

EXPERIMENTAL SET-UP

The industrial building investigated in this paper has a surface of 180 m² (Fig. 1). The building is lightened by means of 8 fluorescent luminaires at all hours of the day and night. The luminaires have an electric power of 58 W and provide an illuminance level of 150 lx for the related area consisted of a walking route and stocking zones. The building is lack of daylight since there is no win-

* On basis of report at the 1st International Conference on Green Technologies and Energy Efficiency". Sakarya, Turkey, 28 September – 01 October.



Fig. 1. Experiment area



Fig. 2. The daylight sources implemented in the ceiling of the building

dow (Fig. 1). Thus two holes are constituted in the ceiling to perform the application of daylighting illumination (Fig. 2).

The current illuminance level of the building is determined via image processing methods. Images of the buildings are captured by a camera mo-

onitoring system simultaneously. Then the greyness level of the images obtained by the camera is correlated to the illuminance level of the building and transformed into an electrical signal by NI USB-6221 I/O.

The control of the automated system is carried out by a PLC. The electric signals by NI USB-6221 I/O are evaluated in PLC to adjust the illumination level requirements of the building, 150 lx, by switching the luminaries on and off.

EXPERIMENT RESULTS

1. Lighting Energy Savings and Sunshine Duration

Energy consumption of the system is observed by PAC3200 analyser. Table 1 presents the monthly consumption, the monthly saving and monthly saving percentages in the experimental period (January 2015-December 2015).

Fig. 3 presents the monthly average daily sunshine hours of Kocaeli during the experimental period. According to the figure, the sunshine hours increase from January to July. In this period, monthly saving percentage increases as well (Table 1). The longest sunshine hours are recorded in July (Fig. 3). In this month, maximum of energy savings is provided (Table 1). After July, the sunshine hours start to decrease and monthly lighting energy saving percentage starts to decrease as well.

Fig. 4 presents the comparison of the seasonal average daily lighting energy consumption before and after automated lighting system. Here the warm period of the year (April-September) is considered as summer and the cold period of the

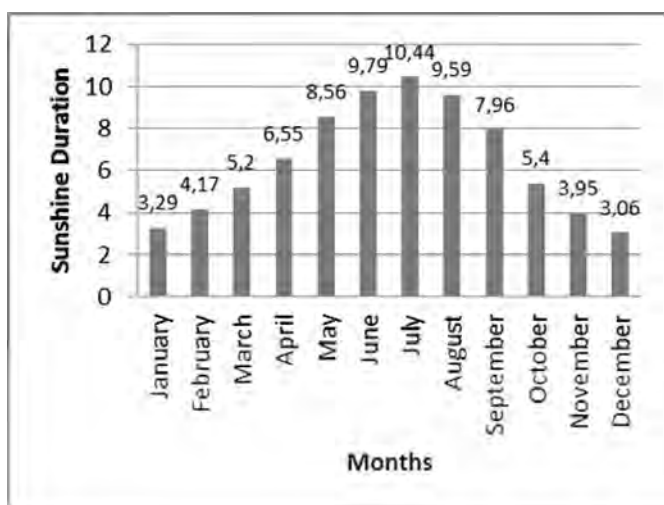


Fig. 3 Monthly average of daily sunshine duration for Kocaeli

Table 1. Monthly energy consumption of the automated lighting system

Month	Monthly Consumption, kWh	Monthly Saving, kWh	Monthly Saving, %
January	437,26	217,78	33,25
February	394,98	197,87	33,40
March	409,94	240,97	37,02
April	370,27	265,48	41,76
May	384,61	273,83	41,89
June	343,82	295,38	46,21
July	325,92	326,42	65,23
August	327,52	330,39	50,22
September	341,82	295,70	46,38
October	408,4	241,44	37,15
November	396,72	234,00	37,10
December	435,36	223,09	33,88

Table 2. Annual energy consumption of the building before and after the experiment

Annual energy consumption before the experiment, kWh	7718,47
Annual energy consumption after the experiment, kWh	4576,62
Difference after the automated system loaded	3141,85

year (October-March) is considered as winter. From the figure it is observed that the monthly consumption dramatically decreases in summer months due to the longer sunshine hours.

The results obtained from Table 1, Fig. 3 and Fig. 4 are indicate that there is a strong relation between the lighting energy consumption and sunshine hours in a daylight responsive lighting control system.

II. Lighting Energy Savings and CO₂ emission

Table 2 presents the annual energy consumption of the building before and after the experiment. From the table it is observed that 3141,85 kWh of energy saving is provided with a daylight responsive automated lighting control system in a year. This saving equals to prevention of 2.042 tons CO₂ emission by the building.

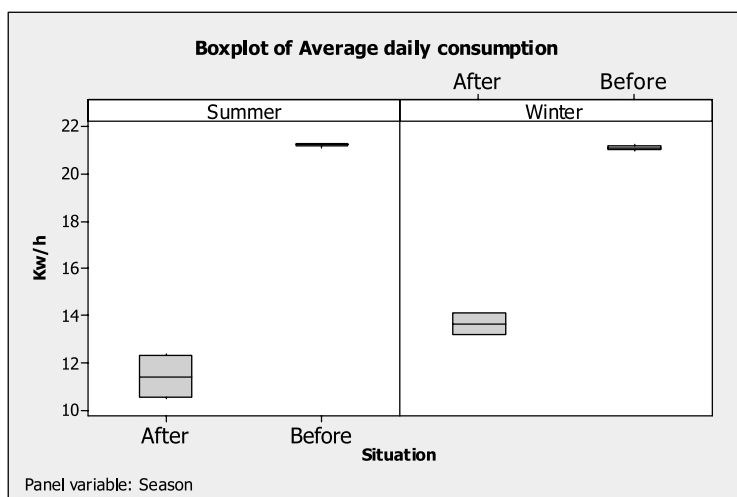


Fig. 4. Seasonal average daily lighting energy consumption before and after automated lighting system

CONCLUSION

The behaviour of a daylight responsive automated lighting control system is observed for a year in this study. The results indicate that energy savings is strongly related to the sunshine duration of the experimental area. On a monthly basis, energy savings increases up to 65.23 % in summer and decreases to 33.25 % in winter.

Comparing to previous similar studies held with continuous dimming systems in same climate conditions [18] this study indicates that no matter, which system is used for light automation, there is always a high probability for a big ratio of energy savings. Whether on-off systems or continuous dimming systems are equipped in working zones up to 45 % of lighting energy saving is possible.

Saving electric energy is also saving the world from greenhouse gas emissions. More than 2 tons of CO₂ emission is prevented by this system just for a 180 m² area. Expanding this result to the whole building or even to the all Industrial area along Kocaeli city would be great addition and help to environmental pollution prevention.

REFERENCES

1. World Energy Resources 2013 Survey: Summary. World Energy Council.
2. Energy Efficiency Market Report 2015. Internat. Energy Agency <http://www.iea.org/publications/free-publications/publication/MediumTermEnergyefficiencyMarketReport2015.pdf>.
3. S.K.H. Chow, D.H.W. Li, E.W.M. Lee, J.C. Lam, Analysis and prediction of daylighting and energy performance in atrium spaces using daylight-linked lighting controls, *Appl. Energy* 112 (2013) 1016–1024.
4. Yun GY, Kim H, Kim JT. Effects of occupancy and lighting use patterns on lighting energy consumption. *Energy and Buildings* 46 (2012) 152–158. doi:10.1016/j.enbuild.2011.10.034.
5. J.D. Jennings, F.M. Rubinstein, D. DiBartolomeo, S.L. Blanc, Comparison of control options in private offices in an advanced lighting control testbed, *Journal of the Illuminating Engineering Society* 29 (2) (2000) 39–60.
6. R.R. Verderber, F.M. Rubinstein, Mutual impacts of lighting controls and daylighting applications, *Energy and Buildings* 6 (1984) 133–140.
7. Yu X, Su Y. Daylight availability assessment and its potential energy saving estimation –A literature review. *Renewable and Sustainable Energy Reviews* 52 (2015) 494–503. <http://dx.doi.org/10.1016/j.rser.2015.07.142>.
8. Onaygil S, Güler Ö. Determination of the energy saving by daylight responsive lighting control systems with an example from Istanbul. *Build Environ.* 2003;38:973–7.
9. Atif MR, Galasiu AD. Energy performance of daylight-linked automatic lighting control systems in large atrium spaces: report on two field-monitored case studies. *Energy and Buildings* 2003;35:441–61.
10. Lee ES, Selkowitz SE. The New York Times Headquarters daylighting mockup: monitored performance of the daylighting control system. *Energy and Buildings.* 2006;38:914–29.
11. Li DHW, Cheung ACK, Chow SKH, Lee EWM. Study of daylight data and lighting energy savings for atrium corridors with lighting dimming controls. *Energy and Buildings* 2014;72:457–64.
12. Li DHW, Wong SL. Daylighting and energy implications due to shading effects from nearby buildings. *Appl Energy* 2007;84:1199–209.
13. Yun GY, Kong HJ, Kim H, Kim JT. A field survey of visual comfort and lighting energy consumption in open plan offices. *Energy and Buildings* 2012;46:146–51.
14. Bodart M, De Herde A. Global energy savings in offices buildings by the use of daylighting. *Energy and Buildings* 2002;34:421–9.
15. Doulos L, Tsangrassoulis A, Topalis F. Quantifying energy savings in daylight responsive systems: the role of dimming electronic ballasts. *Energy and Buildings* 2008;40:36–50.
16. Li DHW, Lam TNT, Wong SL. Lighting and energy performance for an office using high frequency dimming controls. *Energy Convers Manag* 2006;47:1133–45.
17. Chow SKH, Li DHW, Lee EWM, Lam JC. Analysis and prediction of daylighting and energy performance in atrium spaces using daylight-linked lighting controls. *Appl Energy* 2013;112:1016–24.
18. Yavuz, C, Yanikoglu, E, Guler, Ö, “Evaluation of Daylight Responsive Lighting Control Systems According to the Results of a Long Term Experiment”, *LIGHT & ENGINEERING*, Vol. 20, pp. 75–83, December, 2012.



Musa Demirbař

received B.S. degree in Electronics and Communications Engineering from Yıldız Technical University, in 1996. He received M.S. degree in Electronics and Communications Engineering from Istanbul Technical University, in 2003. He finished his Ph.D. in the Department of Electrical and Electronics Engineering at Sakarya University, in 2015. He has been working at Arçelik A.Ş. Cooking Appliances Plant R&D Department since 1997



Türker Feadi Çavuş

received the Electrical Engineering degree from Istanbul Technical University, Turkey in 1995. Later, he obtained his M.Sc. and Ph.D. degrees in Electrical Engineering from Sakarya University (SAU) in 1998 and 2004 respectively. He has been working as an Assistant Professor at SAU Electrical and Electronics Engineering Department since 2005. His current research interests include lighting applications, reliability in energy systems and high voltage technique. Dr. Çavuş is a member of Turkish Chamber of Electrical Engineers



Cenk Yavuz

received the Electrical and Electronics Engineering degree from Sakarya University (SAU), Turkey in 2002. Later, Yavuz obtained his M.Sc. and Ph.D. degrees in Electrical Engineering from SAU in 2004 and 2010 respectively. He is currently an Associate Professor at SAU Electrical and Electronics Engineering Department. His current research interests include daylighting applications, lighting energy savings, energy efficiency and energy quality in lighting. Dr. Yavuz is a member of Turkish National Illumination Committee



Ceyda Aksoy Tırmıkçı received the B.Sc. and M.Sc. degrees from Ege University in 2011 and Sakarya University 2013 respectively. Her present research interests are photovoltaic system applications. She joined the Electrical and Electronics Engineering Department at Sakarya University in 2012 where she is a assistant researcher at present

LIGHTING QUALITY SUPPORTED BY SOFTWARE AND APPLICATION OF INCREASING THE EFFICIENCY*

Mustafa Zeytin and Nazım İmal

Bilecik Şeyh Edebali University,
E-mails: zeytin2000@yahoo.com; nazim.imal@bilecik.edu.tr

ABSTRACT

The quality of lighting made by daylight or other light sources is as important as the physical size. It is known that, people are affected psychologically from the illuminance and correlated colour temperature of the place where they live, and the people who are in places with different colour and design could react different to the same stimulants. Qualitative and quantitative properties of lighting are so important for visualization. Quantitative properties are luminous flux, intensity and illuminance. Likewise the qualitative properties are correlated colour temperature and colour rendering index of the light. At this work, the value of correlated colour temperature and illuminance for a sample medium are optimized by using colour sensor and software. In optimization, the approach to the ideal lighting which is productive and economic is aimed by making data groups with measured data. These data groups are used by PIC microprocessor and PLC compound system so as to make the illuminance approach to demanded values. Measures were done with different dots to see the changing in lighting quality and productivity by determining the best sensor position. The sensor produces some base data with daylight. Energy possession is made in case the daylight data are enough

and no extra lighting source is needed, so measurable possession data are gathered.

Keywords: light, colour, illuminance, colour rendering, set value, PIC, PLC

1. INTRODUCTION

Lighting, which could be made with lots of waste despite insufficient light flux with flaming lighting devices in the past, became an important concept, which was handled together with its quality since the time of the end of 19th century, especially when the electricity began to use as commercial. For the electrical lighting which the quantitative property is more important in the first half of the 20th century, qualitative properties began to be important in the second half of the 20th century.

For a lighted surface, quantitative property is described as illuminance ($E: lx$), qualitative properties are described as colour rendering index (CRI) and luminance (cd/m^2). Therefore, beside a light flux, which comes from a lighting device, specification in colour gets important as much as the flux. For instance, although the productivity of light flux is so much high, the sodium steam discharge lamps are not preferred in indoor lighting.

Colour is called as a physical effect, which can be sensed by a persons' eye and reflected by not being sucked according to the matter that the light crashed and being in wavelengths which makes the light. Colour effect constitutes the fundamental of lighting together with illuminance concept.

¹ On basis of report at the 1st International Conference on Green Technologies and Energy Efficiency". Sakarya, Turkey, 28 September – 01 October.

That is why the lighting and colour quality are the main effective factors directly, optimum solutions must be gathered by evaluating lighting with colour, colour rendering index and illuminance parameters.

In this study, how the lighting and colour levels, which belong to their mediums, can be optimum and how the optimum level gets stable with which parameters were investigated. An application method was developed by making some labours convenient with the aim of implementing of this stability. At the application method developed:

- Determining the best colour and illuminance;
- Assigning the value to the parametric variables according the criteria determined;
- Implementing the algorithmic operations by software according to the values assigned;
- Getting the highest level of productivity;
- Energy possession was done by the daylight effect which was included.

2. LIGHTING QUALITY AND PRODUCTIVITY

With this study, quality lighting which is commanded automatically convenient with the light sources selected with compatible properties (colour rendering index, correlated colour temperature, energy consuming and function) and their logical diagrams and flow charts is aimed. Besides, that is why the daylight effect was included; the productivity in lighting design was increased.

It was implemented that the light was sensed and transformed to a digital data, which was compared with the desired data and the most convenient light sources were turned on according to result of this comparison. A special sensor was used for sensing the light. Colour light sensor, a kind of special sensor, has a structure to able to transform a colour full light to an analogue signal and produces a voltage in DC form on its output. Its working principle is based on sensing the three fundamental colours, which are called as Red, Green, Blue (RGB). It can resolve the voltage output of any colour of RGB, in case that one of them is sensed. Besides, this sensor can divert the output voltage according to the light flux level and produce a total output value according to light flux and colour in the medium.

Placement location of the sensor is critical to the parameters obtained. Therefore, in outdoor lighting applications, sensors must be placed in accordance with the calculated vector coordinates. In this study, since the basis of interior lighting applications, the sensor was placed in a point on the ground, where is received an average horizontal illuminance. If a colour filtering is desired, it will sense the colour of the light which is filtered, and give an output when it senses that colour.

DC voltage, which is gathered from the sensor output, is transformed to 10 bit of data by an electronic analogue-digital transforming card of 10 bits. Thus, sensor bits are made for inputs of PLC (I0.00-I0.09). Analogue-digital circuits, used in application, were implemented with PIC microprocessors. One of the circuits transforms the analogue voltage, which is gathered from the sensor, and the other transforms that of which is gathered from potentiometer to 10 bit of digital data. On Fig. 1, the position of the sensor in application model; on Fig. 2, the scheme of ADC set circuit; on Fig. 3, the working situation of the light sources mounted to the roof of the model are presented.

3. CONTROL CIRCUIT

PIC was used as the main microprocessor in control circuit. Two reference voltages were described for the microprocessor. Reference voltages determine that of in which reference range the analogue voltage would be transformed.

Digital data, which are gathered after transforming, remain in reference range entered.

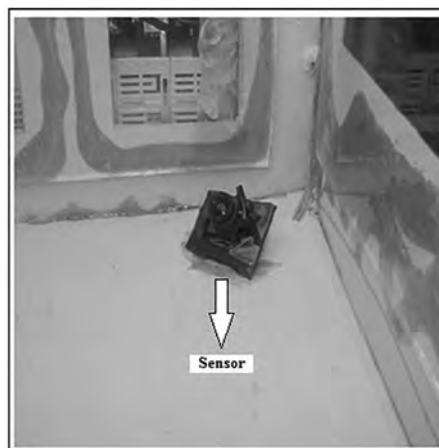


Fig. 1. The position of the sensor in model

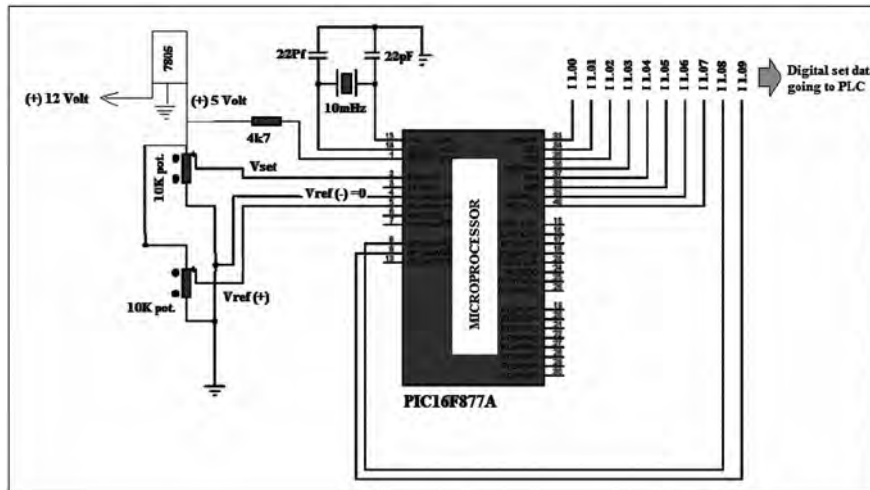


Fig.2. ADC circuit [2]

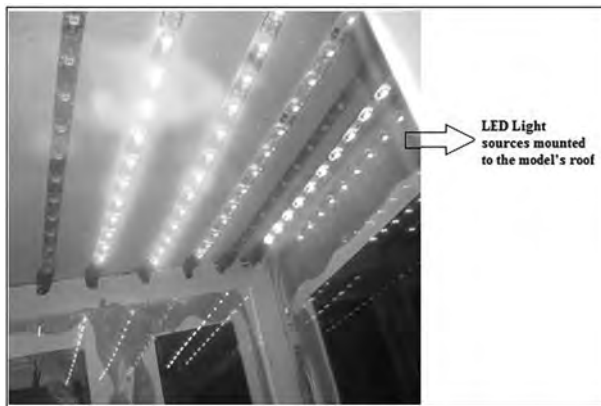


Fig.3. Light sources in different colours

On setting circuit, setting voltage is added by potentiometer according to the medium conditions.

On set circuit, there is a potentiometer so as to put the desired set value into effect. The digital transforming of this set value is made implemented by microprocessor owing to the potentiometer.

Table I. Symbolic equality of light sources

Colour of Light Sources	PLC Output Q(100.0n)... n=queue number	Representative Symbol
Blue	Q(100.00)	a
Green-2	Q(100.01)	b
Green-1	Q(100.02)	c
Red-2	Q(100.03)	d
White	Q(100.04)	e
Red-1	Q(100.05)	f

Reference voltages were determined as 0 and 5 Volts. Because the total voltage of the light sources on the roof of model was about 5 V, it was implemented that the microprocessor would work in the range of 0–5 V. Because the low line reference voltage which is one of the reference voltages to be sent to microprocessor as input, 0 V, the mentioned input was connected to ground. The outputs, which are “logic 1 (analogue 5 V)” were transformed to 24 V of DC value by an integrated circuit called as “ULN2803”. “Common” or “com” voltage of “ULN2803” was energized with 24 V DC and owing to this, the logic 1 bits on the output of microprocessor were sent to input of PLC as 24 V DC. Crystal oscillator frequency was kept in the range of between 10 MHz and 20 MHz.

The outputs of PLC were symbolized as letters so as to be understood easily. Therefore, all combinations were symbolized by letters and there was no need to write the output colour for every combination. On Table 1, it was seen which light source was symbolized with which letter.

All possibilities of light sources were exposed and the voltage data, which are the equity of these possibilities, were measured and saved for PLC program. These were loaded to virtual registers independently in PLC program. These data loaded to registers are the values which the sensor always measure and ones which could divert in any time. These values were compared with the set voltage value desired or arranged in set circuit in PLC. The difference occurred at the result of comparison was compared for second time again with the database in registers.

3.1. PLC programming circuit

PLC programming was done for Omron CQM1-H PLC type. All programs were gathered in “STL” form after being written in ladder diagram. While the data bits, which came from set circuit, were being connected to an input card the bits, which came from sensing circuit, were sent to the other input card of PLC. These digital data which came to every input card, were saved to intern (virtual) PLC relays. All voltage values were gathered one by one and a database was formed by being saved to PLC registers.

PLC calculates what input value is bigger than the other after making a comparison between the data, which come from set and sensing circuits by evaluating the difference between them. It decides what light source or sources will be turned on or off at the amount of the difference.

PLC implements a lighting regulation by using the daylight at this working style. But, while this application is being implemented, the position of the light sources selected and their voltage capacities are too much important. Because PLC works so sensitive, it senses even a little change that comes from the sensor. To minimize the instability some regulations were made with the present sensor but they don't work. So, by making some changes in the program (software), a description for the interval between the voltage values those the sensor produced as a wide range of interval and a more stable working was done.

4. WORKING PROCESS OF THE SYSTEM

Measured data done to work the system are shown on the tables below. The data measured on these tables were gathered while the daylight was getting down. On Table 2, the daylight voltage was read 0,70 V DC in sensing and at 0,50 V DC voltage, it was seen that some light sources were turned on.

At this table, because the colour rendering index was done, PLC program did not turn on any light source. As long as the data measured from the daylight is bigger than the set value, no light source is turned on. When the set value gets bigger than the data from the daylight, PLC program begins to scan the most convenient light sources. System compensation is being done by turning

Table 2. Results of the test of set voltage-1

Set Voltage, Volt DC	Sensing Voltage, Volt DC	Turned on Light Sources
0,50	0,7 (Daylight: 0,7 V)	-
		-
		-
		-
		-
		-

Table 3. Results of the test of set voltage-2

Set Voltage, V DC	Sensing Voltage, VDC	Turned on Light Sources
1,00	1,04 (Daylight: 0,7 V)	a
		b
		-
		-
		-
		-

on the most suitable light sources so as to minimize the difference of voltages between set value and the daylight data.

On the Table 3, the light sources, which are turned on for 1 V of set value while the colour rendering index is getting down, is shown. The set voltage desired here is 0,30 V bigger than the voltage which the sensor read. So, PLC turned on the light source called as “c” and “b” and decreased the difference to 0,04 V. Owing to this, set voltage was done as 1 V of value. The set value was gathered by the daylight (0,70 V) and light sources (0,30 V) turned on.

Similar applications were tested by taking the application module to different mediums. Just as the applications are seen with only one light source, according to the level of lighting and colour sensing some applications with a few light sources even all sources were implemented.

5. LIGHT EFFICIENCY

Nowadays, energy possession became an indispensable element of lighting projects. In this paper, the working integration of light sources

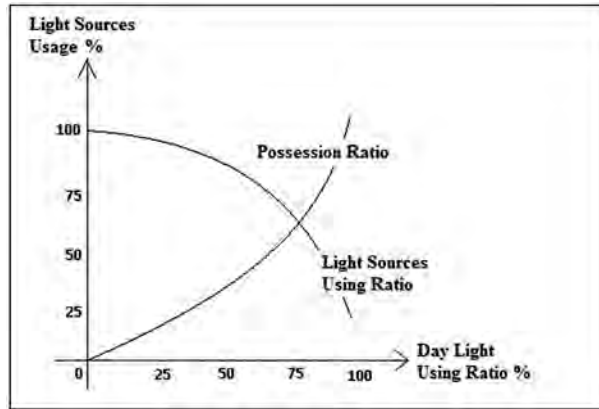


Fig. 4. The relation between possession and the using ratio of light sources.

and daylight was implemented and measurable energy possession was done by turning off some light sources. It was seen that the mentioned possession differed according to the ratio of getting daylight. On Fig. 4, a changing graph of possession and light sources using ratios according to the daylight usage. As it is seen on the graph, this possession ratio could be 100 percent depending on using ratio of daylight. With the increased use of daylight, decrease in the use of LED structures will improve energy efficiency. In this case, LEDs used in the circuit, are aimed to regulate the colour for perceived the light of day.

CONCLUSION

Lighting and colour level in the mediums where people live effect not only human psychology but also increase working productivity of them. Thus, the thing of keeping the desired lighting and colour level in mediums gets fast and easy means getting possession in energy and personal. In application a model medium was done. The total lighting and colour levels in the model medium was measured by a sensor and with these measures a comparison between the desired coloured illuminance and the coloured lighting in the present medium was made. By this comparison, increasing of colour rendering index by compensating the deficient colours is aimed. By increasing the colour rendering index, owing to turning on the less lighting source, an increasing in lighting efficiency was made as well. As it is seen in application, a comparison between the desired and set colour rendering index and illuminances is made and fast convergence to set value is determined.

For different illuminances and colour returns, at measuring data in different dots, it was seen

that, the voltage values increased when the sensor got nearer to light sources and compensated the system by turning on the less light sources. Thus, the voltage value which is gathered by accumulating the voltage values of more than one sensor in different dots and calculating the average value is admitted as the based fundamental voltage value. After an analysis with multi doses to determine the best sensor position, it was thought that a dot, which the light sources were all seen and the daylight was used the most, would be the most efficient dot. In addition, it was seen that the stability of the sensor used is too much important in these kinds of applications. It was determined that the stability of PLC in controlling its outputs changed depending on being stable of the sensor used completely. And it was observed that it would be so important to get care about the sensor used for being sensitive and too stable.

REFERENCES

1. Özbudak Y.B., Gümüş B., Çetin F.D. In Turkish "In indoor lighting, color and lighting relationship" D.Ü. II. Ulusal Aydınlatma Sempozyumu, 2003.
2. Miyasawa N, Nakamura Y, Wakasa N., "Effect of personal adjustment of brightness on the satisfaction of office lighting" *Journal of Light and Visual Environment*, 27, 2, 92–106. *Lighting Research and Technology*, 31, 3, 107–115, 2003.
3. Gençoğlu M.T., Özbay E., In Turkish "Lighting Energy Efficiency Methods", XII. Elektrik, Elektronik, Bilgisayar, Biyomedikal Mühendisliği Ulusal Kongresi, Eskişehir, 2007.
4. Shikakura, T., Marikawa H., Nakamura, Y. "Perception of lighting fluctuations in Office lighting environments" *Journal of Light and Visual Environment*, 27, 2, 75–82, 2003.

5. Katar İ., In Turkish “Microcontrollers Text-books”, 2006.
6. Özbudak Y.B., Gümüş B., Çetin F.D., <http://www.emo.org.tr/ekler/0db17c6772e2a26_ek.pdf/>, 2012.
7. Gabriela R., “Color temperature and illuminance levels in offices” 25th Session of CIE Proceedings, 2, San Diego, 2003.
8. Anonym2, <<http://www.profahmet.tr.gg/PIC16f877-10Bit-ADC.htm/>>, 2012.
9. Anonym1, <http://www.sure-electronics.net/download/DC-SS501_Ver1.0_EN.pdf>, 2012.
10. Duff T. P., “Modular Solid State Lighting Apparatus Platform With Local And Remote Microprocessor Control” United States Patent Application 20160128157, 2016.
11. Ying W.B., “Automatic room light intensity detection and control using a microprocessor and light sensors” IEEE Transactions on Consumer Electronics (Volume: 54, Issue: 3), 2008.



Mustafa Zeytin

graduated electrical and electronics undergraduate and graduate degrees. He works in Bilecik as electrical and electronic engineer. Also, he has been studying on his academic career at the Bilecik Şeyh Edebali University. Academic career stage is preparation of Ph.D. thesis. His field of interest is electrical energy systems, control systems, and lighting



Nazım İmal,

Dr., Assistance Professor in Bilecik Şeyh Edebali University Energy Systems & Electrical and Electronics Engineering Department, his directions of science are electrical power systems and lighting

A CHROMATIC CONCEPTUALISATION OF NATURAL LIFE

Nikolai L. Pavlov

The Moscow Architectural Institute (State Academy), Moscow
E-mail: pavlovn@mail.ru

... research into the possible connections between physiological and cultural processes is still in its infancy.

Edward O. Wilson

ABSTRACT

The article considers the difference between Newton and Goethe's understandings of light spectral composition. Elaborating on the subject, it is suggested that in many cultural traditions certain colours and their combinations represent and symbolise evident origins of natural life and aspects of the structure of the Universe. It can be seen that these colours, apparently, are exactly caused by specific properties of human sight and have a clear priority in the perception system and, accordingly, within the composition of language.

Keywords: colour, nature, physiology, culture

Isaac Newton performed light decomposition experiments using a prism, and discovered a spectral scale of seven primary colours. We still use this scale today. Before Newton, such scales existed in different variations since Antiquity: they usually consisted of three or five primary colours.

A feature of Newton's chromatic scale is that it was easily and naturally integrated into natural numerical series and stimulated the emergence of a cultural numerical series. The seven-day phase of the Moon – the natural lunar cycle – when transposed into the cultural context led to the determination of the seven day week, and hence the lunar month consisting of four weeks.

This basic natural cycle can be traced in many systems of concepts about completeness of life and

about a full life cycle. In Ancient Egypt, temple colonnades which represent the generation of life, for example the temple in Luxor (Ipet Resyt) (Fig. 1), are formed of rows of seven columns to symbolize the full life cycle of a person. Completeness of life is reflected in numerous folklore texts from different cultural traditions connected primarily with ideas of a comprehensive family with seven children. For example, in the Russian tradition: seven from one pod, seven Simeons, seven on benches, seven don't wait for one, etc.

Goethe, in his Theory of Colours retorted heatedly against Newton's scale. Based on the variety he observed, he described a dialectics of colour interaction. In doing so, Goethe consid-



Fig. 1. Temple of Luxor (Ipet Resyt). Colonnade of two rows of seven columns embodying completeness of the human life cycle



Fig. 2. Gold of yellow colour, colour of the sun, colour of a deity:

a – Moscow. The Kremlin. Blagoveshchensky cathedral. Gold domes; *b* – Moscow. Ascension church in Kolomenskoe. The temple is projected from a gold orb-sun; *c* – St Peterburg. The Admiralty building. Gold spike being sun ray is projected from a gold ball-sun; *d* – Germany. Zost. Church of St Patroclus, the Tent is projected from a gold orb-sun; *e* – Myanmar. Shwedagon Pagoda. The huge mortar is projected from a gold bud-sun; *f* – Byzantium. Fatih Jami. The Pantocrator with a gold nimbus in the dome lunette; *g* – Vologda. An icon. A gold nimbus over the head of the sacred; *h* – India. Ajanta. Painting of a cave monastery. Gold nimbus over the head of Buddha; *i* – Persia. A huge gold nimbus over head of the divinified Khosrow II; *j* – Nepal. Kathmandu. Kala Bhairava – all-devouring time deity in a gold aura

red colours both in themselves and colour ratios to be inseparably connected with their perception by human eyes [1, p. 21– 62].

Developing this subject, it can be noted that in many cultural traditions chromatic realities and their perception by humans have formed entire systems, in which colours represent natural origins of life.

In this way yellow is naturally associated with the sun and with sunlight; the solar colour of gold representing an eternal metal. This idea is reflected in language as well. For example, in the In-

do-European language family, colour of the gold-sun is connected with the radical “cr – chr”. In Sanskrit gold is named *chiranya*, in Greek it is *chrysos*¹ (χρυσός). Accordingly, names of yellow pigments are ochre and crown.

Historically, the time of day was determined by the sun. Therefore, the ancient god of time was Cronos, derivative Kronos, who the Time devour-

¹ Accordingly, in Buddhism, as well as in many other traditions, the higher, unshakable celestial stronghold is gold, in Sanskrit it is *charmya*.



Fig. 3. Ancient Greece. Blue is the colour of the sky and the colour of water (celestial ocean). Blue in triglyphs and in drops under taenias and mutules represents a vertical outflow of celestial waters. On the pediment field, blue is the background for statues of gods, representing the colour of the sky

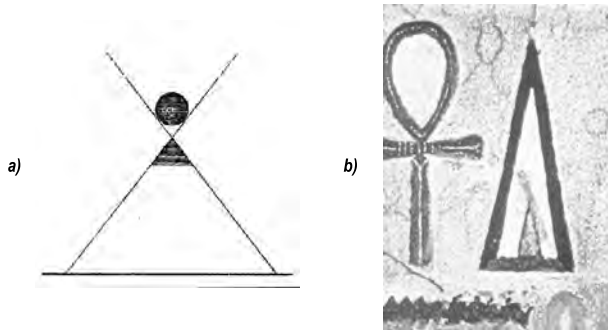


Fig. 4. Ancient Egypt:
 a – a pyramid with gilt vertex is projected from the sun; b – the pyramid hieroglyph outside and inside is edged with green colour: sunlight gives life the all vegetation

ing his own children. A chromatic sacral sun shade of gold is apparently present in the name of the God-Man: the Christ and accordingly also in the term meaning the place of God’s presence: *Khram* (temple) (Rus.), *kirche* (Ge.), *church* (Eng.).

In iconography this subject is expressed by gold, solar nimbuses of God and the characters accompanying Him: angels, evangelists, holy

men. In architecture this subject is directly expressed using golden domes, spires and their gold ball-sun tops, from which as from the sun, the whole temple is projected [2 p. 140 – 161] (Fig. 2).

Time has the colour of the sun, which itself is used to determine time.

The colour blue naturally corresponds with the colour of water and of the sky; the heavenly ocean, from which celestial God’s grace arrives as rain arrives to earth: water is a source of life. In daily antique traditions, time appeared in two ways: as solar time (sun dials) and as the outflow of celestial waters (water clock).

In the tradition of antique temples, the descent of this celestial holy grace was connected with the colour blue within an entire system of architectural elements. A pediment field, against the background of which antique gods were presented in the “celestial world”, was painted in blue, as the colour of the sky and the colour of waters of the celestial ocean. Vertical details of the order representing the outflow of celestial holy grace,

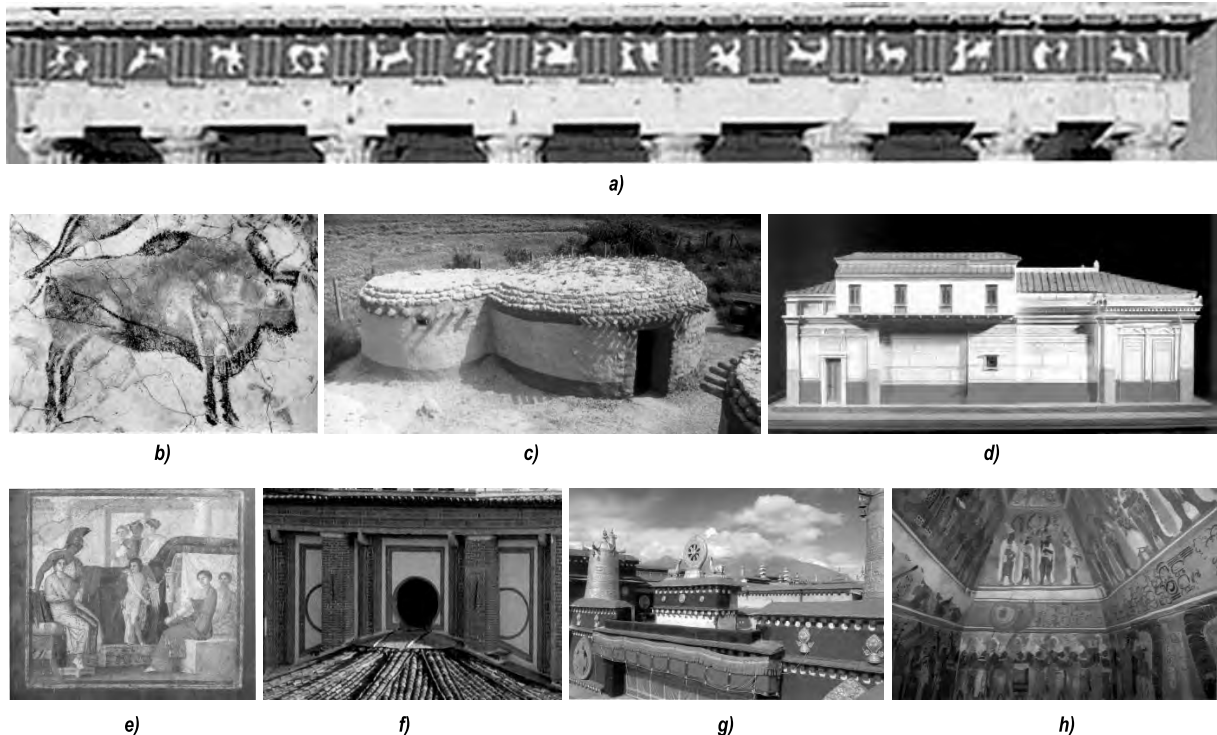


Fig. 5. Red is the colour of blood, colour of animal and human life:

a – Ancient Greece. Parthenon. Metope boom under the temple cornice on the red background expresses the heroic history of the Greeks. Reconstruction; b – Paleolithic Spain. Altamira cave. A chain of bull images on the walls of the primeval cave. Red ochre; c – Neolithic Cyprus. Lempa. A residential building is encircled with red ochre under the cornice and along the socle; d – Ancient Rome. Pompeii. The house is encircled with a red socle. Reconstruction; e – Ancient Rome. Pompeii. The fresco on a villa wall is surrounded by a red frame; f – Renaissance Italy. Milan. Bramante. Church of Santa Maria delle Grazie. Red edges on the facade surface; g – Tibet. Samye Monastery. Red friezes under cornices of the temples; h – Mexico. Mayan culture. Bonampak. A red belt of paintings under the temple vault expresses the heroic history of the Maya

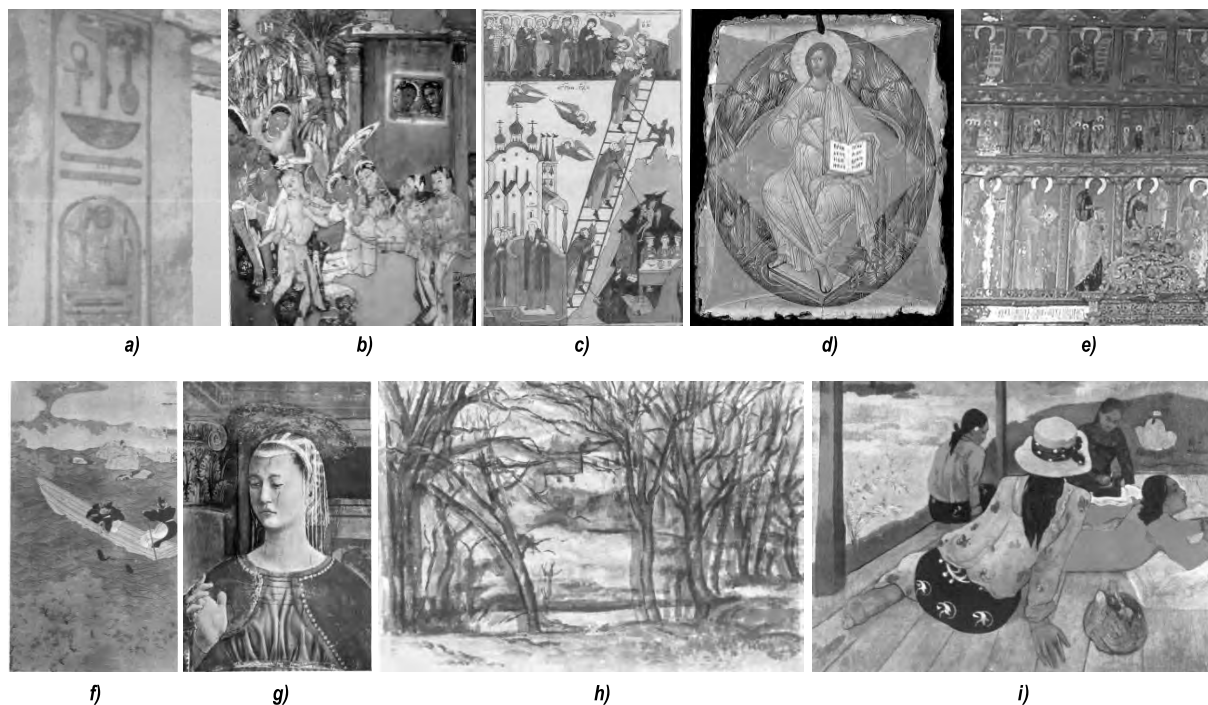


Fig. 6. Combinations of green and red colours represent a harmony of vegetative and animal life. Painting: *a* – Ancient Egypt. A painting in the temple of Rameses III; *b* – Ancient India. Ajanta. A painting on the walls of the cave monastery; *c* – Russia. An icon. Subject of Lestnitsa (stairs); *d* – Russia. An icon. Christ in Majesty; *e* – Russia. An iconostasis; *f* – Japan. A picturesque canvas; *g* – Italy. Renaissance. Piero della Francesca; *h* – France. Cezanne; *i* – France. Gauguin

which was water-time, were painted in blue: tri-glyphs (months of three decades), taenias and drops under them ($6 \times 2 = 12$ drops-months of the year in each bay), mutules and drops under them ($3 \times 6 \times 2$ drops-decades is a year in each bay). In antique architecture, the system of water circulation between the sky and earth was represented as a general ring vertical structure of water circulation and the “hydro-biological natural cycle” [2, p. 253 – 280] (Fig. 3).

Considering the theme of colour mixing proposed by Goethe, it should be stated that yellow associated with sunlight, and blue associated with the colour of water, once mixed create green, which is the colour of vegetative life. Colours of sunlight and of water are represented as two foundations of life on earth. In ancient Egypt, inside a gold or yellow (solar) hieroglyph «pyramid», a little green wedge of vegetative life was located (Fig. 4).

Red being the colour of blood and colour of life (Fig. 5), was already widely used in cave painting of primitive hunters, who used red ochre: recent research has shown that it was specially burnt from ferrous minerals.

The colour red, which was colour of blood and human (animal) life, in the antique temple tradition was expressed by the circle of life represented by horizontal ring structures along the whole perimeter of the temple: a shelf under the cornice, top and bottom shelves of the frieze and circular red slots (annulets) under echinus of Dorian capitals. In the boom of metopes of the ring frieze, which showed the stories of epic battles (Lapiths with centaurs, Greeks with amazons, etc.) red dominated as a background. The same subject was reflected in the ring construction of Greek vases with red figures.

Red-brown terracotta booms under cornices are typical for the Etruscan tradition. Later on in wall paintings of rich Roman villas, separate plots were wrapped in red frames. In these later renditions, lifelike pictures of gods and people were already closed in the vertical plane. Red booms and red frames on facades were typical for the Renaissance as well. For many other traditions distant from Europe, horizontal rich red booms under cornices and in paintings are typical. In the process of painting transformation into secular easel art, they started to make picture frames out

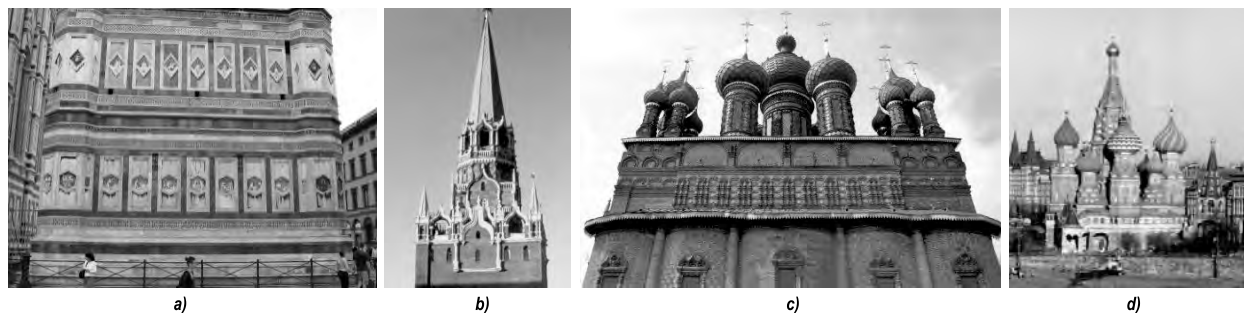


Fig. 7. Combinations of green and red colours represent a harmony of vegetative and animal life. Architecture: *a* – Italy. Florence. Giotto. Bell tower of Santa Maria del Fiore cathedral. Shades of green and red marble; *b* – Russia. Moscow. Spasskaya tower of the Kremlin. Red brick and green tiles; *c* – Russia. Yaroslavl. John the Precursor's church in Tolchkov. Red brick and green tiles; *d* – Russia. Moscow. Intercession cathedral on the Ditch. Red brick and green tiles

of precious mahogany, and then to make pictures more impressive and divine with gilt frames.

A combination of the colour green associated with vegetative life, and the colour red associated with animal (human) life and with blood was perceived as harmonious and represented a natural harmony of these two forms of life.

In painting, different combinations of red and green colours represented this special sort of harmony. In painting, red and green, as well as blue and yellow were considered to be complementary colours. Such combinations are typical not only for different iconographic traditions but also for best paintings of the Italian Renaissance, which grow out of antique and east Christian Byzantine traditions. The harmonious combination of green and red colours is richly presented in Russian iconography and in painting of different cultural traditions (Fig. 6).

Such a harmony in traditional Russian architecture is expressed by combination of red brick and green ceramic tiles. On the ribs of the tented roof of Spasskaya tower of the Moscow Kremlin, green (vegetative) colour is penetrated with inserts of yellow (solar) tiles falling from the gold orb sun (Fig. 7).

Modern research on colour perception shows that these four colours: red and green, yellow and blue are the first in terms of perception intensity and by mention frequency in different languages. It is interesting that as far as perception of these four colours goes, modern science seems to build upon the intuitive conclusions of Goethe. Physiologically, such a selective perception can be explained by there being three types of cones on the retina of a human eye: blue, green and red [3].

As a result, it can be suggested that in human culture these specific colour combinations provided a basis for the chromatic concept of life itself and for some aspects of the structure of the Universe.

Later on, with development and complication of various rituals, with introduction of different local, somewhat arbitrary conventions, secondary chromatic ideas about the decoration of religious and other doctrines, were imposed on these primary concepts.

REFERENCES

1. Goethe I.V. Zur Farbenlehre. Knowledge theory; translation from German of V.O. Lichtenshtadt. – Standard reproduced edition– Moscow: URSS: Librokom, 2014. 195 p.
2. Pavlov N.L. Chancel. Mortar. Temple. An archaic universe in architecture of Indo-Europeans. Moscow, OLMA-PRESS, 2001. 368 p.
3. Wilson E.O. Owners of the earth. The social conquest of Earth. SPb: Piter, 2014. 352 p.



Nikolai L. Pavlov,
Dr. of Architecture,
Professor. Graduated from
the Moscow Architectural
Institute in 1965. Professor
of the Chair “Soviet and
foreign architecture” of the
Moscow Architectural

Institute (State academy). Advisor to the
Russian Academy of Architecture and
Construction Sciences

Current State, Trends and Perspectives of the Development of Light Emitting Diode Technology



Fig. 5. In national park Tsianfoshan, Tsinan, China



Fig. 10. The Green Creative BR30 Cloud LED lamp



Fig. 12. Directions of light emitting diode hothouse radiation use:

a) Minsk vegetable factory (2015): hothouse radiation (Test laboratory of the Centre of light emitting diode and optoelectronic technologies of the National Academy of Sciences of Belarus); b) many-storey systems; c) a device for house use (Test laboratory of the Centre of light emitting diode and optoelectronic technologies of the National Academy of Sciences of Belarus)

Thermal Design of an LED System: A Special Lantern for Turkish Historical Mosques

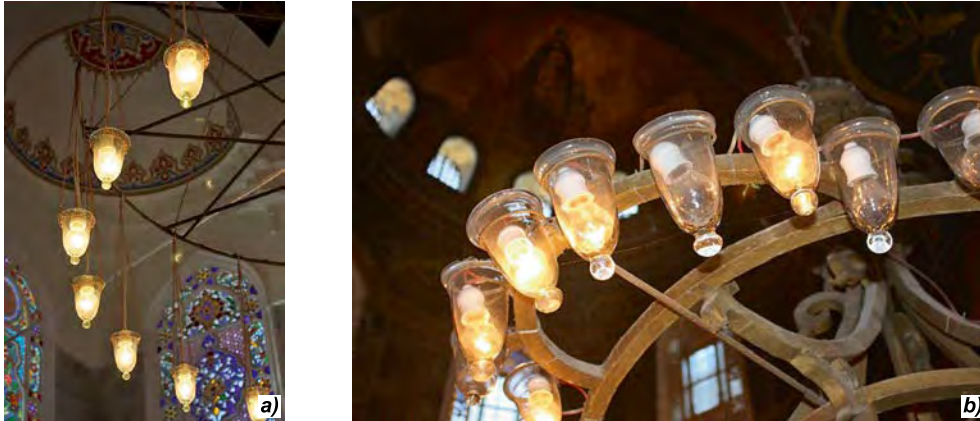


Fig. 1. Lanterns used in the interior lighting of (a) Semsi Ahmed Pasha Mosque, (b) Hagia Sophia Museum

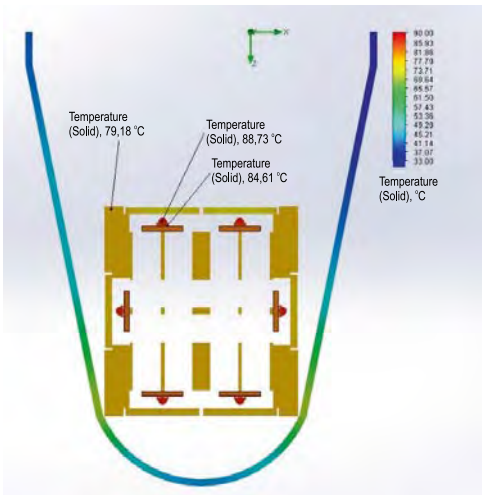


Fig. 12. Temperature distribution of the initial approach

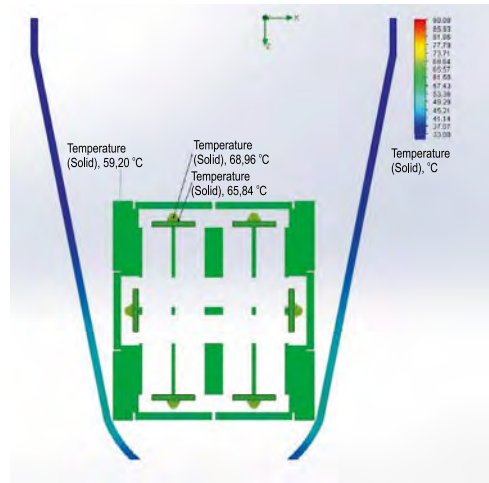


Fig. 13. Temperature distribution of the final approach

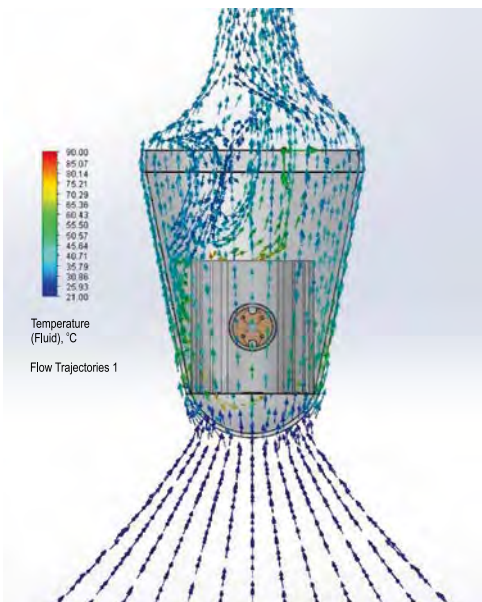


Fig. 14. Air flow in and around the lantern, initial approach

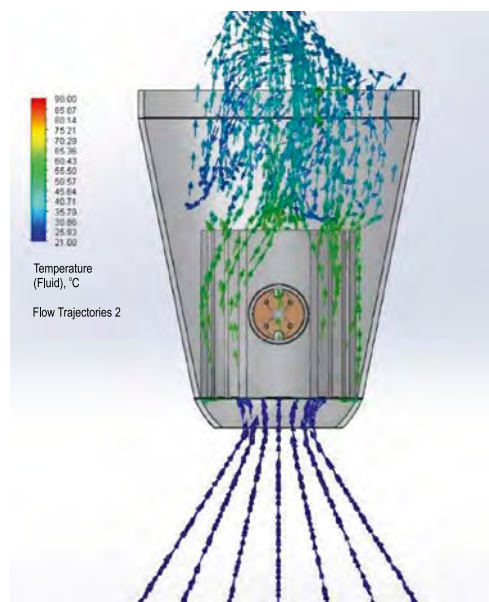


Fig. 15. Air flow in and around the lantern, final approach

A Chromatic Conceptualisation of Natural Life



Fig. 2. Gold of yellow colour, colour of the sun, colour of a deity:

a – Moscow. The Kremlin. Blagoveshchensky cathedral. Gold domes; *b* – Moscow. Ascension church in Kolomenskoe. The temple is projected from a gold orb-sun; *c* – St Peterburg. The Admiralty building. Gold spike being sun ray is projected from a gold ball-sun; *d* – Germany. Zost. Church of St Patroclus, the Tent is projected from a gold orb-sun; *e* – Myanmar. Shwedagon Pagoda. The huge mortar is projected from a gold bud-sun; *f* – Byzantium. Fatih Jami. The Pantocrator with a gold nimbus in the dome lunette; *g* – Vologda. An icon. A gold nimbus over the head of the sacred; *h* – India. Ajanta. Painting of a cave monastery. Gold nimbus over the head of Buddha; *i* – Persia. A huge gold nimbus over head of the divinified Khosrow II; *j* – Nepal. Kathmandu. Kala Bhairava – all-devouring time deity in a gold aura



Fig. 6. Combinations of green and red colours represent a harmony of vegetative and animal life. Painting: *a* – Ancient Egypt. A painting in the temple of Rameses III; *b* – Ancient India. Ajanta. A painting on the walls of the cave monastery; *c* – Russia. An icon. Subject of Lestnitsa (stairs); *d* – Russia. An icon. Christ in Majesty; *e* – Russia. An iconostasis; *f* – Japan. A picturesque canvas; *g* – Italy. Renaissance. Piero della Francesca; *h* – France. Cezanne; *i* – France. Gauguin

Sunlight as an Arranging Factor of Forming Dynamic Architecture



Fig. 2. A heliotrope turning house:

a) general view at night from the south side in winter; b) general view in the daytime from the north side in summer.

URL: <http://mixstuff.ru/archives/43807>



Fig. 4. Examples of the houses following (turning with) the Sun:

a) the *Round the World* two story house; b) a house in La Mece (California, the USA); c) the *Everingham* turning house; d) the *Dome House* (ecohouse)

AVAILABILITY OF DAYLIGHTING IN SCHOOL OPERATING TIME

Mária Ferenčíková¹ and Stanislav Darula²

¹*M & P creative studio s.r.o., Martin, Slovakia*

²*Institute of Construction and Architecture, Slovak Academy of Sciences, Bratislava, Slovakia*
E-mail: mariaferencik@gmail.com

ABSTRACT

Creating an optimal level of daylight in buildings in accordance with the quality of the environment is highly topical issue now. Daylight changes constantly not only every day from sunrise to sunset but also throughout the year. From systematic illuminance measurements at the CIE IDMP stations the daylighting dynamics in exterior also shown. To design and simulate daylighting in the indoor building environment, it is necessary to know the typical local luminous exterior conditions. A new method for evaluating of daylighting in interiors proposed by CEN TC169 / WG11 Daylight is based on occurrences of exterior illuminances at a specific locality, representing climatic parameter median of diffuse exterior illuminance. Paper presents testing this new climatic parameter and proposes its extension to other statistics. Proposed new criteria are demonstrated in a study of the daylighting availability in schools and school facilities and statistically divided from measured one-minute diffuse illuminance data in Bratislava during the period of six years.

Keywords: daylighting, availability of diffuse illuminance, median, school buildings.

List of symbols: d – number of the day in month; D – Daylight Factor; ET – equation of time, hour; $E_{v,d}$ – diffuse horizontal illuminance, lx; $E_{v,g}$ – global horizontal illuminance, lx; $E_{v,d,med}$ – median of diffuse exterior illuminance, lx; E_{vo} – luminous solar constant, lx; $E_{vo,h}$

– luminous solar constant recalculated on the horizontal plane, lx; $F(x_0)$ – cumulative frequency function; J – day in the year; k^a – percentile of diffuse horizontal illuminance $E_{v,d}$, lx; LT – local time, hour; m – number of the month; min – minute in the day; $P(X \leq x_0)$ – probability of occurrence, TST – True Solar Time, hour; t_1 – start time of the school operation; t_2 – end time of the school operation; γ_s – solar altitude, deg; δ – declination, deg; ε – eccentricity factor; λ_{l_0} – geographical longitude of the side, deg

1. INTRODUCTION

Daylight has irrecoverable effects for the human body, which do not have adequate alternative. Its typical characteristics – dynamics, irregular changes in the quantity and quality during a day to stimulate our attention and cannot be exactly replaced by artificial light, which by its monotony leads to reduction alertness, feelings of fatigue and sleepiness and decrease work performance, [1] Therefore, access to daylight in interiors cannot be underestimate and it is important to ensure its in such level and quality that is needed for human health and safety occupation. Currently, the design and evaluation of daylight in buildings is performed in accordance with technical standards in several countries, e.g. in Slovakia, Czech Republic, Germany, U. K., China or Russia. Criteria for the design and evaluation of daylight are based on CIE recommendations [2]. For simplification, the model of the uniform overcast sky with the sky luminance gradation in the ratio

1:3 from horizon to zenith is commonly applied. According to this model, the illuminance during the worst daylight exterior conditions is possible to determine, but it is not possible to satisfactorily evaluate annual availability of daylighting in interiors because exterior illuminance changes are not considered. Conditions of optimal visual comfort in the spaces permanently occupied by people have to be created with respect to various exterior situations occurring during a year, i.e. under overcast skies with a low external illuminance levels, cloudy skies variously covered by clouds or clear skies with direct sunlight [3–7].

A new method of evaluation of interior daylighting is based on determination of statistical characteristics of the exterior illuminance occurrences determined from measurements in certain locations. The established climatic statistical parameter median of diffuse exterior illuminance [8] can be calculated from satellite data and also from regular ground measurements and standardised. On the base of the results of the analysis modelled exterior diffuse illuminance characteristics in school operating time, the statistical method for evaluation of the exterior diffuse illuminance with respect to effective utilization of daylighting in schools was proposed.

2. METHODOLOGY

Daylight availability on the Earth's surface depends on several factors – the solar altitude, cloud type, cloudiness and also atmospheric turbidity. Exterior daily illuminance is permanently changing in all components, global, diffuse and direct. Authors in [9] introduced that the same two daily courses of diffuse and global illuminance $E_{v,d}$ and $E_{v,g}$ were not found in the database of measurements 1994–2006 and every day was identified as original without repetition. Daily illuminance in building interiors is up to now evaluated after Daylight Factor D , criterion which concept is based on the CIE model of the uniform unshaded overcast sky when the impact of direct sunlight is excluded. However, it is important to notice that daylighting should be evaluated on the base of instantaneous data because the human eyes are able to perceive daylight levels at the time of their occurrence not as averaged or cumulative values. Except for the minimum illuminance levels needed in the architectural design and assessment of inte-

rior daylighting the qualitative parameters of daylight and its dynamic changes should also be taken into account.

Experimental results focused to quantification of exterior illuminance changes are published in the scientific papers for a long period, for example in [10–16]. There can be found methods for evaluation exterior illuminance in terms of daylighting design and simulation daily sequences. Authors, e.g. [17–18] analysed daily illuminance courses of $E_{v,d}$ and $E_{v,g}$ in all months in the year. Comparison of individual days confirms very high variability of natural light in terms of the time of occurrence and the measured levels. So, to design and evaluate daylight in buildings very exactly it is necessary to determine the real luminous climate in locality. In the book [19] and work [20] also shown that only system of comprehensive measurements and their processing allow to obtain relevant information about daylight climate. The first complex characterization of year-round courses of diffuse exterior illuminance in Bratislava was published in [21]. At the same time research in [17] and [22] was pointed on availability of annual daylight changes described by statistical methods.

Dynamic daylight conditions can be captured by modelling of the characteristic exterior illuminance courses from data measured on the horizontal plane and on the base of analysis of comprehensive long-term measurements and their statistical processing.

For modelling of the exterior diffuse illuminance availability it is necessary to use inputs in the form:

- Time and date of the day,
- Long-term measured one-minute data of exterior diffuse horizontal illuminance,
- Long-term measured one-minute data of exterior global horizontal illuminance.

The draft of the European lighting standard «Daylighting of Buildings» [8] and [23] prescribes the climate statistical parameter – median of diffuse exterior illuminance $E_{v,d,med}$. Another important parameter for determination of daylighting in building interiors is time of available daylight utilization which depends on the operating times of the occupied building. The operating time of the building (or standard working time) is classified by building category in respect to use of the building and this time determines its daily

operation, i.e. the beginning and the end of occupancy during the day, the weekly operation (Monday to Sunday) also year-round use of the building (January to December).

Standard operating times for lighting in buildings are prescribed in regulation [24] in the Slovak Republic. Different standardized daily operation time have e.g. schools and school facilities (length of daily operation is 7.5 hours), office buildings (9.5 hours) or hospitals (14 hours). Weekly operation time of buildings depend also on the building type, e.g. office buildings are performed five days a week while hotels and hospitals seven days a week. Also, it is different year-round occupancy of buildings, for example, school buildings are occupied only during the school year (it is 10 months, if other holidays during the school year are not considered) but, for example, hospitals are continually performed during a year. To model exterior diffuse horizontal illuminance use as much as exactly it is important to define time intervals corresponding to standard operating times during operating days of each building type from the database of horizontal illuminance measurements.

Modelling the characteristic of exterior diffuse illuminance availability in Bratislava was based on the database containing instantaneous one-minute data of global horizontal illuminance $E_{v,g}$ and diffuse horizontal illuminance $E_{v,d}$ systematically measured in Bratislava during the six-year period – from January 4, 1994 until 31 December 1999. These data were offered for study of daylighting availability without ambition to describe climate changes. Recorded data were strictly checked against Quality Control tests before next processing while tests published in the CIE guide [25] were applied. Probability of $E_{v,d}$ occurrence above the gain limit was calculated after formulae (1).

$$P(E_{v,d} \geq k^\alpha) \text{ for interval } \langle t_1, t_2 \rangle, \quad (1)$$

where k^α – percentile of diffuse horizontal illuminance $E_{v,d}$, lx,

- t_1 – start time of the school operation,
- t_2 – end time of the school operation.

The flow chart for modelling of the annual typical availability of exterior diffuse illuminance in schools and school facilities is shown in Fig. 1. Graphical presentation of results in the form of the graph of the cumulative distribu-

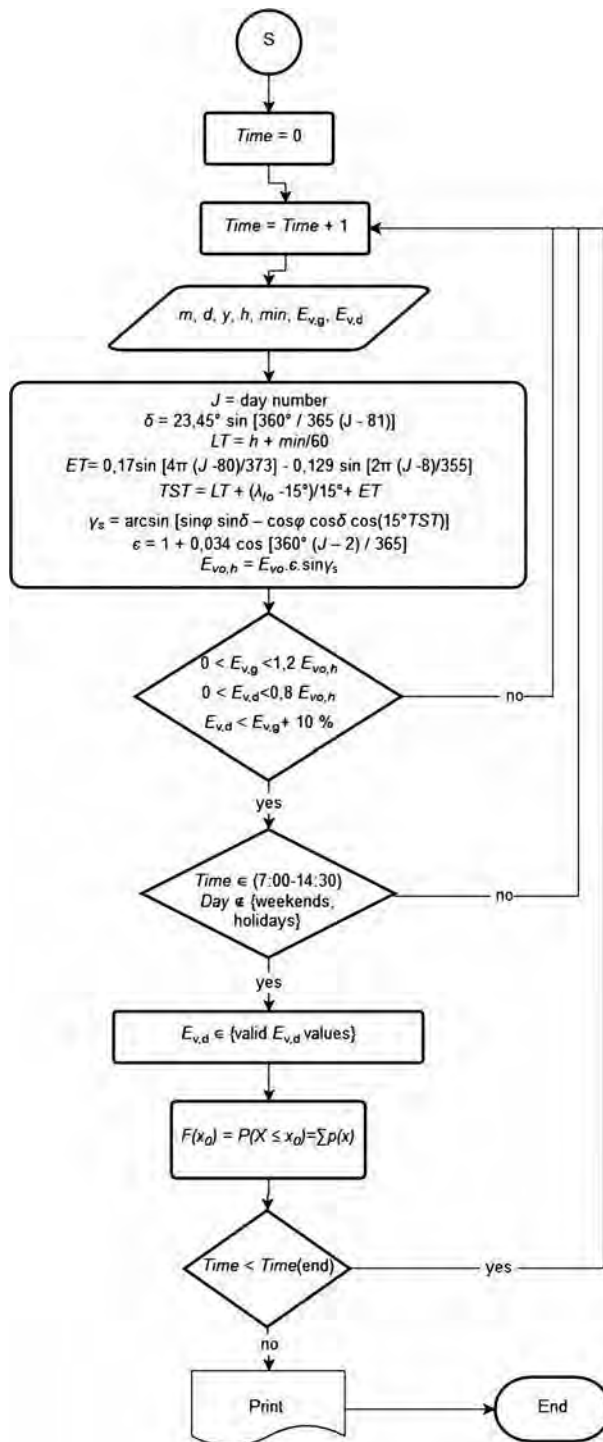


Fig. 1 The flow chart for modelling of the probability of annual exterior diffuse illuminance $E_{v,d}$ occurrence for the schools operating time

tion function is more instructive than tables with many numbers, therefore, this form was used in Fig. 2. Diagram in the Fig. 2 shows the percentage of occurrence of the exterior diffuse horizontal illuminance considering all daylight cloudy, clear, overcast and dynamic situations representing Bratislava luminous climate during 1994 spe-

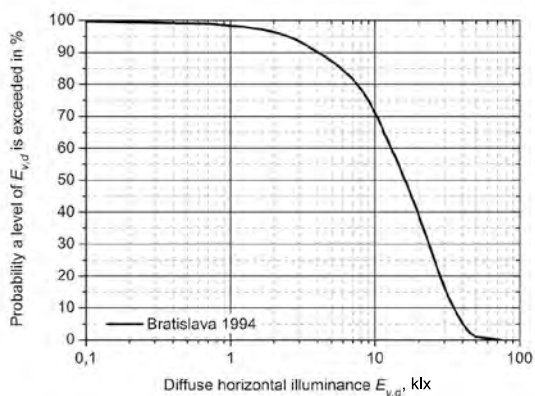


Fig. 2. The probability of $E_{v,d}$ occurrences which were exceeded, the school operating time, Bratislava 1994

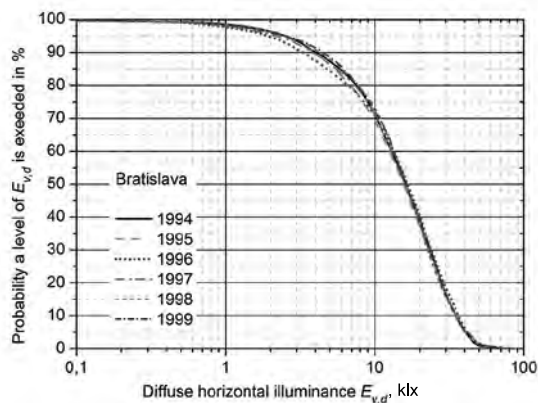


Fig. 3. Probability of the $E_{v,d}$ annual occurrence for school standard operating time, Bratislava 1994–1999

cified for school operating time. The curve also allows to read value of the $E_{v,d}$ median and to find out other statistical characteristics – quantiles or percentiles of the diffuse horizontal illuminances.

For the purposes of the processing $E_{v,d}$ availability in school buildings the standard operating times in the period Monday to Friday excluding national holidays as well as winter and summer vacations was taken into account. Occasional teaching free days were not considered in this study because of their difficult identification and local specification. Exclusion of data from database recorded in the periods when buildings were not occupied allowed express more realistic Bratislava daylight conditions. This way was modelled monthly, yearly characteristic of the exterior diffuse illuminance availability and the derived medians and percentiles for all months in the year.

3. RESULTS

The overview of the characteristic occurrence of illuminance levels was acquire from param-

eterization of the measured $E_{v,g}$ and $E_{v,d}$ values in the period 1994 to 1999. Calculated values of the medians $E_{v,d,med}$ and $E_{v,d}$ percentiles are documented in Tab. 1 for each investigated year. Values of deviation in percentage represent difference between percentage of year and values obtained from whole six year period. In Tab. 2 are presented results obtained from calculations based on the data matrix containing all data measured from January 4, 1994 to December 31, 1999. Graphical presentation of the probability occurrence of exterior diffuse illuminance $E_{v,d}$ either for each month is in Fig. 3 or for whole six-year period is in Fig. 4 respectively. Grey colour of the cell in Tab. 1 indicates minimum deviation in the percentile category.

From comparison of monthly 40th to 90th percentiles and median it can be observed small differences. These vary from 930 lx for 60th percentile (difference between illuminance levels found out in 1998 and 1995) to 1247 lx for 40th percentile (difference between $E_{v,d,1996}^{(40)}$ and $E_{v,d,1995}^{(40)}$), Table 1. Annual values of percentile deviations vary be-

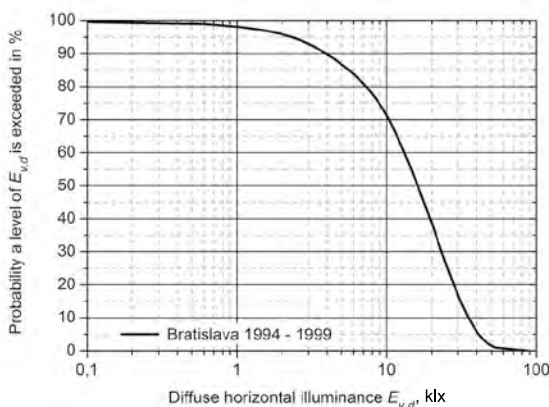


Fig. 4. Probability of $E_{v,d}$ occurrence in school operating time, Bratislava 1994–1999

Table 1. Values of annual medians of diffuse exterior illuminance $E_{v,d,med}$ and 40th – 90th percentiles in lx for the standard school operating time, Bratislava 1994–1999

Percentile, lx	Year					
	1994	1995	1996	1997	1998	1999
40 th	19683	18876	20123	19579	19218	19359
Deviation, %	+ 1,1	–3,1	+ 3,3	+ 0,6	–1,3	–0,6
50 th = $E_{v,d,med}$	16088	15578	16583	15882	16261	16221
Deviation, %	–0,2	–3,3	+ 2,9	–1,4	+ 0,9	+ 0,7
60 th	12904	12502	13432	12812	13432	13406
Deviation, %	–1,5	–4,6	+ 2,5	–2,2	+ 2,5	+ 2,3
70 th	10254	9815	10280	10280	10900	10668
Deviation, %	–1,0	–5,3	–0,8	–0,8	+ 5,2	+ 3,0
80 th	7484	6819	6612	7306	7749	7697
Deviation, %	+ 2,7	–6,4	–9,2	+ 0,3	+ 6,4	+ 5,7
90 th	4070	3926	3302	3823	4288	4494
Deviation, %	+ 3,6	–0,1	–16,0	–2,7	+ 9,1	+ 14,4

Table 2. Values of the median diffuse exterior illuminance $E_{v,d,med}$ and 40th to 90th percentile for standard school operating time, Bratislava 1994–1999

Period	Percentile					
	40 th	50 th = $E_{v,d,med}$	60 th	70 th	80 th	90 th
	lx					
1994–1999	19471	16115	13100	10360	7284	3930

tween –16 % (90th percentile in 1996) to +14.4 % (90th percentile in 1999). The smallest deviations are registered for 40th percentile expressing the highest values of the $E_{v,d}$ illuminance, Table 1. Statistics presented in Table 2 document their importance for daylight design in buildings. If median will be proposed as criterion for window design then interior will be satisfactory illuminated by daylight during 50 % of daylight hours and when exterior illuminance will be higher than 16115 lx. Better daylight conditions in interiors during year can be achieved when criterion for window design will be determined by lower value of illuminance and longer day time for daylight performance. This can be fulfilled by 80th percentile. In this case interiors will be satisfactory illuminated by daylight during 80 % of daylight hours and also early morning and late afternoon when exterior illuminance is higher than 7284 lx.

Annual occurrences of diffuse horizontal illuminance levels in the observed period are very similar as illustrate cumulative functions in Fig. 3. Small shifts between curves representing each year indicate nonsignificant differences of the diffuse exterior horizontal illuminance in Bratislava at the annual level.

After analysing all data, we can conclude that deviation of yearly statistical parameters is the lowest in 1994 (– 1,5 % to + 3,6 %) and in 1997 (– 2,7 % to + 0,6 %), see Table 1. The minimum deviations of percentiles from medians are highlighted in grey. In contrast, the highest deviations were found in 1996 (– 16,0 % to + 3.3 %), which indicates higher occurrence cloudy situations with dynamic illuminance changes during whole year.

Occurrence of exterior illuminance levels in a locality depends also on the orography and climatic conditions. Climate in Bratislava is char-

Table 3. Relative sunshine duration measured in Bratislava

Year	1994	1995	1996	1997	1998	1999
Relative sunshine duration, <i>s</i>	0.410	0.375	0.379	0.434	0.411	0.399

acterised by four typical seasons and moderate Central Europe climate which can be described also by parameters influencing daylighting, e.g. sunshine duration, cloudiness or atmospheric turbidity. Relative sunshine duration measurements in Bratislava show that yearly values change slightly around the value of 0.4. Because design of daylight criteria should respect also specified climate conditions, the influence of sunshine duration *s* on the investigated statistics was studied. In Table 3 are documented values of relative sunshine durations obtained from measurements of $E_{v,g}$ and $E_{v,d}$ at the IDMP CIE station Bratislava while their values were calculated in respect with CIE108:1994 recommendations. Minimum value of *s* was found in 1995 and maximum in 1997.

To apply various percentiles of $E_{v,d}$ for daylight design it was assumed that climatic criteria determine comparable daylight conditions during year to year. Study of relation between sunshine duration *s* and $E_{v,d}$ occurrence expressed by percentiles results any dependence between these variables, Fig. 5. This finding is very important for application of various percentiles for daylight design in various building interiors, e.g. in offices, hospitals, school buildings or spaces for retail.

4. CONCLUSIONS

Research of $E_{v,d}$ – diffuse horizontal illuminance availability based on the data measured continuously during six- year period from 1994

to 1999 showed that the availability of $E_{v,d}$ has typical cumulative character and their mutual comparisons not result significant differences. It was found 50 % occurrence of $E_{v,d}$ levels higher than 16115 lx (value of the six year median $E_{v,d,med}$) and 50 % occurrences of $E_{v,d}$ will be lower in the school standard operating time (7:00 to 14:30). The median exterior diffuse horizontal illuminance $E_{v,d,med}$, is a key parameter for evaluation of daylighting in building in proposed new European standards [8]. For Bratislava, capital city of Slovakia was derived value of $E_{v,d,med} = 16300$ lx. In this standard is recommended to derive $E_{v,d,med}$ from satellite data or ground measurements during the day time, i.e. from sunrise to sunset.

If daylighting in building interiors is design or evaluated after criterion median diffuse exterior illuminance it can be expected that interiors will be illuminated levels higher than 16300 lx over half of the year and during rest half of the year occurrence of illuminance levels will be lower than the median. From definition of the median results that in situations with exterior diffuse illumination levels lower than the median $E_{v,d,med}$ will be interiors insufficiently illuminated by daylight and the supplementary lighting or artificial lighting will have to be used.

In the past it was assumed that the model of the CIE overcast sky presents levels of the exterior diffuse illuminance in the range of $E_{v,d} = 5000-7000$ lx. Schools in Slovakia are occupied for more than 80 to 90 % of operating time. Ap-

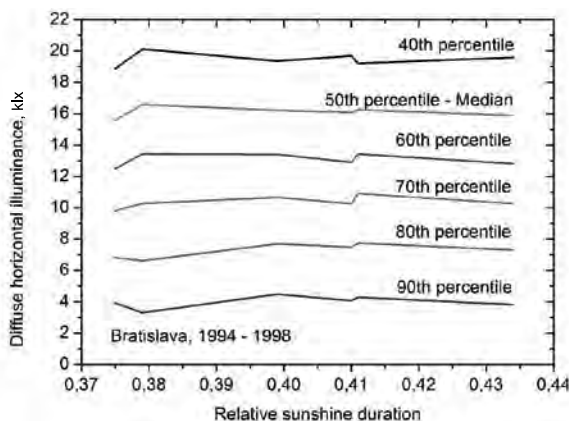


Fig. 5. Relation between relative sunshine duration and horizontal diffuse illuminance

plying Table 1 or Fig. 3 and Fig. 4 corresponding critical illuminance value will be in the range 4000–7500 lx. Traditionally level of $E_{v,d} = 5000$ lx is associated with exterior illuminance under CIE Overcast Sky.

For ensuring healthy lighting the daylight should be applied in the required time, i.e. when buildings are occupied by people – during standard operating time of the building. This means that for good illumination of school interiors by daylight the criterion for the daylight availability should be determined on the basis of 80th to 90th percentile (see Tab. 1 and Tab. 2). These values correspond to the statistical parameters (2) and (3) as was found in the presented study:

$$E_{v,d}^{(80)} = 6612-7697 \text{ lx}, \quad (2)$$

and

$$E_{v,d}^{(90)} = 3301,6-4494 \text{ lx}. \quad (3)$$

The introduction of other statistics as criteria for the evaluation of daylighting in buildings, for example 80th or 90th percentile allows to more efficient use daylight in school interiors. In window design, strictly application of median can results in realization of building constructions with window size, which will limit sufficient indoor daylighting only during half of the year.

Based on the analysis and its results the modeled characteristic availability of diffuse exterior illuminance for the school standard operating time the appropriate statistical method in terms of efficient utilization of daylight in schools was proposed. Application of the new method for evaluation of daylighting in interiors can achieve energy benefits of daylighting in point of view of hygienic aspects and visual comfort, which is very important not only for adults but also for the growth of the young person body.

ACKNOWLEDGMENT

This work was supported by the project VEGA 2/0042/17 and APVV-0118–12.

REFERENCES

1. Boyce, P.R. Human Factors in Lighting. London: CRC Press, 2014.
2. CIE016–1970: Daylight. Vienna: CIE Bureau.
3. Darula, S. Daylighting in the exterior and in the interior. Bratislava: STU, 2011.
4. Ferenčíková, M., Darula, S. Diffuse illuminance during school hours. Proc. Int. Conf. Lumen V4, 2014, Visegrád, Hungary, P19.
5. Valíček, P., Novák, T., Vaňuš, J., Sokanský, K., Martinek, R. Illuminance Evaluation in Automatically Dimmed Interior Lighting Systems. Proc. VI. IEEE Lighting Conference of the Visegrad Countries LUMEN V4 201, Karpacz, pp. 40–44.
6. LI, D.H.W., TSANG, E. K.W. An analysis of daylighting performance for office buildings in Hong Kong. Building and Environment, 2008, 43, 9, pp.1449–1458.
7. Tregenza, P., Standard skies for maritime climates. Lighting Research and Technology, 1999, 31, 3, pp.97–106.
8. prEN17037 Daylight of Buildings, draft July 2016.
9. Darula, S., Kittler, R., Kocifaj, M., Plch, J., Mohelníková, J., Vajkay, F. Osvětlování světlovody (Light guide illumination). Praha: Grada Publishing, a.s., 2009. (In Czech).
10. Enarun, D., Littlefair, P. Luminance models for overcast skies: Assessment using measured data. Lighting Research and Technology. 1995, 27, 1, pp.53–58.
11. Mardaljevic, J. Simulation of annual daylighting profiles for internal illuminance. Lighting Research and Technology. 2000, 32, 3, pp.111–118.
12. Darula, S., Kittler, R., Kambezidis, H., Bartzokas, A. Reconstruction of missing measured illuminance values in regular daylight data recording. Proc. 14th Int, Conf, Light 2003, Liptovský Ján, Dom techniky ZSVTS, Bratislava, pp. 62–70.
13. Ng, E., Cheng, V., Gadi, A., Mu, J., Lee, M. Defining standard skies for Hong Kong. Building and Environment. 2007, 42, 2, 866–876.
14. Alshaibani, K. Finding frequency distributions of CIE Standard General Skies from sky illuminance or irradiance. Lighting Research and Technology, 2011, 43, pp. 487–495.
15. Budak, V.P, Smirnov, P.A. A physical model of the firmament to calculate daylight. Light and Engineering, 2013, 21, pp. 17–23.
16. Kittler, R., Kocifaj, M., Darula, S. Daylight science and daylighting technology. New York: Springer, 2012.
17. Dumortier, D., Fontoynt, M., Avouac-Bastie, P. Daylight availability in Lyon. Proc. Conf. on Energy Performance and Indoor Climate in Buildings, Lyon, 1994, pp. 1315–1320.

18. Darula, S., Kittler, R. Research of the year-round changes of solar and daylight availability for the computer evaluation of sustainable buildings, Daily courses and sunshine duration in Bratislava during 2001–2005 after IDMP measurements. VEGA 2/5093/5 R2006, 1, ICA SAS Bratislava, 2006.
19. Kittler, R., Pulpitlová, J. *Základy využívania slnečného svetla žiarenia (Basis of the utilization of solar radiation)*. Bratislava: Veda, 1988. (In Slovak).
20. Hayman S. *The daylight climate of Sydney*, Ph D. Thesis, University of Sydney, 1996.
21. Darula, S. *Štatistické charakteristiky exteriérovej osvetlenosti v Bratislave podľa meraní počas rokov 1994 a 1995. (Statistical characteristics of exterior illuminance measured during 1994–1995)*. *Světelná technika*, 1997, 30, 3–4, 42–46. (In Slovak).
22. Mardaljevic, J. Simulation of annual daylight profiles for internal illuminance. *Lighting Res. Technol.*, 2000, 32, 3, pp. 111–118.
23. Mardaljevic, J., Christoffersen, J., Raynham, P. A proposal for a European standard for daylight in buildings. *Proc. Int. Conf. Lux Europa 2013*, Krakov, pp. 237–250.
24. Vyhláška č. 364/2012 Z. z. Ministerstva dopravy, výstavby a regionálneho rozvoja Slovenskej republiky, ktorou sa vykonáva zákon č. 555/2005 Z. z. o energetickej hospodárnosti budov a o zmene a doplnení niektorých zákonov v znení neskorších predpisov. (Regulation No. 364/2012 Z. z. Ministry of Transport, Construction and Regional Development of the Slovak Republic on Energy Performance of Buildings). (In Slovak).
25. CIE108:1994. *Guide to recommended practice of daylight measurement*. Vienna: Central Bureau.



Stanislav Darula,

Ph.D. He is a Head of the Building Physics Department in Institute of Construction and Architecture of Slovak Academy of Sciences in Bratislava. Stanislav is a national member of the CIE Div. 3. Also, he is a member of the Presidium and chairmen of the Slovak National CIE TC8 Daylighting, member of the ISES (International Solar Energy Society), member of the SKSI (Slovak Chamber of Civil Engineers), member of the SZSI (The Slovak Union of Building Engineers), member of the SSTS (Slovak Illuminating Engineering Society).

His field of science is research in building physics, daylighting, sun energy utilisation, energy performance of buildings, daylighting design in the buildings. He is an external lecturer at Slovak Technological University in Bratislava and a consultant for daylighting design



Mária Ferenčíková,

Dipl. Ing. was graduated from Slovak University of Technology in Bratislava at Faculty of Civil Engineering in 1991. Since 2002 she is authorized as the civil engineer of Building Structures for the execution of complex architectural and engineering services in the Slovak Chamber of Civil Engineers. At present, she is chief of the M&P creative studio. Her professional interest is focus on the daylight design and daylight solutions in buildings. Currently, she participates in the elaboration of new European standards of Daylight in Buildings within the Slovak National Committee of the CIE

SUNLIGHT AS AN ARRANGING FACTOR OF FORMING DYNAMIC ARCHITECTURE

Natalya A. Saprykina

MARCHI (State Academy), Moscow
E-mail: nas@markhi.ru

ABSTRACT

Examples of use of solar (natural) light as a factor of forming dynamic (kinetic) architecture are considered. These examples show that use of natural light is popular, and methods of its use and embodiment are widespread. It is noted that kinetic orientation is put forward by many design proposals through the use of natural illumination both when building rotation, and when modifying the configuration of architectural objects or their facade structures, thus changing their natural light consumption mode. It is a recognized fact that with the development of new original solutions using kinetic methods based on natural illumination requires reconsidering approaches to the formation of building facades. Modern digital technologies and innovations for collecting and adjusting natural light become important. In particular, this concerns a complex integrated ecological system of automatic control and self-control, which is used to increase comfort, to decrease costs and reduce energy consumption.

Keywords: sunlight in architecture, dynamic architecture, building following (tracing) the Sun, kinetic structural systems, solar digital technologies

Solar (natural) light is one of the tools forming spatial arrangement of architecture, where relative dimensions and spatial measurements can be only determined with illumination. Light in architecture, besides its illumination function, is an eternal material, which is always modern. In design practice and development of the theory is an increasing use of digital light technology as a means of expression in the architecture of large cities¹. Lately, designers working within computer simulation of architectural illumination do not take into account the role of natural light as an important component of the configuration and image of a building.

In the context of new trends in lived space imaging, as well as in the context of present and future architectural development, sunlight becomes an arranging factor of forming architectural objects with a completely new approach. This is a result of the fact that the stability of a building through time and environmental exposure, i.e. its durability was always considered a criterion of building quality. But this feature can be implemented not through stability but through changeability as the main architectural principle. One of the main directions in design practice is the development of flexible transformed space-planning and kinetic structural systems [1]. In this process, a big role is played by the col-

¹ Such as media facades with huge screens built into the architectural appearance of a building, 3D-video mapping technology, which allows projecting static and dynamic video images onto different surfaces, including building facades, and even holography, which allows generating stereoscopic pictures. Among architectural illumination methods, general floodlight, contour and local illumination, light facades and background floodlight are used.

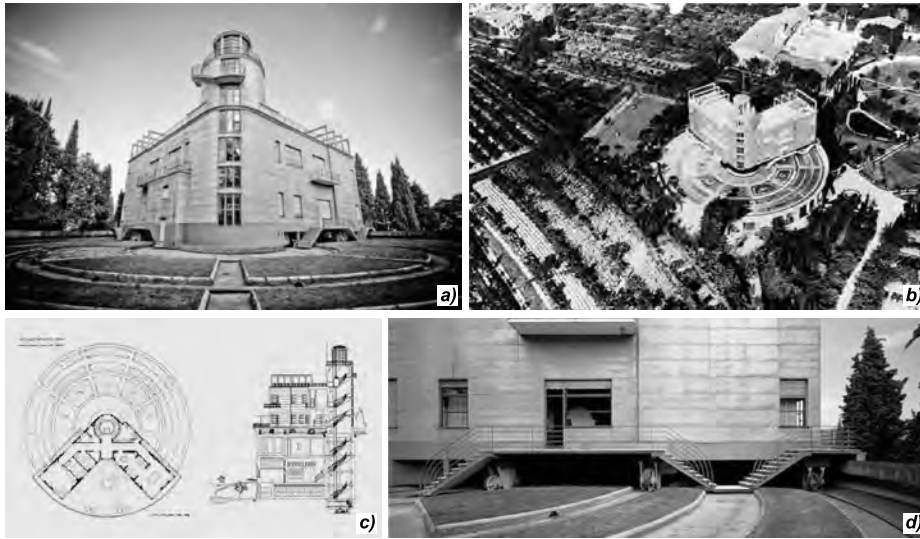


Fig. 1. The Girasole country house: a) facade; b) general view; c) layout and section; d) a facade fragment
 URL: <http://mixstuff.ru/archives/43807>

lection and adjustment of natural light to create a comfortable life environment.

Modern technologies allow developing architectural solutions with movable façade systems for automatic control of illumination, temperature, humidity and other components of the comfort. Swiftly developing technologies make it possible to move ahead and to create not just functional but also self-adjusting, responsive buildings, which change dynamically like elements of the natural world, for example, as sunflowers following the Sun. During their conception, functional and technological approaches prevail.

Illustration of this idea is the *Girasole* country house, which is the first example of dynamic (kinetic) architecture. *Girasole* means sunflower in Italian. This building was designed and constructed by architect Angelo Invernizzi between

1929 and 1935 not far from Verona, Italy. The two story building stands on a round base 44 m in diameter, which is supplied with two diesel engines, which allows the house to follow the Sun at a maximum speed of 4 mm/s (Fig. 1). *Girasole* is a huge mechanical structure, which is fitted with window-blinds with electronic control, and rotates around a central pylon [2].

The concept of a building following the Sun was a feature of many design proposals, patent developments and constructed buildings, which became the very first buildings in history that generated more energy than they consumed. An example is the rotating house of architect Richard T. Foster in Connecticut, USA, designed with the help of Philip Johnson in 1967. Its outlines make it look more like a UFO than a house



Fig. 2. A heliotrope turning house:
 a) general view at night from the south side in winter; b) general view in the daytime from the north side in summer
 URL: <http://mixstuff.ru/archives/43807>



Fig. 3. The *Suite Vollard* turning house:
 a) general views; b) layout of a floor
 URL:
<http://geographyofrussia.com/krutyashhiesya-kvartiry-v-bashne-suite-vollard/>

(the building height is 3.65 m, and the diameter is of about 22 m)².

Another example is the heliotrope turning house, which uses solar energy. It was constructed much later in Freiburg in Breisgau, Germany, in 1994 by architect Rolf Disch, a passionate environmental activist. In winter the facade of the house turns towards the Sun, heating itself, and in summer it turns away from the Sun, providing good thermal insulation (Fig. 2).

The pollutant-free building is equipped with a solar-thermal balcony handrail, a geothermal heat exchanger, two-axial solar photo-electric panels and a thermal power plant (a combined production of electric and thermal energy) [3].

The world's first 50 meter turning house *Suite Vollard* was designed by architect Bruno de Franco between 1995 and 2001 and constructed in the

middle of December, 2004, in Curitiba town, Brazil (Fig. 3). The turning house is built of vinyl and metal structures on a movable foundation installed on supports. A kitchen, a laundry and a bathroom, as well as a control centre with a remote control changing rotation direction and speed, light and air conditioning using voice commands are located there. Water-supply pipes and electric wires are mounted so that it is possible to change their length depending on the rotation angle (they are automatically elongated or shortened similar to a fire hose reeled up). Each separate apartment is equipped with big windows made of several types of glass of a different shade and rotates individually doing the whole revolution in one hour. Sunlight penetrating through 3-millimeter glass paints each sector with the a particular colour creating a certain image [4].

² The house was completely repaired in 2005. URL: http://architectuul.com/architecture/view_image/the-round-house/4845.



Fig. 4. Examples of the houses following (turning with) the Sun:
 a) the *Round the World* two story house; b) a house in La Mece (California, the USA);
 c) the *Everingham* turning house; d) the *Dome House* (ecohouse)

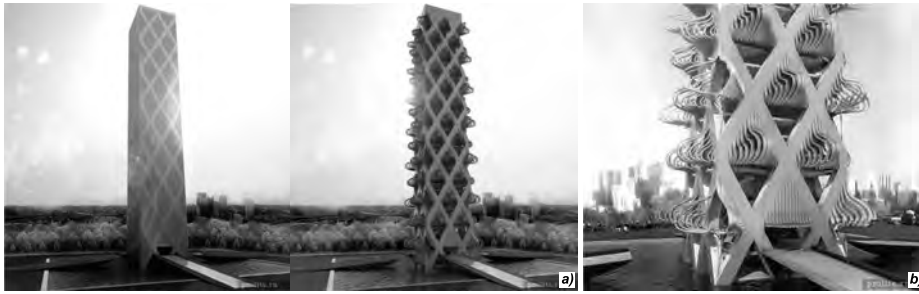


Fig. 5 The *Kinetower* project:

a) general view in steady and transformed states;
 b) a facade fragment as the window structures react to sunlight intensity

URL: <http://www.chaoslend.ru/node/1651>

In design and construction practice around the world, there are many examples of turning houses following the Sun, with varying numbers of floors and of different dimensions, for example:

- A turning two story Round the World house, in Green Gable on Prince Edward island (Canada), 464 sq.m in area (Fig. 4, a);
- A unique turning house belonging to Al and Janet Johnston in La Mece (California, USA), 492 sq.m in area (Fig. 4, b);
- Turning house *Everingham*, constructed of glass and steel in 2006 by Luke Everingham for his family (New South Wales, Australia). The building represents an octagon in plan of 24 m diameter of circumscribed circle and has an electric motor thanks to which it can make a full revolution around its axis in 30–120 minutes. (Fig. 4, c) [4];
- A turning dome ecohouse (*Dome House*) with an autonomous renewable electric power supply made of natural materials by *Dome-space Homes* Company out of natural materials. It stands on a mechanical platform, which can

turn 360°. Its vaulted structure and interior is well thought out by Patrick Marsilli, providing for the maximum use of natural light (Fig. 4, d) [5].

An importance of solar (natural) light as a factor of forming dynamic architecture is seen not only in turning buildings, but also in examples of modifying the configuration of architectural objects themselves or their facade structures when adapting the light consumption mode:

- One of the most interesting concepts in construction of kinetic buildings is challenging static norms by creating changeable configurations which meet user requirements or react to sunlight. The *Kinetower* project (architects *Barbara van Bievliet* and *Xaveer Claerhout*). The external windows react to the intensity of sunlight or to user's control signals just as flowers to react sunrise: they unfold giving the building facade soft features and a completely different appearance [6]. This transformation is possible because of the building material, which is rigid in its normal state but can bend at high temperatures (Fig. 5).

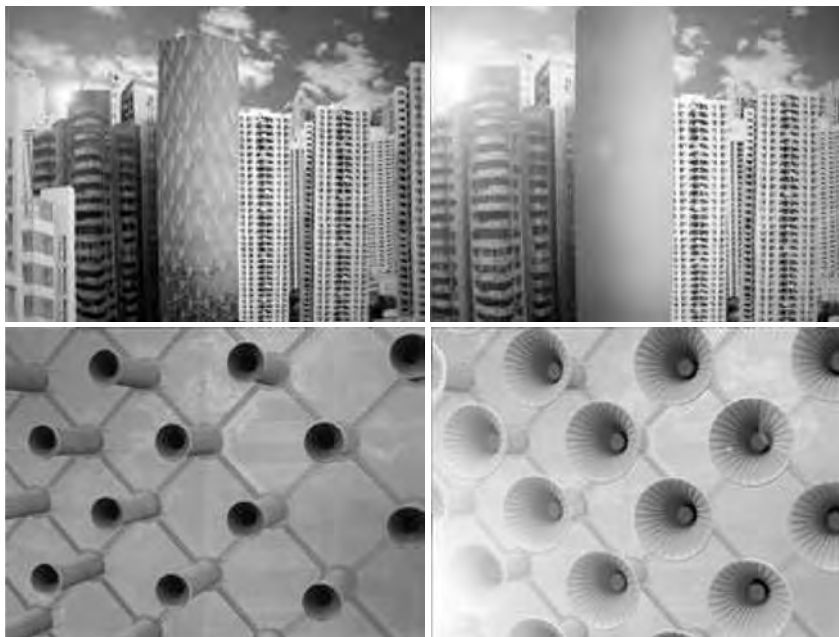


Fig. 6. The Sustainable Habitat – 2020

URL: <http://reality.newsru.com/article/11sep2008/bioskin>



Fig. 7. The *Animated Apertures* project:
a) general view; b) cross section.

URL: <http://green-buildings.ru/ru/dom-s-resnichkami>

- Another example is the *Sustainable Habitat 2020* which is part of the Dutch project of developing environmentally sustainable housing. The building is covered with a bionic «skin» and multiple collecting flowers, which follow the Sun and collect rain water for the building's use. The building is unique due to the special material similar to bioskin or to cell membranes (Fig. 6). The walls of the building have openings with built-in solar batteries, which open in sunny weather like buds. Natural light and air penetrate through them into the rooms, when the weather is overcast, they close [7]. There are no windows in the building facades, however if desired, with the click of a button, a window of any configuration can be designed independently, because wall components are covered with a transparent light-absorbing layer controlled by electronics. The water supply for the house is rain water, which runs into membranes and then passes through cleaning filters. Later on, small reactors can be built into the wall generating biogas from organic waste.

- The Live windows (*Animated Apertures*) project in Lima (Peru) is also quite eccentric. A window in the house is not a plain glazed surface but a three-dimensional object, which is built into the house, like a lens diaphragm, and has structural elements adjusting light passing through it. The window openings have a directed geometry and are connected with certain points in the town environment (the ground, the sky, the horizon, the points of interest). They are also transitional spatial elements between the interior and the facade (Fig. 7). According to the authors, the window openings can radically change spatial percep-

tion within each dwelling, as well as the appearance of the whole building in its surroundings [8].

- The *Animated Apertures* project was born as a research design project, the purpose of which was to reconsider windows from the viewpoint of their functional intention, structural elements, appearance and use of this knowledge for typology of multistory buildings based on expanded boundaries of architecture and town design.

- Another famous example of a dynamically changing architectural object dependent on sunlight is the Quadracci pavilion of the Milwaukee Museum of Art (USA) constructed in 2001 by *Santiago Calatrava*, who is well known for his special relation to light³.

- The pavilion is built with a peculiar movable structure, similar to wings on the roof, called Solar breeze, which opens out in sunny weather and closes with overcast skies and at night (the wingspan is 66 m)⁴.

There are many new solutions appearing in architectural practice. They encourage new approaches to designing buildings facades using kinetic methods, which react to natural illumination:

- In the early 1980s, *Jean Nouvel* in partnership with *Architecture-Studio* Company won a design competition to build the Arab World Insti-

³ S. Calatrava once said: "Light is comfort in the broadest sense of this word, and together with space, light is the key to the future of architecture". URL: <http://www.procbet.ru/article.asp-articleid=55.htm>.

⁴ URL: <http://www.liveinternet.ru/users/4099413/post185810584/>.

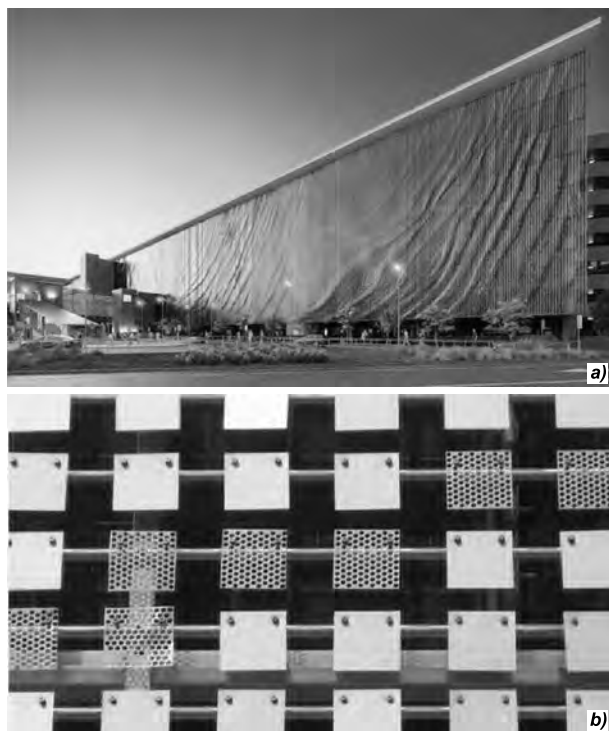


Fig. 8 *The Vertical Lake* kinetic facade:
 a) general view; b) a facade fragment.
 URL: <http://www.lookatme.ru/flow/posts/architecture-radar/110075-kineticheskij-fasad>

tute (Institut du Monde Arab) in Paris, France. After its completion in 1987 it became a popular place both for Parisians and for tourists. One of its remarkable architectural features is its southern wall, which is covered with 240 photo-sensitive aluminium square panels, decorated to resemble an Islamic art style pattern. These panels are apertures, which automatically narrow or expand depending on sunlight intensity, thereby regulating the incoming sunlight and the indoor illumination level⁵. Photo-sensitive components measuring the room's natural illumination level and keeping it constant are built into the panels⁶.

• One kinetic facade design for Brisbane (Australia) uses the wind and sun to achieve a variety of effects (Fig. 8). The idea is proposed by the *Urban Art Projects (UAP)* international design studio together with artist *Ned Kahn* and design group *Brisbane Airport Corporation (BAC)*. The concept of a *Vertical Lake* consists of a vertical array of panels, which changes the relief every

⁵ URL: <http://www.arhinovosti.ru/2011/10/22/institut-arabskogo-mira-ot-zhana-nuvelya-jean-nouvel-parizh-franciya/>.

⁶ In more detail: URL: <http://www.nice-places.com/articles/europe/paris/121.htm>.

second. The array consists of 250 thousand aluminium panels with total area of 5000 m² on the external wall of an eight story car park building in Brisbane airport. The creators of the concept wanted to solve achieve three effects with this kinetic facade: first, the effect of air flows over the surface of the array, when the slightest gust of wind can change the slope angle of each element, creating the impression of ripples on the water; second, inside the parking lot the sunlight passes through the aluminium panels, filling the interior is with patterns of light and shadow; third, the facade design providing ample ventilation, aeration and removal of excessive insolation [9].

• Another example which uses new technologies and future innovations is the campus of the University of Southern Denmark (Kolding, Denmark) with a “smart” facade. This is a complex integrated ecological automated control and self-control system, which generates increased comfort, as well as reduced operational costs and energy saving. A feature of the building designed by *Henning Larsen Architects* bureau, is the unusual triangular configuration of the foundation and the movable kinetic facade elements, which react to changes in temperature and solar illumination (Fig. 9). On the building facade, more than 1500 moveable triangular sun-protection panels are installed. Built in sensors monitor temperature and levels of natural illumination. The sensors are

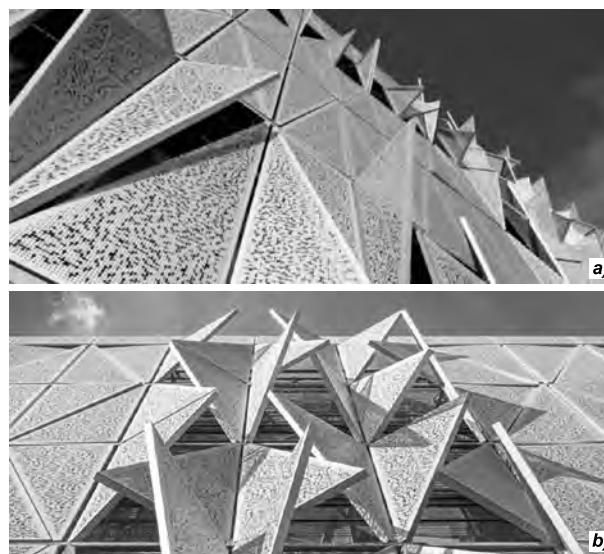


Fig. 9. Triangular in plan campus of the *University of Southern Denmark*

URL: http://stroyka.uz/publish/doc/text116422_kineticheskaya_arhitektura_fasad;
<http://stofasadov.ru/novosti/universitet-v-danii.html>

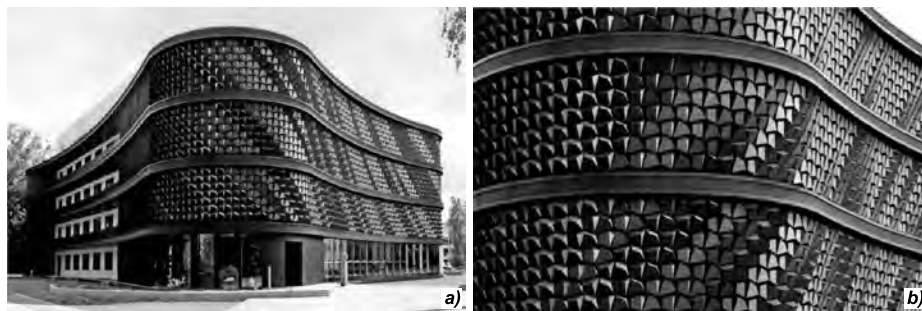


Fig. 10. The FLARE facade membrane:

a) general view; b) a facade fragment

URL: <http://www.arch-platforma.ru/?act=1&cat-g=48&nwid=100>

connected with the movable panel system, which can change position to completely cover, open or slightly open the windows: this avoids the inside the building overheating [10].

- Use of digital technologies allowed Christopher Bauder and Christian Perstil to create the FLARE facade membrane, which was presented by Berlin *WHITEvoid interactive art & design* Company in 2008 at the NEXT exhibition of art and technologies in Aarhus (Denmark). The FLARE is a computer controlled pneumatic facade system (Fig. 10). The system consists of rotating elements, or flakes which together form a dynamic skin for the building, wherein each flake can be at different angle, reacting to its environment. The surface of the flake modules is smooth and shiny, which allows it to reflecting the environment, either catching the sun or turning away to become a dark pixel. When the weather is sunny, the computer system starts the pneu-

matic elements, the flakes turn and the facade becomes «dark», not letting through excess solar rays. The sensors inside and outside the building monitor changes in weather and illuminance, and the appearance of the facade changes with them [11].

- Some dynamically changeable and adaptive architectural façade concepts have already been implemented. Kinetic facades have become one of the most popular topics in modern architecture. The *Ernst Giselbrecht + Partner* Austrian architectural studio has developed an innovative office building project for the *Kiefer Technic Architecture Showroom* (Styria, Austria) (Fig. 11). The office space also includes exhibition areas. Electrically driven facade panels constantly move and adapt to the office needs, adjusting solar illumination of the rooms. The architecture comes to life transforming static sculptural objects into dynamic ones [12].

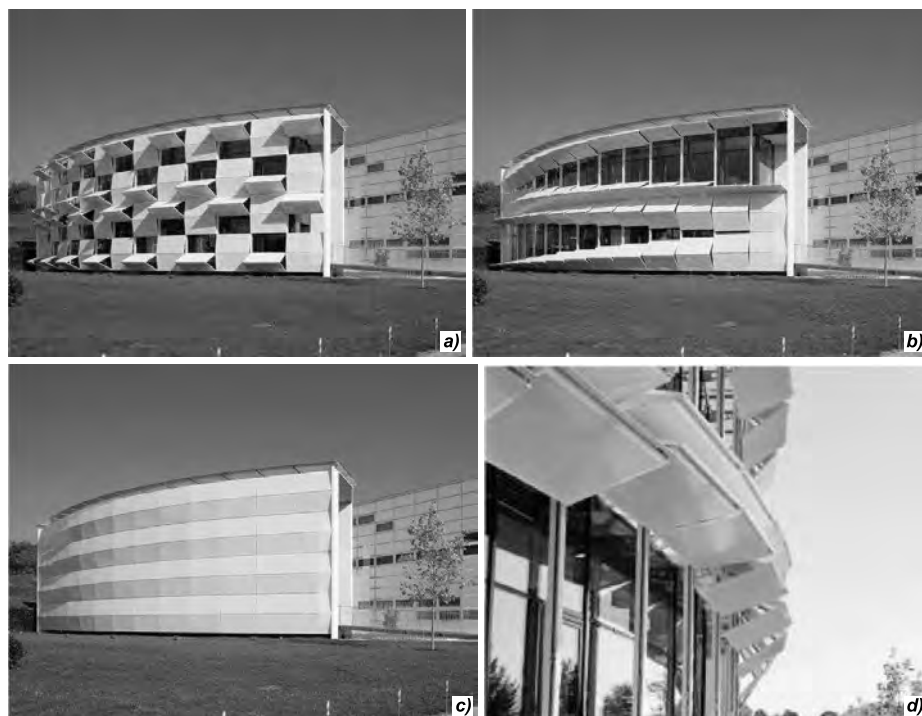


Fig. 11 The Kiefer Technic Architecture Showroom building:

a, b, c – versions of facade transformation; d) a facade fragment while transforming (version b)

URL: <http://ostmetal.info/kineticheskaya-arxitektura-metall-v-dvizhenii-budushhego/>

Natural light can be used cinematically to develop dynamic architecture objects; natural light is the main component of human existence and an extraordinarily powerful tool for an architect. It is also researched thoroughly and considered in designs of static solutions. Many ideas exist on how to «trap» natural light and use it to change space perception throughout a day or a season [13]. Other ideas consider how to create impressions of artificial sunlight to imitate natural illumination in closed spaces: windowless rooms, museums, metro stations⁷, including natural light control. When developing projects with natural light, the most advanced technologies are used: sunlight photometric simulation and imitation.

- One of the examples of the use of simulation in the «control» of natural light⁸ is a natural illumination system for the *High Museum of Art*, Atlanta (USA) constructed according to a project by architect Renzo Piano. The exhibition halls are supplied with openings, which can be described as «light spoons» – curved hatches which disperse natural illumination inside the rooms. To find the best tub-shaped configuration for the light hatches, which «collect» diffused light at the northern side of the building and block direct solar rays at the southern side, a group of specialist carried out many experiments. In 2006 this project obtained two awards of the International association of light designers (IALD).

- It is also worth mentioning the project of Madrid Barajas airport's fourth terminal, which was commissioned by competitive tender in 1997 from the British architectural studio of Richard Rogers and the local bureau *Estudio Lamela*, as well as *Initec* and *TPS* – Spanish and British engineering companies. Wide overhangs of the roof and additional steel elements protect the walls from overheating during the hot summer months. Roundish openings in the ceilings allow natural light to penetrate deep down into the building due to special «canyons» which cut through three above ground passenger terminal levels (there are also three underground cargo levels). At the same

⁷ The designer developed artificial sunlight of «CoeLux». URL: <http://www.sveto-tekhnika.ru/ru/businessnews-3/pages/business/coelux>.

⁸ *Rohir van der Heyde*. Unsurpassed light. Static systems of daylight in architecture and light design//PROCBET. – 2008. – No. 3(4). URL: <http://www.procbet.ru/article.asp-articleid=55.htm>.

time, they do not influence the temperature inside the building in any way⁹.

The considered examples of the use of solar (natural) as a factor of forming dynamic architecture are indicative of the wide variety of the methods of its use. Kinetic aspects are vividly revealed in many design proposals in the ways they deal with natural illumination both when designing buildings in rotation, and when modifying configuration of architectural objects or their facade structures, changing their natural light consumption mode. Furthermore, the recent emergence of new original solutions using kinetic methods based on the effects of natural illumination demonstrates that the traditional approach to building facades is being reconsidered. Use of modern progressive technologies and innovations, in particular of complex integrated ecological systems of automated control and self-control, as well as «solar» digital technologies facilitates increased comfort, and saving running costs and energy resources.

The above listed precedents of using natural light as an important factor in the design of kinetic objects are a result of rapidly developing branches of engineering, mechanics, physics, chemistry and other knowledge fields. Architecture is expanding its sphere of influence sphere as an integrated science with blurring boundaries between architecture and design. Dynamic (kinetic) architecture, which uses the possibilities of natural light, is one for the most recent and interesting directions; it seeks not only to carry out its direct functions but to respond dynamically to the needs of modern people.

REFERENCES

1. *Nazarenko L.A., Chernets V.S., Lesnaya O.I., Kononenko A. Yu.* Illumination role in dynamic architecture of a modern city // Lighting and electric energetics. 2013, № 3–4, pp. 4–10. URL: <http://lepe.kname.edu.ua/index.php/lepe/article/view/260> (addressing date: 11.09.2016 9/11/2016).
2. *Malein M.* Movement architecture / Lecture, November, 2015, in the ZIL Cultural centre, Moscow. URL: http://www.architime.ru/video/kinetic_architecture.htm (addressing date: 8/11/2016).

⁹ <http://ispaniagid.ru/aeropuerto-de-madrid-barajas-glavnyiy-mezhdunarodnyiy-aeroport-ispanii/>.

3. URL: <http://idoorway.mirtesen.ru/blog/43166730751/10-domov>, – brosayuschiy-vy-izov-gravitatsii (addressing date: 7/10/2016), <http://geographyofrussia.com/krutyashhiesya-kvartiry-v-bashne-suite-vollard/> (addressing date: 15.07.2016).
4. URL: <http://mixstuff.ru/archives/43807> (addressing date: 7/14/2016).
5. URL: <http://ecology.md/page/eko-arhitektura-dom-kupol-sledjashhij-za> (addressing date: 9/14/2016).
6. URL: <http://www.chaoslend.ru/node/1651> (addressing date: 9/15/2016).
7. URL: <http://realty.newsru.com/article/11sep2008/bioskin> (addressing date: 8/15/2016).
8. URL: <http://green-buildings.ru/ru/dom-s-resnichkami> (addressing date: 8/15/2016).
9. URL: <http://www.lookatme.ru/flow/posts/architecture-radar/110075-kineticheskiy-fasad> (addressing date: 8/15/2016).
10. URL: http://stroyka.uz/publish/doc/text116422_kineticheskaya_arhitektura_fasad (addressing date: 8/15/2016).
11. URL: <http://www.archplatforma.ru/?act=1&catg=48&nwid=100> (addressing date: 8/15/2016).
12. URL: <http://ostmetal.info/kineticheskaya-arhitektura-metall-v-dvizhenii-budushhego/> (addressing date: 8/25/2016).
13. *Narboni R., Nicholas E.* A light trap in the Eqho tower lobby in La Défense quarter (Paris)// *Svetotekhnika*. 2014, #4, pp. 70–72. URL: <http://www.sveto-tekhnika.ru/fullarticles/pages/fullarticles/eqho> (25.09.2016 addressing date: 9/25/2016).



Nataliya A. Saprykina,

Doctor of Architecture, Professor. She graduated from the MARKHI in 1970. At present, she is the Head of the chair «Elements of architectural design» of the MARKHI (SA), an honoured architect of the Russian Federation, an honorary member of the RAACS and a member of the Moscow Union of Architects

REFLECTIVE FACADES AND THEIR INFLUENCE ON ILLUMINATION OF NEARBY BUILDINGS

Alexei K. Solovyov

MSCU NRU, Moscow
E-mail: agpz@mgsu.ru

ABSTRACT

Architects believe that reflective or specular facades intensify illumination in rooms of the buildings opposite. Is this really so? To establish whether this is the case, typical examples of daylight factor calculations for rooms in building opposite mirror facades are considered. It is found that reference point illuminance increases above a normal diffusely reflecting façade case, only when a large area of the sky is reflected. In other cases, reflective facades cause considerable decrease in illuminance inside buildings which face them.

Keywords: specular reflection, facade, facade luminance, natural illumination, building geometry, diffuse reflection, structural glazing, double-glazed window, double-glazed window deflection, climate loading

1. INTRODUCTION

Reflective specular facades (SF) are one of the newest trends in architecture. Facades can be partly or entirely mirrored. An entirely SF building is an example of the «disappearing architecture», when the surrounding environment is reflected in the façade with trees, buildings, cars, people, and building itself is not seen. The building becomes visible only at night, when electric light shines in its windows. The «disappearing architecture» can be a good instrument for an architect when restoring architectural ensembles and

architecture monuments, if the surrounding buildings are of a great importance.

Specular reflection of facades can be broken by «climate loading», when under the influence of a high external temperature, glass in double-glazed windows are deflected outside, and at low external temperatures, on the contrary, they are deflected inside [1–3]. This breaks the clearness of the reflection. Influence of such scattering on natural illumination conditions in buildings opposite buildings can be minimal but requires analysis.

Studies of room illumination through light shelves have showed [4–6] that the maximum gain in illumination level (IL) is on the top floors, where the light shelf illuminated by the firmament, is visible from reference points. IL gain is minimal when secondary reflections take place.

SFs pose many architectural questions. They are not only an instrument of architectural and artistic solution for surrounding building design but also strongly influence the light environment in rooms of the buildings opposite and in rooms of the mirror façade buildings themselves. On the



Fig. 1. Structural glazing forms an ideal specular surface of a building facade

one hand, reflective façades can considerably raise IL in rooms of buildings opposite them. On the other hand, if the building opposite is tall, then the neighbouring reflective façade can significantly reduce IL in its higher rooms. The following analysis shows the conditions, which lead to increased or decreased IL.

2. CALCULATION METHODS AND RESULTS

Reflective façade buildings, especially with structural glazing (Fig. 1), reflect the environment in a specular manner. It is the content of the reflection which is important: either the high luminance sky, or nearby buildings which have different heights and different façades of different reflecting power. Mirror façade buildings influence the IL in rooms inside buildings which stand right next to them. The reflections of buildings opposite are clearly visible in Fig. 2, in which a building with a normal SF is shown. The luminance of the reflected building is considerably lower than the luminance of the reflected sky.

2.1. Methods

Practicing architects often believe that SFs raise IL in rooms buildings opposite them [7]. Is this really the case? Let's consider several typical cases of building geometry. For simplicity, we will first consider cases where opposite buildings are mutually parallel and their length far exceeds their height and the distance between them. Optical transmission of the opening and inner reflection characteristics will be assumed to be identical in the calculated room. The room, for which the daylight factor is calculated, has windowsill height $h_{\pi} = 1$ m, window height $h_o = 1.5$ m, wall thickness $d_{cr} = 0.5$ m, distance from the window to the floor reference point $d = 3$ m and distance between the buildings $L = 15$ m.

Case 1

The SF has a constant height $H_2 = 24$ m at different height to the building opposite with the calculated room H_1 from 4 to 28 m, with a step of 4 m (all geometrical designations used hereinafter are given in Fig. 3 and 4).

The calculation of the geometrical daylight factor ε is performed according to established for-



Fig. 2. Reflection of opposed buildings in a standard specular facade with transoms

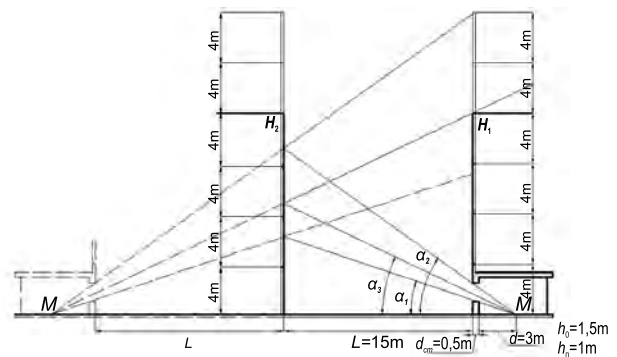


Fig. 3. A diagram for accounting of an opposite building's specular facade (cases 1 and 2)

mulas corresponding to the calculation according to A.M. Danilyuk's diagram #1.

– If only sky or a building opposite is seen through the window from the reference point (r.p.) M , then:

$$\varepsilon = \frac{\cos \alpha_1 - \cos \alpha_2}{2} \cdot 100\%,$$

where $\alpha_1 = \arctg \frac{h_{\pi}}{d}$, $\alpha_2 = \arctg \frac{h_{\pi} + h_o}{d + d_{cr}}$.

– If reflection of the firmament and of a building opposite are visible through the window from the reference point, then the geometrical daylight factor ε_H taking into consideration direct light from the sky, is expressed as follows:

$$\varepsilon_H = \frac{\cos \alpha_3 - \cos \alpha_2}{2} \cdot 100\%,$$

where $\alpha_3 = \arctg \frac{H_1}{d + d_{cr} + 2 \cdot L}$,

as it is seen from Fig. 4.

Table 1. Calculated values in case 1

H_1	α_1	α_2	α_3	ε_H	$\varepsilon_{3Д}$	q	b_ϕ	$K_{3Д,*}$	$K_{3Д}$	e	\bar{e}^{**}	Note	
4	18.43°	35.54°	6.81°	6.75	0	0.817	-	-	-	2.206	1.91	Only sky is reflected	
8			13.43°				-	-	-				
12			19.71°	6.38	0.37	0.826	0.23	1.192	1.18	2.148		A building + the sky are reflected	
16			25.53°	4.43	2.32	0.864		1.344	1.771				
20			30.84°	2.24	4.51	0.898		1.39	1.126	1.327			
24			35.62°	0	6.75	-	0.225	1.33	1.33	0.808		Only a building is reflected	
28	39.88°	-	0.213			0.765							

* $K_{3Д,0}$ is a coefficient, which accounts for the change of the daylight factor inner reflected component (e) in a room in the case of full shadowing of the firmament by the building opposite as seen from the reference point (determined by Table B.6 of the Building Regulations [8])

** \bar{e} is the daylight factor value when shadowed by a normal facade with $\rho_\phi = 0.4$

According to the Building Regulations (BR) [8], daylight factor

$$e = (\varepsilon_H \cdot q + \varepsilon_{3Д} \cdot b_\phi \cdot K_{3Д}) \cdot \tau_o \cdot r_o / K_3,$$

where τ_o is the general light transmission factor, $\varepsilon_{3Д}$ is the geometrical daylight factor taking into consideration light reflected from the opposed building (it is calculated according to the correspondent BR formula [8]), b_ϕ is average relative luminance of the opposite building's facade (according to the correspondent BR Table [8]), $K_{3Д}$ is the coefficient, which accounts for changes of inner reflected daylight factor component in the room with the availability of the building opposite (it is calculated according the correspondent BR formula [8]), K_3 is the calculation coefficient which accounts for the daylight factor and decreased illuminance during operation as a result of the pollution and aging of translucent fillings in the light openings, as well decreasing reflective properties of the room surfaces (determined according to Table 3 of the Building Regulations [9]), r_o is the coefficient, which accounts for day-

light factor increase in the case of lateral illumination due to light reflected from the room's surface and from the underlying layer adjacent to the building. This coefficient, is used according to BR Tables B.4 and B.5. [8], q is the coefficient which represents non-uniform luminance of the CIE cloudy sky:

$$q = \frac{1 + 2 \sin \theta}{3} \cdot \frac{9}{7},$$

where $\theta = (\alpha_2 + \alpha_3)/2$.

Further, we assume for simplicity that $\tau_o = 1$, $K_3 = 1$, $r_o = 1$ and add SF reflection factor $\rho_{3ЭРК}$ to formula for e as a common multiplier, equal to 0.4, which is typical for i -glass.

We determine b_ϕ value according to the relevant BR Table [8] for a building reflected in the mirror facade, i.e. for the building with the calculated room. For this building we determine $K_{3Д}$ value by considering redistribution of luminous fluxes inside the studied room due to reflection from the mirror facade using another BR Table [8]. Had the opposed building not specu-

Table 2. Calculated values in case 2

H_I	α_1	α_2	α_3	ϵ_H	ϵ_{3D}	q	b_ϕ	$K_{3D,0}^*$	K_{3D}	e	\bar{e}^{**}	Note	
4	18.43°	35.54°	6.81°	6.75	0	0.817	–	–	–	5.51	5.51	Direct component only (e_H)	
8			13.43°				–	–	–			Direct component only (e_H)	
12			19.71°	6.38	0.37	0.826	0.213	–	1.18	5.37	5.36	Direct component. (e_H) + reflected component (e_{3D})	
16			25.53°	4.43	2.32	0.864		–	1.126	4.48	4.38	Direct component. (e_H) + reflected component (e_{3D})	
20			30.84°	2.24	4.51	0.898		–	1.26	2.52	3.22	Only a building + direct sky are reflected	
24			35.62°	0	6.75	–		–	1.33	0.765	1.91	0.765	Only a building is reflected
28			39.88°			–		–	1.33				

* $K_{3D,0}$ is the coefficient, which accounts for the change of the daylight factor inner reflected component (\bar{e}) in a room in the case of full shading of the firmament by the building opposite as seen from the reference point (determined by Table B.6 of the Building Regulations [8])

** \bar{e} is the daylight factor value when shadowed by a normal facade with $\rho_\phi = 0.4$

lar but normal facade with typical reflection factor $\rho_\phi = 0.4$, then through a window from the reference point we would see the opposed building wall only. To be compared, e calculation for this case was carried out.

The calculated e values for specular and normal facades are given in Table 1, from which it is clear: if the reference point reflects the sky only from the specular facade, then the SF raises e in the studied room (approximately by 15 % in this

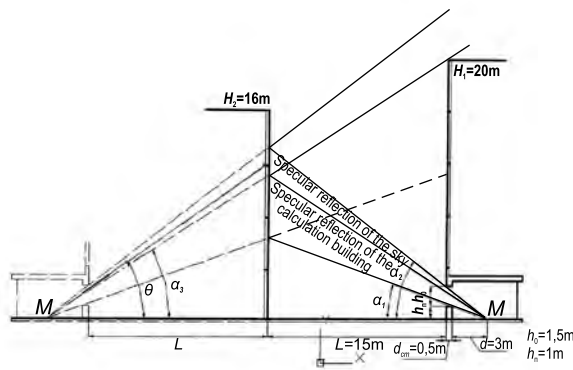


Fig. 4. A diagram for calculation in the example with a specular façade building opposite

case), and of course the higher the ρ_{ϕ} , the greater e becomes.

With increasing H_1 , when the building with the studied room begins to be reflected in the SF, consequently reducing the portion of the sky seen in the SF, e in the reference point M decreases. If $H_1 \geq 22$ m in case the building opposite has a mirror facade, e considerably decreases (in our situation approximately by 40 %). Generally, SF only raises e when L is equal to height H_1 excess over reference point M .

Case 2

H_2 varies when H_1 is constant at $H_1 = 28$ m. Unlike case 1, at small H_2 here in reference point M , only direct component e from the sky light can take place.

2.2. Results

The e calculation results both with SF and with a normal facade of the building opposite are given in Table 2. It can be seen from the table that in our case at $H_1/L = 0.67$, in reference point M , only e direct component takes place, which is the same for both these facades. With growth of H_2 in excess over the reference point M , its e value gradually decreases because of a reduction of the solid angle, under which the open sky site is visible through the light opening. In the event that an opposed building has a reflective, as soon as the open sky is no longer seen from the reference point with H_2 growth, e abruptly decreases. Decrease of e in our case is the same as in case 1 considered above, i.e. it is approximately equal to 40 %.

As it can be seen from Tables 1 and 2, the calculated e value found according to the BR [8], does not depend on H_1 . What actually happens is that

the facade (including SF) of the opposed (shading) building is illuminated with a section of firmament, the size of which depends on H_1 , and therefore both b_{ϕ} and hence e depend on H_1 .

Today, when there is a possibility of mathematically simulating illumination conditions using a computer in the case of shadowing by a building opposite, a correction of the BR Table B.2 [8] for determination of b_{ϕ} is necessary, and it is vital to take H_1 into account.

This correction is especially important relative to the central districts of cities with their restrained urban conditions, and it can facilitate the work of architects and designers regarding reconstruction of these districts.

To understand, the influence of nearby mirror facades on illumination conditions in rooms of buildings opposite them, it is necessary to construct a scale cross-section of the building's context with a cross-section of the specific room and construct a beam diagram of solid angles of direct and reflected light coming through the opening to the reference point (Fig. 4).

Let us now consider a worked example

Let $H_1 = 20$ m, $H_2 = 16$ m, $L = 15$ m, $d = 3$ m, $h_{\pi} = 1$ m, $h_o = 1.5$ m, $d_{cr} = 0.5$ m and $\rho_{\text{зепк}} = 0.4$. Calculated values $\alpha_1 \approx 18.43^\circ$, $\alpha_2 \approx 35.84^\circ$, $\alpha_3 = \arctg[20/(3+0.5+2 \cdot 15)] \approx 30.84^\circ$, $\epsilon_H \approx 2.4\%$, $\epsilon_{\text{зл}} \approx 4.5\%$, $\epsilon_H \approx [(\cos 30.84^\circ - \cos 35.84^\circ)/2] \cdot 100\% \approx 2.4\%$, $\epsilon_{\text{зл}} \approx [(\cos 18.84^\circ - \cos 30.84^\circ)/2] \cdot 100\% \approx 4.5\%$, $\theta \approx (35.84^\circ + 30.84^\circ)/2 \approx 33.34^\circ$, $q \approx 0.9$, $b_{\phi} \approx 0.18$, $K_{\text{зл}} \approx 1.23$ and $e \approx 3.156\% \cdot 0.4 \approx 1.26\%$.

With a normal facade of the building opposite with $\rho_{\phi} = 0.4$, $e \approx 1.53\%$, i.e. more than with an SF.

At $H_1 = 24$ m, a reflection of the sky is not visible from the reference point. The building is only seen with the room containing this point. With ZF, $e \approx 0.67\%$, and with a normal facade at $\rho_{\phi} = 0.4$, $e \approx 1.68\%$. Even at $\rho_{\text{зепк}} = 1$, which in principle is impossible, calculated $e \approx 1.68\%$, i.e. could only come near to e value in case of a normal, diffusely reflecting facade.

Therefore, in this example, the reflective facade reduces illuminance at the reference point.

REFERENCES

1. Calculation of climate load on a double-glazed window as exemplified by Moscow // Scientific review, 2013, #9, pp. 190–194.

2. *Straty P.V., Boriskina I.V., Plotnikov V.V.* Climate load on double-glazed windows // MSCU Bulletin, 2011, #2–2, p. 262.

3. *Straty P.V., Plotnikov V.V., Boriskina I.V.* Study of double-glazed window deflection under the influence of the climate load atmospheric component // Home construction, 2011, #4, pp. 33–36.

4. *Stetsky S.V., Chen-Guanlun.* Optimum structural, planning and geometrical solutions of light shelves for multi-storey production buildings // Industrial and civil construction, 2013, #2, pp. 84–85.

5. *Stetsky S.V., Chen-Guanlun.* Creation of high-quality light environment in rooms of production buildings for climatic conditions of south-east China // Messenger of the MSCU, 2012, #7, pp. 16–25.

6. *Stetsky S.V., Chen-Guanlun.* Structural and planning solutions of multi-storey production buildings with a support of natural illumination through light shelves in them // Industrial and civil construction, 2014, #3, pp. 70–72.

7. *Grishchenko G.D., Kasyanov V.F.* Formulation of the problem concerning application of light guides and reflected light by facades to improve insolation conditions and to increase daylight factor when reconstructing urban development // Svetotekhnika, 2015, #3, pp. 27–30.

8. Building Regulations СП 23–102–2003 “Natural illumination of residential and public buildings”.

9. Building Regulations СНиП 232–05–95 * «Natural and artificial illumination».



Alexei K. Solovyov,

Doctor of Technical Science, Professor, graduated from the MSCU of V.V. Kuybyshev in 1965. At present, he is the Professor of the Chair of «Architecture of civil and industrial buildings» of the MSCU Federal state budgetary educational institution of higher vocational training, a member of the European Academy of Sciences and Arts and of the editorial board of the Light and Engineering journal. He has titles “Honourable builder of the Russian Federation» and “Honoured higher education worker of the Russian Federation”

A COMPARATIVE ANALYSIS OF THE INFLUENCE ARTIFICIAL ILLUMINATION ON BEHAVIOUR OF LABORATORY ANIMALS

Mikhail V. Osikov¹, Oksana A. Gizinger², Olga I. Ogneva¹, Olga R. Bokova²,
and Victoria G. Chudinova²

¹ Southern Ural State Medical University

² Southern Ural State University (National Research University)

E-mail: ogizinger@gmail.com

ABSTRACT

The article presents the results of a comparative ethological study of the influence of light emitting diode and fluorescent light sources on laboratory animals. The researches were carried out on 46 guinea pigs. Their behaviour and activity was observed in the Open field test, and cognitive function was assessed using Morris's Water maze. The results showed that under conditions of both fluorescent and light emitting diode illumination, the animals didn't exhibit symptoms of alarm, decrease in investigatory-exploratory behaviour, indicators of decrease of training ability and long-term memory. On the contrary, improvement in spatial orientation on the 30th day of the researches in comparison with the 10th and 20th days of the observations was noticed. A comparative ethological analysis of the state of the animals showed that indicators reflecting spatial orientation using external reference points improved with light emitting diode and fluorescent illumination, compared to natural illumination.

No statistically significant difference between light emitting diode illumination and fluorescent illumination was revealed in terms of their influence on animal spatial orientation.

Keywords: light emitting diode illumination, fluorescent illumination, laboratory animals, behavioural activity, ethological status

SIGNIFICANCE

The increased use of light emitting diode sources is a priority direction for the development of energy saving illumination, which is connected with their operation benefits [4, 5, 6]. Research into the biomedical effects of illumination over the last few years has shown that light of the visible spectrum interval affects some physiological and psychophysiological processes in a human body [7, 9, 10]. The authors have previously demonstrated that desynchronosis under fluorescent illumination conditions was observed to change the state of an animal subject on the tenth day of the experiment, compared to light emitting diode sources [4,5]. However, a comparative analysis of the influence of light emitting diode and fluorescent sources of artificial light is important. The interest of biologists and physiologists in this topic is supported by the annual growth and wide application of light emitting diode light sources in place of fluorescent, which definitely creates a need for more comparative research into their influence on behaviour, activity and cognitive function of animals [12].

The research objective is to carry out a comparative ethological evaluation of the state of laboratory animals under conditions of artificial light from light emitting diodes and fluorescent illumination.

Table 1. Main characteristics of artificial illumination sources used for the study

Indicator	Light emitting diode illumination sources	Fluorescent illumination sources
Manufacturer	«ISAlight – Office 32», Automation Engineering Systems Open Company, Russia	«LLAlight – Office 30», Automation Engineering Systems Open Company, Russia
Colour-rendering index, Ra	75	75
Radiation colour, K	4500 (neutral-white)	4500 (neutral-white)
Luminous flux pulsation,%	Less than 4 % (1 %)	Less than 5 %
Illuminance level, lx	400	420

MATERIALS AND METHODS

For the researches, forty six guinea pigs were taken from the nursery of laboratory animals of the Microgen FSUO scientific and production association of the Ministry of Health of the Russian Federation. The guinea pigs were under vivarium standard conditions and were fed using a typical diet according to the standards confirmed by the Order of the Ministry of Health of the USSR # 1179 of 10.10.1983. They had free access to food and water. All experimental work with the animals was performed in accordance with the European Convention for the Protection of Vertebrate Animals used for Experimental and other Scientific Purposes (ETS123, 18.03.1986), including provisions of Appendix A of 15.06.2006 and Directive 2010/63/EU of the European Parliament and Council of the European Union on the protection of animal used for scientific purposes of 22.09.2010. Experiments were carried out under *in vivo* conditions with nonlinear reproductive male guinea pigs of 300 ± 50 g mass. Guinea pigs were chosen as research subjects because, unlike others experimental animal (rats, mice), they exhibit daytime activity [8,15,16]. The light perception and colour perception of guinea pigs is close to the chromatic sensitivity of a human eye, which makes them appropriate for the study of light-associative changed states [13, 14,15].

The study used fluorescent and light emitting diode sources. Their main characteristics are presented in Table 1.

Artificial sources were placed at a distance of 250 cm above the animals' cages so that the luminous flux could uniformly illuminate the perimeter.

Natural indoor illuminance at cage level changed during the day according to the season (August-September) and to the annual features of photoperiodicity of the Southern Ural region: in the morning (08:00–09:00) 50–200 lx; in the afternoon (10:00–16:00) up to 800 lx on clear days, and 500 lx in overcast days; in the evening (18:00–20:00) 150–300 lx. The duration of a natural light day was between 12 and 14 hours.

For the purposes of the study, the forty-six guinea pigs were randomly divided into groups: group 1 ($n = 8$) consisted of animals under natural illumination (NI) conditions (12 hours of natural light / 12 hours of darkness), group 2 ($n = 20$) consisted of animals under standard stable illumination conditions (12 hours of light / 12 hours of darkness). This mode (SSFI) was created by fluorescent lamps. Group 3 ($n = 18$) consisted of animals under standard stable illumination conditions. This mode (SSLEDI) was created by light emitting diode lamps. The state of the animals was studied using the Open field and Morris's Water maze test actographs [2]. An evaluation of the animals under NI, SSFI and SSLEDI conditions was carried out on the 10th, 20th, and 30th day of the experiment. The total duration of the experiment was 30 days.

The Open field test was performed in order to study the behaviour of experimental animals under new (stress inducing) conditions and allowed estimating first a level of emotional and behavioural reactance of the animals, and secondly strategy of investigatory-exploratory behaviour using intensity and dynamics of separate behavioural elements [13].



Fig. 1. Open field test

The actograph (Fig. 1) represents an open square site of 80×80 cm size bordered along its perimeter with opaque boards. The floor of the arena is divided into 16 squares. Each square has one opening at its centre 3 cm in diameter intended to reveal a species-specific component of research activity of the rodents (hole exploratory behaviour). The animal under test was placed in the Open field in its angular square at the arena wall. The test lasted 30 minutes. Every animal was tested once [14].

During the test process, the sequence of the behaviour and actions was recorded: horizontal activity (HA), which is number of squares crossed; vertical activity (VA), which is number of times an animal stands on its hind feet with the support of the arena board and without support; research activity (RA), which is the number of peeps into the holes on the arena floor; number of grooming actions (GR); and, number of fecal boluses (FB). Behavioural actions and vegetative reactions were recorded using a digital video camera. The obtained data were processed using the Real Timer computer program of Open Science Research-and-production complex Open Company, Russia.

Morris's Water maze test is used to study animal cognitive function state and spatial navigation ability [15]. To carry out the test, a pool 180 cm in diameter and 60 cm in height is filled with water (Fig. 2). Water in the pool is tinted opaque with milk in order to remove the possibility of seeing the underwater platform. The water temperature was $24 \pm 2\text{C}^\circ$. To simplify orientation of the animals in the space, the pool walls have fixed images of black-and-white geometric shapes (circle, square, triangle and rhombus). A platform of translucent organic glass of 15×15 cm size was placed at the centre of the pool's northern sector (near to the rhombus shape), lower than water level by 1 or 2 cm. The test was carried out with the invisible platform, without the platform and for visual perception. Movements of the animals were recorded by means of a video camera placed over the pool. In the Morris's Water maze, three test series were performed: 4–10 days of the experiment, 14–20 days of the experiment and 20–30 days of the experiment. Different animals took part in each series of the tests.

In the test with invisible platform, daily over the course of four days, the animals were given two attempts each to search for the platform invisible from the water surface. The starting point for the animal start in the pool was changed every day. Average time of the platform search and average length of the search trajectory were recorded. Calculation of the animal movement trajectory was carried out using the Any-maze program (Stoelting Co., the USA). On the fifth day, two tests were made: a test for visual perception and test without a platform.

Within the test for visual perception, in the southern sector (opposite to the sector, in which the platform was placed), a black platform was installed, which was 1.5 cm higher than the water level.

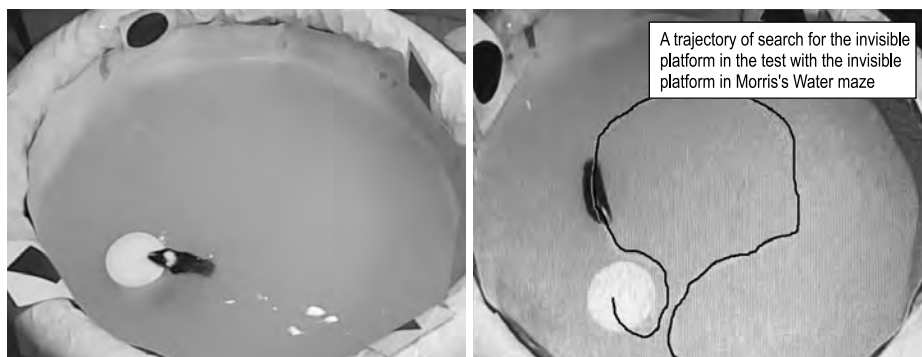


Fig. 2. Morris's Water maze test

vel: the time the animal took to find the platform, was recorded.

In the test without a platform, the animals were placed in the southern sector of the pool. The length of time an animal stayed in each sector, and the percentage of animals staying in the sector were recorded. The sample characteristic is presented in the $M \pm m$ format, where M is arithmetic mean value of a criterion; m is standard error of the mean. To analyse the distribution normalcy the Shapiro-Wilk test was used, to check the hypotheses about equality of general dispersions the Levene test was used. Check of statistical hypotheses in the groups was carried out using the Mann-Whitney test (U), and Wald-Wolfowitz Run Test (WW).

The differences were considered to be significant at $p \leq 0.05$. At $p > 0.05$, the hypothesis about insignificance of statistical differences was accepted.

RESULTS AND DISCUSSION

The Open field test revealed an increase of horizontal activity on the 10th day and on the 30th day of observations under conditions of fluorescent illumination in comparison with natural light; also an increase of vertical activity was observed on the 10th day, a decrease in the number

of grooming actions was observed on the 20th day, and a decrease in the number of fecal boluses on the 30th day of the experiment was also noticed (Table 2).

The increase of horizontal and vertical activity on the 10th day suggests active investigatory-exploratory behaviour and an absence of feelings of alarm amongst the animals, which reflects the exploratory behavioural component. A decrease in grooming on the 20th day can only be interpreted in conjunction with change in other indicators. Taking into consideration that other parameters did not differ from indicators of the group investigated under natural illumination conditions, it can only be concluded that the animals don't exhibit characteristics of alarm and their investigatory-exploratory behaviour wasn't influenced. On the 30th day, a combination of an increase in horizontal activity increase and a decrease in the number of fecal boluses reflecting vegetative reaction of an animal shows that there are no criteria of alarm and oppression of investigatory-exploratory behaviour.

So the animals didn't show signs of alarm and oppression of investigatory-exploratory behaviour on the 10th, 20th and 30th days.

Under conditions of standard stable light emitting diode illumination in comparison with natural illumination, it was found that during the

Table 2. Indicators of the Open field test under the standard stable fluorescent illumination ($M \pm m$) conditions

Indicators	Group 1 NI (n = 8)	Group 2 SCFI		
		10 th day (n = 6)	20 th day (n = 8)	30 th day (n = 6)
Horizontal activity, number of actions	19.25 ± 4.96	29.67 ± 2.79 *	23.00 ± 3.11	29.33 ± 4.15 *
Vertical activity, number of actions	1.50 ± 0.18	2.67 ± 0.21 *	1.67 ± 0.42	2.00 ± 0.37
Exploratory activity, number of actions	3.50 ± 0.62	5.00 ± 0.97	2.67 ± 0.21	3.33 ± 0.21
Grooming, number of actions	3.37 ± 0.46	1.67 ± 0.42	1.33 ± 0.21 *	2.67 ± 0.76
Fecal boluses, number of actions	7.37 ± 0.80	5.00 ± 1.32	5.33 ± 0.76	4.33 ± 0.42 *

Note. * – Significant ($p < 0.05$) differences as compared with NI group.

Table 3. Indicators of the Open field test under standard stable light emitting diode illumination conditions (M ± m)

Indicators	NI group	SSLEDI group		
		10 th day	20 th day	30 th day
Horizontal activity, number of actions	19.25 ± 4.96	28.67 ± 2.20 *	34.33 ± 5.06 *	31.33 ± 2.49 *
Vertical activity, number of actions	1.50 ± 0.18	2.67 ± 0.42 *	3.67 ± 0.76 *	2.67 ± 0.22 *
Exploratory activity, number of actions	3.50 ± 0.62	5.33 ± 0.76	6.00 ± 0.97 *	3.67 ± 0.56
Grooming, number of actions	3.37 ± 0.46	3.00 ± 0.37	3.67 ± 0.76	1.33 ± 0.21 *
Fecal boluses, number of actions	7.37 ± 0.80	6.00 ± 0.97	5.67 ± 0.56	5.00 ± 0.73

Note. * – Significant (p < 0.05) differences as compared with NI group.

Open field test, horizontal and vertical activity of animals increased on the 10th, 20th and 30th days of the observation, exploratory activity increased on the 20th day, the number of grooming actions decreased on the 20th day of the experiment (Table 3).

Increase of horizontal and vertical activity on the 10th and 20th days as well as an increase of exploratory activity on the 20th day suggests active investigatory-exploratory behaviour of the animals. On the 30th day, the decrease of grooming action number against a background of high indicators of horizontal and vertical activity as a whole is indicative of the absence of alarm and oppression criteria of investigatory-exploratory behaviour. Thus, there were no animal indicators of alarm and oppression of investigatory-exploratory behaviour on the 10th, 20th and 30th days of the experiment.

With standard stable fluorescent illumination during Morris’s Water maze test with the in-

visible platform, reduction of the platform search time on the 30th day was observed, length of the trajectory of the platform search did not change (Table 4, 5).

In the test for visual perception, a reduction of search time for the visible platform on the 20th and 30th days of the experiment (Fig. 3) was observed.

In the test without a platform, no time differences of animals staying in the underwater platform location area for all periods of the experiment was revealed (Table 6).

So in some tests in Morris’s Water maze under standard stable fluorescent illumination conditions, an improvement of the animal’s orientation in space was observed on the 20th and 30th days. There was no indicators decreased training ability or long-term memory in all periods of the experiment.

When studying animal cognitive function under standard stable light emitting diode illumina-

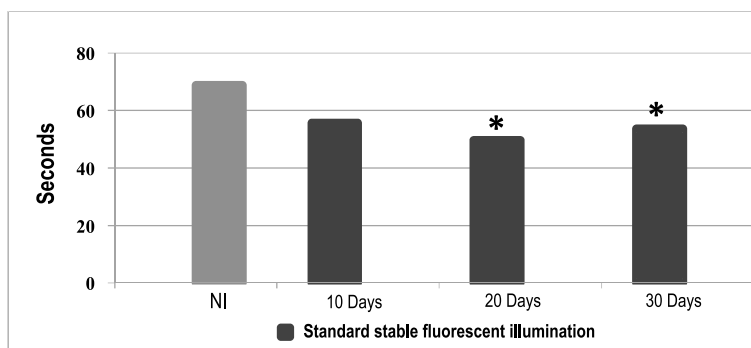


Fig. 3. Time of searching for the visible platform within the test for visual perception under standard stable fluorescent illumination conditions
Note. * – Significant (p < 0.05) differences as compared with NI group.

Table 4. Time of searching for the platform within the test with invisible platform in Morris’s Water maze test under standard stable fluorescent illumination ($M \pm m$) conditions

Indicators	Group 1 NI (n = 8)	Group 2 SSFI		
		10 th day (n = 6)	20 th day (n = 8)	30 th day (n = 6)
First day, s	86.38 ± 1.71	86.83 ± 1.10	75.25 ± 5.13	84.33 ± 3.58
Second day, s	76.81 ± 4.06	78.83 ± 5.64	59.63 ± 7.15	64.00 ± 3.18 *
Third day, s	58.31 ± 6.16	60.33 ± 5.24	60.13 ± 5.57	46.67 ± 5.57 *
Fourth day, s	35.19 ± 5.45	22.50 ± 2.69	46.87 ± 3.92	18.17 ± 2.89 *

Note. * – Significant ($p < 0.05$) differences as compared with NI group.

Table 5. Length of trajectory when searching for the platform hidden under the water in Morris’s Water maze under standard stable fluorescent illumination ($M \pm m$) conditions

Indicators	Group 1 NI (n = 8)	10 th day (n = 6)	Group 2 SSFI	
			20 th day (n = 8)	30 th day (n = 6)
First day, m	19.62 ± 1.25	20.03 ± 1.92	18.48 ± 1.88	22.22 ± 1.73
Second day, m	17.49 ± 0.87	18.09 ± 1.13	17.53 ± 1.31	19.23 ± 1.11
Third day, m	14.68 ± 1.04	14.36 ± 1.42	13.89 ± 0.94	13.15 ± 1.11
Fourth day, m	13.54 ± 0.39	14.30 ± 1.27	12.80 ± 0.75	11.27 ± 0.30

tion conditions during the test with the invisible platform in Morris’s Water maze, search time for the platform on the 10th and 20th days didn’t differ from the natural illumination group (Table 7). On the 30th day, search time was the lowest compared to the natural illumination group for all days of the experiment. When analyzing the length of search trajectory for the invisible platform, no difference from the natural illumination group

on the 10th, 20th and 30th days for all periods of the experiment was revealed (Table 8).

During the test for visual perception, searching time of the visible platform decreased in comparison with the natural illumination group on the 10th, 20th and 30th day of the experiment (Fig. 4).

When estimating the test without a platform, the portion of time an animal stayed in the area, where the invisible platform was previously lo-

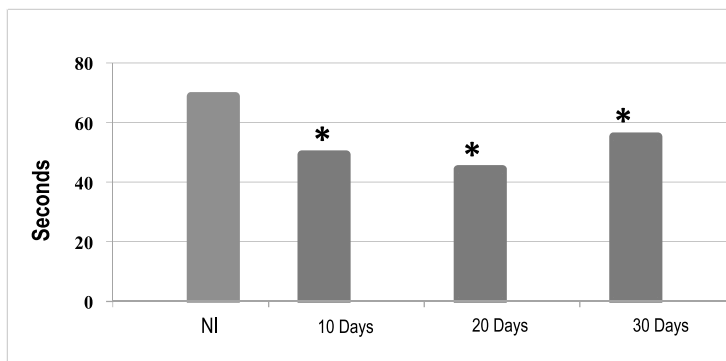


Fig.4. Searching time for the visible platform in the test for visual perception under light emitting diode illumination conditions
Note. * – Significant ($p < 0.05$) differences as compared with NI group

Table 6. Portion of time an animal stayed in the area of the underwater platform during the test without the platform in Morris’s Water maze under standard stable fluorescent illumination conditions (M ± m)

Indicators	Group 1 NI (n = 8)	Group 2 SSFI		
		10 th day (n = 6)	20 th day (n = 8)	30 th day (n = 6)
Time portion,%	69.30 ± 5.88	71.33 ± 2.56	70.25 ± 3.71	71.33 ± 3.04

Table 7. Search time for the platform hidden under the water in Morris’s Water maze test under standard stable LED illumination conditions (M ± m)

Indicators	Group 1 NI (n = 8)	Group 3 SSLEDI		
		10 th day (n = 6)	20 th day (n = 8)	30 th day (n = 6)
First day, s	86.38 ± 1.71	73.17 ± 4.25	83.83 ± 1.69	58.67 ± 4.23 *
Second day, s	76.81 ± 4.06	62.67 ± 3.22	60.50 ± 10.05	21.83 ± 9.39 *
Third day, s	58.31 ± 6.16	48.00 ± 3.80	48.33 ± 5.01	17.33 ± 2.38 *
Fourth day, s	35.19 ± 5.45	43.33 ± 5.75	46.50 ± 6.32	14.33 ± 3.01 *

Note. * – Significant (p < 0.05) differences as compared with NI group.

Table 8. Length of search trajectory for the platform hidden under water in Morris’s Water maze under standard stable LED illumination conditions (M ± m)

Indicators	Group 1 NI (n = 8)	SSLEDI group		
		10 th day (n = 6)	20 th day (n = 8)	30 th day (n = 6)
First day, m	19.62 ± 1.25	21.56 ± 1.66	20.07 ± 2.09	21.74 ± 1.66
Second day, m	17.49 ± 0.87	17.94 ± 0.93	19.06 ± 1.40	19.45 ± 1.04
Third day, m	14.68 ± 1.04	14.34 ± 1.21	14.99 ± 1.06	13.32 ± 1.08
Fourth day, m	13.54 ± 0.39	13.46 ± 1.87	12.00 ± 1.04	11.56 ± 0.35*

Note. * – Significant (p < 0.05) differences as compared with NI group.

cated, on the 10th, 20th and 30th day did not differ from the natural illumination group (Table 9).

Comparative ethological analysis of the state of the animals under artificial illumination conditions observed that indicators reflecting spatial orientation by external reference points was raised earlier under light emitting diode illumination, than under fluorescent illumination, name-

ly on the 10th day, however, variance of these differences is not statistically significant. A possible explanation of the obtained results is the fact that artificial sources create a constant illuminance level of the object and a constant light incidence angle on the object, which allows perceiving objects with a fewer errors of the size, shape and colour. And all this helps to memorise them better [11,12].

Table 9. Portion of time an animal stayed in the previous location of the underwater platform in Morris's Water maze test under standard stable LED illumination conditions ($M \pm m$)

Indicators	NI Group	SSLEDI Group		
		10 th day	20 th day	30 th day
Time portion, %	69.30 ± 5.88	68.00 ± 5.80	69.33 ± 3.90	66.67 ± 8.89

CONCLUSIONS

Under conditions of standard stable fluorescent and light emitting diode illumination in comparison with natural light, animals did not show signs of alarm, oppression of investigatory-exploratory behaviour, decrease of training ability and long-term memory. On the contrary, an improvement in spatial orientation was noted.

A comparative ethological analysis of the animals' state showed that indicators reflecting spatial orientation using external reference points were raised in the case of light emitting diode and fluorescent illumination, compared to natural illumination. No statistically significant difference between light emitting diode and fluorescent illumination was revealed in terms of their influence on animal orientation.

ACKNOWLEDGMENT

The work was carried out with financial support from the Ministry of Education and Science of the Russian Federation (state contract #14.516.11.0091 of 01.07.2013) and Federal Government Budgetary Institution Fund of assistance to development of small enterprises in scientific and technical sphere under the "У.М.Н.И.К" program 2013–2015.

REFERENCES

1. Buresh Ya. Methods and main experiments on studying brain and behaviour / Ua. Buresh, O. Bureshova, D.P. Houston. Moscow: Vyshaya Shkola, 1991, pp. 119–122.
2. Gizinger O.A. Research approaches in the illumination safety field under megapolis conditions / O.A. Gizinger, M.V. Osikov, O.R. Bokova, E.V. Dolin, O.I. Ogneva // Semiconductor light engineering. 2013, V.21, # 1. pp. 60–61.
3. Osikov M.E. Ethological status and cognitive function in case of experimental desynchronosis under light emitting diode illumination conditions [Electronic

resource] / M.V. Osikov, O.A. Gizinger, O.I. Ogneva, A.A. Fedosov // Fundamental researches. 2015, #1, 7, pp.1392–1396. Access mode: <http://fundamental-research.ru/ru/article/view?id=37977> (16.02.2016).

4. Osikov M.V. Immune status and behavioural activity in case of experimental desynchronosis under fluorescent illumination conditions / M.V. Osikov, O.A. Gizinger, O.I. Ogneva // Russian immunologic journal, 2015, V.9 (18), # 2 (1), pp. 301–303.

5. Deinego V.N.. Light of energy saving and light emitting diode lamps and human health / V.N. Deinego, V.A. Kaptsov // Hygiene and sanitary. 2013, # 6, pp. 81–84.

6. Zakgeim A.L. Light emitting diode systems of illumination: energy efficiency, visual perception, health safety / A.L. Zakgeim // Svetotekhnika. 2012, # 6, pp. 12–21.

7. Osikov M.V. Medical-and-biologic and sanitary-and-hygienic aspects of innovative technologies of street, interior and industrial illumination / M.V. Osikov, L.F. Telesheva, O.A. Gizinger, O.I. Ogneva, et al. // Izvestiya vyshixh uchebnykh zavedeniy. Ural region. 2012, #4, pp.181–187.

8. A method of evaluation of artificial light exposure according to the the state of factors of peripheral blood and congenital immunity using models of laboratory animals: application #2014117407 / O.A. Gizinger, M.V. Osikov, O.I. Ogneva. #2556556. Registered 16.06.2015.

9. Ronchi L.R. Both warm, and cold light, and fine circadian structure // Svetotekhnika 2014, # 3, pp. 11–16.

10. Sliny D.H. Influence of new lighting devices on health and safety of people // Svetotekhnika, 2010, # 3, pp. 49–50.

11. Reference book on light engineering / under editorship of Yu.B. Aizenberg. – the third revised edition. Moscow: Znack, 2006, 972 p.

12. Sudakov S.K. Determination of anxiety level of rats in the Open field, Elevated plus – maze and Fogel's tests / S.K. Sudakov, G.A. Nazarova, E.V. Alekseeva et al. // Bul. of experimental biology and medicine. 2013, V. 155, # 3, pp. 268–270.

13. Jacobs, G.H. Evolution of colour vision in mammals // Philos. Trans. R. Soc. Lond. B Biol Sci. 2009. Vol. 364. № 1531, pp. 2957–2967.

14. Jacobs, G.H. Influence of cone pigment coexpression on spectral sensitivity and colour vision in the

mouse / G.H. Jacobs, G.A. Williams, J.A. Fenwick [et al.] / Vision Res. 2004. Vol. 44. № 14, pp. 1615–1622.

15. Morris, R.G. Developments of a water-maze procedure for studying spatial learning in the rat // J. Neurosci. Methods. 1984, Vol. 11, № 1, pp. 47–60.

16. Ostrin, L.A. Pharmacologically Stimulated Pupil and Accommodative Changes in Guinea Pigs / L.A. Ostrin, M.B. Garcia, V. Choh [et

al.] // Invest Ophthalmol. Vis. Sci. 2014. Vol. 55, № 8, pp. 5456–5465.

17. Shuboni, D.D. Acute effects of light on the brain and behavior of diurnal *Arvicantis niloticus* and nocturnal *Mus musculus* / D.D. Shuboni, S.L. Cramm, L. Yan, C. Ramanathan, B.L. Cavanaugh, A.A. Nunez, L. Smale / Physiol. Behav. 2015, Vol. 138, pp. 75–86.



Mikhail V. Osikov,

Dr. of Medical Science, Professor of Pahtophysiology chair of Southern Ural State Medical University, member- correspondent of Russian Academy of Natural Science, graduated from Chelyabinsk State medical Academy



Oksana A. Gizinger,

Dr. of Biological Science, Professor of the Microbiology, Virology, Immunology, and Clinic laboratory diagnostics chair, senior research associate of SI of Immunology, Chelyabinsk



Olga I. Ogneva,

post graduate student of Southern Ural Medical University, graduated from Chelyabinsk State Medical Academy, RF



Olga R. Bokova,

graduated from Sverdlovsk Architecture Institute, architect, Associate Professor of the Design chair of Southern Ural State University (National Research University)



Victoria G. Chudinova,

architect, Ph.D. in architecture, Associate Professor of the Architecture chair of Southern Ural State University (National Research University), member of the Union of architects of Russia

MODELING THE SPECTRUM OF A LUMINAIRE INCLUDING A DICHROIC FILTER BY SPECTRAL RAY TRACING

Guy Durinck, Frédéric B. Leloup, Jan Audenaert and Peter Hanselaer

*KU Leuven, ESAT/Light&Lighting Laboratory, Technology Campus Ghent,
Gebroeders De Smetstraat 1, 9000 GHENT, Belgium
E-mail: guy.durinck@kuleuven.be*

ABSTRACT

Ray tracing is a useful tool in the optical design of luminaires. Usually simulations are performed at one wavelength. However, in some luminaires optical components are incorporated to alter the spectrum of the light source. In a retail environment, luminaires equipped with a dichroic filter are commonly used to enhance the attractiveness of products. In this paper, spectral ray tracing is used to model the spectral radiant intensity distribution of such a luminaire. A geometric model of the luminaire, the spectral distribution of the lamp and the spectral scattering and transmission properties of the reflector and the filter are used as input parameters. The spectral radiant intensity at several emission angles as modelled by spectral ray tracing is compared with the experimentally determined values. A very good agreement is found. Furthermore, ray tracing simulations reveal detailed information about effect of light recycling in the luminaire on the emission spectrum.

Keywords: spectral ray tracing, retail lighting, optical modelling

INTRODUCTION

Monte Carlo ray tracing is frequently used as a tool to validate the optical performance of optical systems and virtual prototypes of luminaires [1,2,3]. In many cases, the optical properties of the materials in the design are more or less

wavelength independent, allowing the ray tracing calculations to be performed at one wavelength in order to strongly reduce the simulation time. However, for some special purpose luminaires, the spectrum emitted by the light source is, by design, altered by one or several optical components of the luminaire. Typically in retail lighting, both coloured filters combined with a classic light source, and spectrally designed solid state lighting sources are implemented. It is well documented that consumer acceptance of a food product strongly depends on the visual appearance of the product, and that the perceived colour of the product is one of the most important visual cues [4]. Particularly, consumers perceive fresh meat and some types of dark coloured fresh fish as more appealing when illuminated with a radiant spectrum dominated by red light [5,6]. A computer model of the optical behaviour of a filter based luminaire for the illumination of food products needs to take into account the combined influence of the light source, the optics and the filter, on the spectrum of the light emitted by the luminaire. Therefore, a ray tracing model of such a device needs to account for the entire visual spectrum of the light source. In this paper, a luminaire for retail lighting of meat products (Flexio from LUNOO NV) equipped with a Philips SDW-T 100W lamp and a dichroic filter is discussed. The filter is especially designed to be used in combination with the SDW-T lamp for the illumination of meat products. An interference filter has the advantage over a colour filter based on light absorption that al-

most no light is lost in the filter. However, a typical disadvantage of a such filter is that the spectral transmission depends on the angle of incidence. This results in the spectrum of the light emitted by the luminaire to be function of the emission angle. At small emission angles this effect is not visible but at larger angles a colour shift becomes visually apparent. In this work, the spectral radiant intensity of the luminaire is experimentally determined with a goniophotometer setup at several emission angles and calculated at the same emission angles by Monte Carlo ray tracing. The simulation takes into account the spectral surface scattering properties of the reflector material, and the dependency of the spectral reflection and transmission properties of the interference filter on the angle of incidence. The discharge lamp is modelled with a relatively simple geometric model. Additionally the effect of light recycling by the reflector of light initially reflected by the interference filter is investigated.

EXPERIMENTAL SET-UP AND MEASUREMENTS

The surface of the reflector material scatters light in a wide angular pattern around the specula direction. The angular scattering properties need to be modelled accurately to enable realistic ray tracing simulations [7,8]. Surface scattering properties are mathematically modelled by the Bidirectional Reflectance Distribution Function (BRDF), which is defined as the ratio of the infinitesimal radiance $dL_{e,s}$ of the ir-

radiated sample in a particular viewing direction, to the infinitesimal irradiance $dE_{e,i}$ on the sample by a collimated beam from a particular direction (equation 1). The index e indicates the radiometric property while the indices i and s indicate incident and scattered light respectively. Because surface scattering can be wavelength dependent, the BRDF is a function of 5 variables: θ_s and ϕ_s are spherical coordinates defining a particular scatter direction relative to the surface normal, θ_i and ϕ_i are spherical coordinates defining the direction of the incident beam, and λ is the wavelength:

$$BRDF(\theta_i, \phi_i, \theta_s, \phi_s, \lambda) = \frac{dL_{e,s}(\theta_i, \phi_i, \theta_s, \phi_s, \lambda)}{dE_{e,i}(\theta_i, \phi_i, \lambda)} \left[\frac{1}{sr} \right]. \tag{1}$$

Under particular circumstances the generic expression for the BRDF (1) is transformed into a practical expression (2), $\Phi_{e,s}$ and $\Phi_{e,i}$ represent the scattered and incident radiant flux, respectively, Ω_s being the solid angle subtended by the detector, and θ_s the angle between the surface normal and the scatter direction [9]:

$$BRDF(\theta_i, \phi_i, \theta_s, \phi_s, \lambda) = \frac{\Phi_{e,s}}{\Phi_{e,i} \Omega_s |\cos(\theta_s)|} \left[\frac{1}{sr} \right]. \tag{2}$$

Spectrally resolved BRDF measurements are carried out with an in house designed and

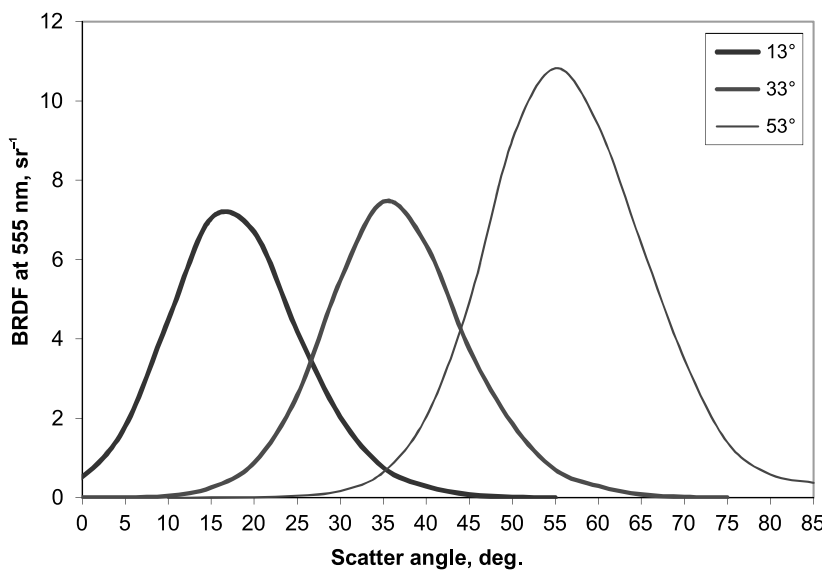


Fig. 1. BRDF of the reflector material as a function of scatter angle at a wavelength of 555nm at an incident angle of: 13°, 33° and 53°

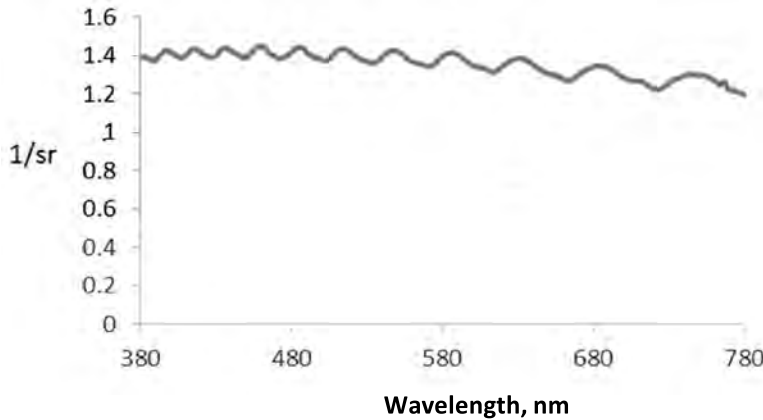


Fig. 2. BRDF (in units 1/sr) of the reflector material as a function of wavelength at an angle of incidence of 53 degree and scatter direction 75 degree to the surface normal

constructed gonioradiometer [10]. In Fig. 1 the BRDF of the reflector material is shown as a function of scatter angle for a number of incidence angles. The surface scatter data are shown at a wavelength of 555nm. The spectral behaviour of the BRDF for a particular angle of incidence, i.e., 53°, and scatter direction 75° to surface normal, is depicted in Fig. 2. For all incidence angles and all scatter angles, the BRDF exhibits small amplitude oscillations. The interference filter used in the luminaire consists of a number of thin transparent layers with different indices of refraction. The multilayer uses constructive and destructive interference to transmit light at certain wavelengths at certain angles of incidence and to reflect the same wavelengths at other angles of incidence. The interference filter is supported by a transparent glass plate with negligible absorption and scattering. Absorption in the multilayer itself is of the order of magnitude of 3 % while the scattering is neg-

ligible [10]. The filter exhibits only regular transmission and specular reflection which are characterized by the transmission and reflection coefficients (Equations 3 and 4). The reflection and transmission coefficients are experimentally determined with the BRDF measurement set up.

$$T(\lambda, \theta) = \frac{\Phi_{e,t}}{\Phi_{e,i}} \tag{3}$$

$$R(\lambda, \theta) = \frac{\Phi_{e,r}}{\Phi_{e,i}} \tag{4}$$

In Equations (3) and (4), the indices *i*, *t* and *r* respectively refer to the incident, transmitted and reflected flux. The index *e* is used to indicate radiant flux (W), not luminous flux (lm). The transmission and reflection coefficients are measured as a function of wavelength for a number of in-

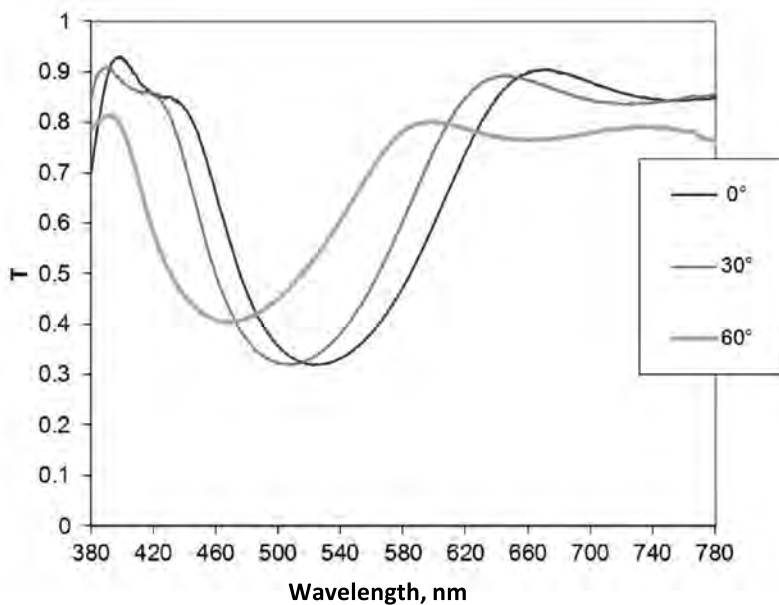


Fig. 3. Transmission coefficient of the interference filter as a function of wavelength for three angles of incidence

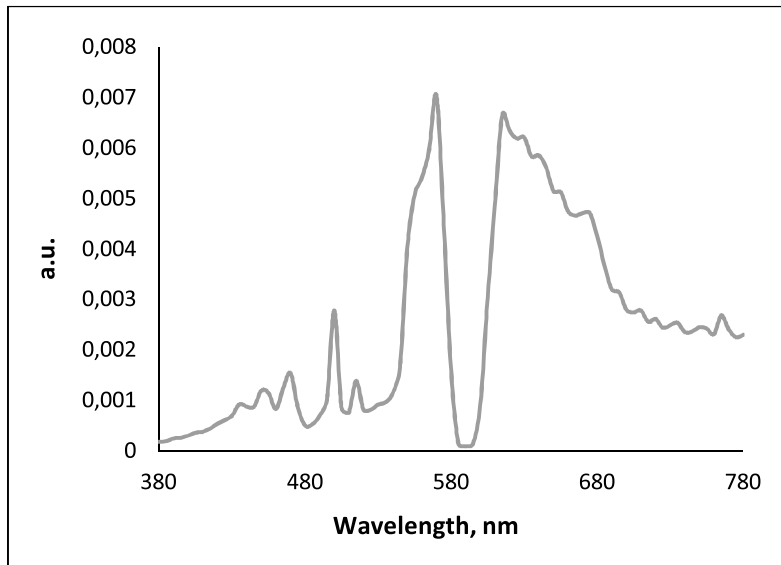


Fig. 4. Normalized measured spectrum of the SDW-T lamp, expressed in arbitrary units

cidence angles. In Fig. 3, the measured regular transmission coefficient is shown for three incidence angles. Notice that the transmission coefficient as a function of wavelength depends significantly on the incidence angle.

To measure the emission spectrum of the luminaire as a function of emission angle the luminaire is mounted in a CIE type 1 goniophotometer [11] which can rotate the lighting fixture around a horizontal and vertical axis. The light is captured by a Topcom 100 camera positioned in the far field at a distance of 8.72m from the luminaire. The captured light is transferred by an optical fibre to an Oriel Multispec spectrograph. Because the detection system is positioned in the far field and the complete lighting fixture is located within the field of view, the recorded spectrum is interpreted as the spectral radiant intensity spectrum of the luminaire. The emission spectrum of the naked SDW-T lamp is measured by the same procedure. The spectrum of the lamp, in arbitrary units, normalized to one is shown in Fig. 4.

SPECTRAL MONTE CARLO RAY TRACING

A commercial software package, TracePro® from Lambda Research Corporation, is implemented to perform the Monte Carlo ray tracing. The geometry of the luminaire is modelled in the software package using CAD-files of the reflector, as supplied by the manufacturer, and a generic model of an SDW-T lamp, as available in the software package's library. The geometric model

of the luminaire is shown in Fig. 5. The surface of the cylindrical gas discharge tube in the lamp is considered to be the light source and is modelled as a Lambertian surface source. This relatively simple source model is acceptable because the source is small and positioned at a relatively large distance from the reflector. Furthermore the emission spectrum of the lamp does not vary strongly with emission angle. If the latter was the case a much more advanced spectral source model based on spectral ray files would be required [12,13]. The surface scatter data for the reflector material and the transmission and reflection coefficient of the interference filter are transferred into the appropriate format and imported in the ray tracing software. The scatter data are somewhat simplified as it is impractical to include the small oscillations that are slightly different for each angle of incidence. Therefore, the BRDF is assumed to be constant between 380nm and



Fig. 5. Model of the luminaire used in the ray tracing simulations

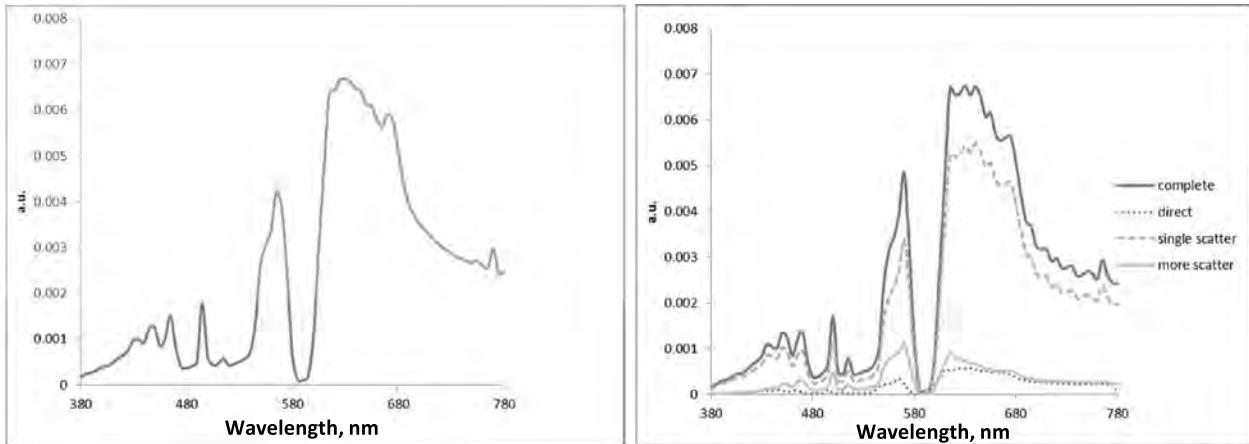


Fig. 6. Measured (left) and simulated spectrum (right) of light emitted at emission angle 0 degree and captured at a distance of 8.72m from the luminaire; light that is scattered once dominates the spectrum and the multiple scatter component is more important than the direct light contribution

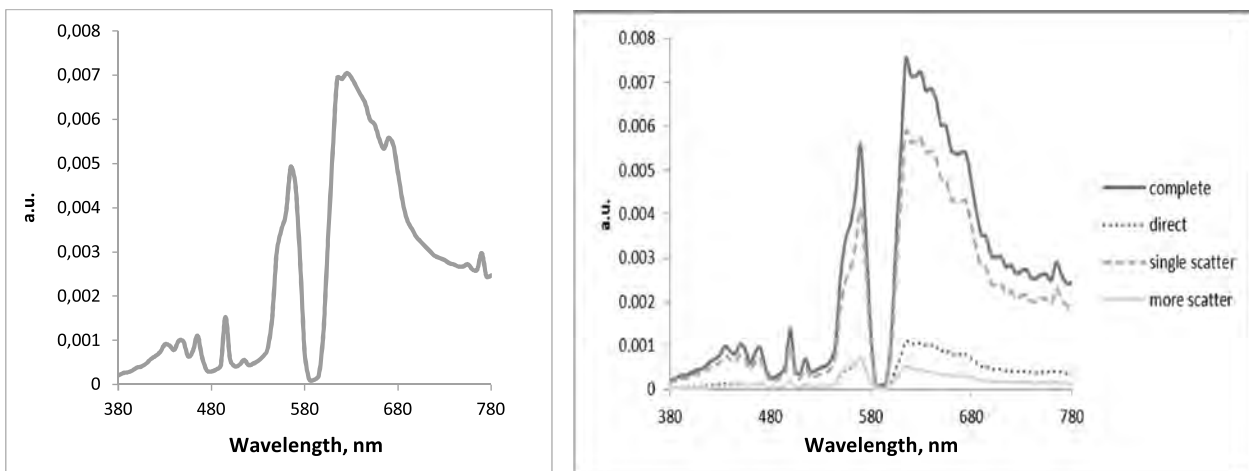


Fig. 7. Measured (left) and ray traced spectrum (right) of light emitted at emission angle of 30° and captured at a distance of 8.72m; the intensity spectrum is dominated by light that is scattered once and the direct light contribution is more important than the multiple scatter component

570nm, and to decrease linearly between 570nm and 780nm in such a way that the total integrated scatter (TIS) agrees with the experimental value. To model the detector, a disk shaped target with diameter 3mm (i.e. the same dimensions as the entrance aperture of the Topcom 100 camera) is created in the model and positioned at a distance of 8.72m from the luminaire. Because of the small dimensions of the ray tracing target and the large distance to the light source, the probability of a random ray hitting the target is extremely small, making classic source to target ray tracing impractical. Therefore a technique frequently applied in computer graphics, reverse ray tracing, is implemented [14]. In reverse ray tracing rays are traced backwards through the optical system, i.e. from target to source, and a history of the events encountered by the rays (e.g. Fresnel reflection,

surface scatter, etc...) is logged. If and when a ray impinges on the source, a flux is assigned to it according to the emission properties of the source. From this emitted flux, and taking into account the complete history of the ray, the flux observed at the target is calculated. To model the emission spectrum of the SDW-T lamp, 1 million rays per wavelength are traced at 81 wavelengths in the range 380nm – 780nm with 5nm increments. The relative radiant flux at each wavelength is weighted according to the emission spectrum of the discharge lamp.

RESULTS AND DISCUSSION

Both the measured and simulated spectra are normalized such that the integrated spectra equal unity. The spectra found by reverse ray tracing

Table 1. CIE (u' , v') chromaticity coordinates calculated from the measured and simulated spectra. The difference in chromaticity between simulation and experiment increases with emission angle

emission angle	experiment	simulation	$\Delta_{(u',v')}$
0 degree	$u'=0.3125$ $v'=0.5088$	$u'=0.3119$ $v'=0.5086$	0.0006
30 degree	$u'=0.3097$ $v'=0.5196$	$u'=0.3163$ $v'=0.5191$	0.0066
60 degree	$u'=0.1982$ $v'=0.5360$	$u'=0.2087$ $v'=0.5365$	0.0105

can be deconstructed in component spectra corresponding to light taking different paths through the optics [15]. Three component spectra are considered: the direct light contribution (i.e. light that travels directly from source to target, through the filter), light that is scattered once by the reflector and afterwards transmitted through the filter before being detected, and light that is scattered more than once by the reflector before passing through the filter and reaching the target. In Figs. 6, 7 and 8 a comparison is made between the measured and calculated spectra, expressed in arbitrary units, at 0, 30 and 60 degree emission angle. A good agreement is found between the simulated spectrum and the measured spectrum in all three situations. From the simulations, it becomes clear that the relative contribution of the three component spectra to the entire spectrum changes as a function of emission angle. The spectrum emitted at 0 degree is dominated by light that is scattered once by the reflector. The component corresponding to light that is scattered several times by the reflector materi-

al is larger than the direct light contribution. At an emission angle of 30 degree the direct light contribution has become larger than the multiple scatter contribution, but the spectrum is still dominated by light that is scattered once by the reflector. At an emission angle of 60 degree the line of sight between the detector and the gas discharge tube is blocked by the reflector, and the direct light contribution is zero. However, part of the inner side of the reflector is still visible from the detector position and light reaches the detector after being scattered at least once by the reflector. From the ray tracing simulations it becomes clear that the spectrum is now dominated by light that is scattered several times by the reflector surface.

The chromaticity of light stimuli and the chromaticity difference of light sources is, as recommended by the CIE, preferably expressed in the CIE (u' , v') chromaticity diagram [16].

The chromaticity difference between two light sources, A and B, is expressed by Equation (5).

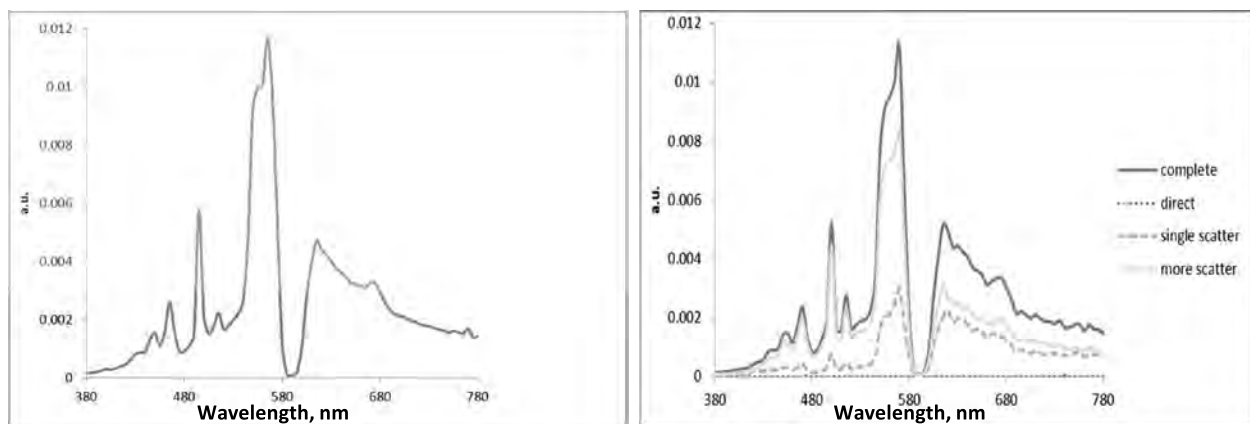


Fig. 8. Experimentally determined (left) and simulated spectrum (right) of light emitted at an emission angle of 60 degree and captured at a distance of 8.72m from the luminaire; the spectrum is dominated by light that reaches the detector after multiple scattering events, there is no direct light contribution

Table 2. CIE (u', v') chromaticity coordinates corresponding to the experimental spectrum, the simulated spectrum of the luminaire, the simulated spectrum excluding light recycling and the spectrum found by multiplying the original lamp spectrum with the 0 degree transmission coefficient of the interference filter (also shown are the differences between the chromaticity of the measured light and the chromaticity corresponding to the calculated spectra)

	Measured spectrum	Simulated spectrum	Simulated spectrum without recycling	(lamp spectrum) x (transmission coefficient)
Chromaticity	u'=0.3125 v'=0.5088	u'=0.3119 v'=0.5086	u'=0.3271 v'=0.5056	u'=0.3289 v'=0.5058
Chromaticity difference with measured spectrum		$\Delta_{(u',v')}$ = 0.0006	$\Delta_{(u',v')}$ = 0.0150	$\Delta_{(u',v')}$ = 0.0166

$$\Delta_{(u',v')} = \sqrt{(u'_A - u'_B)^2 + (v'_A - v'_B)^2} \tag{5}$$

The just noticeable difference in chromaticity (at 50 % probability) corresponds to a difference in chromaticity coordinates of 0.0013. In Table 1, the (u', v') chromaticity coordinates calculated from the measured and simulated spectra and the chromaticity difference between simulation and experiment are shown. Notice that the chromaticity difference increases with emission angle. This is probably caused by the statistical noise inherent to the ray tracing procedure. In each reverse ray tracing session, 1 million rays per wavelength are launched but because of the different geometry the number of rays that actually reaches the light source is different. At emission angle zero, typically 29 % of the rays arrive at the source, but at 30 degree emission, only 19 % of the rays hit the light source, and at 60 degree emission less than 1 %

of the rays contribute to the simulated spectrum. As the number of rays that contribute to a simulated spectrum decreases with emission angle, the noise on the simulated spectra increases with emission angle.

It is interesting to have a look at the impact of the recycling of light on the spectrum. Light emitted by the source is back reflected by the interference filter to the reflector. At the reflector surface it scatters at least once, impinges on the filter again, is transmitted, and contributes to the spectral radiant intensity of the luminaire. In order to investigate if light recycling has an impact on the emission spectrum of the luminaire, the ray tracing model is adapted. In the model, the interference filter is removed from the luminaire and repositioned at a large distance (8m) from the reflector but parallel with its original configuration. In this configuration the line of sight from the detector, through the interference fil-

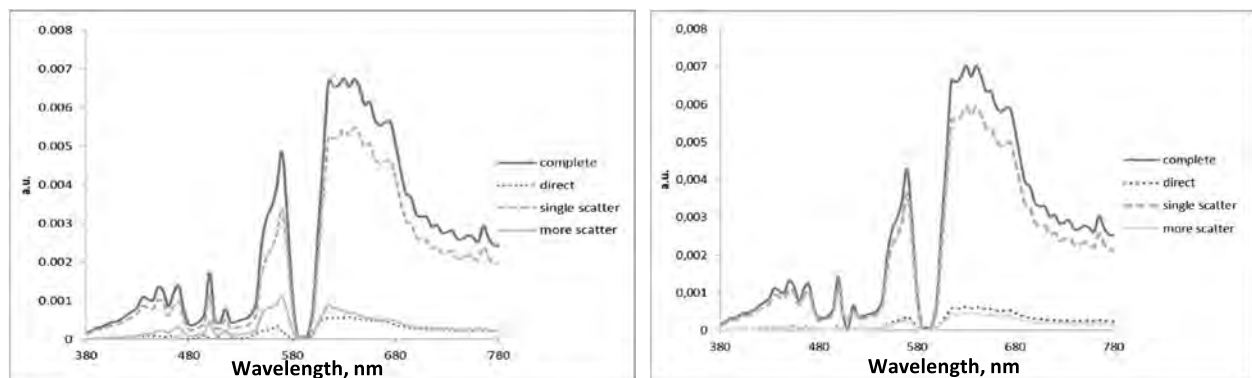


Fig. 9. Emission spectra at 0 degree emission angle found from ray tracing calculations of the luminaire (left) and in the modified geometry excluding light recycling (right); notice that in the situation excluding light recycling, the contribution of the more scatter component is significantly reduced

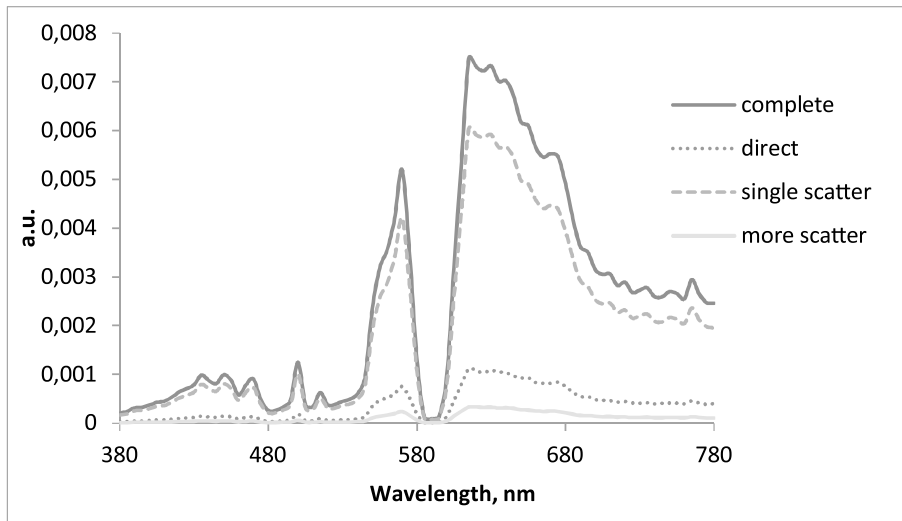


Fig. 10. Simulated spectrum of the emitted light at 30 degree emission angle without light recycling

ter, to the reflector and the lamp is not altered but light that is reflected by the filter will not reach the reflector and disappear from the simulation, thus eliminating light recycling. In Fig. 9, the simulated emission spectra at 0 degree emission angle are compared. In the modified geometry, the contribution to the spectrum of light that is scattered multiple times is of the same order of magnitude as the direct light component while in the classic luminaire geometry the multiple scatter component dominates the direct light component in the wavelength range 540–650nm. This is suggesting a difference in chromaticity of the light between both cases. It should be noted that, since the properties of the reflector material are practically independent of wavelength, the spectrum without light recycling is the spectrum that would be observed while viewing the light source

through the interference filter without any other optics present. In Table 2 the CIE (u' , v') chromaticity coordinates of the experimentally observed spectrum, the simulated spectrum, the simulated spectrum without recycling and the spectrum obtained by multiplying the spectrum of the lamp with the transmission coefficient of the dichroic filter are listed. Also the chromaticity difference between the measured spectrum and the other spectra is shown. From the table it is clear that the chromaticity of the light emitted by the luminaire cannot be found by simply multiplying the emission spectrum of the lamp with the transmission coefficient of the filter, this despite the fact that the scattering properties of the reflector are practically independent of wavelength. The simulations show that light recycling by the optics of the luminaire has a significant influence on the

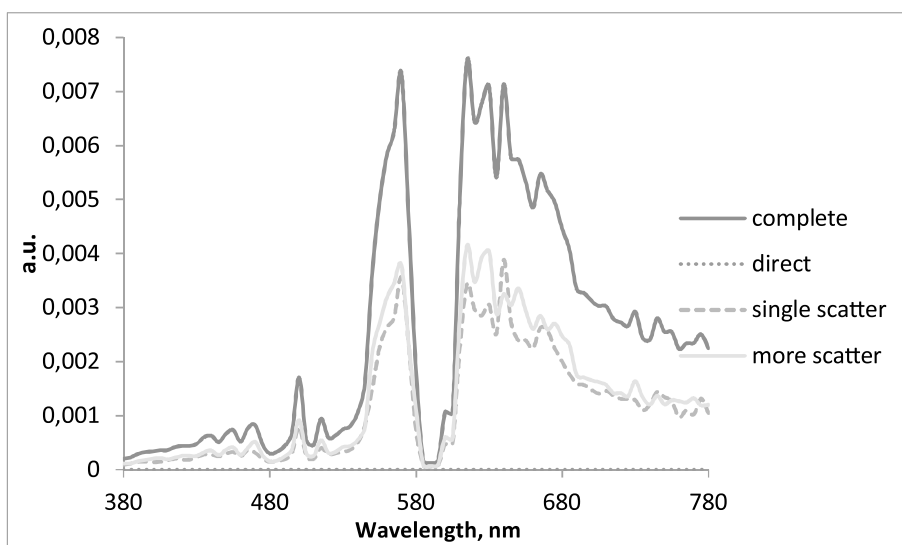


Fig. 11. Simulated emission spectrum, excluding light recycling, at emission angle 60 degree

spectrum and chromaticity of the light. The simulated spectra at 30 degree and 60 degree emission angle have more statistical noise and thus the chromaticity corresponding to these spectra is less in agreement with the experimental data (Table 1). The spectra are shown in Fig. 10 and Fig. 11. At emission angle 30 degree, the spectrum without light recycling shows a reduction of the contribution of light that is scattered several times by the reflector surface. However, the overall shape of the spectrum and the relative contribution of each of the components is not altered significantly relative to the spectrum shown in Fig. 7. In this particular situation the effect of light recycling is relatively small. The situation at 60 degree emission angle is quite different (Fig. 11) and the spectrum excluding light recycling is completely different. In this case the line of sight from detector to the gas discharge tube, the actual light source, is blocked by the reflector and the spectrum with light recycling is strongly dominated by light that is scattered several times. Excluding light recycling causes the single scatter contribution and the multiple scatter contribution to be of equal importance, which results in a completely different spectrum.

CONCLUSION

Spectral Monte Carlo ray tracing can be used to accurately model the angle dependent spectrum of luminaires containing spectrally non-neutral optical components such as interference filters. The spectra resulting from computer simulations correspond very well to the measurements and additionally yield interesting information about how the spectrum is composed of light taking different paths in the luminaire and how this composition changes with the emission angle. The phenomenon of light recycling in the luminaire is investigated by repeating the computer simulations with a slightly altered geometry that excludes this phenomenon. It is found that light recycling is of significant importance to explain the spectral radiant intensity and the chromaticity of the emitted light. This type of modelling contributes to a better understanding of unwanted spectral shifts in luminaires and additionally provides a useful tool for the optical design of lighting systems.

REFERENCES

1. Lee X.H., Moreno I. and Sun C.C. High-performance LED street lighting using microlens arrays. *Optics Express*, 2013, 21(9), pp.10612–10621.
2. Wang K., Chen F., Liu Z., Luo X. and Liu S. Design of compact freeform lens for application specific light emitting diode packaging. *Optics Express*, 2010, 18(2), pp.414–425.
3. Vandeghinste F., Durinck G., Forment S., Deconinck G. and Hanselaer P. A narrow beam reflector for a two-dimensional array of power light emitting diodes. *Leukos*, 2008, 4(4), pp. 243–254.
4. Imram N. The role of visual cues in consumer perception and acceptance of a food product. *Nutrition & Food Science*, 1999, #5, pp.224–228.
5. Barbut S. Effect of illumination source on the appearance of fresh meat cuts. *Meat Science*, 2001, #59, pp.187–191.
6. Barbut S. Effect of three commercial light sources on acceptability of Salmon, Snapper and Sea Bass filets. *Aquaculture*, 2004, 236, pp. 321–329.
7. Audenaert J., Leloup F.B., Durinck G., Deconinck G. and Hanselaer P. Bayesian deconvolution method applied to experimental bidirectional transmittance distribution functions. *Meas. Sci. Technol.* 2013, #24, 035202(9p).
8. Audenaert J., Leloup F.B., Van Giel B., Durinck G., Deconinck G. and Hanselaer P. Impact of the accurateness of bidirectional reflectance distribution function data on the intensity and luminance distributions of a light emitting diode mixing chamber as obtained by simulations. *Optical Engineering* 2013, #52(9), pp. 095101–1 – 095101–7.
9. ASTM 2002. Standard practice for angle resolved optical scatter measurements on specula or diffuse surfaces. *ASTM E1392–96*, 2002, 12p
10. Leloup F.B., Forment S., Dutré P., Pointer M. and Hanselaer P. Design of an instrument for measuring the spectral bidirectional scatter distribution function. *Applied Optics*, 20084, #7(29), pp. 5454–5467.
11. CIE1996. The photometry and goniophotometry of luminaires. *CIE121–1996*.
12. Rykowski R.F. Spectral ray tracing from near field goniophotometer measurements. *Light & Engineering*, 2011, V.19, #1, pp.23–29.
13. Jacobs V.A., Audenaert J., Bleumers J., Durinck G., Rombouts P. and Hanselaer P. Rayfiles including spectral and colorimetric information. *Optics Express*, 2015, 23(7), pp. A361-A370.

14. Dutré P., Bekaert P. and Bala K. Advanced Global Illumination. A K Peters Ltd, 2006.

15. Durinck G., Leloup F.B., Audenaert J. and Hanselaer P. Spectral ray tracing to model the spectrum of a luminaire equipped with an interference filter. Pro-

ceedings of the 6th International Conference on Optical Measurement Techniques for Structures & Systems OPTIMESS2015, Antwerp, 8–9 April 2015, pp. 85–93

16. CIE2014. Chromaticity Difference Specification for Light Sources. CIE TN001:2014. 5p.



Guy Durinck

obtained a Master of Science in physics at University Ghent (Belgium) in 1989 and a Ph.D. in physics at KU Leuven (Belgium) in 1999. He is currently a research scientist at the Light & Lighting Laboratory (KU Leuven) and a lecturer at KU Leuven and University College Odisee. His current research interests are in the design of lighting and illumination optics and in optical modelling by ray tracing. He teaches courses in mathematics, general physics and physical optics



Frédéric B. Leloup

graduated as a master in industrial engineering in 2001 and obtained his Ph.D. in engineering in 2012. He is currently a research support co-ordinator at the Light & Lighting Laboratory, affiliated to KU Leuven. His research focuses on the soft metrology of appearance, investigating possible correlations between optical parameters which, either singly or in combination, correspond to attributes of visual appearance (colour, gloss, texture, etc.), and on issues related to quality aspects of testing and calibrations laboratories



Jan Audenaert

graduated as a master in information and communication technology from Katholieke Hogeschool (KAHO) Sint-Lieven (Gent) in 2009. In 2010 he started a Ph.D. at the Light & Lighting laboratory (KU Leuven) after being granted a scholarship from the Agency for Innovation by Science and Technology in Flanders (IWT). He obtained his Ph.D. in engineering from KU Leuven in 2014. Currently he is active at the Light & Lighting laboratory as R&D consultant with a main research focus on ray tracing and near-field goniophotometry



Peter Hanselaer,

full professor at KU Leuven, was born in 1959 and received his Ph.D. in Physics at University of Gent (B) in 1986. In 1997, he founded the Light & Lighting Laboratory. His main research areas are lighting, perception and appearance, optical design, light sources and optical metrology. He was recently appointed as Editor of CIE Division 1 and as chair of the Doctoral Committee of the Faculty of Engineering Technology. Peter is teaching the master courses photonics, optical fibre communication and lighting

MATHEMATICAL SIMULATION OF LIGHTING INSTALLATIONS USING A COMPUTER

Victor S. Zheltov and Vladimir P. Budak

The Moscow Power Institute NRU, Moscow
E-mail: budakvp@gmail.com

ABSTRACT

The last 30 years in the development of lighting installations (LI) computer simulation methods are analysed. Simulation efforts began from attempts at automation for routine LI design stages by means of a computer. The article describes the challenges which arise with these methods, and ways of solving them, which are implemented in current programs that visualise spatial and angular distribution of the light field in the LIs on the display screen based on numerical solution of the global illumination equation, which records strictly light characteristics in the geometrical optics approach.

Keywords: lighting installations, global illumination theory, radiosity, luminous emittance, ray tracing, instant radiosity, Monte-Carlo method

1. FROM DESIGN TO SIMULATION OF LIGHTING INSTALLATIONS

One feature of current scientific and technological progress is the digital revolution: converting all knowledge systems into a digital configuration of files, databases, calculation programs and computer-aided engineering systems. In the early days of computer technologies, in the late nineteenth and twentieth centuries, computer programs automated the work of design engineers by taking on otherwise time-consuming calculations. More recently developed digital technologies have led to the emergence of revolutionary new algorithms and programs opening new ave-

nues for the creation and development of many systems. Now literature uses the term “second digital revolution”, as a result of which computers will perform functions which were never intended to be automated, for example, control of driverless vehicles.

One of the most important fields in lighting engineering is the design of lighting installations (LI); and here the digital revolution has come about in the brightest and most dramatic way. As mentioned earlier, in the early stages, some standard and most routine LI design procedures were transferred to computers. At this stage an idea arose: if programs calculate illumination, and therefore luminance (in the assumption that all surfaces reflect light diffusely, which was generally accepted when calculating LIs), then having displayed this distribution, we will see an image of the installation. However, it turned out to be the case. Fig. 1 shows a synthetic image of a simple scene: a table covered with a stripy cloth, on which a metal hemisphere and a glass cylinder stand. The all space is illuminated with a parallel light beam. In Fig. 1a this scene is displayed in the view, which would be obtained when carrying out calculations based on the inverse square law, which at that time was the generally accepted LI calculation procedure. It can be seen that this image does not look realistic at all; the eye does not perceive the hemisphere as metal, and the cylinder as glass. The main reasons for this incorrect perception of the scene are the hard shadows and the absence of reflections of objects within each other. Such a method of synthetic image calcula-

tion in computer graphics was named the local illumination model [1]. It is obvious that for realistic visualization, an algorithm which takes into account repeated reflections (transmissions) in the scene is necessary: a global illumination [1].

Therefore, the real digital revolution in LI calculation took place not only due to development of computer facilities but also due to mathematical methods. In 1986 *J. Kajiy* formulated a visualization equation representing Fredholm's second kind equation [2]:

$$L(r, \hat{l}) = L_0(r, \hat{l}) + \frac{1}{\pi} \oint L(r, \hat{l}') \sigma(r; \hat{l}, \hat{l}') |(\hat{N}, \hat{l}')| d\hat{l}' \quad (1)$$

where $L(r, \hat{l})$ is luminance of light field in \mathbf{r} point in the direction \hat{l} , $\sigma(r; \hat{l}, \hat{l}')$ is luminance factor of a surface element in \mathbf{r} point in the direction \hat{l} with a directed illumination of this element using a parallel light beam in the direction \hat{l}' . It is often named bidirectional function of dispersion (reflection or transmission), L_0 is straight line (directly from the sources) of the luminance component, \hat{N} is normal in \mathbf{r} point to an element of the scene surface. Hereinafter the «lid» over a vector will designate single direction vectors playing an extremely important role in lighting engineering. Circulatory integral in (1) means an integration over the full solid angle, the element of which is designated as $d\hat{l}'$.

Equation (1) is closed for determining a required luminance distribution $L(r, \hat{l})$, however it is difficult to use it for the development of numerical methods as we are interested in spatial luminance dependence, and integration in the equation comes over a solid angle. Using luminance invariance along the viewing beam and the ratio between solid angle $d\hat{l}'$ and an element square d^2r' cut out by it from the surface reflecting light to \mathbf{r} point, it is easy to obtain a new form of equation (1) which is called the global illumination equation (GIE) [3]:

$$L(r, \hat{l}) = L_0(r, \hat{l}) + \frac{1}{\pi} \int_{\Sigma} L(r', \hat{l}') \sigma(r; \hat{l}, \hat{l}') F(r, r') \Theta(r, r') d^2r' \quad (2)$$

where $F = \frac{|(\hat{N}(r), (r-r'))| |(\hat{N}(r'), (r-r'))|}{(r-r')^4}$ is el-

ementary form factor, or efficiency coefficient, $\Theta(\mathbf{r}, \mathbf{r}')$ is function of element d^2r' visibility from \mathbf{r} point. The Σ symbol designates all surfaces, which repeated reflections are taken into consideration.

Determination of Σ is non-trivial, because we always exclude from the LI calculation some real surfaces, for example, the corridor when calculating a room or the street when calculating a natural illumination. A set of the considered surfaces is accepted as the illumination scene.

An exact solution for GIE (2) is still not found today. Therefore, in practice it is solved numerically. For this purpose, all surfaces included into the illumination scene are replaced with a grid of flat edges. And the integral in equation (2) is replaced with a final sum, which reduces the integrated equation to a linear algebraic equation system. This method solving the equation in mathematics is known as the finite element method [4]. To increase the accuracy of the solution, one should divide the scene over space into very small spatial and angular elements, which means that it is necessary to solve a very large system of millions of equations. Due to the inevitability to round-off any computer operation, such a problem becomes mathematically incorrect. The only possible stable method of solving such a system is the iteration method, which is physically equivalent to ray tracing. It should be noticed that for the first time, the method of energy calculation of optical systems using ray tracing is proposed in [5], and the correspondent calculation of light devices is proposed in [6, 7].

If the described scene is calculated by the ray tracing method, accounting for eight collisions (rereflections and transmissions), then we obtain the image given in Fig. 1b. A reasonable question arises: how many reflections should be taken into consideration? Fig. 1c shows an image obtained when accounting for 64 reflections. It is easy to notice that using 64 collisions is essential for realistic reproduction of the scene image. And this is correct for simple scenes as well. It is obvious that in spaces with indoor illumination, where walls, ceiling and floor are located opposite to each other, the number of reflections to account for can reach thousands. For compu-

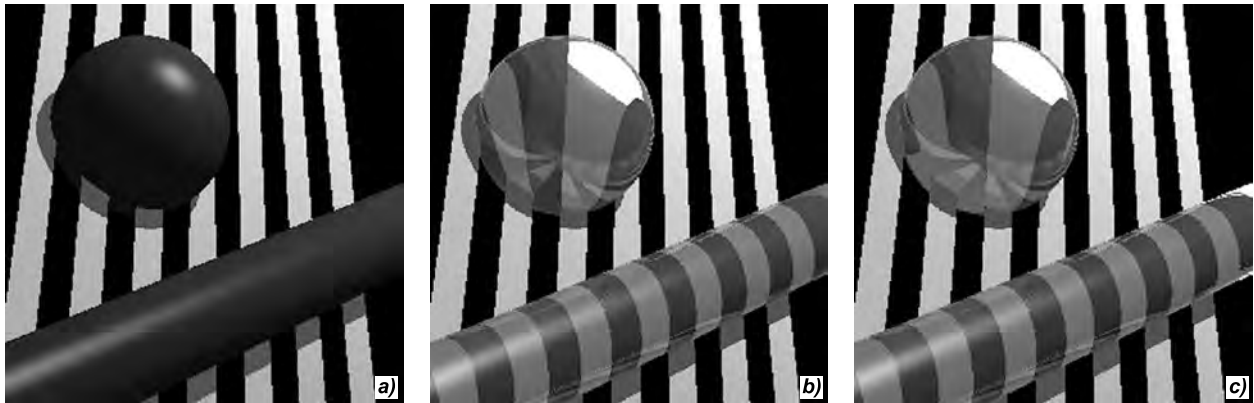


Fig. 1. Visualisation of an simple illumination scene, taking into account different numbers of reflection multiplicity:
a) single reflection; b) eight reflections; c) 64 reflections

ters of from the 1980^s and early 1990^s this scale was impossible.

The situation becomes significantly simpler, if we assume that an illumination scene only consists of diffusely reflecting surfaces: $\sigma(r; \hat{l}, \hat{l}') = \sigma(r)$. In this case luminance does not depend on direction \hat{l} and unambiguously is connected with luminosity of the verge by reflected light $M(\mathbf{r}) = \pi L(\mathbf{r})$, which allows to transform (2) as follows:

$$M(\mathbf{r}) = M_0(\mathbf{r}) + \frac{\sigma(\mathbf{r})}{\pi} \int_{\Sigma} M(\mathbf{r}') F(\mathbf{r}, \mathbf{r}') \Theta(\mathbf{r}, \mathbf{r}') d^2 \mathbf{r}', \quad (3)$$

where $M(\mathbf{r})$ is luminosity in \mathbf{r} point, $M_0(\mathbf{r})$ is initial luminosity in \mathbf{r} point in approach of one reflection directly from the light sources. Equation (3) was derived for the first time in LI calculation theory and named the equation of radiosity [8].

Radiosity equations are also solved by replacing the integral with a final sum but owing to absence of luminance angular dependence, the number of equation decreases by thousands of times, which made such a solution accessible for computers of the 1990^s. In lighting engineering, the radiosity method in finite differences was for the first time formulated in work [9], and integrated equation (3) was derived in [10] and GIE was for the first time obtained in work [11] by Soviet thermophysicist G.L. Polyak for radiant heat exchange in furnaces, however, it did not influence the development of computer graphics.

Solution of the radiosity equation using the final element method was named the radiosity method. In this case, surface finite elements are

connected by finite beams, and not by infinitely thin beams of the tracing method. This significantly reduced counting duration. For the first time radiosity method was implemented in the *Lightscape* program, and today the radiosity method is the cornerstone of key software products for LI simulation: *DIALux* [12] and *Relux* [13].

These programs go beyond calculating illumination values in some points of the scene but display the light field over the whole scene volume. Hence the light field distribution within the scene, when taking into account multiple reflections, depends not only on the light sources but also on the objects in the space and their mutual positions. So in these programs, it is not just the LI project which is implemented but its real, «live» model, and the design process is replaced by simulation.

GIE and methods of its solution are at the base of both computer graphics programs for visualisation of virtual objects, and of LI simulation programs. GIE exactly allows computing light fields over the all illumination scene, and synthetic image creating process itself represents visualisation of the spatial-and-angular luminance distribution. And one can say that dreams of descriptive geometry creators Gaspard Monge (1746–1818) and Julius Plücker (1801–1868) in order that formulas would expressed beauty of the real world, were embodied.

2. RADIOSITY ERA

After the implementation of the radiosity method, it became a standard for all computer graphic programs to create synthetic images of three-dimensional spaces. The main attractive feature of the method is that synthetic images, created us-

ing solution (3) by the radiosity method, take an acceptable length of time and correspond to the object picture quality. Discrepancy of the display screen luminance interval with the luminance interval in the illumination scene before displaying caused an inevitability of luminance scaling, which results in photorealistic but not visual displays of the scene as human eyes are complex non-linear receivers. However, people long ago had got used to judge objects by their pictures, which allows them seeing a being designed object before its creation.

In any lighting project, there are always three interested parties: customer, designer and the project author. Each of them describes and estimates LI quality using his/her own terminology. The picture (a synthetic image on the screen) creates a uniform communication platform and a language of understanding between them. This fact was decisive, and LI simulation programs quickly force out other LI design methods.

The radiosity method became the first method which allowed accounting for multiple reflections in the diffuse approach; the reflection diffuse model became the cornerstone of this method. However, no less essential is the fact that visualisation is based on LI calculation by the radiosity method, which significantly improves the normal technique. In this way the designer can work with parameters of light fields in all parts of the space, rather than just illuminance or luminance values in separate points. This makes it possible to show the light field distribution in various configurations: tables, isoluxes, pseudo colours, which avoids the disadvantages of photorealistic reproduction i.e. the image on the screen is scaled, contrasted and changes by colour. This solves the main problem of LI design: light, unlike any other design object, is invisible, and only the created LI will allow seeing all the objects as a whole.

In its turn, an object image in conjunction with light distribution analysis facilities have made it possible to design LIs not only based on illuminance or luminance values at determined points in the space but also to consider illumination quality: discomfort, light rhythm, accents, etc. LI simulation programs, which enable calculation and analysis of light field distribution over the space and create the scene image, have opened wide opportunities for LI design. As a matter of fact, we have witnessed the advent of a new approach to LI

creation and respectively, the emergence a new profession: light design.

Further development of LI simulation programs and light design revealed serious problems in the radiosity method:

- A correct discomfort determination requires an exact calculation of luminance distribution in glare spots from large surfaces. Within the radiosity method, calculation of multiple reflections is carried out in the assumption of a diffuse reflection from all of the surfaces, and the presence of glare is specified at the final stage of calculation – visualisation – at reverse ray tracing. This means generating glare is more likely in a synthetic image, without giving a quantitative assessment of luminance distribution.

- The radiosity method is almost ineffective if transparent surfaces are present in the space, which is becoming more and more common: glass facades, transparent office partitions, etc.

- With increasing scene complexity, the labour input required for the radiosity method increases significantly faster than for the ray tracing method, and after a certain threshold, the tracing method becomes much more effective. It does not allow simulating complex scenes by the radiosity method: big polyzonal sites, building storeys, streets and so on.

3. RAY TRACING

Another method for GIE solution was developed for computer graphics tasks. Its purpose was a realistic visualisation of three-dimensional scenes. One of the significant methods has become the method of photon cards [14]. This method is based on consideration of radiation transfer by photon particles moving along light rays and transferring discrete portions of light energy. At the initial stage, photons are emitted by a light source according to its radiation energy distribution. In the simulation process, photons are traced in the scene and collide with various elements of the scene. Depending on the properties of the surface material, photons are subject to various impacts: diffuse reflection, specular reflection, refraction or absorption. A specific impact coming about a photon is selected based on surface material properties and on the Russian Roulette statistical method [14]. Every diffusely reflected photon is recorded in a list. After some statis-

tics are accumulated, a photon card is constructed as having some structure of spatial division, which allows a quick finding N next photons. At the last stage, luminance collection takes place.

Having used the known ratio between incident radiation luminance and flux:

$$L(r, \hat{l}') = \frac{d^2\Phi(r, \hat{l}')}{\cos\theta d\omega d\hat{l}' dA}, \quad (4)$$

equation (1) can be rewritten as follows:

$$L(r, \hat{l}') = L_0(r, \hat{l}') + \frac{1}{\pi} \int \sigma(r; \hat{l}, \hat{l}') \frac{d^2\Phi(r, \hat{l}')}{dA}. \quad (5)$$

Incident flux $\Phi(r, \hat{l}')$ can be approximated using the photon card after collecting N photons closest to point \mathbf{r} :

$$L(r, \hat{l}') \approx L_0(r, \hat{l}') + \frac{1}{\pi} \sum_{i=1}^N \sigma(r; \hat{l}, \hat{l}') \frac{\Delta\Phi(r, \hat{l}')}{\Delta A}, \quad (6)$$

where ΔA is area of the hemisphere formed around point \mathbf{r} with radius equal to the distance to the most distant photon.

As a result, the photon card method allows simulating GIE itself and obtaining luminance taking into account multiple diffusive-directed reflections. In this case, all other processes of interaction with material (specular reflection, refraction, etc) should be approached by other methods. The version of luminance collection considered above leads to noisy results.

In order to eliminate the noise, a final collection is used. Within the final collection method, a number of rays is emitted from the preset point into the hemispherical space, and luminance is collected in those places in the hemisphere where rays were. Based on the obtained luminance values, luminance for the preset point is calculated. This makes it possible to reduce noise level considerably [14] but the scope of the calculation increases.

In the 2000s, the photon card method was frequently and regularly used in computer graphics, and later it also found its place in light engineering. The photon card method became the basis of the new product *DIALux Evo* [12]. There were

two main prerequisites for transition to *DIALux* from the finite element method: limitations of the reflection model and limitations of scene size.

In recent years, the idea has arisen in lighting community that the simulation of indoor and external illumination should not be considered separately, and large inner spaces should not be simulated separately. Illumination modelling should be a uniform inseparable process for the whole object and should be considered as an integral whole. However, this prerequisite was limited for a long time due to the complexity of the radiosity method when simulating large objects. Computation time grows proportionally to the number of elements squared. Within the photon card method, this dependence is less typical, and in some approaches, it reduces itself to growth of the calculation volume in the process of ray tracing only, when it is necessary to search through a greater number of objects. The emergence of *DIALux Evo* based on the photon card method should allow moving to another LI simulation level. However, in reality, this has not occurred in modern engineering practice.

For today, specially optimised libraries of ray tracing exist, which take into consideration architectural features of modern central and graphic processing units, for example, *Intel Embree* [15]. These libraries allow designers of modern lighting programs to overlook a number of the most complex optimisation questions and concentrate on the solution of their own applied problems.

Lately in computer graphics, the *Instant Radiosity* method has featured prominently for the first time stated within phenomenological approach in 1997 in A. Keller's work [16]. In this work, Keller considered qualitatively the process of simulating multiple GIE reflections (1) based on constancy of the set of secondary sources in the space and the on calculation of their contribution to luminance for the studied point. However, as it is shown in our work [17], this method is based on the well-known local assessments proposed for the first time in atomic physics [18]. Local assessments have gained their further powerful development when solving radiation transfer equation in atmosphere and ocean optics [19].

GIE can be written down as a space integral and expanded into Neuman's series. After some transformations, the obtained expansion can be written down as [17]:

$$\begin{aligned}
L(r, \hat{l}) = & L_0(r, \hat{l}) + \\
& + \frac{1}{N} \sum_{i=1}^N \left(\frac{1}{\pi} \frac{L_0(r_{1i}, \hat{l}_{1i})}{p_1(r_{1i}, \hat{l}_{1i})} \frac{\sigma(r; \hat{l}_{1i}, \hat{l}) G(r_1, r)}{p_2(r_{1i}, \hat{l}_{1i} \rightarrow r, \hat{l})} \right. \\
& + \frac{1}{\pi^2} \frac{L_0(r_{1i}, \hat{l}_{1i})}{p_1(r_{1i}, \hat{l}_{1i})} \frac{\sigma(r_{2i}; \hat{l}_{1i}, \hat{l}_{2i}) G(r_{1i}, r_{2i})}{p_2(r_{1i}, \hat{l}_{1i} \rightarrow r_{2i}, \hat{l}_{2i})} \times \\
& \left. \times \frac{\sigma(r; \hat{l}_{2i}, \hat{l}) G(r_{2i}, r)}{p_2(r_{2i}, \hat{l}_{2i} \rightarrow r, \hat{l})} + \dots \right) \quad (7)
\end{aligned}$$

This expression can be interpreted as Markovian chain. As a result of creating the Markovian chain, one can assess at each chain element in the equation nucleus determining probability of departure from the trajectory to the studied points $\mathbf{r}, \hat{\mathbf{l}}$. Accumulating the statistics, we directly obtain luminance in the preset points in the preset directions [17]. We implemented the proposed method of local assessments within this work, and the scene visualisation example is given in Fig. 2. The scene was carried out by means of this method.

At present, other GIE simulation methods are also extensively developed. One can notice two of them: the *path tracing* method and *Metropolis light transport* calculation method [20]. The methods and their implementation can be divided into two main classes: shifted and non-shifted. Non-shifted methods are broadly developed in applied visualisation tasks, in cinema, in computer games and in simulators; i.e. in such tasks, where exact spatial and angular luminance distri-

bution is not as important but a «photorealistic» image is.

4. PER ASPERA AD ASTRA

The rapid development of GIE simulation methods has found applications in cinema, television, architectural design and in many other applied tasks but not in engineering practice of LI lighting design. The situation seems to be paradoxical: in computer graphics tasks luminance is calculated taking into account multiple reflections using modern methods, while in light engineering, illuminance is mainly used. At the same time, this state of affairs is quite logical.

The modern regulatory documents for indoor illumination, both Russian [21], and European [22] use illuminance as a normalised characteristic and illuminance uniformity as its derivative. It should be noted that a human eye does not react to illuminance but sees luminance. As to luminance, it is normalised for external illumination only, for example, in the illumination of highways or in architectural illumination [23]. This can be easily explained: when standard documents were drawn up, there was no possibility to simulate luminance taking into account multiple reflections. There were neither simulation methods, nor necessary computing facilities. Development of computer facilities and of mathematical simulation methods allowed solving GIE, however, it was solved with caution to the regulatory documents. Why calculate spatial and angular luminance distribution, if illuminance, an in-

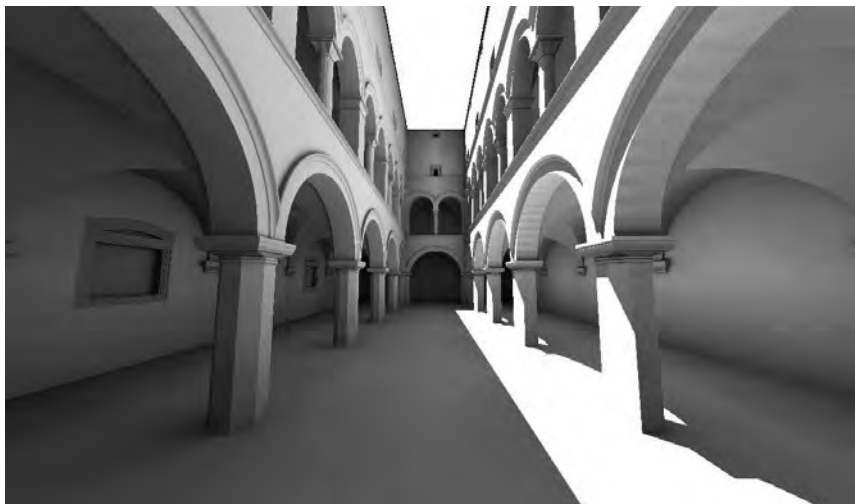


Fig. 2. Visualisation of the standard test three-dimensional *Dabrovic Sponza* scene using local assessments of the Monte-Carlo method

tegral characteristic, is normalised? This brings us into a vicious circle. *DIALux Evo*, which based on a method which allows simulating luminance but has not found its place in engineering practice, becomes a confirmation of this fact.

The situation with rationing of quantitative characteristics is reflected in the quality characteristics as well. In modern engineering practice, the Unified Glare Rating (*UGR*) is mainly used [21].

$$UGR = 8 \lg \left[\frac{0,25 \sum_{i=1}^N \frac{L_i^2 \omega_i}{p_i^2}}{L_a} \right], \quad (8)$$

where L_i is luminance of the glare source, cd/m^2 , ω_i is the angular size of glare source, sr , p_i is the index of the glare source position relative to the sight line, L_a is adaptation luminance, cd/m^2 . When simulating with the existing software, only the light sources themselves will be taken into consideration, whereas glares on the reflecting surfaces will not be included in the glare rating.

This results in a situation when design is quantitatively developed without proper consideration of illuminance as a characteristic perceived by a person in the space, and quality questions completely rely on the experience and intuition of the designer. The new GIE simulation methods allow revising regulatory documents and forming both new quantitative indices normalising spatial-and-angular luminance distribution, and new quality characteristics obtained from it.

The evolution of LI lighting simulation, which began with a technological revolution in the nineteenth century, comes to its logical conclusion, and the next stage of development will become revolutionary again. A result of this step will be the transition from LI design relative to a preset illuminance distribution to design relative to a preset illumination quality.

Another important direction for LI simulation program development should be the transition from photorealistic image synthesis to a realistic one based on the use of uniform chromaticity scale systems. This will make it possible to obtain LI images which are based on the laws of light and colour similarity, and how they are perceived by the human eye. This will enable the customer and the designer to compare various illumination options and to select the best by their visual perception. This is a separate big subject, which

is beyond the scope of this review of modern LI simulation methods using a computer.

REFERENCES:

1. *Foley, J.D., van Dam, A., Feiner, S.K., Hughes, J.F.* Computer Graphics: Principles and Practice. Addison-Wesley Professional, 1994.
2. *Kajiya, J.T.* The rendering equation // Computer Graphics (Proc. SIGGRAPH'86). 1986. Vol. 20, # 4, pp. 143–150.
3. *Budak V.P.* Computer graphics – a lighting computer project // Svetotekhnika, 1999, #1, pp. 22–25.
4. *Gallager R.* Finite element method. Foundations. Moscow: Mir, 1984.
5. *Medvedev V.E., Paritskaya G.G.* Calculation of illuminance in images // Optics and spectroscopy. 1966, Vol. 22, #5, pp. 638–642.
6. *Kusch O.K., Mitin A.I.* Calculation of light distribution of specular symmetric surfaces with an extended light source using a computer // Svetotekhnika, 1976. #6, pp. 3–5.
7. *Korobko A.A., Kusch, O.K.* Use of the Monte-Carlo method in lighting calculations // Svetotekhnika, 1986, #10, pp. 14–17.
8. *Goral, C., Torrance, K., Greenberg, D., Battaile, B.* Modeling the interaction of light between diffuse surfaces // Computer Graphics, 1984, Vol. 18, # 3, pp. 213–222.
9. *Yamauti, Z.* The light flux distribution of a system of inter-reflecting surfaces // Journal of the Optical Society of America, 1926, Vol.13, # 5, pp. 561–571.
10. *Moon, P.* On Interreflections // Journal of the Optical Society of America, 1940, Vol. 30, # 2, pp.195–205.
11. *Polyak G.L.* Radiant heat exchange of bodies with arbitrary indicatrices of surface reflection / in book: Convective and radiant heat exchange. – Moscow: Academy of Sciences of the USSR, 1960, pp.118–132.
12. www.dialux.de.
13. www.relux.biz.
14. *Christensen, N. J., Jensen, H. W.* A Practical Guide to Global illumination and Photon Maps // Siggraph, 2000, Course 8, July 23, 77 p.
15. *Wald, I., Woop, S., Benthin, C., Johnson, G.S., Ernst, M.* Embree – A Kernel Framework for Efficient CPU Ray Tracing // ACM Transactions on Graphics (proceedings of ACM SIGGRAPH), 2014, Vol. 33, # 4, Article 143 (July 2014), 8 p.
16. *Keller A.* Instant radiosity // Proc. SIGGRAPH, 1997, pp. 49–56.

17. Budak, V., ZheltoV, V., Notfulin, R., Chembaev, V. Relation of Instant Radiosity Method with Local Estimations of Monte Carlo Method // WSCG 2016, pp. 189–197.

18. Kalos, M.H. On the Estimation of Flux at a Point by Monte Carlo // Nuclear Science and Engineering, 1963, Vol. 16, #.1, pp. 111–117.

19. Monte-Carlo method in atmospheric optics / Under the editorship of G.I. Marchuk, Novosibirsk: Nauka, 1976.

20. Pharr, M., Humphreys, G. Physically based rendering from theory to implementation, Morgan Kaufmann Publishers, 2010.

21. GOST P 55710–2013 «Illumination of working places in buildings. Standards and methods of measurements».

22. EN12464–1:2002 “The Lighting of Workplaces”.

23. GOST P 55706–2013 «External utilitarian illumination. Classification and standards».



Victor S. ZheltoV,

Ph.D., graduated from the Chair “Light and Engineering” of the Moscow Power Institute in 2005. At present, he is an assistant lecture at the same chair of MPI



Vladimir P. Budak,

Dr. of technical science, Prof., graduated from the Chair “Light and Engineering” of the Moscow Power Institute in 1981. At present, he is the Professor of the same chair of MPI and Editor in Chief of Light & Engineering Journal

AN APPROXIMATE FORMULA FOR ANGULAR DISTRIBUTION OF IRRADIANCE FROM AN IRREGULAR SURFACE WITH COMPLEX REFLECTION INDICATRIX

Sergei V. Alkov, Mikhail L. Belov, and Viktor A. Gorodnichev

Moscow State Technical University of N.E. Bauman, NRU
E-mail: belov@bmstu.ru

ABSTRACT

Using the photometric approach, an approximate expression for angular distribution of irradiance from an irregular anisotropic surface with local reflection indicatrix is obtained. The indicatrix has both diffuse (wide in the angular sense), and quasispecular components when radiating the surface by means of a radiation beam from an arbitrary direction. It is shown that the angular distribution of irradiance is significantly influenced by the characteristics of surface roughness inclinations, incidence angle, and direction of the radiation beam, as well as parameters of diffuse and quasispecular components of the local reflection indicatrix.

Keywords: radiation beam, irradiance, angular distribution, irregular anisotropic surface, local reflection indicatrix, diffuse and quasispecular indicatrix components

INTRODUCTION

Calculation of the angular distribution of energy photometric parameters of radiation reflected by surfaces is of interest for the creation of certain devices and systems: vision (laser and night vision), illumination and radiation, optical location, optical monitoring, etc. [1–5].

In the optical spectral range, most cases addressing this problem use irregular surface models either with specular or with Lambert reflection indicatrices of local sites [3–6].

A more general irregular surface model has a complex reflection indicatrix of local sites. It has both wide angular and specular or quasispecular components [7–10]. However, in previous works using this model of reflection indicatrix of local sites to calculate angular distribution of energy photometric parameters, the surface was considered isotropic.

In this article, using the photometric approach (based on use of radiometric values radiance and irradiance) for calculations, an approximate expression is deduced for irradiance angular distribution from an irregular and generally anisotropic surface with a complex local reflection indicatrix having both diffuse (wide angular), and quasispecular components when radiating the surface with a radiation beam from an arbitrary direction.

FORMULATION OF THE PROBLEM

Let there be a three-dimensional random-irregular surface S , which is irradiated with a radiation beam from an arbitrary direction. An approximate expression for irradiance $E(\vec{r})$ created by radiation reflected by the surface can be obtained using the general expression [4] registered according to a two positions layout (when the radiation source and receiver are separated in space) with a receiver of unit area and of 2π vision field solid angle:

$$E(\vec{r}) = \int_S d\vec{R} \int_{2\pi} d\Omega(\vec{m}) L_r(\vec{R}, \vec{m}) L_{ref}(\vec{R}, \vec{m}) \cos\theta, \quad (1)$$

where $L_{ref}(\vec{R}, \vec{m})$ is radiance (R) of reflected radiation from the surface in point \vec{R} in direction \vec{m} coming to the observation point \vec{r} ; $d\vec{\omega}(\vec{m})$ is an element of the solid angle; θ is the angle between normal to S surface in point \vec{R} and direction to the observation point \vec{r} ; $L_r(\vec{R}, \vec{m})$ is the value of sr^{-1} . If multiplied by $1 \text{ W}\cdot\text{m}^{-2}$, the obtained value will have meaning of R created on the surface element S by radiation incident from a «fictitious» source [4, 5] with parameters of the receiver registering an irradiance in the observation point of a unit area, of 1 W radiation flux and of 2π vision field solid angle.

An expression similar to (1) was also obtained when considering optical location of solid bodies [11].

Within the photometric approach R, $L_{ref}(\vec{R}, \vec{m})$ in the case of a uniform reflecting surface can be presented as [4]

$$L_{ref}(\vec{R}, \vec{m}) = \chi(\vec{n}, \vec{m}) L_o(\vec{R}, \vec{m}), \quad (2)$$

where $\chi(\vec{n}, \vec{m})$ is local reflection indicatrix, i.e., indicatrix relating to an elementary site of irregular surface, which is much greater than the radiation wavelength but much smaller than the surface roughness dimensions; \vec{n}, \vec{m} are vectors characterising direction of the incident and of the reflected radiation; $L_o(\vec{R}, \vec{m})$ is R of the reflected radiation for an ideal reflector (Lambert surface with albedo equal to one).

R distribution $L_o(\vec{R}, \vec{m})$ appears as follows [4]:

$$L_o(\vec{R}, \vec{m}) \equiv L_o(\vec{R}) = \frac{E_s(\vec{R})}{\pi}, \quad (3)$$

where $E_s(\vec{R})$ is irradiance of a surface elementary site created by radiation ray (RR) incident on the surface.

Local reflection indicatrix characterises diffusing properties of local sites of large-scale surface S .

If besides Lambert component (with which R is distributed uniformly within the hemisphere based on a local surface site), local indicatrix of the real surface has a significant specular component, then as indicatrix models $\chi(\vec{n}, \vec{m})$, the following expression can be used (see, e.g., [8]):

$$\chi(\vec{n}, \vec{m}) = \frac{A}{\alpha + \beta} \left[\alpha + \beta \frac{\pi}{\cos \theta_{spec}} \delta(\vec{m} - \vec{m}_{spec}) \right], \quad (4)$$

where A is albedo of an elementary reflecting site; α and β is a portion of Lambert and specular reflection for the elementary reflecting site, $\alpha + \beta = 1$; \vec{m}_{spec} is vector of specular reflection dependent on the vector of incident radiation direction \vec{n} and on normal vector \vec{k} to the reflecting site; $\vec{m}_{spec} = \vec{n} - 2\vec{k}(\vec{k}\vec{n})$; θ_{spec} is angle between the normal to the reflecting site \vec{k} and vector \vec{m}_{spec} .

As to the reflection indicatrix of a more general type than (4), both the diffuse (wide angular), and quasispecular component can have parameters changing their angular width (the similar indicatrix was used in [9]):

$$\begin{aligned} \chi(\vec{n}, \vec{m}) = & A \frac{1}{\alpha \frac{2}{n+2} + \beta} [\alpha (\vec{k}\vec{m})^n + \\ & + \beta \frac{1}{\cos \theta_{spec} \Delta^2} \exp\{-\frac{(\vec{m} - \vec{m}_{spec})^2}{\Delta^2}\}], \end{aligned} \quad (5)$$

where n is the parameter characterising the angular width of the reflection indicatrix diffuse component, $n > 0$; Δ is the parameter characterising the angular width of the reflection quasispecular component.

The first summand in (5) describes diffuse (wide angular) component of the local indicatrix, and the second describes quasispecular (narrow angular) component of the local indicatrix, which at the limit ($\Delta \rightarrow 0$) changes into specular component.

Indicatrices (4) and (5) are normalized by the following condition: $\frac{1}{\pi} \int_0^{2\pi} \int_0^{\pi/2} \chi(\vec{n}, \vec{m}) \cos \theta d\Omega(\vec{m}) = A$.

At $n = 0$ and $\beta = 0$, expression (5) changes into expression for reflection indicatrix of the Lambert surface: $\chi(\vec{n}, \vec{m}) \equiv A$. At $\alpha = 0$ in formula (5), reflection quasispecular component only remains, which changes into specular at $\Delta \rightarrow 0$.

At $\beta = 0$ and at an arbitrary n , formula (4) changes into expression [12]:

$$\chi(\vec{n}, \vec{m}) = A \frac{n+2}{2} \cos^n \theta, \quad (6)$$

where θ is the angle between normal to an elementary site of the irregular surface and observation direction.

Fig. 1 [12] shows the nature of the $\cos^n\theta$ function change. The function determines angular dependence of reflection indicatrix (6) for different n parameter values (the correspondent values of parameter n are noted by each curve). It can be seen from Fig.1 that within the used model, local reflection indicatrix can change from a wide Lambert's (for which $\chi(\vec{n}, \vec{m}) \equiv A$) to very narrow.

In the article, an approximate formula for angular distribution of illuminance from an irregular anisotropic surface is obtained based on the integral expression (1) using expressions (2) and (3) for reflection indicatrix of local sites (5).

FORMULA FOR THE ANGULAR DISTRIBUTION OF ILLUMINANCE FROM AN IRREGULAR SURFACE

Using expressions (2), (3) and (5) (as in [4]), from (1) we obtain an approximate expression for irradiance $E(\vec{r})$ created by radiation reflected from an occasionally irregular surface, with a local indicatrix (5). In doing so, we consider that angular RR width and angular width of quasispecular component of the local indicatrix is much less than the mean square value of surface S inclines and that radiation source and observation point are on the same plane (XOZ):

$$E(\vec{r}) \cong \frac{A}{\pi} \frac{1}{(\frac{2}{\alpha} + \beta)} \frac{1}{z_r^2} \left\{ \alpha \int_{S_o} d\vec{R} E_s(\vec{R}'_{o\zeta}) (\vec{k}(\vec{R}_o) \vec{m})^n + \beta \int_{S_o} d\vec{R} E_s(\vec{R}'_{o\zeta}) \frac{1}{\cos\theta_{spec} \Delta^2} \exp\left\{-\frac{(\vec{m} - \vec{m}_{spec})^2}{\Delta^2}\right\} \right\}, \quad (7)$$

where $\vec{R}'_{o\zeta} = \{[R_{ox} \text{ctg}\theta_s - \zeta(\vec{R}_o)] \sin\theta_s, R_{oy}\}$; S_o is the projection of irregular surface S on plane $Z = 0$; $\vec{R}_o = \{R_{ox}, R_{oy}\}$ is the vector on surface S_o ;

$E_s(\vec{R}) = (\vec{n}\vec{k}) E_s^n(\vec{R})$; $E_s^n(\vec{R})$ is the irradiance distribution in the cross-section of a radiation beam in Gaussian approach [4]

$$E_s^n(\vec{R}) \cong \frac{P_o}{\pi \alpha_s^2 z_s^2} \exp\left(-\frac{R^2}{\alpha_s^2 z_s^2}\right);$$

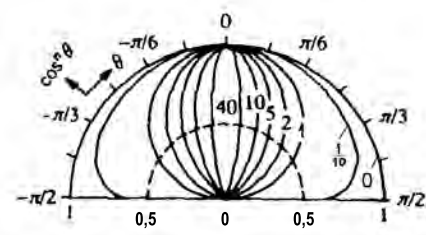


Fig. 1. Nature of the changing $\cos^n\theta$ function

P_o and α_s is the source radiation flux and angular width of the radiation beam; z_s and z_r are inclined distances from the radiation source (along optical axis of the radiation beam from the observation point to the surface optical spot centre); $\zeta(\vec{R}_o)$ is S surface height in point \vec{R}_o ; $\vec{k} = \{k_x, k_y, k_z\}$ is the unit vector of the normal to a local site of irregular surface S ; θ_s is the angle between the normal to S_o surface and direction to the radiation source.

When calculating (7), it was considered that inclined distances from the radiation source (along the radiation beam optical axis) and from the observation point to the centre of the illuminated spot on the surface are much more than roughness height of surface S .

Observation point position \vec{r} in (7) is characterised by the distance to z_r surface and by vector \vec{m} .

As a model of irregular surface we will use the model of three-dimensional uniform anisotropic randomly irregular surface. Such a surface can be expressed as a function, where z is surface height in point \vec{R} . Let stochastic function $\zeta(\vec{R})$ be unambiguous and quite smooth, and let it be characterised by probability density $W(\xi)$. Similarly, the surface incline field $\vec{\gamma} = \{\gamma_x, \gamma_y\}$ is characterised

by probability density $W(\gamma_x, \gamma_y)$. ($\gamma_x = \frac{\partial \zeta}{\partial x}$ and $\gamma_y = \frac{\partial \zeta}{\partial y}$, $\gamma_x = \frac{\partial \zeta}{\partial x}$ and $\gamma_y = \frac{\partial \zeta}{\partial y}$ values determine

tangents of slope angles of surface $z = \zeta(\vec{R})$ to the plane $Z = 0$).

Surface height and inclination distribution laws will be considered normal. Normal laws of height and incline distribution reflect the rather obvious fact that for most surfaces the probability of large deviations from the mean (of heights or inclinations) is always very low.

Let's consider the surface to be plain on average. Then the only statistical characteristics of a randomly irregular surface are surface dispersions of heights $\langle \zeta^2 \rangle$ and of inclinations $\langle \gamma_{x,y}^2 \rangle$. Here angular brackets mean averaging over the total surface.

Averaging E values over heights and inclines of a randomly irregular surface S (considering it smoothly irregular), we will obtain the following approximate formula for average irradiance \bar{E} . We also consider that mean square values of the surface heights are much less than RR dimensions on the surface:

$$\bar{E}(\vec{r}) \cong \frac{Aa_s}{z_s^2 z_r^2 C_s \cos \theta_s} \frac{1}{\alpha \frac{2}{n+2} + \beta} [\alpha F(\theta_s, \theta_r) + \frac{\beta q^4}{8q_z^4 \langle \gamma_x^2 \rangle \langle \gamma_y^2 \rangle^{1/2}} \exp(-\frac{q_x^2}{2q_z^2 \langle \gamma_x^2 \rangle})], \quad (8)$$

where $q_x = (\sin \theta_s - \sin \theta_r)$; $q_z = -(\cos \theta_s - \cos \theta_r)$; $\vec{r} = \{z_r, \theta_r\}$; θ_r is the angle between normal to S_o surface and direction to the observation point; for an isotropic surface with diffuse component of local indicatrix $[(n + 2)/2] \cdot \cos^n \theta$ type and inclination dispersion $\langle \gamma_{x,y}^2 \rangle \equiv \gamma_o^2$

$$F(\theta_s, \theta_r) = F_{is}(\theta_s, \theta_r, n) = \cos^n \theta_r (2\gamma_o^2)^{-n/4} \exp(\frac{1}{4\gamma_o^2}) [\cos \theta_r \cos \theta_s (2\gamma_o^2)^{-1/4} \times \times W_{\frac{n+1}{4}, \frac{n-1}{4}}(\frac{1}{2\gamma_o^2}) + \frac{1}{2} \sin \theta_r \sin \theta_s (n+1)(2\gamma_o^2)^{1/4} \times \times W_{\frac{n+3}{4}, \frac{n-3}{4}}(\frac{1}{2\gamma_o^2})]; \quad (9)$$

and for anisotropic surface with a diffuse component of local indicatrix coinciding with Lam-

bert's, and inclination dispersions $\langle \gamma_x^2 \rangle, \langle \gamma_y^2 \rangle$ (see eqn. 10), where

$$a = 4(\frac{1}{\langle \gamma_x^2 \rangle} + \frac{1}{\langle \gamma_y^2 \rangle})^{-1}; \mu = 0,5a\delta; \delta = 0,5(\frac{1}{\langle \gamma_x^2 \rangle} - \frac{1}{\langle \gamma_y^2 \rangle});$$

$\Gamma(k)$ is gamma function; $W_{n, m}(x)$ is Whittaker's function.

In a limiting case of the plain Lambert surface ($n = 0, \beta = 0, \langle \gamma_{x,y}^2 \rangle \rightarrow 0$) expression (8) coincides with the similar earlier result [5]. The limiting case does not describe a plain smooth surface (8), because provided that angular width of radiation beam is much less than mean square value of surface inclinations. In a special case of accidentally irregular locally Lambert surface ($n = 0, \beta = 0$) formula (8) coincides with the results in [13].

For an irregular, accidentally isotropic surface, formula (8) is consistent with the correspondent results of work [9], and for a local indicatrix having Lambert and specular components [14].

As formula (8) is obtained provided that mean square value of surface heights $\langle \zeta^2 \rangle$ is much less than the radiation beam's dimensions on the surface, and angular width of quasispecular component is much less than the mean square value of surface inclinations, then $\langle \zeta^2 \rangle$ and $\Delta 2$ values were not included in the approximate formula (8).

Averaging in formula (8) is generally performed according to the implementation ensemble of random surfaces.

However, if not only mean square values of surface heights but also dimensions of surface roughnesses are much less than the radiation beam dimensions on the surface, then a real experiment averaging is carried out due to the large size of the S surface optical spot.

$$F(\theta_s, \theta_r) = F_{an}(\theta_s, \theta_r) = \frac{a \exp(\frac{1}{2a})}{4(\langle \gamma_x^2 \rangle \langle \gamma_y^2 \rangle)^{1/2}} \sum_{k=0}^{\infty} \frac{a^{-k}}{k!} (\frac{\mu}{2})^{2k} \{ \sin \theta_s \sin \theta_r a^{1/4} \times \times \frac{\Gamma(2k+2)}{\Gamma(k+1)} W_{-k-\frac{3}{4}, k+\frac{3}{4}}(\frac{1}{a}) - \sin \theta_s \sin \theta_r a^{-1/4} \frac{\Gamma(2k+3)}{\Gamma(k+2)} \frac{\mu}{2} W_{-k-\frac{5}{4}, k+\frac{5}{4}}(\frac{1}{a}) + \times + 2 \cos \theta_s \cos \theta_r a^{-1/4} \frac{\Gamma(2k+1)}{\Gamma(k+1)} W_{-k-\frac{1}{4}, k+\frac{1}{4}}(\frac{1}{a}) \}. \quad (10)$$

4. CALCULATIONS RESULTS AND THEIR DISCUSSION

The main difficulty of angular distribution calculations of irradiance from irregular surface with complex reflection indicatrix according to the approximate formula (8) is that (9) and (10) contain special functions (Whittaker's functions $W_{n, m(x)}$).

When calculating, it was taken into consideration that S surface is smoothly irregular ($\langle \gamma_{x,y}^2 \rangle^{1/2} \ll 1$), and Whittaker's functions are approximated by expressions based on asymptotic series for Whittaker's functions [15] (only three terms of series the were considered).

It leads to a rather simple and tight expressions for a smoothly irregular surface with $\langle \gamma_{x,y}^2 \rangle^{1/2} \ll 1$. For example, for an isotropic surface with a diffuse component of local indicatrix of $[(n + 2)/2] \cdot \cos^n \theta$ type and with an inclination dispersion of $\langle \gamma_{x,y}^2 \rangle \equiv \gamma_o^2$, approximate expression for $F_{is}(\theta_s, \theta_r, n)$ has the following appearance:

$$\begin{aligned}
 F_{is}(\theta_s, \theta_r, n) &\approx \\
 &\approx \cos \theta_s \cos^{n+1} \theta_r \left\{ 1 - \frac{\gamma_o^2}{8} [(n+3)^2 - (n-1)^2] + \right. \\
 &+ \frac{\gamma_o^4}{128} [(n+3)^2 - (n-1)^2] [(n+7)^2 - (n-1)^2] \left. \right\} + \\
 &+ \sin \theta_r \sin \theta_s \cos^n \theta_r (n+1) \\
 &\gamma_o^2 \left\{ 1 - \frac{\gamma_o^2}{8} [(n+5)^2 - (n-3)^2] \right\}.
 \end{aligned}$$

Fig. 2 illustrates angular distribution of illuminance from an irregular surface with a local reflection indicatrix $\chi(\vec{n}, \vec{m}) = A \frac{n+2}{2} \cos^n \theta$ (i.e. without a quasispecular component). Fig. 2 presents calculation results of M value dependence on the observation angle θ_r ; the relation of irradiance \bar{E} from the surface with local reflection indicatrix $\chi(\vec{n}, \vec{m}) = [(n + 2)/2] \cdot \cos^n \theta$ to irradiance from the surface with local-Lambert reflection indicatrix:

$$M \cong \frac{n+2}{2} \frac{F_{is}(\theta_s, \theta_r, n)}{F_{is}(\theta_s, \theta_r, n=0)}.$$

The calculations were carried out with the following parameter values:

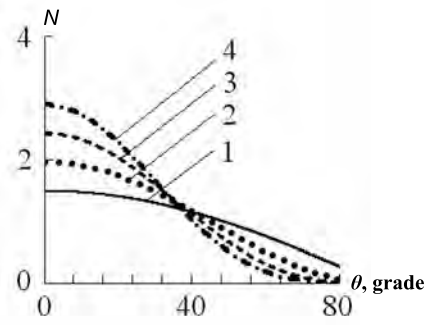


Fig. 2. Angular distribution of irradiance from an irregular surface with local reflection indicatrix $\chi(\vec{n}, \vec{m}) = A \cdot [(n + 2)/2] \cdot \cos^n \theta$

$$\theta_s = 40^\circ; \langle \gamma_x^2 \rangle^{1/2} = \langle \gamma_y^2 \rangle^{1/2} = 0.1;$$

$$1 - n = 1; 2 - n = 2; 3 - n = 3; 4 - n = 4.$$

It can be seen from Fig. 2 that parameter n characterising the angular width of the diffuse indicatrix component significantly influences angular irradiance distribution. And at angles $\theta_r \leq 40^\circ$, irradiance \bar{E} grows with n and can be much greater than the irradiance from the surface with local-Lambert reflection indicatrix, and at $\theta_r > 40^\circ$, with n growth, \bar{E} decreases. This situation is illustrated by Fig. 3, in which M calculation dependence on n at three different θ_r values is shown. The calculations were carried out at the following parameter values:

$$\theta_s = 40^\circ; \langle \gamma_x^2 \rangle^{1/2} = \langle \gamma_y^2 \rangle^{1/2} = 0.1;$$

$$1 - \theta_r = 0^\circ; 2 - \theta_r = 40^\circ; 3 - \theta_r = 80^\circ.$$

As formula (8) is obtained for smoothly irregular surface ($\langle \gamma_{x,y}^2 \rangle^{1/2} \ll 1$), distribu-

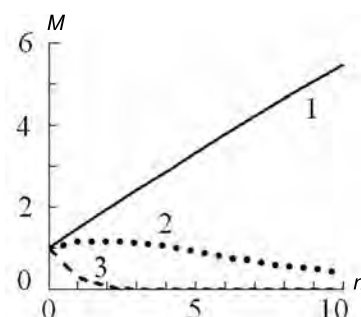


Fig. 3. M value dependence on n parameter

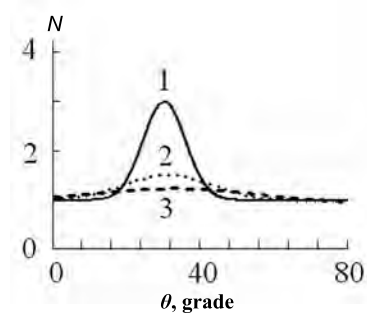


Fig. 4. Irradiance angular distribution at different mean square values of surface inclinations

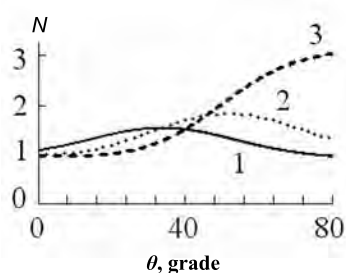


Fig. 5. Influence of θ_s surface radiation angle on irradiance angular distribution

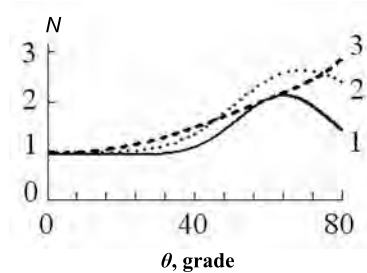


Fig. 6. Influence of radiation direction on angular distribution irradiance from an anisotropic surface

tion of irradiance from an irregular surface with local reflection indicatrix $\chi(\vec{n}, \vec{m}) = A \cdot [(n + 2)/2] \cdot \cos^n \theta$ (without a quasispecular component) slightly depends on the mean square values of surface inclines $\langle \gamma_{x,y}^2 \rangle^{1/2}$.

The situation changes, when the indicatrix has a quasispecular component.

Figs. 4–6 show the influence of a quasispecular local reflection indicatrix component of elementary reflecting surface sites on angular irradiance distribution \bar{E} . Here results of N value calculation dependence on θ_r angle are given: the relation of irradiance \bar{E} from an anisotropic surface with local indicatrix having a quasispecular component and a diffuse component coinciding with Lambert's, to the irradiance from an isotropic surface with locally Lambert's reflection indicatrix only:

$$N \cong \frac{1}{\alpha + \beta} \frac{[\alpha F_{an}(\theta_s, \theta_r) + \frac{\beta q^4}{8q_z^4 (\langle \gamma_x^2 \rangle \langle \gamma_y^2 \rangle)^{1/2}} \exp(-\frac{q_x^2}{2q_z^2 \gamma_{ox}^2})]}{F_{is}(\theta_s, \theta_r, n=0)}$$

Fig. 4 shows irradiance angular distribution with three different mean square values of surface inclinations. The calculations are carried out at the following parameter values: $\theta_s =$

$30^\circ; \alpha = 0.97; \beta = 0.03, 1 - \langle \gamma_{x,y}^2 \rangle^{1/2} = 0.05;$

$2 - \langle \gamma_{x,y}^2 \rangle^{1/2} = 0.1; 3 - \langle \gamma_{x,y}^2 \rangle^{1/2} = 0.15.$

It can be seen that along the direction close to the specular reflection angle ($\theta_r = -\theta_s$), a peak appears, the height and width of which is strongly dependent on the irregular surface inclination mean square value (and certainly on the portion of the specular component local surface reflection indicatrix).

Figs. 5 and 6 illustrate the dependence of angular irradiance distribution on angle θ_s (Fig. 5) and on radiation direction (Fig. 6). Regarding Fig. 5, the calculations were carried out with the following parameter values: $\alpha = 0.95; \beta = 0.05;$

$1 - \theta_s = 30^\circ; 2 - \theta_s = 45^\circ; 3 - \theta_s = 60^\circ; \langle \gamma_x^2 \rangle^{1/2} =$

$= 0.15; \langle \gamma_y^2 \rangle^{1/2} = 0.1.$ And surface radiation was

made within one plane: XOZ . As to Fig. 6, surface radiation was simulated in three planes: **1** – within XOZ plane; **2** – within a plane forming 45° with XOZ and YOZ planes; **3** – within YOZ

plane; $\theta_s = 60^\circ; \alpha = 0.95, \beta = 0.05; \langle \gamma_x^2 \rangle^{1/2} = 0.1;$

$\langle \gamma_y^2 \rangle^{1/2} = 0.2.$

From Fig. 5 and 6 can also be seen that the nature of irradiance angular distribution depends on angle θ_s and on the radiation direction in a complex fashion.

And with θ_r growth, irradiance can increase (as the reflection peak of the quasispecular component with θ_r increase has not yet been reached).

CONCLUSION

Using the photometric approach, an approximate expression for angular distribution of irradi-

ance from an irregular anisotropic surface is obtained with local reflection indicatrix when radiating a surface with a beam from an arbitrary direction. The indicatrix has both diffuse and quasi specular components. It is shown that the irradiance angular distribution depends in a complex fashion on the surface roughness inclination characteristics, on the radiation angle and direction, on parameters of local reflection indicatrix diffuse and quasispecular components.

REFERENCES

1. Reference book on lighting engineering / Under the editorship of Yu.B. Ayzenberg. The 3rd revised edition, – Moscow: Znak, 2006. – 972 p.
2. *Karasik V.E., Orlov V.M.* Laser systems of vision. – Moscow: Publishing house of the MSTU of N.E. Bauman, 2013, 478 p.
3. Optoelectronic systems of environmental monitoring / Under the editorship of V.N. Rozhdestvin. Moscow: Publishing house of the MSTU of N.E. Bauman, 2002, 528 p.
4. Foundation of pulse laser location / Under the editorship of V.N. Rozhdestvin. Moscow: Publishing house of the MSTU of N.E. Bauman, 2010, 572 p.
5. Elements of the theory of light scattering and optical location / Under the editorship of V.M. Orlov. Novosibirsk: Nauka, 1982, 225 p.
6. *Toporets A.S.* Optics of rough surface. L.: Machinostroyeniye, 1988. 191 p.
7. *Ticconi F., Pulvirenti L., Pierdicca N.* Models for Scattering from Rough Surfaces. URL: <http://cdn.intechopen.com/pdfs-wm/16082.pdf> (addressing date: 9/21/2016).
8. *Kopilovich L.E., Fuks I.M.* Scattering indicatrices and albedo of strongly rough surfaces // Proceedings of high education institutions. Radiophysics. 1981. V. 24, #7. pp. 840–850.
9. *Belov M.L., Orlov V.M.* On the power registered by lidar when sounding in surface atmosphere with a combined scattering indicatrix // Optics of Atmosphere. 1991. V.4, #10, pp. 1066–1069.
10. *Labunets L.V.* Digital models of target images and of signal implementation in optical locational systems. Moscow: Publishing house of the MSTU of N.E. Bauman, 2007. 216 p.
11. *Varshavchik M.L.* Influence of atmosphere diffusing properties on measurement error of effective area of of solid body scattering // Optical-and-mechanical industry. 1988. #3, pp. 8–10.
12. Inverse problems in optics / Under the editorship of G.P. Bolts. Moscow: Machinostroyeniye, 1984, 199 p.
13. Imitation simulation in problems of optical remote sounding / Under the editorship of V.E. Zuev. Novosibirsk: Nauka, 1988. 164 p.
14. Scattering of laser beam on accidentally-irregular surface with a complex local reflection indicatrix in turbulent atmosphere // Bulletin of the MSTU. Instrument making series. 2007. #2, pp. 63–67.
15. *Gradstein I.S., Ryzhik I.M.* Tables of integrals, sums, series and products. Moscow: Nauka, 1971. 1108 p.



Sergei V. Alkov,
Ph.D., Associate Professor.
He is graduated from the Kursk Polytechnical Institute in 1978. At present, he is the Dean of the Radio Electronics, Laser and Medical Equipment

Department of the MSTU of N.E. Bauman NRU. Field of scientific interest: optical and optoelectronic devices and systems



Mikhail L. Belov,
Doctor of Technical Science, Professor.
He is graduated from the Moscow Power Institute in 1973. At present, the Chief researcher of the Radioelektronika and Laser

Technology NRU «MSTU of N.E. Bauman». Field of scientific interest: optical and optoelectronic devices and systems



Victor A. Gorodnichev,
Doctor of Technical science, senior research associate.
Graduated from the Moscow State University of M.V. Lomonosov in 1976. The Head of the Radioelektronika and

Laser Technology department of the MSTU of N.E. Bauman Scientific Research Institute NRU. Fields of scientific interest: optical and optoelectronic devices and systems

STUDY ON THE COMPARISON OF TWO SPECTRAL REFLECTANCE RECONSTRUCTION METHODS BASED ON AGILE SPECTRUM IMAGING AND LIQUID CRYSTAL MODULATION

Leihong Zhang¹, Bei Li^{1*}, Haojun Zhang², Yi Kang¹, Wenjie Zhan¹, Wenjuan Yi¹,
and Zhiwen Chen¹

¹*College of Communication and Art Design, University of Shanghai for Science and Technology, Shanghai 200093, China*

²*Shanghai Radio Equipment Research Institute, Shanghai 200090, China*

**E-mail: 443956507@qq.com*

ABSTRACT

Spectral reflectance plays an important role in colour representation of the object. There are a lot of methods to reconstruct spectral reflectance. Two spectral reflectance reconstruction methods based on agile spectrum imaging and liquid crystal modulation are compared in this paper. CIE1931 colour difference, Root Mean Square Error and Spectral Goodness of Fit Coefficient are adopted as three evaluating indicators to compare the two methods. From the results of the comparison, the method based on agile spectrum imaging is better than the method based on liquid crystal modulation in the aspects of the max, average and standard deviation of the colour difference and Root Mean Square Error. What's more, the average Spectral Goodness of Fit Coefficient of the method based on agile spectrum imaging is 0.9967, which is 1.4 % larger than the method based on liquid crystal modulation and reach the standard of spectral reconstruction. The comparison of these two methods contributes to the further study on reconstructing spectral reflectance and acquiring multispectral images by single bucket.

Key words: spectral reflectance reconstruction, agile spectrum imaging system, sine modulation, liquid crystal modulation

INTRODUCTION

The colour of an object is mainly determined by 3 factors: light source, spectral reflectance [1] and observer. Objects with different spectral reflectance can express the same colour, which is called the phenomenon of metamerism. Images with the same colour and different spectrum may have colour difference in different environments. Spectral reflectance plays an important role in accurately describing the colour information of objects. And spectral reflectance reconstruction of objects can avoid the phenomenon of metamerism and accurately reappear the colour. Nowadays, there are a lot of spectral reflectance reconstruction methods. Filter [2–3] and camera are used to acquire the image signal which can reconstruct the spectral reflectance, but its system is complex and the cost is high; the different spectral bands of modulated LED [4] light source is used to irradiate the colour block, which can reconstruct the spectral reflectance. But modulating the light source and acquiring different spectral band light source are difficult. As a result, many researchers have done a lot of researches on different methods to acquire spectral reflectance in recent years. Yitzhak August and Adrian Stern [5] studied on the method of reconstructing the spectral reflectance of compressed sensing based on liquid crystal modulation. By com-

binning with the liquid crystal modulation device, single pixel detector and compressed sensing algorithm, they achieved a high accuracy of spectral reflectance reconstruction. Leihong Zhang et al. [6] studied the method based on modulation light source and single pixel detector technology, using sparse prior properties to reconstruct the spectral reflectance, which simplified the measuring device and reduce the cost. Liheng Bian et al [7] studied the method using the agile spectrum imaging system for multi spectral imaging and using the correlation imaging algorithm to reconstruct its spectral reflectance, which realized the spectral reflectance reconstruction of large size image.

Different spectral reflectance obtaining methods have different advantages and disadvantages. Therefore, choosing a method that can accurately reconstruct the spectral reflectance is necessary. But for a variety of reconstruction methods, no scholars have made a comparative study of this. Obtaining multi spectral images and reconstruct the spectral reflectance based on single bucket detector can reduce the demand of the high resolution and high sensitivity array detector, which can also reduce the cost of system and increase the signal to noise ratio of the system, and have great application prospects. As a result, the multispectral images of the two methods based on agile spectrum imaging and liquid crystal are all acquired by sing bucket detector. The methods of reconstructing spectral reflectance are compared in three aspects: colour difference, Root Mean Square Error and Spectral Goodness of Fit Coefficient. By comparison, the accuracy and reliability of the two methods in reconstructing spectral reflectance were analyzed, which contributes

to the study on acquiring multispectral images by single bucket in the future.

1. The spectral reflectance reconstruction method based on agile spectrum imaging

The agile spectrum imaging system is used to modulate the input light source. After that, the modulated light source is used to illuminate the colour block, and the spectral reflectance of an object can be reconstructed by the echo signal acquired by a single bucket detector. Fig. 1 [7] is a simple diagram of experimental device for agile spectrum imaging system. The light source passes through the grating and gradient type modulation film, and then irradiates the colour block. The single bucket detector is used to receive the reflected spectral signal. The agile spectrum imaging system consists of light splitting gratings and gradient type modulation rotary wheel. First of all, the light emitted by the light source passes through the grating to separate the spectrum at different wavelengths. After converged by lens, it forms a «rainbow plane» in the gradient type modulation film. In short, the spectrum that is near the wave is gathered together. Next, the gradient type modulation rotary wheel is used to modulate the spectrum at different wavelengths. The centre to edge of the gradient type modulation film modulate spectrum in different wavelength. In the process of rotation, the transmittance of the spectrum modulated by the modulation rotary wheel is sinusoidal with time, which can produce the sine modulation matrix with time as the horizontal coordinate and transmission as the vertical coordinate. After irradiating the modulat-

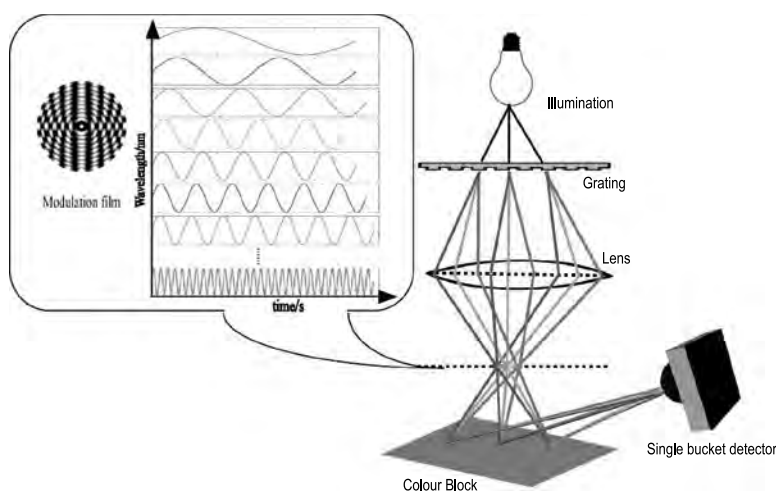


Fig. 1. The follow chart of the method based on agile spectrum imaging

ed light source spectrum to colour block, the reflected spectral signal is acquired by single bucket detector.

The modulation matrix is obtained by grating and gradient type modulation rotary wheel, which separates the spectrum at different wavelengths and modulate the light source. And the method of calculating the modulation matrix is shown in formula 1. In formula 1, $I_{\lambda_n t_m}$ represents sine curve of each modulation, and each sine curve is a single wavelength curve. T is cycle and t is time. n represents the n^{th} sinusoidal function with modulation frequency. In this paper, $n=1,2,3,\dots,31$, m is the sampling frequency of time dimension. The modulation matrix is shown in formula 2. In this formula, each row's time is invariant but the wavelength changes, and each column's wavelength is invariant but the time changes. The matrix $I_{\lambda_n t_m}$ is comparable with the transpose of matrix I .

$$I_{\lambda_n t_m} = \sum_{n=1}^{T/2} \sin\left(\frac{2\pi n}{T} t\right). \quad (1)$$

$$L_{\lambda_n t_m} = \begin{bmatrix} I_{\lambda_1 t_1} & I_{\lambda_2 t_1} & \dots & I_{\lambda_n t_1} \\ I_{\lambda_1 t_2} & I_{\lambda_2 t_2} & \dots & I_{\lambda_n t_2} \\ \vdots & \vdots & \ddots & \vdots \\ I_{\lambda_1 t_m} & I_{\lambda_2 t_m} & \dots & I_{\lambda_n t_m} \end{bmatrix}. \quad (2)$$

The pseudo inverse method is used to reconstruct the spectral reflectance, and the calculation method is shown in formula 3. In formula 3, \hat{R} is the reconstructed spectral reflectance, D_1 represents the response signal detected by the single bucket detector, S_1 is the spectral power distribution of the light source, $L_{\lambda_n t_m}$ is the sine modulation matrix computed above and $pinv$ represents calculating the pseudo inverse of the matrix.

$$\hat{R} = pinv\left(S_1 L_{\lambda_n t_m}\right) \cdot D_1. \quad (3)$$

2. The spectral reflectance reconstruction method based on liquid crystal modulation

The experimental equipment of the spectral reflectance reconstruction method based on liquid crystal modulation mainly consists of liquid crystal phase retarder and single bucket detector. In the device, the function of the liquid crystal device is to modulate the input spectral signal. Besides, the spectral detector is used to obtain the spectral signal of the output.

Fig. 2 is the schematic diagram of spectral reflectance reconstruction system based on liquid crystal modulation. In this system, the input spectral signal (spectral signal of the light source) is used to irradiate the colour block after modulated by the liquid crystal phase retarder, and the reflected spectral signal is obtained by the single bucket detector. In liquid crystal phase retarder, there exist the transparent cells filled with a solution of LC molecules, which functions just like a variable wave plate. The alignment layer in the absence of an applied voltage determines the orientation of the liquid crystal molecules. Voltage that being applied between the electrodes induces birefringence, and the optical retardation is proportional to the induced birefringence [5]. In short, changing the voltage applied to the orientation layer can modulate the input spectral signal. And different amplitude and frequency variation can produce different effects on the final modulation.

Δn is used to represent the changing of the applied voltage of the alignment layer, which can be calculated by formula 4, where n_0 represents the ordinary refraction coefficient, and n_i is the

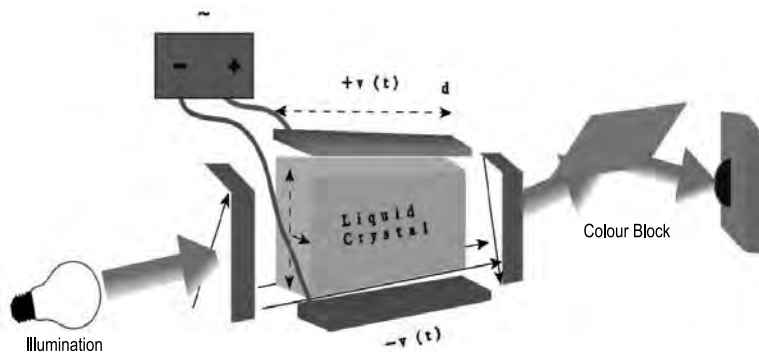


Fig. 2. The follow chart of the method based on liquid crystal modulation

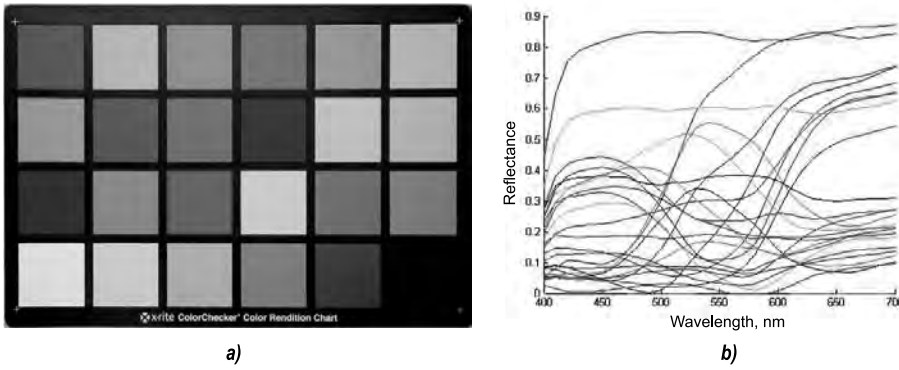


Fig. 3. The RC24 colour charts (a) and their spectral reflectance (b)

extraordinary refraction coefficient. Suppose d is the gap of the given cell, the phase difference in the λ wavelength can be computed by formula 5. In formula 5, λ is the wavelength and η_i is the correspondingly phase difference.

$$\Delta n_i = n_i - n_0, \tag{4}$$

$$\eta_i = (2 \cdot \pi \cdot \Delta n_i \cdot d) / \lambda. \tag{5}$$

In the method of spectral reflectance reconstruction based on agile spectrum imaging system, the modulation matrix is modulated by sine decomposition. But in the method based on liquid crystal modulation, the modulation matrix is proportional to the square of the sine function. Formula 6 express the relationship between the modulation matrix P_i and the phase difference η_i .

$$P_i(\lambda) \propto \sin^2(\eta_i(\lambda)/2). \tag{6}$$

As a result, the modulation matrix P_i can be expressed in formula 7. P_i is a $M \times N$ matrix, where M is the modulation frequency and N is the sampling times (see eqn. 7).

The equation for reconstructing spectral reflectance is shown in formula 8.

$$P = \begin{bmatrix} \sin^2\left(\frac{1}{2}\eta_1(\lambda_1)\right) & \dots & \sin^2\left(\frac{1}{2}\eta_1(\lambda_N)\right) \\ \vdots & \sin^2\left(\frac{1}{2}\eta_i(\lambda_j)\right) & \vdots \\ \sin^2\left(\frac{1}{2}\eta_M(\lambda_1)\right) & \dots & \sin^2\left(\frac{1}{2}\eta_M(\lambda_N)\right) \end{bmatrix}. \tag{7}$$

$$\hat{R} = pinv(S_2 M) \cdot D_2, \tag{8}$$

where S_2 is spectral power distribution of light source, M represents the modulation matrix, D_2 is the value obtained by a single bucket detector, and $pinv$ represents calculating the pseudo inverse of the matrix.

3. Simulation experiment

The two spectral reflectance reconstruction methods mentioned above is simulated in the simulation experiment. And the experimental object that we adopted is the GretagMacbech company 24 colour charts of Colour Checker RC (hereinafter referred to as RC24). Colour charts RC24 contains the common colour of the natural world, which are almost the most commonly used samples in optical experiments. Fig. 3(a) is the RC24 colour charts and Fig. 3(b) is the spectral reflectance of them.

The same light sources modulated by different methods can produce different effect. In the final analysis, the difference between the two modulation methods is the modulation matrix. In the method based on agile spectrum imaging, the matrix is accord with sine function. But in the method based on liquid crystal modulation, the modulation matrix is proportional to the square of the sine function. Besides, the generated wave-

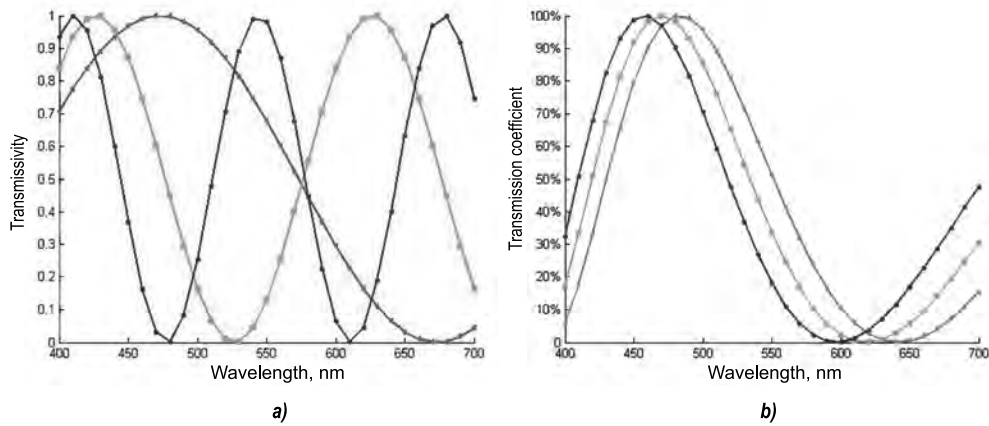


Fig. 4. The modulation matrixes of the two methods

form of these two matrix modulation methods is not the same. Fig. 4 shows the different waveforms generated using different modulation matrices. The horizontal coordinates in Fig. 4 (a) and 4 (b) all express wavelength, which is limited in 400~700nm, the vertical coordinate represents

spectral transmission coefficient. In this experiment, the 400~700nm of the visible light is adopted as the experiment object, which interval is 10nm.

Figs. 4(a) and 4(b) show the single wavelength modulation function of the spectral reflectance

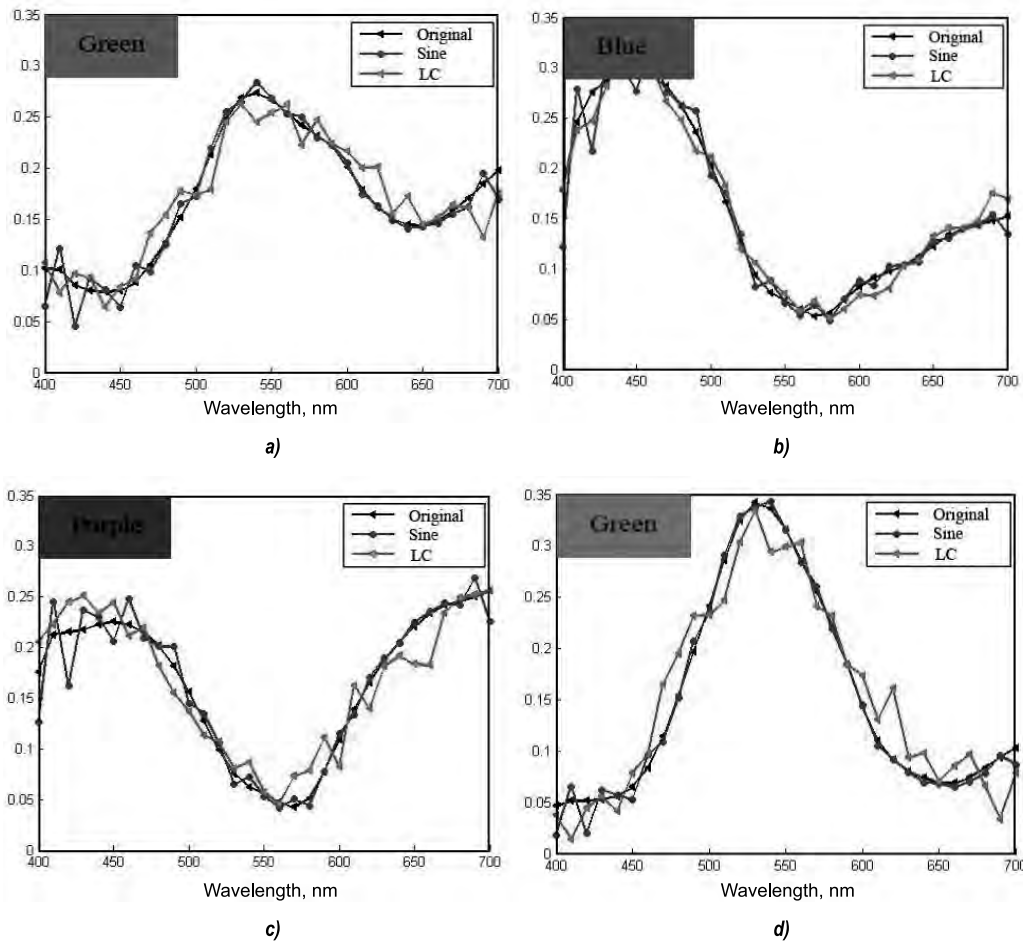


Fig. 5. Examples of the reconstruction of spectral curves of RC24 colour charts: (a) fourth colour chart; (b) the eighth colour chart; (c) the tenth colour chart; (d) the fourteenth colour chart

reconstruction method based on agile spectrum imaging (a) and liquid crystal modulation (b) respectively. It can be seen that the cycles of 3 sine modulation curves in Fig. 4(a) are different. But in Fig. 4(b), the cycles of the 3 single wavelength modulation curves are almost identical, and the cycle has increased trend with the increase of wavelength.

Fig.5 shows some spectral reconstruction results of RC24 colour charts, which are modulated by those two methods. Figs. 5(a), 5(b), 5(c) and 5(d) represent the spectral reflectance reconstruction effect graphs of the fourth, eighth, tenth and fourteenth colour charts of RC24 colour charts respectively. And in Fig.5, the black curve is the original spectral reflectance, the blue one is the spectral reflectance, which is modulated by agile spectrum imaging. Similarly, the last red one is the spectral reflectance, which is reconstructed by the method based on liquid crystal modulation. The horizontal coordinate of Fig. 5 is wavelength which is limited in 400~700nm, and the vertical coordinate represents the reflectance.

From all the pictures in Fig. 5, it can be seen that the reconstruction effect of the method based on agile spectrum imaging is much better than the method based on liquid crystal modulation. Especially in the wavelength of 450~700nm, the reconstructed spectral reflectance curves of the method based on agile spectrum imaging are almost coincident with the original spectral reflectance. On the comparison, the reconstruction effect of the method based on liquid crystal modulation is a little worse, which has the larger fluctuation amplitude with the original spectral reflectance. But for 450~700nm, the reconstruction effect is not good enough. Error is mainly concentrated in this range of wavelength even for the method based on agile spectrum imaging, which has excellent spectral reflectance reconstruction effect in range of wavelength 450~700nm.

As for the evaluating indicators, in this study, colour difference, Root Mean Square Error and the Spectral Goodness of Fit Coefficient are adopted to compare the spectral reconstruction methods mentioned above. And the colour difference is evaluated from the chroma aspects. Moreover, Root Mean Square Error and the Spectral Goodness of Fit Coefficient are evaluated from the view of spectrum.

3.1. Comparison of colour difference

As the most commonly used spectral reflectance reconstruction method, colour difference [8–11] is well-known, and it is also used as an index to evaluate the above two methods. In this paper, the CIE1976 colour difference formula is used to calculate the colour difference. In formula 9, ΔE_{ab}^* represents the colour difference and ΔL represents the luminance difference. As for a , the positive direction of a represents red, the negative direction of a represents green. At the same time, the positive direction of b represents yellow, and the negative represents blue.

$$\Delta E_{ab}^* = \sqrt{(\Delta L)^2 + (\Delta a)^2 + (\Delta b)^2} \quad (9)$$

The analysis results of colour difference are shown in Table 1. The reconstructed spectral reflectance \hat{R} and the original spectral reflectance R are compared under D50, D65 [12] and standard A light source. Some conclusions can be contained from the results of Table 1:

- Whether it is under D50, D65 light source or standard A light source, the average, maximum and the standard deviation of colour difference of the reconstruction method based on agile spectrum imaging are all the smallest.
- Colour difference of original spectral reflectance and the reconstructed spectral reflectance based on liquid crystal modulation method is slightly larger than that of the agile spectrum imaging method.
- The average colour differences of the two reconstruction methods are all less than 3, which is acceptable.

Under D50 light source, the average colour differences of RC24 colour charts computed by the above two spectral reconstruction methods are shown in Fig. 6. In Fig. 6, the histogram represents colour difference of the spectral reflectance reconstruction method based on agile spectrum imaging, which is limited in 0–0.9, and its value is far less than 3. The grey line graph represent colour difference generated by the method based on liquid crystal modulation. Although the maximum colour difference is 10, but the minimum colour difference is less than 1, and we can see that the average value is about 2.9 from Table1.

Table 1. Colour difference under different light sources

Methods	ΔE_{ab}^* Under D50			ΔE_{ab}^* Under D65			ΔE_{ab}^* Under SA		
	Max	Mean	Std.	Max	Mean	Std.	Max	Mean	Std.
Sine	0.7953	0.5326	0.1810	0.8733	0.5991	0.2032	0.6551	0.4236	0.1299
Liquid Crystal	10.3731	2.9113	2.3140	14.0966	2.9062	2.8605	6.7783	2.8601	1.9055

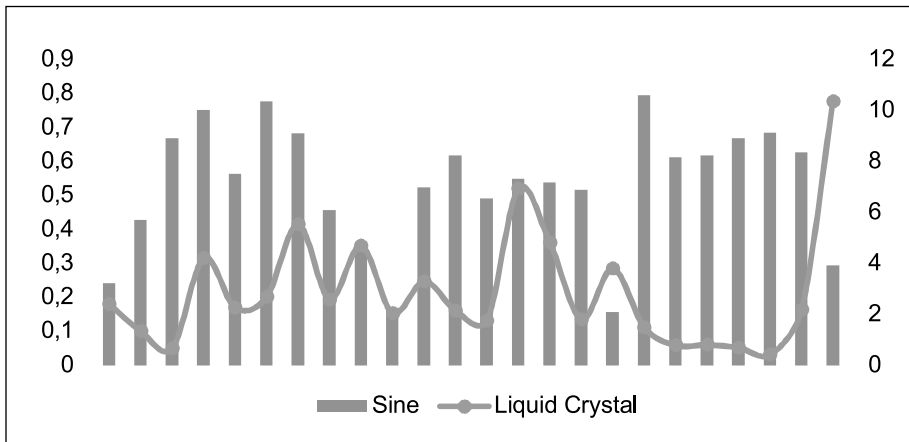


Fig.6. Mean colour difference of the two methods

3.2. Comparison of Root Mean Square Error

Root Mean Square Error [13–16] is used to do a quantitative analysis of the effect of modulation and reconstruction. The reconstructed spectral reflectance is closer to the original spectral reflectance if the Root Mean Square Error is near to 0. And the calculation formula is shown in formula 10. In formula 10, R represents the original spectral reflectance of RC24 colour charts, and \hat{R} is the spectral reflectance reconstructed by different methods. N is the dimension of spectral reflectance and in this simulation experiment $N = 31$.

$$RMSE = \sqrt{\frac{\sum (R - \hat{R})^T (R - \hat{R})}{N}} \tag{10}$$

The average, maximum and standard deviation value of Root Mean Square Error calculated by formula 10 of the two different modulation methods are listed in Table 2. In Table 2, sine represents the spectral reflectance reconstruction method based on agile spectrum imaging and liquid crystal represents the method based on liquid crystal modulation. It can be seen in Table 2, whether it is the average, maximum or standard deviation value of Root Mean Square Error, the values for method based on liquid crystal modulation is larger than for the method based on agile spectrum imaging for all parameters. That indicates the reconstruction effect of this method is worse.

Root Mean Square Error of RC24 colour charts reconstructed by the two methods mentioned above are shown in Fig. 7, which varies from 0 to 0.09. In Fig. 7, the bar graph represents the method base on liquid crystal modulation,

Table 2. RMSE comparison of two methods

Methods	RMSE		
	Mean	Max.	Std.
Sine	0.0142	0.0190	0.0032
Liquid Crystal	0.0269	0.0782	0.0190

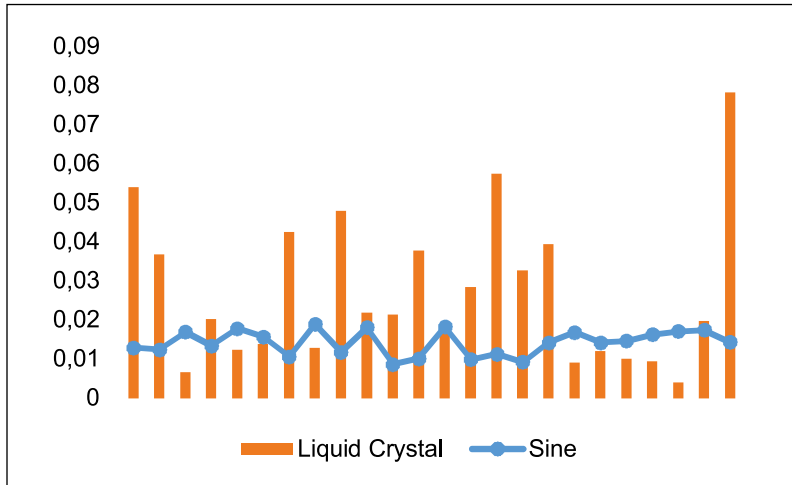


Fig.7. Mean RMSE of the two methods

and the grey polyline is the method based on agile spectrum imaging. Even though for some colour charts such as the third, fifth, eighteenth to twenty-second, the Root Mean Square Error of the method based on agile spectrum imaging are larger than the method based on liquid crystal modulation. But overall, the Root Mean Square Error of RC24 colour charts produced by the method based on agile spectrum imaging are uniform, which range is 0.01 to 0.02 and smaller than the method based on liquid crystal modulation.

It can be concluded from Table 2 and Fig. 7 that the spectral reflectance reconstruction method based on agile spectrum imaging is better than the method based on liquid crystal modulation from the aspect of Root Mean Square Error.

The causes of different Root Mean Square Error of the two methods are analyzed from the aspect of different modulation matrix. Through the calculation of software, the modulation matrix of the method based on agile spectrum imaging is full rank, but the method based on liquid crystal is not. And the pictures of the two modulation matrixes are shown in Fig. 8. Fig. 8 (a) and

8 (b) represent the modulation matrixes of the method based on agile spectrum imaging and the method based on liquid crystal modulation respectively. The horizontal coordinates express the wavelength which range is 400~700nm. And vertical coordinate in Fig. 8(a) is time, but it is sampling times in Fig.8 (b). In Fig. 8, different colours represent different values, which can be seen in the colour bar in the right of the two pictures. The differences of the two modulation matrixes can be intuitively seen in Fig. 8. The colour distribution of Fig. 8 (a) is more complex which indicates the values are more random. But in Fig. 8 (b), the values in the range of 0.4 to 0.5 have a ring distribution around the lower right corner. And the values are larger than 0.6 and are smaller than 0.1 appear a cross distribution, the distribution is more uniform and regular that indicates the worse randomness.

Numerical value and corresponding number of the two modulation matrixes are shown in Fig. 9. Fig. 9 (a) represents spectral reflectance reconstruction method based on agile spectrum imaging, and Fig. 9 (b) represents the method

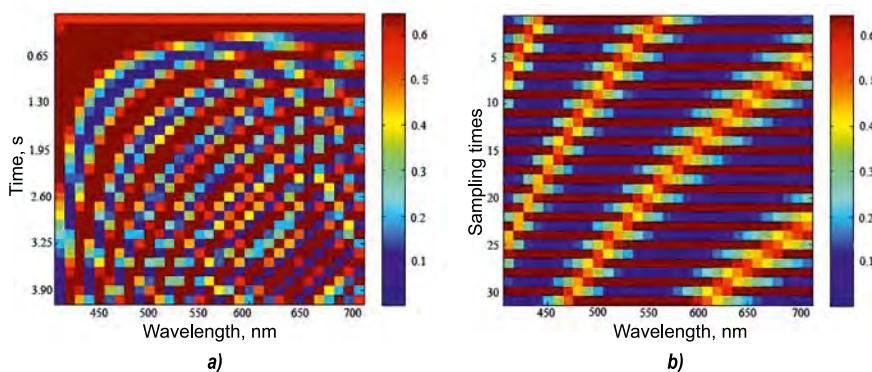


Fig. 8. The two modulation matrixes:
(a) – the modulation matrix of the method based on agile spectrum imaging (b) – the modulation matrix of the method based on liquid crystal modulation

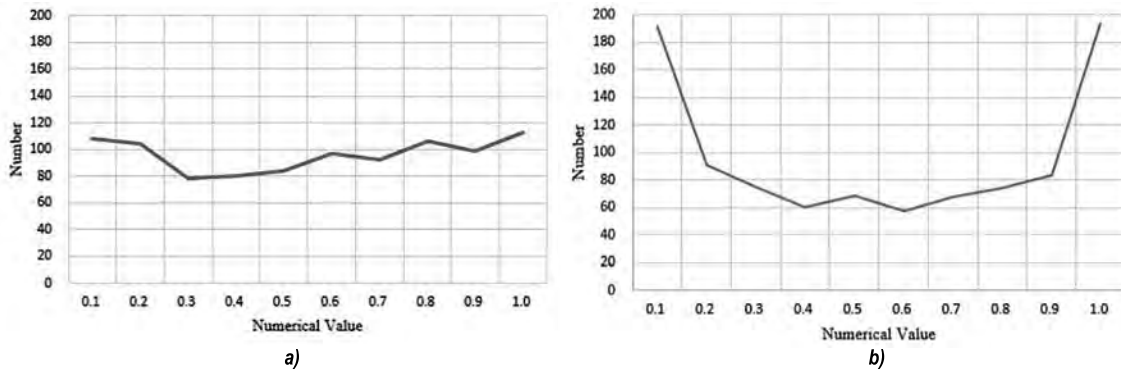


Fig. 9. The numerical values of two modulation matrixes: (a) the modulation matrix of the method based on agile spectrum imaging; (b) the modulation matrix of the method based on liquid crystal modulation

based on liquid crystal modulation. Here, horizontal ordinate represents the numerical value, and longitudinal coordinates represent the number of times that appear in the matrix. It is shown in Fig. 9 (a), that the occurrences of all the values are limited nearly in 80 –120. In the modulation matrix of the method based on liquid crystal modulation, the occurrence of 0.1 and 1 are higher, nearly 200 times, and the fluctuation range of its values is 40~200. It can be seen from Figs. 8 and 9 that the modulation matrix of the method based on agile spectrum imaging is more random. As a result, the Root Mean Square Error of this method is smaller than that of the method based on liquid crystal modulation.

3.3. Comparison of Spectral Goodness of Fit Coefficient

Spectral Goodness of Fit Coefficient (SGFC) [17] is another index to measure the effect of spectral reflectance reconstruction, which is short for SGFC. The more accuracy of SGFC is close to 1, the precision of reconstruction is the higher. SGFC of spectral reconstruction method could reach 99 %, which is considered that the reconstruction effect is acceptable. When the SGFC of spectral reflectance reconstruction is reaching 99.99 % and above, reconstruction effect is won-

derful. The expression of SGFC is shown in formula 11. Here, R_λ and \hat{R}_λ respectively represent the original spectral reflectance and reconstructed reflectance. And \sum represents sum all the numerical values up.

$$SGFC = \frac{\left| \sum_{\lambda} R_{\lambda} \hat{R}_{\lambda} \right|}{\sqrt{\sum_{\lambda} R_{\lambda}^2} \sqrt{\sum_{\lambda} \hat{R}_{\lambda}^2}} \quad (11)$$

The maximum, minimum and average values of SGFC of the two reconstruction methods based on agile spectrum imaging and liquid crystal modulation are list in Table.3. It can be seen from Table. 3 that the average and the minimum of SGFC of the method based on agile spectrum imaging are both larger than the method based on liquid crystal modulation. But the maximum SGFC of the method based on liquid crystal modulation is slightly larger than that of the method based on agile spectrum imaging. For the spectral reflectance reconstruction method based on agile spectrum imaging, the maximum, the minimum and the average of SGFC is all larger than 0.99, and it reaches the requirement of reconstruction accuracy. But the average SGFC of the reconstruction method based on liquid crys-

Table 3. SGFC comparison of two methods

Methods	SGFC		
	Mean	Max.	Min.
Sine	0.9967	0.9988	0.9944
Liquid Crystal	0.9834	0.9998	0.9053

tal modulation is only about 0.98, and its minimum value is about 0.9, which shows the SGFC of the method based on liquid crystal modulation is poor. Thus, from the aspect of SGFC, just as analyzed above, the effect of the spectral reflectance reconstruction based on agile spectrum imaging is better than the method based on liquid crystal modulation.

4. CONCLUSION

Spectral reflectance reconstruction is now widely used in all professions and trades, and it is very important to choose a good reconstruction method. In this paper, the spectral reflectance reconstruction method based on the liquid crystal modulation and the method based on agile spectrum imaging are compared and analyzed. The two methods are compared from three indexes: colour difference, the Root Mean Square Error and the Spectral Goodness of Fit Coefficient. From the view of chromatics, colour difference is a good way to show us the advantages and disadvantages of the spectral reflectance reconstruction methods, and other two kinds of indexes are used to analyze it from the angle of spectrum. On the one hand, the maximum, mean and standard deviation of the colour difference of the method based on agile spectrum imaging are the smallest. On the other hand, for Root Mean Square Error, the maximum and standard deviation of the spectral reflectance reconstruction method based on agile spectrum imaging are also the smallest. Analyzed from the view of Spectral Goodness of Fit Coefficient, the conclusion is the same. In summary, the spectral reflectance reconstruction method based on agile spectrum imaging is better than the method based on liquid crystal modulation, and it can be widely used in spectral reflectance reconstruction.

5. ACKNOWLEDGMENTS

This study is supported by the National Natural Science Foundation of China (Grant No. 61405115), the Natural Science Foundation of Shanghai (Grant No. 14ZR1428400), and the Innovation Project of Shanghai Municipal Education Commission (Grant No. 14YZ099), National Basic Research Program of China (973 Program) (Grant No. 2015CB352004).

REFERENCES

1. Barakzahi M, Amirshahi S H, Peyvandi S, et al. Reconstruction of total radiance spectra of fluorescent samples by means of nonlinear principal component analysis[J]. *Journal of the Optical Society of America A Optics Image Science & Vision*, 2013, 30(9):1862–70.
2. Kim B G, Werner J S, Siminovitich M, et al. Spectral Reflectivity Recovery from Tristimulus Values Using 3D Extrapolation with 3D Interpolation[J]. *Journal of the Optical Society of Korea*, 2014, 18(5):507–516.
3. Funamizu H, Shimoma S, Yuasa T, et al. Effects of spatiotemporal averaging processes on the estimation of spectral reflectance in color digital holography using speckle illuminations[J]. *Applied Optics*, 2014, 53(30):7072–80.
4. Lin M C, Tien C H. Spectral image reconstruction by a tunable LED illumination[J]. *Proc SPIE*, 2013, 8870(5):441–443.
5. August Y, Stern A. Compressive sensing spectrometry based on liquid crystal devices[J]. *Optics Letters*, 2013, 38(23):4996–9.
6. Zhang L, Liang D, Li B, et al. Study on the key technology of spectral reflectivity reconstruction based on sparse prior by a single-pixel detector[J]. *Photonics Research*, 2016, 4(3).
7. Bian L, Suo J, Situ G, et al. Multispectral imaging using a single bucket detector[J]. *Physics*, 2015, 6.
8. Zhang L, Liang D, Pan Z, et al. Study on the key technology of reconstruction spectral reflectance based on the algorithm of compressive sensing[J]. *Optical & Quantum Electronics*, 2014, 47(7):1–14.
9. Amiri M M, Amirshahi S H. A hybrid of weighted regression and linear models for extraction of reflectance spectra from CIEXYZ tristimulus values[J]. *Optical Review*, 2014, 21(6):818–825.
10. Zhang L, Liang D, Li B, et al. The study of key technology on spectral reflectance reconstruction based on the algorithm of adaptive compressive sensing[J]. *Laser Physics*, 2016, 26(4):045201.
11. Raju Shrestha, Jon Yngve Hardeberg, Alamin Mansouri. One-shot multispectral color imaging with a stereo camera[J]. *Digital Photography VII*, 2011, 7876:298–306.
12. Wu Guang Yuan, Liu Zhen, Zhang Jian Qing. Spectral colour reproduction from CIE tristimulus values using a node address array selection technique[J]. *Image Processing and Pattern Recognition*, 2015, 8(9):141–150.
13. Chen S, Ong Y H, Lin X, et al. Optimization of advanced Wiener estimation methods for Raman reconstruction from narrow-band measurements in the presence of fluorescence background[J]. *Biomedical Optics Express*, 2015, 6(7):2633–48.

14. Agahian F, Funt B. Outlier modelling for spectral data reduction[J]. Journal of the Optical Society of America A Optics Image Science & Vision, 2014, 31(7):1445–52.

15. Yoo Ji-Hoon, Kyung Wang-Jun, Ha Ho-Gun. Estimation of reflectance based on properties of selective spectrum with adaptive Wiener estimation[J]. Proc Spie, 2013, 8652(2):86520–86527.

16. Chen S, Lin X, Yuen C, et al. Recovery of Raman spectra with low signal-to-noise ratio using Wiener estimation[J]. Optics Express, 2014, 22(10):12102–14.

17. Kandi S. Gorji. Representing Spectral Data Using Lab PQR Color Space in Comparison with PCA Method[J]. 2011, 4:95–106.



Leihong Zhang,

Dr., Associate Professor. He is a teacher in University of Shanghai for Science and Technology. The main research contents are spectral reflectance reconstruction based

on compressed sensing algorithm, correlation imaging algorithm and hyper spectral reconstruction algorithm



Bei Li

After graduating from QuFu Normal University, she went to University of Shanghai for Science and Technology. As a graduate student, her main research interests are spectral reflectance reconstruction and single bucket detector



Haojun Zhang, Dr.

He is a senior engineer in Shanghai radio equipment research institute. His main research contents are laser active imaging system and composite detection system. And he also hosts four national projects



Yi Kang

is graduated from the QuFu Normal University. He is studying at University of Shanghai for Science and Technology. Currently he is conducting research on the ghost imaging and compressive sensing



Wenjie Zhan

is graduated from the Chizhou University. He is studying at University of Shanghai for Science and Technology. His main research contents are ghost imaging and spectral reflectance reconstruction



Wenjuan Yi, Bachelor.

At present, she is in University of Shanghai for science and technology with main research direction: spectral reflectance reconstruction based on compressed sensing algorithm, principal component analysis (PCA)



Zhiwen Chen, Bachelor.

After graduating from Qibao high school, she went to University of Shanghai for science and technology. She is major in Printing Engineering and spectral reflectance reconstruction

DESIGN AND IMPLEMENTATION OF OPTICAL RECEIVER FOR VISIBLE LIGHT COMMUNICATION TO REDUCE AMBIENT LIGHT NOISE

Kadirvel Sindhubala* and Baba Vijayalakshmi

ECE Department, B.S. Abdur Rahman University, Chennai, India

**E-mail: sindhumtech@yahoo.com*

ABSTRACT

In the recent years, visible-light communication (VLC) has engrossed amount of researchers as for power conservation and the new archetype in the field of optical wireless communication. However, ambient light noise due to indirect sunlight and fluorescent light is a major concern that affects the performance of the communication system in an indoor environment. This paper develops a project to design and implement new optical receiver for visible light communications (VLC) to reduce the ambient light noise. Using the proposed experimental system, data rate of 10 Kbps and a distance of 0.40 m is achieved between the transmitter and receiver.

Keywords: ambient light noise, fluorescent light, indirect sunlight, optical receiver, visible-light communication (VLC)

1. INTRODUCTION

In the future, traditional home and office lighting will soon be replaced by longer life time, low power consuming, and health hazardless light emitting diode (LED) devices. The fast switching capability of LED devices makes it possible to transmit huge amounts of data at high speed. Thus LED can be used for both illumination and communication purpose. This technology is called visible-light communication (VLC). VLC technologies are identified as supplement technology for radio frequency (RF) based communication used

in critical environment like hospitals, underwater communications etc. [1–4].

One of the main challenges existing in the VLC system is the ambient light noise from the sunlight and other artificial light sources contributed at the receiver side. In an indoor environment, the ambient light noise sources include indirect sunlight and fluorescent lamps driven by conventional ballast. Hence ambient light noise reduction technique is necessary to reduce the in band interference that occurs from other lighting sources and to improve the performance of the communication system.

Earlier methods use optical filter, low pass filter, high pass filter, etc. [5–8] to reduce the ambient light, but it does not mitigate the noise completely and it still affects the performance of the communication system. Wavelet neural network, adaptive filtering, wavelength filtering, OFDM also reduces the ambient light noise but the optical receiver structure is complex [9–12]. Miller code, Filter based sensor array has also been used previously to reduce the noise, but no practical experimentation is performed [13–14]. Hence the VLC receiver structure designed must be simple, low cost, it must improve the performance of the communication system and it must have the potential to reduce the ambient light noise in the indoor environment.

In our proposed method, two photodiodes with the trans-impedance amplifier are arranged in such a way photodiode1 receives the transmitted signal and ambient light whereas photodiode2

is placed on the opposite side at an angle of 180° , it receives only the ambient light. Difference amplifier is used in the next stage to mitigate the ambient light noise and recover back the received signal with the reduction of ambient light noise. Hence it reduces the cost, simple to implement, efficient noise reduction when compared to the existing methods.

The paper is structured as the following sections; Section 2 describes the proposed indoor VLC system with the ambient light noise reduction technique. In section 3, the testing and the results of the transmission link are discussed. Finally, section 4 concludes the paper.

2. SYSTEM DESCRIPTION OF PROPOSED INDOOR VLC SYSTEM

VLC systems primarily consist of transmitter and receiver. Line of sight (LOS) channel model is preferred between the transmitter and receiver. Fig.1. shows the overall block diagram of the proposed VLC system with the ambient light noise reduction.

2.1. Transmitter design

LM555 timer is used to produce the OOK signals of 10 kHz. On-Off keying (OOK) modulation is chosen because of its simplicity and reduced power consumption compared to other modulation schemes. The LED driver takes the input signal and drives the white LED. The LED driver consisting of resistor prevents the high current flowing through the white LED. We have used 1W high power white LED of forward current 0.35A and viewing angle 90° , and light intensity of 80 lm. Thus the input electrical signal is con-

verted into the optical signal in the transmitter stage. Fig.2. shows the circuit diagram of the proposed VLC transmitter.

2.2. Line of sight (LOS) channel

In this proposed work, the LOS wireless channel is considered between the transmitter and receiver. LOS Channel DC gain for the LED source [15] is given by

$$H(0) = \begin{cases} \frac{A(m+1)}{2\pi d^2} \cos^m(\varnothing) \cos(\psi), & 0 \leq \psi \leq \psi_c \\ 0 & \psi > \psi_c \end{cases}, \quad (1)$$

where d is the distance between the transmitter and receiver, ψ_c is the angle of incidence with respect to the receiver axis, \varnothing is the FOV of the receiver.

The received power is given by

$$P_r = H(0) \cdot P_i, \quad (2)$$

where $H(0)$ is the DC channel gain and P_i is the transmitted optical power of LED source.

2.3. Receiver design

The proposed, VLC receiver design employs two commercially available low cost monolithic photodiode and single supply trans-impedance amplifier (OPT101) of 0.09×0.09 inch cell with maximum responsivity at 650nm.

- OPT101–1: for detecting the optical signal and ambient light noise;

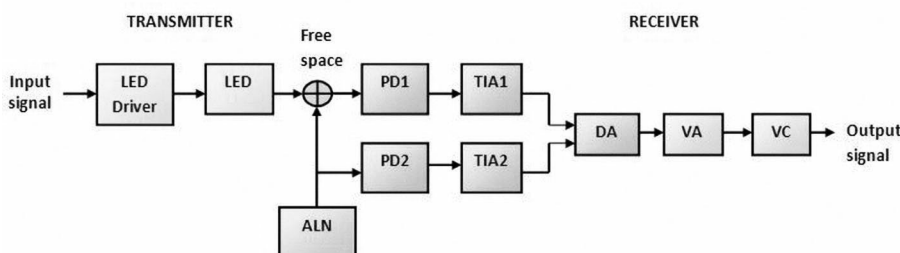


Fig.1. Block diagram of the proposed indoor VLC system with the ambient light noise reduction
 ALN: Ambient light noise PD; Photodiode TIA; Trans-impedance amplifier DA; Difference amplifier VA;
 Voltage amplifier VC; Voltage comparator

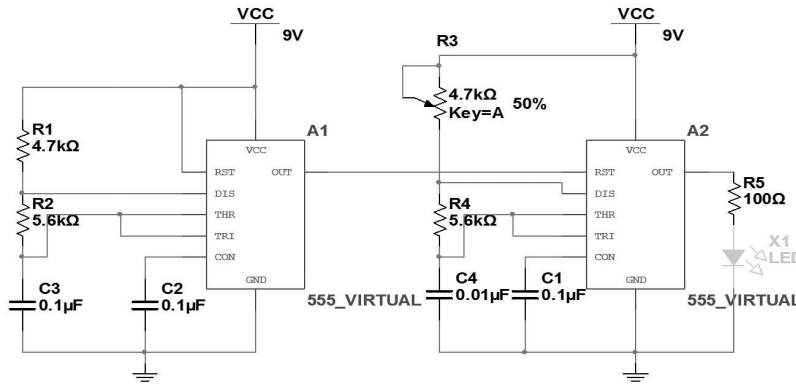


Fig.2. Circuit diagram of proposed VLC transmitter

- OPT101–2: detecting the ambient light noise.

The arrangement of OPT101–1 and OPT101–2 is kept in such a way no transmitted signal falls on the OPT101–2 and it detects only the ambient light. These two are kept opposite to each other at an angle of 180°. The photodiode converts the received optical signal into electrical signal. TIA converts the photocurrent produced by the photodiode into voltage. Next stage is the difference amplifier, which mitigates the ambient light noise. The received signal is weak at this stage. Hence it is amplified using voltage amplifier. Finally the signal is sent through the voltage comparator to reconstruct the digital signal. Voltage amplifier, difference amplifier, and voltage comparator is implemented using LM324 quadruple operational amplifier. LM324 is chosen due to four op-amps in a single package, wide bandwidth of 1 MHz and large DC voltage gain of 100 dB. Fig.3 shows the block diagram of the proposed VLC receiver with the ambient light noise reduction circuit.

2.3.1. Mathematical analysis

The photocurrent produced at the photodiode1 (PD1) is given by the eq. (3)

$$I_{PD1} = I_s + I_n, \tag{3}$$

where I_s is the photocurrent due to LED signal and I_n is the photocurrent due to indirect sunlight and fluorescent lamp.

$$I_s = R \cdot P_i, \tag{4a}$$

$$I_n = R \cdot P_n, \tag{4b}$$

where R is the responsivity of the photodiode1 (PD1), P_i the input optical power of the LED and P_n is the ambient light noise power.

Trans-impedance amplifier1 (TIA1) converts the photocurrent produced from PD1 into voltage. The output voltage produced at the TIA1 stage is given by eq. (5)

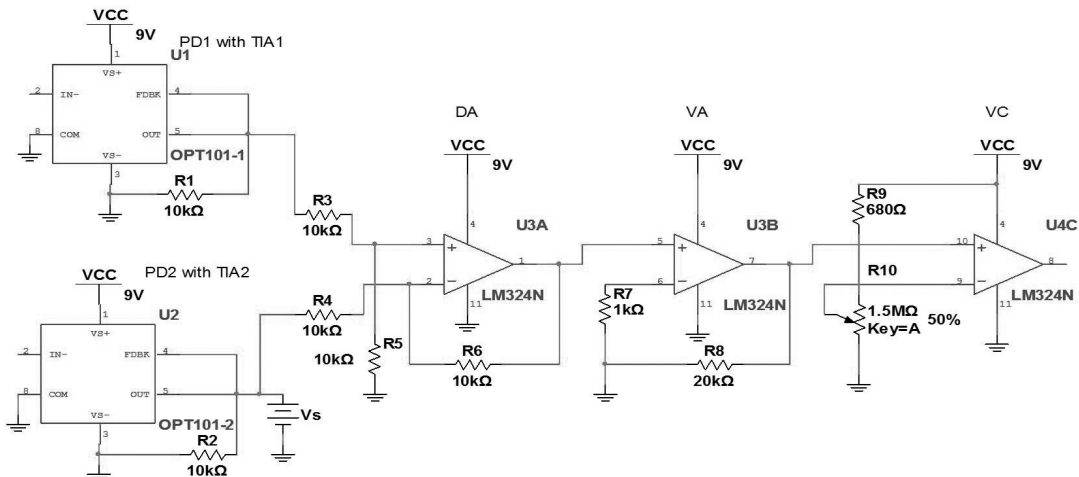


Fig.3. Circuit diagram of proposed VLC receiver

$$V_{out1} = R_f \cdot I_{PD1}, \quad (5)$$

where R_f is the feedback resistance and I_{PD1} is the photocurrent produced at the PD1.

The photocurrent produced at the photodiode2 without the input signal is given by the eq. (6)

$$I_{PD2} = I_n, \quad (6)$$

where I_n is the photocurrent produced due to indirect sunlight and fluorescent lamp inside the indoor environment.

$$I_n = R \cdot P_n, \quad (7)$$

where R is the responsivity of the photodiode2 (PD1) and P_n is the ambient light noise power.

Trans-impedance amplifier (TIA2) converts the photocurrent produced at PD2 into voltage. The output voltage produced at the TIA2 stage is given by eq. (8)

$$V_{out2} = R_f \cdot I_{PD2}, \quad (8)$$

where R_f is the feedback resistance and I_{PD2} is the photocurrent produced at the PD2.

The difference amplifier is used to reduce the ambient light noise and helps to restore back the original signal. The output voltage produced at the difference amplifier stage is given by eq. (9)

$$V_{DA} = V_{out1} - V_{out2}, \quad (9)$$

$$V_{DA} = R_f \cdot I_{PD1} - R_f \cdot I_{PD2}, \quad (10)$$

$$V_{DA} = R_f \cdot I_s + I_n - R_f \cdot I_n, \quad (11)$$

$$V_{DA} = I_s \cdot R_f, \quad (12)$$

Voltage amplifier is used to amplify the signal received from the difference amplifier (DA) stage. The output voltage at the voltage amplifier stage is given by eq. (13)

$$V_{VA} = A_v (V_{DA}) \quad (13)$$

Where A_v the voltage is gain and V_{DA} is the voltage at the DA stage.

Thus the transmitted OOK signals are recovered back at the receiver side using a voltage comparator with the mitigation of optical background noise sources such as indirect sunlight and conventional fluorescent lamp operating at 50 Hz in indoor environment.

3. EXPERIMENTATION AND RESULTS

The experimentation is carried out inside the electronics laboratory of B.S. Abdur Rahman University to characterize the performance of an indoor VLC system. The tests are conducted with indirect sunlight coming through the windows and fluorescent light driven by conventional ballast is turned on. The experiment is carried out at the input frequency of 10 kHz and communication distance of 0.40m is achieved between the transmitter and receiver. The results are discussed in the subsequent section (Figs 4-10).

The OOK signals are transmitted via white LED where the electrical signal is converted into an optical signal. Fig.4a and Fig.4b represents the time-domain waveform and spectrum of the input signal. The optical signal is transmitted using the free space channel and the OPT101-1 detects the optical signal and the surrounding ambient light Fig.5a and Fig.5b. shows the time-domain waveform and spectrum of the OPT101 signal. OPT101-1 converts the optical signal from LED and ambient light into corresponding voltage. In an indoor environment considered, the ambient light noise sources are from indirect sunlight and fluorescent light lamps operated by conventional ballast. The indirect sunlight induces strong direct current (DC) and the rectified sine wave form is emitted from the fluorescent light lamp operated by conventional ballast. Thus, ambient light noise reduction technique becomes essential to reduce this ambient light noise.

Hence another OPT101-2 is used on the opposite side of OPT101-1 at an angle of 180° to track the ambient light induced on OPT101-1. The arrangement must be such that both the OPT101 must track the same amount of ambient light. In our case, the room in which the experiment is carried out OPT101-1 tracks more ambient light compared to OPT101-2 and the sunlight is a time varying component, hence the DC source is used at the output of OPT101-2 to make the tracking levels of ambient light equal.

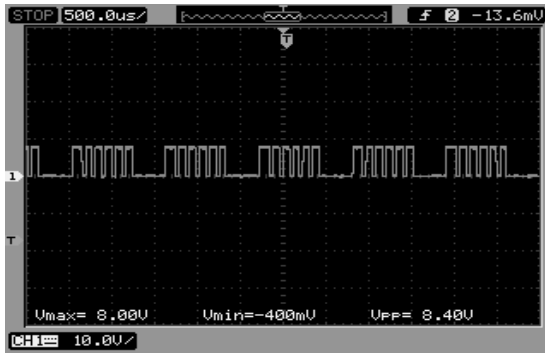


Fig.4a. Time-domain waveform of the input signal

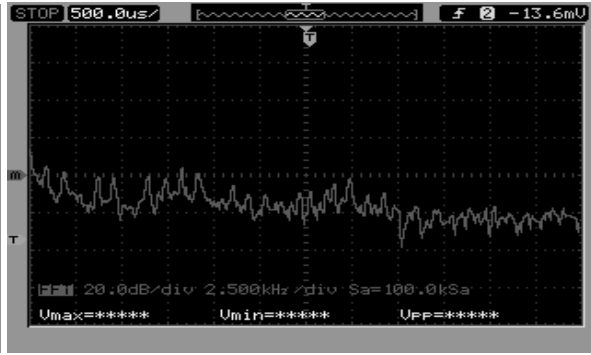


Fig.4b. Spectrum of the input signal



Fig.5a. Time-domain waveform of the OPT101-1 signal

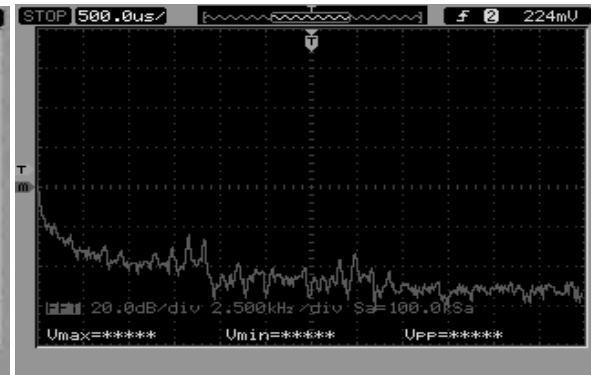


Fig.5b. Spectrum of the OPT101-1 signal



Fig.6a. Time-domain waveform of the OPT101-2 signal

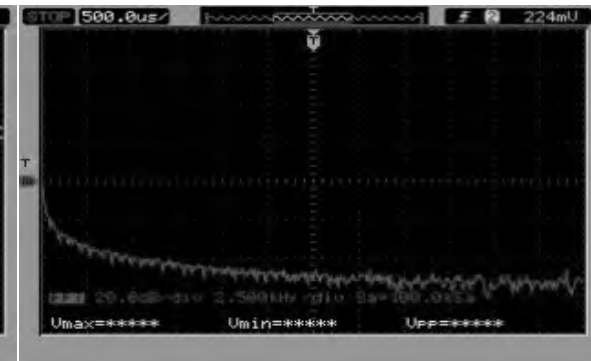


Fig.6b. Spectrum of the OPT101-2 signal

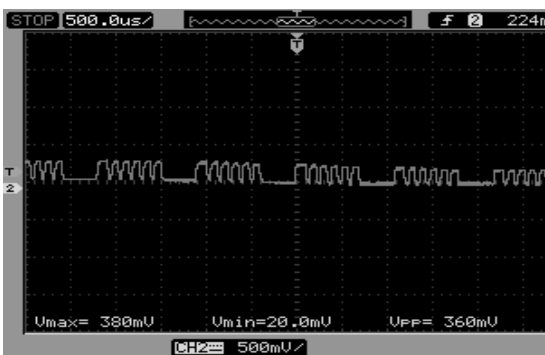


Fig.7a. Time-domain waveform of the difference amplifier signal



Fig.7b. Spectrum of the difference amplifier signal



Fig.8a. Time-domain waveform of the voltage amplifier signal

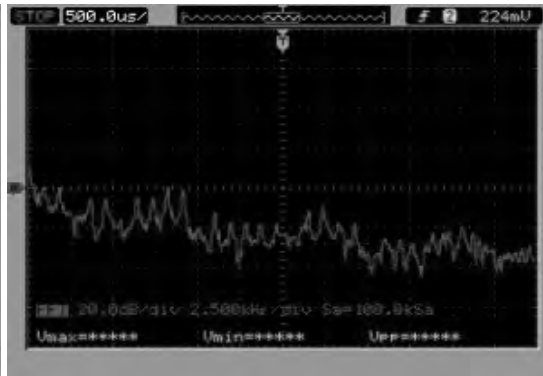


Fig.8b. Spectrum of the voltage amplifier signal



Fig.9a. Time-domain waveform of the voltage comparator signal



Fig.9b. Spectrum of the voltage comparator signal

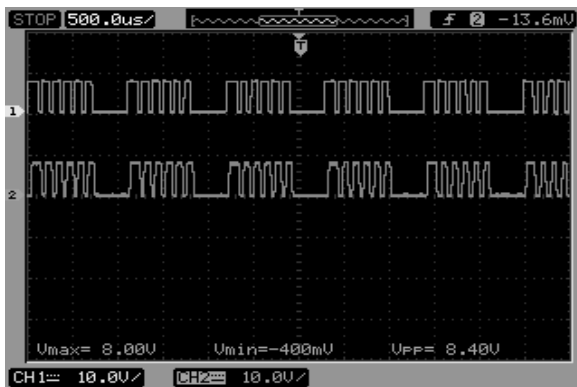


Fig.10a. Time-domain waveform of the input and output signal



Fig.10b. Spectrum of the input signal

Thus, OPT101–2 tracks the voltage of the signal received from ambient light noise. Fig.6a and Fig.6b show the time domain waveform and spectrum of the OPT101–2 signal. Difference amplifier (DA) helps to mitigate the ambient light noise and restore back the received signal. Fig.7a. shows the time domain waveform and spectrum of the difference amplifier (DA) signal.

The signal received is very weak only in the order of mV (360 mV). Hence voltage ampli-

er is used to amplify the weak signal of 360mV to 7.20V signal. Fig.8a and Fig.8b show the time-domain waveform and spectrum of voltage amplifier signal. Voltage comparator is used to convert the amplified signal into digital signal. Fig.9a and Fig.9b show the time-domain waveform and spectrum of voltage comparator signal. Thus the transmitted signal is recovered back at the receiver with the mitigation of ambient light noise. Fig.10a, Fig.10b, Fig.10c show the time-do-

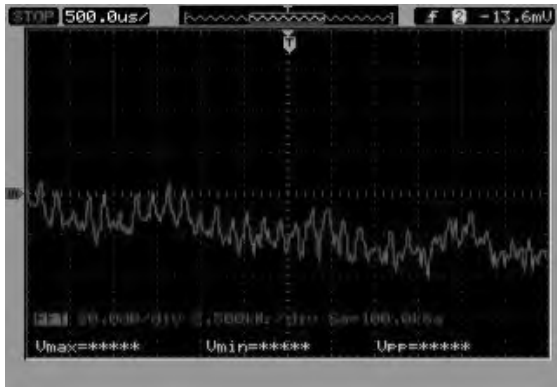


Fig.10c. Spectrum of the output signal

main waveform and spectrum of the input signal and the output signal. Fig.11 shows the experimental indoor VLC system using ambient light noise reduction technique at the receiver side.

Fig.12 shows the graph of the output voltage produced at OPT101-1 with the different vertical distance between the transmitter and receiver. For this measurement, we calculated the performance from 0 to 0.40m distance.

Fig.12 shows that the received output voltage decreases to the increase in distance between the transmitter and receiver.

Fig.13 shows the graph of the optical power of LED with the different vertical distance between the transmitter and receiver up to 0.40m. This measurement was carried out at normal room light condition.

Fig.13 shows that the optical power from LED decreases to the increase in distance between the transmitter and receiver.

In our experimental work, we are restricted by some 0.40m distance because we don't use reflector or magnifying lens and we have used 1W LED with 9V/0.35A supply. However the distance can be further increased by using more number of LEDs, or reflector, or magnifying lens.

4. CONCLUSION

In an indoor environment, ambient light noise from indirect sunlight and fluorescent light degrade the performance of the VLC system. A new optical receiver design for OOK modulation with the ambient light noise reduction is proposed. The design is based on two photodiode with TIA placed opposite to each other at an angle of 180° and difference amplifier to mitigate the ambient light noise. Experimental results show

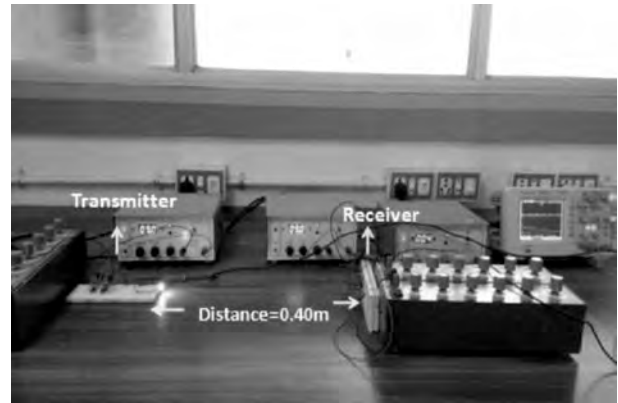


Fig.11. Experimental indoor VLC system using the proposed receiver

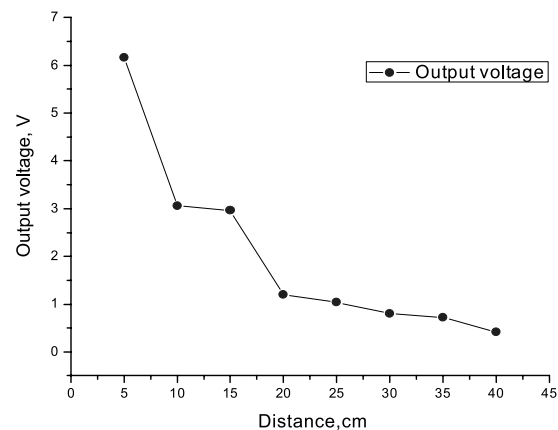


Fig.12. Output voltage produced at the OPT101-1 with the distance

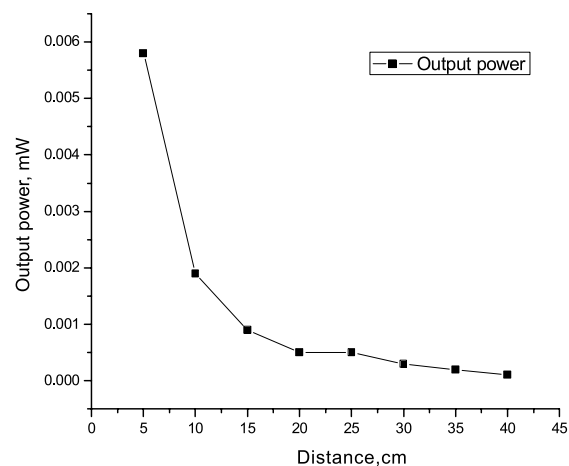


Fig.13. Optical power with the distance

that the proposed VLC receiver is practical and useful to reduce the ambient light noise. The communication distance can be further improved by using more number of high power LEDs, or reflector, or magnifying lens.

REFERENCES

1. Dhatchayeny, D.R., Sewaiwar, A., Tiwari, S.V., Chung, Y. Experimental Biomedical EEG signal Transmission Using VLC. *IEEE sensors journal*, 2015, V15, pp.5386–5387.
2. Cheong, Y.K., Weing, X., YounChung, W. Hazardless Biomedical sensing Data Transmission Using VLC. *IEEE sensors journal*, 2013, V13, pp.3347–3348.
3. Asada, H.H., Rust, I.C. A dual-use visible light approach to integrated communication and localization of underwater robots with application to non-destructive nuclear reactor inspection. *IEEE international conference on Robotics and Automation*, 2012, pp.2445–2450.
4. Murai, R., Sakai, T., Kawano, H., Matsukawa, T., Honda, Y., Kitano, K.C, Campbell, K.C. A novel visible light communication system for enhanced control of autonomous delivery robots in a hospital. *IEEE/SICE International Symposium on System Integration (SII)*, 2012, pp. 510–516.
5. Shahin Uddin, M., Cha, J., Kim, J., Min Jang, Y. Mitigation Technique for Receiver Performance Variation of Multi-Color Channels in Visible Light Communication. *IEEE Sensors Journal*, 2011, V11, pp.6131–6144.
6. Cui, K., Chen, G., He, Q., Xu, Z. Indoor optical wireless communication by ultraviolet and visible light. *Proc. of SPIE*, 2009. V7464, pp.74640D-1–74640D-9.
7. Kim, N., Jing, C., Zhou, B., Kim, Y. Smart Parking Information System Exploiting Visible Light Communication. *International Journal of Smart Home*, 2014, V8, pp.251–260.
8. Yong Tan, Y., Jung, S., Chung, W. Real Time Biomedical Signal Transmission of Mixed ECG Signal and Patient Information using Visible Light Communication. *IEEE EMBS conference*, 2013.
9. Rajbhandari, S., Anthony, P., Haigh. Ghassemlooy, Z., Popoola, W. Wavelet-Neural Network VLC Receiver in the Presence of Artificial Light Interference. *IEEE Photonics Letters*, 2013, V25.
10. Chow, C.W., Yeh, C.H., Liu, Y.F., Huang, P.Y. Background Optical Noises Circumvention in LED Optical Wireless Systems Using OFDM. *IEEE photonics Journal*, 2013, V5.
11. Ya'nez, V.G., Torres, J. R., Alonso, J.B., Borges, A.R., Sa'nchez, C.Q., Gonza'lez, C.T., Jime'nez, R.P., Rajo, F.D. Illumination interference reduction system for VLC Communications, *Proc. WSEAS Int. Conf. Math. Methods, Comput. Tech. Intell. Syst*, 2009, pp. 252–257.
12. Yang, S.H., Kim, H.S., Son, Y.H., Han, S.K. Reduction of optical. Interference by wavelength filtering in RGB-LED based indoor VLC system. *Proc. OECC*, 2011, pp. 551–552.
13. Chang, C., Su, Y., Kurokawa, U., Ichoi, B. Interference Rejection Using Filter-Based Sensor Array in VLC System. *IEEE Sensors Journal*, 2012, V12, pp.1025–1032.
14. Cailean, A., Cagneau, B., Chassagne, L., Popa, V., M. Dimian. Evaluation of the noise effects on Visible Light Communications using Manchester and Miller coding. *International Conference on development and application systems*, 2014.
15. Komine, T., Nakagawa, M. Fundamental Analysis for Visible – Light Communication System using LED Lights. *IEEE Transactions on Consumer Electronics*, 2004, V50, #1, pp.100–106.

**Kadirvel Sindhubala**

received her B.E. degree in Electronics and Communication Engineering from Anna University in 2009 and M.Tech. in Communication Engineering from VIT University in 2011. From 2011 to 2013 she

worked as software engineer at Cognizant technology solutions. Currently, she is involved in her research on visible light communications at B.S. Abdur Rahman University, Chennai, India. She has Published 5 papers in various International journals, National journals and in conferences. Her current research includes optoelectronics, Visible Light Communication and optical communication

**Baba Vijayalakshmi**

received her AMIETE degree in Electronics and Telecommunication Engineering from IETE New Delhi in 2000 and M.E. in optical communication from Anna University, Chennai. She carried her research work in

3D scene generation using two 2D images through DRDO sponsored project. Since 2003, she has been a faculty in Electronics and Communication Engineering Department of different engineering colleges at Tamilnadu. Currently, she is serving as a professor in Electronics and Communication Engineering Department at B.S. Abdur Rahman University, Chennai. More than 24 papers are published in various International journals, National journals and in conferences. Her current research interests include image processing, Visible Light Communication, optical communication, perceptual image analysis, 3D scene generation

CONTENTS

VOLUME 25

NUMBER 3

2017

LIGHT & ENGINEERING
(SVETOTEKHNKA)

Vol. 25, No.3, 2017 is devoting to the selected papers from the partnership of Light&Engineering Journal from CHINA, which are focused in the scope of the journal.

PARTNERS OF LIGHT & ENGINEERING JOURNAL

Editorial Board with big gratitude would like to inform international lighting community about the Journal Partners Institute establishment. The list with our partners and their Logo see below.

The description of partner's collaboration you can found at journal site

www.sveto-tehnika.ru

GENERAL PARTNER



BL GROUP holding



PLATINUM PARTNERS



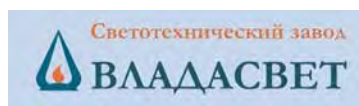
ГЛОБАЛ
ЛАЙТИНГ

GOLD PARTNERS

FAGERHULT



SILVER PARTNERS



BRONZE PARTNERS

